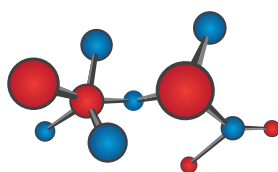


**SMS 2024**  
SMART MATERIALS AND SURFACES



**Nanomed**  
2024



**EGF 2024**  
European Graphene Forum

**SENSORS**  
2024



# SMS 2024 / NANOMED 2024 / EGF2024 / SENSORS 2024 JOINT CONFERENCES

**23 - 25 October 2024**  
**Barcelona, Spain**

## **Book of Abstracts**

Organizer



**SETCOR**  
Conferences & Exhibitions

**SMS / NanoMed / Sensors / EGF 2024**  
**Joint International Conferences Program**  
**23 - 25 October 2024, Barcelona - Spain**

<b>Wed. 23 Oct. 2024</b>		
<b>08:00 - 12:00</b>	<b>Conference Registration</b>	
<b>09:00 - 09:30</b>	<b>Welcome Coffee Break</b>	
<b>SMS 2024 / EGF 2024 / Sensors 2024 / NanoMed 2024 Joint Plenary Session I</b>		
<b>RUBÍ Conference Room RUBÍ (- 1 Floor)</b>		
<b>Session Chairs:</b> <b>Prof. Lucia Baldino, University of Salerno, Italy</b> <b>Prof. T Venkatesh, Stony Brook University, USA</b>		
<b>10:00 - 10:30</b>	Nanoengineered Biomaterials for Medicine and Beyond <b>K. Vasilev</b>	<b>Prof. Krasimir Vasilev</b> , Flinders University, <b>Australia</b>
<b>10:30 - 11:00</b>	Scalable High-Throughput Mechanical Exfoliation for Cost-Effective Production of van der Waals Nanosheets Y. Sozen, E. Zamora, J.J. Riquelme, Y. Xie, C. Munuera and <b>A. Castellanos-Gomez</b>	<b>Dr. Andres Castellanos Gomez</b> , ICMM-CSIC, <b>Spain</b>
<b>11:00 - 11:30</b>	Moiré Multilayers — Towards Topological Quasicrystals <b>M. Koshino</b>	<b>Prof. Mikito Koshino</b> , Osaka University, <b>Japan</b>
<b>11:30 - 12:00</b>	Detailed structural, chemical composition and optoelectronic properties studies of 2D materials via TEM. <b>R. Arenal</b>	<b>Dr. Raul Arenal</b> , University of Zaragoza, <b>Spain</b>
<b>12:00 - 12:30</b>	Towards new 2D quantum materials from single-layer chemically expanded graphenic lattices <b>S.T. Bromley</b>	<b>Prof. Stefan T. Bromley</b> , University of Barcelona, <b>Spain</b>
<b>12:00 - 14:00</b>	<b>Lunch Break - Rossini Room (Ground floor)</b>	
<b>SMS 2024 / Sensors 2024 / NanoMed 2024 Joint Session I. A: Materials synthesis, characterization and properties</b>		
<b>Session Chairs:</b> <b>Prof. Rumen Krastev, Reutlingen University, Germany</b> <b>Prof. Tae June Kang, Inha University, Incheon, Rep. of Korea</b> <b>Prof. Athar Hussain, Netaji Subhas University of Technology, India</b>		
<b>14:00 - 14:15</b>	Role of Phenolic Functional Group in Peptide-Based Bimodal Memristors <b>S. D. Namgung</b>	<b>Prof. Seok Daniel Namgung</b> , Chung-Ang University, Seoul, <b>Rep. of Korea</b>
<b>14:15 - 14:30</b>	Integration of cubic switches as active layer into memristor prototypes through electrochemical methods <b>S.F. Russi</b> , T. Petenzi, C. Methivier, J. Landoulsi, L. Fillaud, E. Maisonhaute, N. Daffe, J. Dreiser, Y. Li, V. Malytskyi and R. Lescouëzec	<b>Mrs. Sofia Frida Russi</b> , Sorbonne University, <b>France</b>
<b>14:30 - 14:45</b>	Nanofabrication of large-scale stretchable surface relief diffraction gratings Y. Bdour and <b>R.G. Sabat</b>	<b>Prof. Ribal Georges Sabat</b> , Royal Military College of Canada, <b>Canada</b>
<b>14:45 - 15:00</b>	Self-assembling colloids a new route to photonic structures <b>A. Chiappini</b> , A. Carpentiero, M. Bollani, R. Mudi, B.M. Squeo, M. Pasini, C. Botta, L. Pasquardini, B.N. Shivakiran Bhaktha, K. Debnath and T. Virgili	<b>Dr. Andrea Chiappini</b> , IFN-CNR CSMFO Lab & FBK Photonics Unit, <b>Italy</b>
<b>15:00 - 15:15</b>	Curminoid-based active surfaces towards the preparation of sensors <b>A. González-Campo</b> , R. Gimeno-Muñoz and N. Aliagaa	<b>Dr. Arántzazu González-Campo</b> , Institute of Materials Science of Barcelona, <b>Spain</b>
<b>15:15 - 15:30</b>	Chemical 'Click' sintering of noble nanoparticles for direct fabrication of nanoporous electrodes for (bio)sensing applications <b>M. Urban</b> , G. Rosati, G. Maroli, F. Della Pelle, A. Bonini, L. Sajti, M. Fedel, R. Blanch Rivera and A. Merçoçi	<b>Mr. Massimo Urban</b> , Catalan Institute of Nanoscience and Nanotechnology (ICN2), Barcelona, <b>Spain</b>

<b>15:30 - 15:45</b>	Lanthanide doped up-converting nanoparticles for bioimaging and thermal sensing <b>L. Mancic</b> , I. Dinic, M. Tomic, M. Vukovic, M. Lazarevic, M. Bukumira and M. Rabasovic	<b>Dr. Lidija Mancic</b> , Institute of Technical Sciences of SASA, <b>Serbia</b>
<b>15:45 - 16:00</b>	Influence of Electron-Phonon Interaction on Optoelectronic properties of Halide Double Perovskite <b>B.R. Sahoo</b> and P. A. Bhohe	<b>Mr. Bikash Ranjan Sahoo</b> Indian Institute of Technology Indore, <b>India</b>
<b>16:00 - 16:30</b>	<b>Afternoon Coffee Break</b>	
<b>Session Chairs:</b> <b>Dr. Andrea Chiappini, IFN-CNR CSMFO Lab &amp; FBK Photonics Unit, Italy</b> <b>Prof. Athar Hussain, Netaji Subhas University of Technology, India</b>		
<b>16:30 - 16:45</b>	Stamping Platinum Electrodes - a new method for modifying the geometry of electrochemical sensors <b>K. Jedlińska</b> , J. Eidenschink, F.-M. Matysik and B. Baś	<b>Dr. Katarzyna Jedlińska</b> , AGH University of Krakow, Kraków, <b>Poland</b>
<b>16:45 - 17:00</b>	Zinc Oxide Nanotubes doped by Palladium by Combining Electro-spinning and Atomic Layer Deposition Techniques for H <sub>2</sub> production <b>X. Sandua</b> , L. Badouric, I. Pellejero, P.J. Rivero, M. Bechelany and R. Rodríguez	<b>Mr. Xabier Sandua</b> , Public University of Navarre, <b>Spain</b>

Wed. 23 Oct. 2024

**SMS 2024 / NanoMed 2024 - Session I. B:  
Smart coatings and Surfaces / Biomaterials/ Bionanomaterials**

Conference Room DIAMANT (- 1 Floor)

**Session Chairs:**

**Prof. Krasimir Vasilev, Flinders University, Australia**

**Prof. Ping Xiao, University of Manchester, UK**

**Dr. Federico Barrino, University of Palermo, Italy**

14:00 - 14:30	Smart design with graded nanostructures for enhanced wear resistance of surfaces exposed to extreme conditions T. Yang, <b>T. A. Venkatesh</b> and M. Dao	<b>Prof. T Venkatesh</b> , Stony Brook University, <b>USA</b>
14:30 - 14:45	Development and Characteristics of sub-Stoichiometric High Entropy Carbonitride Coatings for Friction Applications <b>N. C. Zoita</b> , M. Dinu and A. C. Parau	<b>Dr. Nicolae C. Zoita</b> , National Institute of Research and Development for Optoelectronics- INOE 2000, <b>Romania</b>
14:45 - 15:00	Nanostructured polymer particle coatings for biological studies and sensing <b>E. Rosqvist</b> and J. Peltonen	<b>Dr. Emil Rosqvist</b> , Åbo Akademi University, <b>Finland</b>
15:00 - 15:15	Hydrodynamic testing of viscous drag reduction by bioinspired hybrid coatings <b>A. Rodríguez-Ortiz</b> , P. Pinilla-Cea and J.C. Suárez-Bermejo	<b>Dr. Álvaro Rodríguez Ortiz</b> , Universidad Politécnica de Madrid, <b>Spain</b>
15:15 - 15:30	Design and Development of Novel Additive Manufactured Structures with Optimised Properties for Biomedical Applications <b>V. Spinelli</b> , V. Gallicchio, C. Marino, V. D'Antò, G. Spagnuolo and S. Rengo	<b>Dr. Vincenzo Spinelli</b> , University of Naples, <b>Italy</b>
15:30 - 15:45	Development of magnetic molecular imprinted polymer systems for biomedical applications <b>C. Ciarlantini</b> , G. Carnevale, E. Lacolla, I. Francolini, M. Fernández-García, C. Muñoz-Núñez, A. Muñoz-Bonilla and A. Piozzi	<b>Dr. Clarissa Ciarlantini</b> , University of "La Sapienza", Rome, <b>Italy</b>
15:45 - 16:00	4D printing of triple-shape memory polymer using a thermal stimulus for biomedical applications <b>S. Shankar Mohol</b> and P. Mohan Pandey	<b>Mr. Shubham Shankar Mohol</b> , Indian Institute of Technology Delhi, <b>India</b>
16:00 - 16:30	<b>Afternoon Coffee Break</b>	
<b>Session Chairs:</b>		
<b>Prof. T Venkatesh, Stony Brook University, USA</b>		
<b>Dr. Valentina Castagnola, Italian Institute of technology, Italy</b>		
16:30 - 16:45	Flexible nanostructured electrodes for neural interfacing including core-shell nanowires including core-shell nanowires <b>N. Rodríguez-Díez</b> , B.L. Rodilla, A. Arché-Nuñez, S. Ruiz-Gómez, P. Ocón, L. Pérez and M. T. González	<b>Mrs. Noelia Rodríguez Díez</b> , Fundación IMDEA, <b>Spain</b>
16:45 - 17:00	Sol-Gel Synthesis of Silica-based Biomaterials with different weight percentages of Rosmarinic Acid <b>F. Barrino</b> , F. Giuliano, F. Sedita and C. Dispenza	<b>Dr. Federico Barrino</b> , University of Palermo, <b>Italy</b>
17:00 - 17:15	Graphene oxide is biocompatible and strengthens gelatine through non-covalent interactions with its amorphous region H. Jin Sim, K. Marinkovic, P. Xiao and <b>H. Lu</b>	<b>Dr. Hui Lu</b> , The University of Manchester, <b>UK</b>
17:15 - 17:30	Characterization of lyophilized, extruded histidylated liposome, a versatile platform for mRNA delivery <b>A. Ngalle Loth</b> , M. Maroquenne, Ayoub Medhmedj, C. Pichon, Delphine Logeart- Avramoglou and F. Perche	<b>Mr. Albert Ngalle Loth</b> , University of Orleans, <b>France</b>
17:30 - 17:45	Synthesis and Characterization of Cadmium Sulphide Nanoparticles with Antimicrobial Assay <b>E.U. Ekwujuru</b> , M. G. Peleyeju, C. Ssemakalu, M. E. Monpathi and M. J. Klink	<b>Ms. Ezinne Ekwujuru</b> , Vaal University of Technology, <b>South Africa</b>



Wed. 23 Oct. 2024

**EGF 2024 - Session I. C:**  
**Graphene and 2D Materials synthesis, characterization, and properties**

Conference Room CORAL + CRISTAL (-1 Floor)

**Session Chairs:**

**Dr. Raul Arenal, University of Zaragoza, Spain**

**Dr. Emiliano Bonera, Università degli Studi di Milano Bicocca, Italy**

14:00 - 14:30	Chemistry of 2D Materials for Patterning and Building of Heterostructures <b>E.M. Pérez</b>	<b>Prof. Emilio M. Pérez Alvarez,</b> IMDEA Nanoscience, <b>Spain</b>
14:30 - 14:45	Tuning the exchange coupling in graphene-based synthetic antiferromagnets <b>M. Hsouna,</b> C.A. Brondin, TO. Menteş, A. Locatelli and N. Stojić	<b>Ms. Maha Hsouna,</b> The Abdus Salam International Centre for Theoretical Physics, <b>Italy</b>
14:45 - 15:00	Band Gaps Engineering in the 2D Mo(S1-X,TeX)2-Alloy Adsorbed on Graphite, or Sandwiched Between Layers of Graphene <b>B. P. Burton</b>	<b>Dr. Benjamin Burton,</b> NIST, <b>USA</b>
15:00 - 15:15	Emergent cavity junction around metal-on-graphene contacts <b>Y. Zhao,</b> M. Kapfer, K. Watanabe, T. Taniguchi, O. Zilberberg and B. S. Jessen	<b>Mr. Yuhao Zhao,</b> ETH Zurich, <b>Switzerland</b>
15:15 - 15:30	The Effects of Drying Method and Gelation Time on Reduced Graphene Oxide Aerogels <b>S. Mallia,</b> A. Agius Anastasi and D. A. Vella	<b>Mr. Sean Mallia,</b> University of Malta, <b>Malta</b>
15:30 - 15:45	The Chemistry of Graphene Oxide and its derivatives, a multi-purpose nanolaboratory <b>F. Amato,</b> A. Motta, L. Giaccari, P. Altimari and A. G. Marrani	<b>Dr. Francesco Amato,</b> University "La Sapienza", Rome, <b>Italy</b>
15:45 - 16:00	A continuous approach to developing new pathways for the synthesis of graphene derived materials <b>S. Kellici</b>	<b>Dr. Suela Kellici,</b> London South Bank University, <b>UK</b>
16:00 - 16:30	<b>Afternoon Coffee Break</b>	
<b>Session Chairs :</b>		
<b>Prof. Emilio M. Pérez Alvarez, IMDEA Nanoscience, Spain</b>		
<b>Prof. Mikito Koshino, Osaka University, Japan</b>		
<b>Dr. Emiliano Bonera, Università degli Studi di Milano Bicocca, Italy</b>		
16:30 - 16:45	Nonionic, Cationic and Anionic Surfactants-Assisted Liquid Exfoliation of Graphite into Few-Layer Graphene: Impact of Ultrasound, Solvents and Surfactants <b>M. Saeed,</b> A. Ismail, M. AlSaeedi and Sh. Ahmad	<b>Dr. Maryam Saeed,</b> Kuwait Institute for Scientific Research, <b>Kuwait</b>
16:45 - 17:00	Effect of Graphene Reinforcement on the Tribological and Fracture Behaviours of Silicon-Based Nanocomposites <b>H. Abo El-Einein,</b> A. Berrais, A. Weibel, C. Laurent, B. Berthel and M.I. De Barros Bouchet	<b>Mr. Hussein Abo El-Einein,</b> Ecole Centrale de Lyon, <b>France</b>
17:00 - 17:15	Multi-Probe Evaluation of the Mechanical Response of Monolayer Graphene <b>J. Varillas,</b> J. Lukeš, A. Manikas, J. Maňák, Jiří. Dluhoš, Z. Melníková, C. Galiotis, O. Frank and M. Kalbáč	<b>Dr. Javier Varillas,</b> J. Heyrovský Institute of Physical Chemistry, <b>Czech Rep.</b>
17:15 - 17:30	Laser-induced graphene on biocompatible polymers <b>T. Vičentić,</b> M. V. Pergal, M. Rašljčić Rafajilović, A. Gavran, S. D. Ilić and M. Spasenović	<b>Ms. Teodora Vicentic,</b> University of Belgrade, <b>Serbia</b>
17:30 - 17:45	Development of new substrates for super-resolution studies of supported Lipid Bilayers (slb) by graphene induced energy transfer <b>H. Evcı</b>	<b>Mr. Hüseyin Evcı,</b> J. Heyrovsky Institute of Physical Chemistry, <b>Czech Rep.</b>

Thu. 24 October 2024

**EGF 2024 / SMS 2024 Session II. A:  
Graphene properties and applications  
Functional / Multifunctional, Hybrid, Composites and Responsive Materials**

Conference Room RUBÍ (-1 Floor)

**Session Chairs:**

**Prof. Mikito Koshino, Osaka University, Japan  
Prof. Emilio M. Pérez Alvarez, IMDEA Nanoscience, Spain**

09:00 - 09:30	Thermal properties of Xenon measured by optothermal Raman spectroscopy <b>E. Bonera</b>	<b>Dr. Emiliano Bonera,</b> Università degli Studi di Milano Bicocca, <b>Italy</b>
09:30 - 10:00	Interfacial Ferroelectricity in van der Waals semiconductors and their heterostructures <b>V. Falko</b>	<b>Prof. Vladimir Falko,</b> Manchester University, <b>United Kingdom</b>
10:00 - 10:15	Low resistance laser-reduced graphene oxide: electrical and mechanical characterization for flexible electronic applications <b>M. G. Bonando,</b> N. M. M. Fernandes, S. S. Piva, R. J. E. Andrade, C. C. C. Silva and L. A. M. Saito	<b>Mr. Matheus Guitti Bonando,</b> Mackenzie Presbyterian University, <b>Brazil</b>
10:15 - 10:30	Manufacturing and Thermal Simulation of Graphene Doped Carbon Fiber Reinforced Composites for Through Thickness Heat Transfer <b>J. M. J. Gugliuzza,</b> S. Carosella and P. Middendorf	<b>Mr. Jakob Gugliuzza,</b> University of Stuttgart, <b>Germany</b>

10:30 - 11:00

Morning Coffee Break

**Session Chairs:**

**Prof. Mikito Koshino, Osaka University, Japan  
Dr. Emiliano Bonera, Università degli Studi di Milano Bicocca, Italy  
Prof. Vladimir Falko, Manchester University, United Kingdom**

11:00 - 11:30	On the origin of cyclic instability of SMA actuators <b>P. Šittner,</b> O. Tyc, E. Iaparova, O. Molnarová and L. Heller	<b>Dr. Petr Šittner,</b> Czech Academy of Sciences, <b>Czech Rep.</b>
11:30 - 11:45	Hybridization of Materials and Processes by means of Additive Manufacturing Technologies <b>T. Moritz,</b> U. Scheithauer, A. Günther, L. Gottlieb, E. Schwarzer-Fischer and J. Abel	<b>Dr. Tassilo Moritz,</b> Fraunhofer Institute for Ceramic Technologies and Systems, <b>Germany</b>
11:45 - 12:00	Moiré Engineering in Twisted WTe <sub>2</sub> Structures <b>S.J. Kheirabadi,</b> F. Gity, P.K. Hurley and L. Ansari	<b>Dr. Sharieh J. Kheirabadi,</b> University College Cork, <b>Ireland</b>

12:00 - 14:00

Lunch Break - Rossini Room (Ground floor)

Group Photo at 13:45

**Smart Materials and Surfaces / Sensors 2024 Session II. B:  
New Materials for sensors and actuators: Sensing the Future with New Materials**

**Session Chairs:**

**Dr. Petr Šittner, Czech Academy of Sciences, Czech Republic  
Dr. Andrea Chiappini, IFN-CNR CSMFO Lab & FBK Photonics Unit, Italy**

14:00 - 14:30	Conducting research on the use of curcuminoid-based surfaces as sensors <b>N. Aliaga-Alcalde</b>	<b>Prof. Nuria Aliaga-Alcalde,</b> Institute of Materials Science of Barcelona, <b>Spain</b>
14:30 - 14:45	Engineering Porosity for Tuning Electromechanical Properties in Piezoelectric Systems K. S. Challagulla and <b>T. A. Venkatesh</b>	<b>Prof. T Venkatesh,</b> Stony Brook University, <b>USA</b>
14:45 - 15:00	Combined optical and conductivity properties of ZnO for gas sensor devices <b>Z. Shao,</b> K. Jacob, M. Jakoobi, V. Collière, L. Vendier, Y. Coppel, K. Fajerweg, J-D. Marty, A. Ryzhikov, C. Mingotaud and M. L. Kahn	<b>Mr. Zhigang Shao,</b> CNRS-University of Toulouse, <b>France</b>
15:00 - 15:15	Toward Highly Sensitive Biosensing Systems Based on Perovskite Fluorescent Labels	<b>Mr. William Teixeira,</b> Polytechnic University Valencia, <b>Spain</b>

	<b>W. Teixeira</b> , C. Collantes, P. Martínez, J. Carrascosa, V. González-Pedro and M-J. Bañuls and A. Maquieira	
<b>15:15 - 15:30</b>	Printing technologies at the forefront of analytical tools and sensors innovation <b>F. Paré</b> , G. Gabriel and M. Baeza	<b>Mr. Franc Paré</b> , Autonomous University Barcelona, <b>Spain</b>
<b>15:30 - 15:45</b>	Wearable Textile-based Chemiresistive pH Sensors with MXene-Chitosan Composite <b>P. Kumar</b> , G. M. Stojanović, M. Gupta and H. F. Hawari	<b>Dr. Pradeep Kumar</b> , University of Novi Sad, <b>Serbia</b>
<b>15:45 - 16:00</b>	Smart Patch for Continuous Monitoring and Stretchable Electronics in Enhancing Patient Outcomes <b>A. Ben-Aissa</b> , M. Moreno, B. Molina, M. Alique and A. Moya	<b>Dr. Alejandra Ben-Aissa Soler</b> , Eurecat, <b>Spain</b>
<b>16:00 - 16:30</b>	<b>Afternoon Coffee Break</b>	
<b>SMS / NanoMed / Sensors 2024 Joint Session II. C: Biosensors and sensors for medical applications</b>		
<b>Session Chairs:</b> <b>Prof. Nuria Aliaga-Alcalde</b> , Institute of Materials Science of Barcelona, Spain <b>Dr. Petr Sittner</b> , Czech Academy of Sciences, Czech Republic		
<b>16:30 - 17:00</b>	MOF-based sensors with enhanced electroconductivity: application for vascular endothelial growth factor (VEGF) detection <b>R. Antiochia</b> , M.C. di Gregorio, V. Gigli, T. Gentili, C. Tortolini, A.M. Isidori and M. Nuti	<b>Prof. Riccarda Antiochia</b> , University of Rome "La Sapienza", <b>Italy</b>
<b>17:00 - 17:15</b>	Non-invasive, minimalistic, and self-operated glucose sensor for point-of-care testing in saliva <b>E. G. San Vicente</b> , D. Martin Prats, X. Palmer, R. Grinyte and J. M. Cabot	<b>Ms. Elena G. San Vicente</b> , LEITAT Technological Centre- Barcelona, <b>Spain</b>
<b>17:15 - 17:30</b>	Introducing all-inkjet-printed microneedles for in-vivo biosensing <b>G. Rosati</b> , P.B. Deroco, M.G. Bonando, G.G. Dalkiranis, K. Cordero-Edwards, G. Maroli, L.T Kubota, O.N. Oliveira Jr, L.A. Miyazato Saito, C.C.C. Silva and A. Merkoçi	<b>Dr. Giulio Rosati</b> , Catalan Institute of Nanoscience and Nanotechnology, <b>Spain</b>

**Conference Dinner**  
**Conference venue hotel**  
**24 Oct. 2024 from 19:30**

<b>Thu. 24 October 2024</b>		
<b>NanoMed / Sensors joint Session II. D: Bioinspired, Biomimetic bioactive biomaterials Intelligent drug delivery and release system</b>		
<b>Conference Room DIAMANT (-1 Floor)</b>		
<b>Session Chairs:</b> <b>Prof. Luca Gentilucci, University of Bologna, Italy</b> <b>Prof. Vesselin N. Paunov, Nazarbayev University, Kazakhstan</b>		
<b>09:00 - 09:30</b>	biomimetic approach for designing superhydrophobic surfaces <b>J. Rumeau</b>	<b>Prof. Jannick Rumeau</b> , University of Lyon, <b>France</b>
<b>09:30 - 10:00</b>	Design of Nanomaterials for Radiation Therapy <b>G. Tobías-Rossell</b>	<b>Dr. Gerard Tobías-Rossell</b> , Institut de Ciència de Materials de Barcelona (ICMAB-CSIC), <b>Spain</b>
<b>10:00 - 10:30</b>	Bioinspired nanovesicles as bioengineered hybrid tools against cancer cells <b>V. Cauda</b>	<b>Prof. Valentina Cauda</b> , Polytechnic University of Turin, <b>Italy</b>
<b>10:30 - 11:00</b>	<b>Morning Coffee Break</b>	
<b>11:00 - 11:30</b>	Emerging nanotechnologies for targeting pathogenic bacterial biofilms <b>V.N. Paunov</b>	<b>Prof. Vesselin N. Paunov</b> , Nazarbayev University, <b>Kazakhstan</b>
<b>11:30 - 11:45</b>	Using Label-Free Single Particle Tracking to Characterise the Effect of Cell Layers on Nanoparticle Diffusion in Experimental Models G. Schleyer, E.A. Patterson and <b>J.M. Curran</b>	<b>Ms. Genevieve Schleyer</b> , University of Liverpool, <b>UK</b>
<b>11:45 - 12:00</b>	Platinum nanozymes against central nervous system dysfunctions <b>L. Boselli</b> , G. Tarricone, G. Mirra, L. Cursi, V. Castagnola, F. Benfenati and P.P. Pompa	<b>Dr. Luca Boselli</b> , Italian Institute of technology, <b>Italy</b>
<b>12:00 - 14:00</b>	<b>Lunch Break - Rossini Room (Ground floor)</b>	
<b>Group Photo at 13:45</b>		
<b>SMS / NanoMed / Sensors 2024 joint Session II. E: Biomaterials / NanoBioMaterials / Bioimaging / Biosensors</b>		
<b>Session Chairs:</b> <b>Prof. Jannick Rumeau, University of Lyon, France</b> <b>Dr. Valentina Castagnola, Italian Institute of technology, Italy</b>		
<b>14:00 - 14:30</b>	Integrin-Targeting Peptides for the Design of Cell- Eager Nanostructured Biomaterials <b>L. Gentilucci</b> and T. He	<b>Prof. Luca Gentilucci</b> , University of Bologna, <b>Italy</b>
<b>14:30 - 14:45</b>	Destination brain: trans- and paracellular strategies to overcome the blood-brain barrier <b>V.Castagnola</b> , M. Trevisani, S. Vercellino, L. Boselli, L. Pappagallo, F. De Chirico, A. Danielli, A. Berselli, G. Alberini, L. Maragliano and F. Benfenati	<b>Dr. Valentina Castagnola</b> , Italian Institute of technology, <b>Italy</b>
<b>14:45 - 15:00</b>	Control of protein adsorption, cell adhesion and growth on polysaccharide based multilayer films by incorporation of graphene oxide <b>T. Andreeva</b> and R. Krastev	<b>Dr. Tonya Andreeva</b> , Reutlingen University, <b>Germany</b>
<b>15:00 - 15:15</b>	Exploring the Protein Surface Interactions of a Protein Inspired by a Natural Glue <b>D. Ayed</b> , Z. Khalil, C. R. Picot, M. Weidenhaupt, F. Bruckert, R. Mathey, Y. Hou-Broutin and C. Vendrely	<b>Dr. Dhekra Ayed</b> , CNRS- University Grenoble Alpes, <b>France</b>
<b>15:15 - 15:30</b>	Locally Selective Immobilisation of DNA Origami for Raman Spectroscopy based Biosensors <b>J. Hann</b> , M. Janssen, C. Meinecke, S. Hartmann, A. Heerwig, D. Reuter and M. Mertig	<b>Ms. Julia Hann</b> , University of Technology Chemnitz, <b>Germany</b>
<b>15:30 - 15:45</b>	Multi-scale nanoimprinted nanopillar structures within a microfluidic device fabrication with surface functionalization <b>H.O. M. Chu</b> , P. Goldberg Oppenheimer and L. M. Grover	<b>Dr. Hin On Chu</b> , University of Birmingham, <b>UK</b>

15:45 - 16:00	Advanced Integrated Multipurpose Spectroscopic Lab-on-a-chip for Timely Detection of Extracellular Vesicles as Key-Markers of Inflammatory Bowel Disease <b>E.Buchan</b> , J.J.S.Rickard, M.R.Thomas and P.Goldberg Oppenheimer	<b>Dr. Emma Buchan</b> , University of Birmingham, <b>UK</b>
<b>16:00 - 16:30 Afternoon Coffee Break</b>		
<b>Session Chairs:</b> <b>Prof. Jannick Rumeau, University of Lyon, France</b> <b>Dr. Federico Barrino, University of Palermo, Italy</b>		
16:30 - 17:00	Multifunctional Stimuli-Responsive Systems for Sensing <b>L.L. del Mercato</b>	<b>Dr. Loretta L. del Mercato</b> , Institute of Nanotechnology of CNR, Italy
17:00 - 17:30	Validation of an Intracranial Raman Spectroscopic Probe for In-Situ Monitoring of Traumatic Brain Injury <b>C. A. Stickland</b> , Z. Sztranyovszky, J. J. S. Rickard and P. Goldberg Oppenheimer	<b>Ms. Clarissa Stickland</b> , University of Birmingham, <b>UK</b>
17:30 - 17:45	CMOS-Compatible Electrochemical ELISA Platform for Semi-continuous Cytokine Monitoring in Organ-on-Chip Systems <b>S. J. Zapiain-Merino</b> , A. Torosyan, K. Jans, R. Vos, L. Lagae and O. Henry	<b>Mr. Santino Zapiain</b> , IMEC - Leuven, <b>Belgium</b>

**Conference Dinner**  
Conference venue hotel  
24 Oct. 2024 from 19:30

Thu 24 Oct. 2024

**NanoMed 2024 Session II. F:  
Nanomaterials for Biomedical / Tissue engineering, drug, and gene delivery**

Conference Room CORAL + CRISTAL (-1 Floor)

**Session Chairs:**

**Prof. Valentina Cauda, Polytechnic University of Turin, Italy**  
**Prof. Anna Laurenzana, University of Florence, Italy**  
**Prof. Krasimir Vasilev, Flinders University, Australia**

14:00 - 14:30	Production and Characterization of Deformable Vesicles for Transdermal Application <b>L. Baldino, S. Sarnelli and E. Reverchon</b>	<b>Prof. Lucia Baldino, University of Salerno, Italy</b>
14:30 - 14:45	Potential neuroprotective effects of intranasally delivered multi-walled carbon nanotubes <b>S.Fiorito, M.Soligo and D.Uccelletti</b>	<b>Dr. Silvana Fiorito, Sapienza University- CNR, Italy</b>
14:45 - 15:00	PIC micelles encapsulating medical Cu-64 as a Drug Delivery System for Cancer Therapy <b>M.A.G. Mikhail, N. Hayashi, T. Eto, K. Tsukada, A. Kishimura, and H. Kamizawa6</b>	<b>Mrs. Mary Mikhail, Kyushu University, Japan</b>
15:00 - 15:15	Release of indocyanine green from nanostructured absorbable patch manufactured by bio-printer <b>A. de Nigris, G. Quero, G. P. Vanoli and L. Ambrosone</b>	<b>Dr. Antonio de Nigris, University of Molise, Italy</b>
15:15 - 15:30	Developing Experimental Models to Characterise the Diffusion of Nanoparticles Through Complex Environments using a Novel Real-Time Label-Free Tracking Platform <b>M. Lorenzo López, V.R. Kearns, E.A. Patterson and J.M. Curran</b>	<b>Ms. Moira Lorenzo Lopez, University of Liverpool, UK</b>
15:30 - 15:45	Gold Nanoparticles and endothelial progenitor cells: a win-win alliance for targeting tumors <b>C. Anceschi, E. Frediani, J.Ruzzolini, F. Margheri, A. Chillà, F. Ratto, P. Armanetti, L. Menichetti, M. Del Rosso, G. Fibbi and A. Laurenzana</b>	<b>Dr. Cecilia Anceschi, University of Florence, Italy</b>

16:00 - 16:30

Afternoon Coffee Break

**Session Chairs:**

**Prof. Lucia Baldino, University of Salerno, Italy**  
**Prof. Krasimir Vasilev, Flinders University, Australia**

16:30 - 17:00	Yin/Yang effectiveness of gold nanoparticles in controlling tumor progression and promoting vascularization in vasculopathies <b>A. Laurenzana, C. Anceschi, F. Scavone, A. Chillà, E. Frediani, F. Margheri, F. Ratto, C. Borri, M. Del Rosso, T. del Rosso and G. Fibbi</b>	<b>Prof. Anna Laurenzana, University of Florence, Italy</b>
17:00 - 17:15	Synthesis of nanostructured polymer systems for quantification of circulating biomarkers <b>P. Mastella, S. Luin and F. Beltram</b>	<b>Mr. Pasquale Mastella, Scuola Normale Superiore and CNR-Nano, Italy</b>
17:15 - 17:30	Perfluorocarbon-PLGA particle ultrastructure affects pH sensitivity in 19F NMR and MRI <b>A. Mali, M. Daal, N. Ziolkowska, N. Stumpe, N. Larreina Vicente, N.K. van Riessen, V.V.S. Pillai, F.S. Ruggeri, C. Cadiou, F. Chuburu, D. Jirak, P.B. White and M. Srinivas</b>	<b>Ms. Alvja Mali, Wageningen University and Research, The Netherlands</b>

Conference Dinner  
Conference venue hotel  
24 Oct. 2024 from 19:30



Fri. 25 Oct. 2024

**SMS / EGF 2024 Session III.A:  
Applications for energy and environment**

Conference room DIAMANT (-1 Floor)

**Session Chairs:**  
**Prof. Vladimir Falko, Manchester University, United Kingdom**  
**Prof. Rumen Krastev, Reutlingen University, Germany**

09:30 - 10:00	Anaerobic Biodegradation of Pharmaceutical Herbal Waste Using Batch Test Study <b>A. Hussain</b> , M. Priyadarshi and P. Das	<b>Prof. Athar Hussain</b> , Netaji Subhas University of Technology, <b>India</b>
10:00 - 10:30	<b>Morning Coffee Break</b>	
10:30 - 10:45	Ca(OH) <sub>2</sub> pellets with mesoporous alumina as a binder for thermochemical energy storage <b>D. Castro</b> , E. S. Sanz-Pérez, L. Briones and J. M. Escola	<b>Mr. David Castro</b> , Rey Juan Carlos University, <b>Spain</b>
10:45 - 11:00	Ecological enhancement of PVDF electroactive phase with plant-sourced ZnO for sustainable energy harvesting <b>H. Rejdali</b> , I. Salhi, M. Boutaous, J. Jay, A. Hajjaji and F. Belhora	<b>Ms. Hajar Rejdali</b> , University Chouaib Doukkali, <b>Morocco</b>
11:00 - 11:15	Covalent immobilization of EDTA onto graphene oxide and its application for heavy metal removal A. Al-Shammakhi, <b>E-S I. El-Shafey</b> , B. Al-Wahaibi, S.N.F. Ali	<b>Prof. El-Said I. El-Shafey</b> , Sultan Qaboos University, <b>Oman</b>
11:15 - 11:30	PEO coatings for photocatalytic remediation of water <b>D. Czekanowska</b> , C. Blawert, M. Serdechnova, A. Bamburov, R. Vasilic and P. Głuchowski	<b>Ms. Dominika Czekanowska</b> , Graphene Energy LTD, <b>Poland</b>
11:30 - 11:45	Biodegradation of 2-Chlorophenol by anaerobic reduction on graphene oxide membranes supported on tubular ceramic filtration elements. <b>D. Guevara</b> , J. Font and F. Stüber	<b>Ms. Daniela Guevara Correa</b> , Rovira i Virgili University, <b>Spain</b>
11:45 - 12:00	Efficient CoZnCr@MXene based electrocatalyst for High-Current-Density Alkaline Water Splitting at Industrial Temperature <b>P. Chauhan</b> and Z. Sofer	<b>Dr. Payal Chauhan</b> , Univ. of Chemistry and Technology, <b>Czech Rep.</b>



Fri. 25 Oct. 2024

**Sensors 2024 Session III.B: gas sensors, physical sensors, etc**

Conference room CORAL + CRISTAL (-1 Floor)

**Session Chairs:**

**Prof. Riccarda Antiochia, University of Rome "La Sapienza", Italy**  
**Prof. Sang Sub Kim, Inha University, Rep. of Korea**

<b>09:30 - 09:45</b>	Enhancement of Sensing Properties of Semiconductor Resistive Gas Sensors by Surface Treatment H. Woo Kim and <b>S. Sub Kim</b>	<b>Prof. Sang Sub Kim, Inha University, Rep. of Korea</b>
<b>09:45 - 10:00</b>	Development of an electrochemical oxygen micro sensor for industrial application <b>A. Benayache, V. Martini, C. Marlot and K. Aguir</b>	<b>Ms. Amira Benayache, Aix Marseille Univ, France</b>
<b>10:00 - 10:30</b>	<b>Morning Coffee Break</b>	
<b>10:30 - 10:45</b>	Optimizing Gas Sensing Response: High-Temperature Gradient Laser Annealing of Block Copolymer-Templated Metal Oxide Nanowires <b>P. Pula</b> and P.W. Majewski	<b>Mr. Przemyslaw Pula, University of Warsaw, Poland</b>
<b>10:45 - 11:00</b>	Experimental Investigation of Thermal Tuning for Laterally Excited Bulk Acoustic Wave MEMS Resonators using SOI Bulk Heating <b>M. Bengashier, O. Casha, I. Grech, R. Farrugia, J. Micallef and E. Gatt</b>	<b>Mrs. Munira Bengashier, University of Malta, Malta</b>
<b>11:00 - 11:15</b>	Impact of Optical Fiber Design on the Performance of Interferometric Temperature Sensors at Elevated Temperature <b>S. Pevec, M. Njegovec, V. Budinski, V. Žužek, J. Bojkovski and D. Donlagic</b>	<b>Dr. Simon Pevec, University of Maribor, Slovenia</b>
<b>11:15 - 11:30</b>	A modular gamma-ray scanner consisting of two linear CsI+SiPM arrays for radioactive waste sorting <b>G. Elio Poma, C. Rita Failla, L. Giovanni Cosentino, F. Longhitano, G. Vecchio and P. Finocchiaro</b>	<b>Dr. Gaetano Elio Poma, INFN-LNS, Italy</b>

N.	Poster Title	Author, Affiliation, Country
1.	Sol gel microencapsulated additives for auto-healing coatings of galvanized stainless steel <b>L. Florentino</b> , O. Conejero and R. B. de la Rua	<b>Mrs. Lucia Florentino</b> , Idonial technology Centre, Spain
2.	Development of hybrid sol-gel coatings with improved anticorrosion properties for Cr-free passivation of galvanized steel <b>M. Prado</b> , P. Sánchez and O. Conejero	<b>Mrs. Marta Prado Garcia</b> , Idonial Technology Centre, Spain
3.	Short Electrospun Cellulose Acetate Nanofibers as Seed Coating Applications <b>P.A.M. Chagas</b> , G. B. Medeiros, W. P. Oliveira and M.L. Aguiar	<b>Dr. Paulo A.M. Chagas</b> , Federal University of São Carlos, Brazil
4.	Structural, mechanical, wear and anticorrosive properties of protective multilayers based on TiSi carbo-nitrides used for the development of cutting tools <b>L.R. Constantin</b> , A. C.Parau, M. Dinu, I. Pana, C. Vitelaru, D. M. Vranceanu and A ; Vladescu Dragomir	<b>Dr. Lidia R. Constantin</b> , INOE 2000, Romania
5.	The Impact of Plasma Treatment on Magnesium's Corrosion Resistance and Biocompatibility <b>A. Kocijan</b> , J. Kovač, I. Junkar, M. Resnik, V. Kononenko and M. Conradi	<b>Dr. Aleksandra Kocijan</b> , Institute of Metals and Technology, Ljubljana, Slovenia
6.	Tribological properties of laser-textured Ti6Al4V alloy upon addition of MoS2 nanotubes under water and oil lubrication: introducing the concept of green tribology <b>M. Conradi</b> , B. Podgornik, A. Kocijan, M. Remškar and D. Klobčar	<b>Dr. Marjetka Conradi</b> , Institute of metals and technology, Ljubljana, Slovenia
7.	Bipolar Current Collectors of Carbon Fiber Reinforced Polymer for Laminates of Energy Storage Structural Composites B. Jun So, G. Shin, Y. Choi, H. Lee and <b>T. June Kang</b>	<b>Prof. Tae June Kang</b> , Inha University, Incheon, Rep. of Korea
8.	Containment of Heavy Metal Diffusion from River Yamuna to the Surrounding Geology using Bentonite Based Nanomaterial <b>M. Priyadarshi</b> , P. Das and A. Hussain	<b>Ms. Manjeeta Priyadarshi</b> , Netaji Subhas University of Technology, India
9.	CoPt alloys catalysts for Methanol Oxidation Reaction (MOR): influence of material shape onto their catalytic properties <b>O.G. Dragos-Pinzaru</b> , G. Buema, M. Tibu, F. Borza, G.Ababei, G. Stoian, C. Hlenschi, I. Tabakovic and N. Lupu	<b>Dr. Oana G. Dragos Pinzaru</b> , National Institute of R&D for Technical Physics, Romania
10.	Effect of Complete Dealumination on Acidic, Textural and Adsorption Properties of BEA Zeolite <b>M. Mihaylov</b> , O. Lagunov, V. Zdravkova, E. Ivanova, I. Spassova and K. Hadjiivanov	<b>Prof. Mihail Mihaylov</b> , Institute of General and Inorganic Chemistry- Sofia, Bulgaria
11.	Oxidation of Hydrogen Sorbed in Reduced Nanoceria <b>E. Ivanova</b> , M. Mihaylov, N. Drenchev, K. Chakarova and K. Hadjiivanov	<b>Mrs. Elena Ivanova</b> , Institute of General and Inorganic Chemistry, Sofia, Bulgaria
12.	Green synthesized Au-Ag core-shell nanoparticles as catalyst for reductive degradation of carmoisine V. Moroşan, B. Moldovan and <b>L. David</b>	<b>Prof. Luminita David</b> , "Babeş-Bolyai" University, Cluj-Napoca, Romania
13.	Comparative study of the graphene morphology on the effective electroelastic behavior of PVDF matrix composites <b>S. Elbarnaty</b> , W. Azoti, JPM. Correia and S. Ahzi	<b>Mr. Salah Elbarnaty</b> , University of Strasbourg, France
14.	Hydrogenated graphene superlattices: electronic and optical properties <b>V. A. Saroka</b> , L. A. Chernozatonskii and O. Pulci	<b>Dr. Vasil Saroka</b> , University of Rome Tor Vergata, Italy
15.	pH sensor for the in-situ environmental measurements <b>N. Lenar</b> , R. Piech and B. Paczosa-Bator	<b>Dr. Nikola Lenar</b> , AGH University of Krakow, Poland
16.	FDM technology and the effect of printing parameters on the tensile strength of ABS parts <b>M. Daly</b> , M. Tarfaoui, M. Chihi and C. Bouraoui	<b>Mr. Mohamed Daly</b> , ENSTA Bretagne, France
17.	Advanced Deep Learning Framework for Damage Detection in 3D-Printed AEROSIL-Infused Polycarbonate Under Dynamic Loading <b>Y. Qarssis</b> , A. Karine, M. Nachtane and M. Tarfaoui	<b>Mr. Youssef Qarssis</b> , ENSTA Bretagne, France

18.	Numerical Simulation for Assessing Wave Energy Converter Structural Resistance and Hydrodynamic Behavior <b>M. Karkab</b> , A. Ghennioui, K. Bouziane, O. Jellouli and M. Tarfaoui	<b>Mr. Mohammed Karkab</b> , ENSTA Bretagne, <b>France</b> .
19.	Polymethyl Methacrylate Fresnel Lenses to Focalize Ultrasound at Megahertz <b>M. Ghasemishabankareh</b> , F. Torres and N. Barniol	<b>Mr. Mohammadamir Ghasemishabankareh</b> , Autonomous Univ. Barcelona, <b>Spain</b>
20.	Investigation of a QCM sensing system using the concentration of low-concentration biomarker gas <b>H. Ito</b> , S. Hashimoto and T. Katsuno	<b>Dr. Hirofumi Ito</b> , Toyota Central R&D Labs, <b>Japan</b>
21.	Automatic skin cancer diagnosis using a robotic hyperspectral sensor. C. Sáez, O. Sanmartín, A. García and <b>R. Díaz</b>	<b>Mr. Ricardo Díaz</b> , Sensor and Robotic Department-AINIA, Valencia, <b>Spain</b>
22.	Electrospun carbon nanofibers doped with metal nanoparticles used as sensors for highly sensitive voltametric drug determination <b>J. Smajdor</b> , M. Zambrzycki, M. Marzec, B. Paczosa-Bator and R. Piech	<b>Dr. Joanna Smajdor</b> , AGH University of Science and Technology, <b>Poland</b>
23.	Optimising Raman Spectroscopy for Early Detection of Microbial Spoilage in Meat <b>D. Bhowmik</b> , J. Rickard and P. Goldberg Oppenheimer	<b>Ms. Debarati Bhowmik</b> , University of Birmingham, <b>UK</b>
24.	Reliability Analysis of Hydrogen Pressure Sensor for Automotive Applications <b>H. Lee</b> , C. Han, J. Lee, K. Lee, and H. Sagong	<b>Dr. Hojoon Lee</b> , Korea Automotive Technology Institute, <b>Rep. of Korea</b>
25.	Development of an Integrated Self-Diagnostic System for Water Quality Measurement Sensors <b>K.-Y. Hwang</b> and S. Bae	<b>Dr. Kyung-Yup Hwang</b> , BLUESEN Co. Ltd., <b>Rep. of Korea</b>
26.	Integrating Satellite, Ground Sensors, and AI for Surface Water Protection: The EcoNet Project G. Grasso, D. Zane, B. Brunetti, <b>S. Foglia</b> , G. Ferrara, V. La Pegna, D. De Santis, D. Cappelli, M. Frezza, I. Petracca, F. Del Frate, G. Licciardi, P. Sacco, D. Tapete and R. Dragone	<b>Dr. Sabrina Foglia</b> , CNR-ISMN, <b>Italy</b>
27.	Biosynthesis of cellulose using Antarctic bacterial strains <b>M.C. Biondini</b> , A. Vassallo, M. di Sessa, M. Zannotti, R. Giovannetti and S. Pucciarelli	<b>Dr. Maria Chiara Biondini</b> , University of Camerino, <b>Italy</b>
28.	Characterization of a blue pigment isolated from an Antarctic Rhodococcus bacterial strain <b>M. di Sessa</b> , M. Chiara Biondini, A. Vassallo, M. Zannotti, S. Pucciarelli and R. Giovannetti	<b>Mrs. Martina di Sessa</b> , University of Camerino, <b>Italy</b>
29.	Antimicrobial effect on coated catheter surface <b>Á. Deák</b> , L. Janovák, D. Szabó, L. Rovó, A. Zore, A. Abram and K. Bohinc	<b>Dr. Ágota Imre-Deák</b> , Univ. of Szeged, <b>Hungary</b>
30.	Advancements in Biodegradable Magnesium-Based Implants: Enhancing Biocompatibility and Corrosion Resistance through Alloy Development T. Tański, <b>A. Woźniak</b> , P. Snopiński, K. Cesarz-Adreczke and M. Król	<b>Dr. Anna Woźniak</b> , Silesian University of Technology, <b>Poland</b>
31.	Tailoring Fibrinogen Adsorption on Layer-by-Layer Films: the impact of hydrophilicity and film structure of cross linked PAA/PAH multi-layers B. Borisova, Andreeva, R. Tzoneva and <b>R. Krastev</b>	<b>Prof. Rumen Krastev</b> , Reutlingen University, <b>Germany</b>
32.	Development of a Novel Photothermal Material Using Gold Nanoparticles Synthesized Inside a Hydrogel for Biomedical and Biocatalytic Applications <b>M.J. Martínez-Tomé</b> , A. Balah Tahiri, M. Rubio-Camacho, J. Gómez, C.R. Mateo, R. Esquembre	<b>Dr. María José Martínez Tomé</b> , Miguel Hernández University, <b>Spain</b>
33.	Antioxidant Effect of New Green Synthesized Bimetallic Nanoparticles using Phytocompounds from Goji Fruits <b>B. Moldovan</b> , V. Morosan, L. David and I. Baldea	<b>Dr. Bianca Moldovan</b> , Babeş-Bolyai University, <b>Romania</b>
34.	Design and development of cyclodextrin nano-sponges based in situ gelling systems to co-deliver polyphenols for candidiasis therapy S. V Paramshetti, M. Angolkar, <b>A. Al Fatease</b> and R.A.M Osmani	<b>Prof. Adel Al Fatease</b> , King Khalid University, <b>Saudi Arabia</b>
35.	Synthesis of Photo-crosslinked Nanoparticulate Polymer Supports Using Cyclodextrin and Chitosan Derivatives <b>C-L. Logigan</b> , C. Peptu and C-A. Peptu	<b>Dr. Corina-Lenuta Logigan</b> , Gheorghe Asachi Technical University, <b>Romania</b>
36.	Innovative Nanoparticulate Polymer Supports via Thiol–Ene Polymer Conjugation for Enhanced Drug Delivery <b>C-A. Peptu</b> , C. Peptu and L. Corina-Lenuta	<b>Dr. Catalina A. Peptu</b> , Gheorghe Asachi Technical University, <b>Romania</b>

37.	Novel Egg Protein-Based Nanoplatfoms as Drug Delivery Systems for Personalized Medicine <b>F. Seidita</b> , F. Barrino, M. Mangione, P. Picone, D. Nuzzo, A. Girgenti, D. Chmielewska, M. Walo, S. Cabo Verde and C. Dispenza	<b>Dr. Federica Seidita</b> , Università degli Studi di Palermo, <b>Italy</b>
38.	Reprogramming human ferritin nanoparticles for multivalent inhibition of PCSK9: a novel strategy to enhance LDL cholesterol clearance. <b>C. Cappelletti</b> , A. Incocciati, S. Masciarelli, F. Liccardo, R. Piacentini, S. Botta, L. Bertuccini, B. De Berardis, F. Fazi, A. Boffi, A. Bonamore and A. Macone	<b>Ms. Chiara Cappelletti</b> , Sapienza University of Rome, <b>Italy</b>
39.	ROS responsive dextran-thioketal conjugate nanocarriers for the delivery of various low and high molecular weight hydrophilic payloads <b>S. Nayak</b> , E. Pirlet, N. Caz, E. Wolfs, A. Bronckaers, W. Maes and A. Ethirajan	<b>Mr. Sourav Nayak</b> , Hasselt University, <b>Belgium</b>
40.	Fluorometholone loaded Solid Lipid Nanoparticles: a new strategy for ocular delivery of anti-inflammatory drugs <b>R. Da Ana</b> , J. Fonseca, S. Cravo, F. Fathi5, E. Sanchez-Lopez, M.B.Oliveira, M. Garcia and E. Souto	<b>Ms. Raquel da Ana</b> University of Porto, <b>Portugal</b>
41.	Innovative Gold-Liposome Nanohybrids: Revolutionizing Photothermal Nanoplatfoms with Tunable Plasmonic Properties <b>M. Rubio-Camacho</b> , C. Cuestas-Ayllón, R. Esquembre, M.J. Martínez-Tomé, J.M. de la Fuente and C. R. Mateo	<b>Mrs. Marta Rubio Camacho</b> , Miguel Hernández University, <b>Spain</b>
42.	Optimization of Lipid Nanoparticles for RNA Encapsulation: Influence of the Nature and Content of Ionizable Lipid M. Frohly, C. Favre, E. Lacazette, F. Montury and <b>L. Sanchez Gonzalez</b>	<b>Dr. Laura Sanchez Gonzalez</b> , CEA NanO'up Plateform, <b>France</b>
43.	Improving antibiotics quantification using label-free SERS-based microfluidic platform. Challenges of therapeutic drug monitoring at intensive care units. <b>R. Slipets</b> and M. Pytlarz	<b>Mr. Roman Slipets</b> , Technical University of Denmark, <b>Denmark</b>
44.	Microphysiological systems based on liver on chip for drug discovery and testing. E. Guerrero, A. Rigat, P. Monterde, X. Barceló and <b>J. M. Cabot</b>	<b>Dr. Joan Marc Cabot</b> , Leitat, Barcelona, <b>Spain</b>
45.	Influence of the Nature and Content of Bile Salts on the Properties of Bilosomes Developed for Nose-to-brain Applications <b>J. Aussourd</b> , C. Favre, F. Montury and L. Sanchez Gonzalez	<b>Ms. Justine Aussourd</b> , CEA NanO'up Plateform, <b>France</b>
46.	Development of photosensitizing nanoparticles of nanodiamonds using femtosecond lasers <b>R. C. Queiroz</b> , C. R. Hurtado, G. R. Hurtado, A. M. dos Santos, M. F. Diniz, H. C. Junqueira, A. U. Fernandes, H. Besser, W. Pfleging and D. B. Tada	<b>Ms. Rafaela Campos Queiroz</b> , Karlsruher Institute of Technology, <b>Germany</b>
47.	Lipophilic molecular rotor to assess the viscosity of oil core in nano-emulsion droplets <b>M. Elhassan</b> , C. Faivre, H. Anton, G. Conzatti, P. Didier, T. Vandamme, A. S. Elamin, M. Collot and N ; Anton	<b>Mr. Mohamed Elhassan</b> , University of Strasbourg, <b>France</b>
48.	Nanovehicles for a combined cell differentiation therapy and cancer stem cell-targeting drugs: towards a new way to prevent resistance and tumor recurrence in glioblastoma (TARG-DIFFERENT). <b>T. Fernandez-Cabada</b> , P. Melón, M. Mulero-Acevedo, P. Alfonso-Triguero, A. P. Candiota and J. Lorenzo	<b>Dr. Tamara Fernandez Cabada</b> , Autonomous University of Barcelona, <b>Spain</b>
49.	Shining Light on Cancer Treatments: Integrated Photonic Biosensors for Immunotherapy Monitoring <b>A. Morgado</b> , V. Gil-Ocaña, L. Rueda Calzada, Y. Aceta and A. Con-de-González	<b>Dr. Anjara Morgado</b> , Bioherent S.L, <b>Spain</b>
50.	NIR responsive gold nanorod for targeted cancer photothermal therapy <b>S. Gul</b> , F. Barbero, A. Bellone, G. Perrone, R. Mazzoli and I. Fenoglio	<b>Ms. Shagufta Gul</b> , University of Turin, <b>Italy</b>
51.	Self-targeted magnetic nanoparticles for combined magnetothermal therapy and immunotherapy in cancer treatment <b>X. Xie</b> , C-C. Fong and M. Yang	<b>Ms. Xulin Xie</b> , City University of Hong Kong, <b>China</b>
52.	New Insight in the radius of influence in Electric Force Microscopy <b>L. Lehnert</b> , R. Thoelen and H. Möbius	<b>Mr. Lukas Lehnert</b> , Univ. of Applied Sciences Kaiserslautern, <b>Germany</b>
53.	Hydrogen-like atoms with shielded ions in the tight-binding approximation <b>B. Freinkman</b>	<b>Dr. Boris Freynkman</b> , Independent researcher, <b>Russia</b>
54.	A miniaturized, wireless and implantable sensory system to screen bone healing. <b>E. G. San Vicente</b> , C. Hennemann , J. Disser, R. Grinyte, N. Marjanovi and J. M. Cabot	<b>Ms. Elena G. San Vicente</b> , LEITAT Technological Centre- Barcelona, <b>Spain</b>

## Oral Presentation and Poster terms

### For the Oral Presentation:

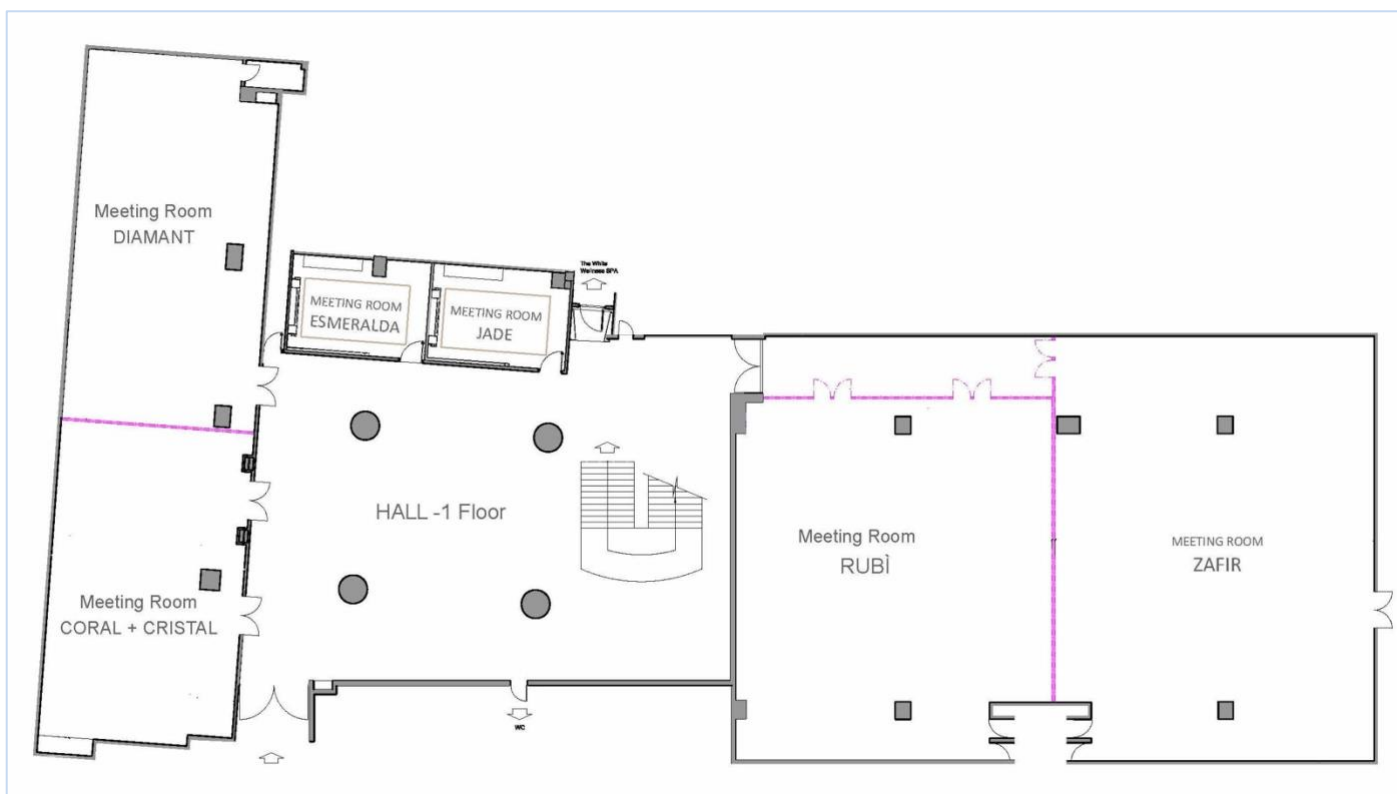
Duration of each talk type (including 2 to 3 minutes for Questions/Answers):

- Keynote talk: 30 minutes. Oral presentation: 15 minutes.
- We do not impose a template for the oral presentation.
- You need to carry your presentation in USB key or external disk and **use the available presentations laptop** at the conference room.
- **Do not plan to use your own laptop.**

### For the Poster:

- Poster dimensions must be within **100cm high X 80cm wide**.
- We do not impose a template for the poster content.
- Please display your poster at your poster board number as per the conference program.

## Conference Venue Floorplan (-1 Floor)



**SMS 2024 / EGF 2024 / Sensors 2024  
/ NanoMed 2024 Joint Plenary  
Session I**



# Nanoengineered Biomaterials for Medicine and Beyond

K. Vasilev<sup>1</sup>

<sup>1</sup> College of Medicine and Public Health, Flinders University, Sturt Road, Bedford Park, South Australia 5042, Australia, Australia  
E-mail: [krasimir.vasilev@flinders.edu.au](mailto:krasimir.vasilev@flinders.edu.au)

## Abstract:

In this keynote talk, I will give an overview of recent progress from my team on development of advanced nanoengineered surfaces and materials capable of controlling infection and inflammation, and are utility in other medical technologies such as drug delivery, tissue engineering and diagnosis of diseases. Over the last few years, we have created the means to control the entire spectrum of surface properties including chemical, physical, mechanical and topographical. We do that by nanoengineering and tailoring traditional plasma polymer films using tools from nanotechnology. By controlling surface properties, we are able to address medical challenges that are often encountered with implantable devices such as infection and inflammation. We have developed four distinct classes of antibacterial surfaces that are suitable for application on various medical devices, which can be classified based on their mechanism of action as non-stinky, contact killing, antimicrobial compound releasing and stimuli responsive. I will provide examples and describe the strategies used to achieve such surfaces, including some that are translated onto commercial devices in collaboration with industry. We have strong interest in understanding the inflammatory responses to biomaterial surfaces, and particularly, the interplay between surface nanotopography and chemistry in regulating these physiological processes. We found that when these parameters are used in an optimal way, we can achieve surfaces that lead to reduction of inflammation and enhance healing. Recently, we have also revealed that the mechanism of surface nanotopography induced modulation of inflammation is related to unfolding of adsorbed proteins. In the case of fibrinogen, for instance, surface nanotopography induced unfolding leads to the exposure of otherwise concealed peptide sequences that activate the MAC-1 receptor of macrophages. I will also give examples of how we use our surface nanoengineering approaches to create diagnostic devices which have been translated to industry. I will also give examples of how the tools generated by our work facilitate progress in other medical area, such as

reproduction, and how we apply our expertise to advance fields beyond biomedical.

**Keywords:** biomaterial coatings, antibacterial surface, medical devices, infection, tissue engineering, inflammation, diagnostics, plasma deposition.

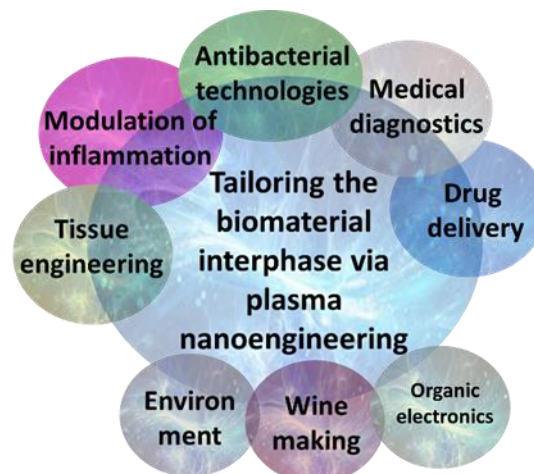


**Figure 1:** Applications of Plasma Nanoengineering.

## Selected references:

1. Visalakshan et al *Advanced Functional Materials* 29 (14), 1970088 (2019)
2. Chen et al *ACS Nano* 11 (5), 4494-4506 (2017)
3. Taheri et al *Biomaterials* 35 (16)4601–4609 (2014)
4. Mierczynska-Vasilev et al *Food Chemistry* 275, 154-160 (2019)
5. Wahono et al *Environmental Pollution* 240, 725-732 (2018)
6. Bright et al *Nano Letters* 22, 16, 6724–6731 (2022)
7. Truong et al *ACS Nano* 17 (15), 14406-14423 (2023)
8. Hayles et al *npj Biofilms and Microbiomes* 9 (1), 90 (2023)
9. Nguyen et al *Advanced Functional Materials* 2310539 (2023)
10. Pham et al *Small* 2305469 (2023)



# Scalable High-Throughput Mechanical Exfoliation for Cost-Effective Production of van der Waals Nanosheets

Yigit Sozen, Esteban Zamora, Juan J. Riquelme, Yong Xie, Carmen Munuera and Andres Castellanos-Gomez

Instituto de Ciencia de los Materiales de Madrid, Spain

## **Abstract:**

Efforts in nanoscience have long sought scalable methods for producing van der Waals materials, following the landmark discovery of graphene via mechanical exfoliation. While this technique offers superior material quality, its scalability is limited by challenges in controlling thickness and lateral size. In this talk, we will introduce a novel approach utilizing a roll-to-roll setup and an automated, massive parallel exfoliation process to address these limitations. Our method yields adhesive tapes densely populated with nanosheets of van der Waals materials over large areas, achieving a notable balance between large lateral size, scalability, and cost-efficiency. Notably, our technique avoids harsh treatments and is compatible with air-sensitive materials.

Through successful fabrication of field-effect transistors and flexible photodetectors in large batches, we demonstrate the practicality and versatility of our approach. By providing a low-cost, scalable pathway for producing large-area films, our method promises significant advancements in the fabrication of high-performance nanoscale devices.

# Moiré Multilayers — Towards Topological Quasicrystals

M. Koshino

Department of Physics, Osaka University, Osaka, Japan

## Abstract:

Two-dimensional moiré materials exhibit a long-range moiré pattern resulting from lattice mismatch, which profoundly influences their electronic properties. In addition to the extensive study of twisted moiré bilayers in the past decade, the scope of investigation has extended to encompass multilayer systems including three or more layers. Particular attention has recently been directed toward twisted trilayer which consists of three layers arranged in a specific rotational configuration. A twisted trilayer is characterized by two distinct twist angles between adjacent layers, where the resulting multiple moiré patterns generate a quasiperiodic structure that lacks conventional periodicity.

After a brief introduction of the conventional moiré bilayer systems, we will present systematic theoretical studies on the lattice relaxation and the electronic structures in general twisted trilayer graphenes [1]. We show that the relaxed lattice structure forms a patchwork of moiré-of-moiré domains, where a moiré pattern given by layer 1 and 2 and another pattern given by layer 2 and 3 become locally commensurate (Fig. 1). The electronic band calculation reveals an emergence of one-dimensional states sharply localized at the boundaries between supermoiré domains, and they are identified as a topological boundary state between distinct Chern insulators. We also show the application to the TMDC trilayers. The theoretical scheme serves as a fundamental tool and guiding principle for topological band engineering in twisted multilayers beyond graphene trilayers.

In the latter part, we will explore the electronic structure of hBN/graphene/hBN trilayer system with arbitrary twist angles. We find that the electronic spectrum displays fractal minigaps akin to the Hofstadter butterfly. Each of minigaps is uniquely labeled by six topological numbers associated with the quasicrystalline Brillouin zones, and these numbers can be expressed as second Chern numbers through a formal connection with the quantum Hall effect in four-dimensional space [2,3].

**Keywords:** 2D materials, graphene, twisted bilayer graphene, moiré pattern, edge states, topological materials.

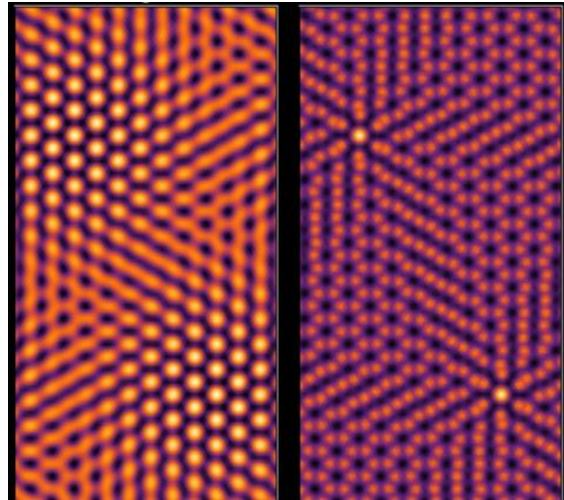


**Figure 1:** Moiré-of-moiré domain formation in twisted trilayer graphene. The left and right panels illustrate the moiré pattern in the rigid and relaxed lattices, respectively

## References:

1. N. Nakatsuji, T. Kawakami, M. Koshino, *Phys. Rev. X* **13**, 041007 (2023).
2. M. Koshino, H. Oka, *Phys. Rev. Research* **4**, 013028 (2022)
3. H. Oka and M. Koshino, *Phys. Rev. B* **104**, 035306 (2021)

# Towards new 2D quantum materials from single-layer chemically-expanded graphenic lattices

Stefan T. Bromley<sup>1,2</sup>

<sup>1</sup> Departament de Ciència de Materials i Química Física & Institut de Química Teòrica i Computacional (IQTC), Universitat de Barcelona, c/ Martí i Franquès 1-11, 08028 Barcelona, Spain.

<sup>2</sup> Institució Catalana de Recerca i Estudis Avançats (ICREA), Passeig de Lluís Companys, 23, 08010 Barcelona (Spain).

Email: s.bromley@ub.edu

## Abstract

Graphene displays a weakly correlated semimetallic electronic structure associated with its extended  $\pi$ -system of highly delocalised electrons. Early theoretical proposals to increase the electronic correlation in graphene suggested expanding the graphenic lattice to induce increased electron-localisation and the emergence of new gapped electronic states (e.g. antiferromagnetic/AFM). For pristine graphene, the high in-plane strains required to induce such states are experimentally unattainable. An alternative approach is to “insert” additional carbon atoms between the trigonal  $sp^2$  nodes of the 2D honeycomb lattice (i.e. chemically expanding the graphenic lattice). This procedure leads to a family of 2D materials known as graphynes. We have recently shown that many graphynes indeed display non-graphenic correlated gapped AFM states [1]. Such correlated graphynes are, however, chemically reactive and difficult to stabilize. Here, we focus on a class materials based on protected trigonal  $sp^2$  carbon nodes. This can be achieved by using persistent radical building blocks (e.g. triphenylmethyl radicals) to construct such 2D materials (i.e. 2D covalent organic radical frameworks – 2D CORFs) in a bottom-up fashion. We show that the resulting chemically-expanded graphenic materials have the potential to exhibit a range of correlated electronic states (e.g. AFM Mott insulator, quantum spin liquid, exotic magnetic states) which, moreover, can be tuned by mechanical and chemical means [2,3,4]. 2D CORFs could thus provide a new single-layered materials platform for future carbon-based quantum technologies.

## References

1. G. Lleopart, M. Lopez-Suarez, I. de P. R. Moreira, S. T. Bromley, *J. Chem. Phys.* 157 (2022), 214704.
2. I. Alcón, J. Ribas-Arino, Ibério de P.R. Moreira, S. T. Bromley, *J. Am. Chem. Soc.* 145 (2023) 5674.
3. I. Alcón, R. Santiago, J. Ribas-Arino, M. Deumal, I. de P. R. Moreira, S. T. Bromley, *Nat. Commun.* 12 (2021) 1705.
4. R. Santiago, I. Alcón, J. Ribas-Arino, M. Deumal, I. de P. R. Moreira, S. T. Bromley, *Adv. Funct. Mater.* (2021) 31, 202004584

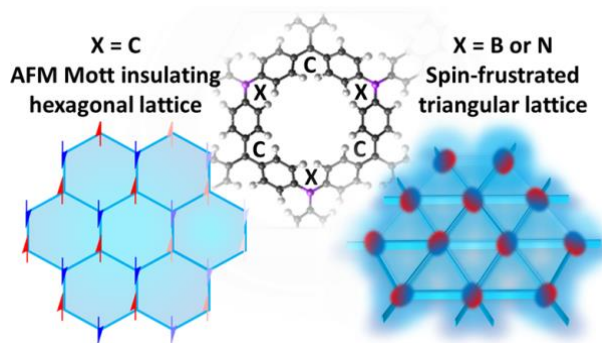


**Figure 1:** AFM Mott insulating / spin-frustrated states in chemically-expanded graphenic lattices [2].

**SMS 2024 / Sensors 2024 / NanoMed  
2024 Joint Session I. A:  
Materials synthesis,  
characterization and properties**

# Role of Phenolic Functional Group in Peptide-Based Bimodal Memristors

S. D. Namgung<sup>1\*</sup>

<sup>1</sup> School of Electrical and Electronics Engineering, Chung-Ang University, Seoul, Republic of Korea

## Abstract:

Neuromorphic computing, an emerging approach for handling large data volumes, has drawn attention due to memristors' potential in realizing this technology. However, memristor operation is inherently stochastic, affecting device control. To bridge the gap between synthetic devices and biological systems, we create a bimodal memristor using bioderived peptide materials.

In biological systems, tyrosine plays a crucial role in proton-coupled electron transfer (PCET)<sup>1</sup>. Unlike synthetic-material-based electronics, where protons and electrons are not simultaneously coupled, tyrosine enables highly efficient charge transfer. Recent research shows that tyrosine-rich peptides (TRPs) significantly influence resistive switching in peptide memristors.<sup>2</sup> By designing specific amino acid sequences, we can improve power consumption and variability. Additionally, memristors exhibit bimodality through proton injection without a voltage sweep.

We specifically investigate the impact of the phenolic hydroxyl group in tyrosine on resistive-switching properties, specifically related to proton mediation. We compare two peptide-based bimodal memristor sequences: YYACAYY (Y7C) and FFACAFF (F7C), analyzing both voltage and humidity modes. (Figure 1) Our findings demonstrate that the phenolic hydroxyl group reduces set voltage and humidity due to proton mediation during electrochemical metallization. This sequence design allows tailoring of proton-coupled reactions, resulting in low power consumption and improved resistive-switching control—a valuable strategy for brainlike computing hardware.

**Keywords:** memristor, memory device, neuromorphic system, peptide, phenolic functional group, tyrosine-rich peptides, tyrosine, phenylalanine.

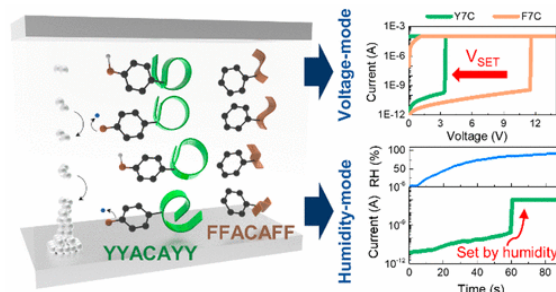


**Figure 1:** The schematic of a peptide memristor operating via electrochemical metallization involves the phenolic hydroxyl group in tyrosine (green) facilitating the redox reaction of Ag/Ag<sup>+</sup> through protonation/deprotonation. In contrast, the benzene group in phenylalanine (brown) does not assist electrochemical metallization due to the absence of a phenolic OH group, resulting in a redox process dominated solely by voltage.

## References:

1. Martin S., Stenbjörn S., Henriette W., Yunhua X., Licheng S., Leif H. (2005) Switching the Redox Mechanism: Models for Proton-Coupled Electron Transfer from Tyrosine and Tryptophan, *J. Am. Chem. Soc.* 127, 11, 3855-3863
2. Song M.-K. Namgung S. D., Choi D., Kim H., Seo H., Ju M., Lee Y. H., Sung T., Lee Y.-S., Nam K. T., Kwon J.-Y., (2020) Proton-Enabled Activation of Peptide Materials for Biological Bimodal Memory. *Nat. Commun.* 11, 5896,

# Integration of cubic switches as active layer into memristor prototypes through electrochemical methods

S.F. Russi<sup>1</sup>, T. Petenzi<sup>3</sup>, C. Methivier<sup>2</sup>, J. Landoulsi<sup>2</sup>, L. Fillaud<sup>3</sup>, E. Maisonhaute<sup>3</sup>, N. Daffe<sup>4</sup>, J. Dreiser<sup>4</sup>, Y. Li<sup>1</sup>, V. Malyskiy<sup>1</sup>, R. Lescouëzec<sup>1</sup>

<sup>1</sup> IPCM, CNRS UMR 8232, Sorbonne Université, 4 place Jussieu, 75005 Paris, France

<sup>2</sup> LRS, CNRS UMR 7197, Sorbonne Université, 4 place Jussieu 75005 Paris, France.

<sup>3</sup> LISE, CNRS UMR 8235, Sorbonne Université, 4 place Jussieu, 75005 Paris, France

<sup>4</sup> Paul Scherrer Institut, CH-5232 Villigen PSI, Switzerland

## Abstract:

Prussian blue analogues (PBAs) are well-known 3D inorganic polymers which have been extensively investigated because of their tuneable electronic and magnetic properties together with their nano-porosity. However, their integration into microelectronic devices is sometimes made difficult by their insolubility in organic solvents.

As an alternative, our group works on molecular scale PBAs, octametallic units based on  $\text{Fe}_4\text{Co}_4$  cages which are robust in solution and can be therefore integrated in nanomaterials. Similarly to the polymeric parent compound PBAs, the  $\pi$ -character of the cyanide bridge ensures the electronic communication between the metal centres resulting in the occurrence of a photo- or thermally-induced metal-to-metal Electron Transfer Coupled to a Spin Transition (ETCST). Moreover, differently from the polymer, the cube assembly can be studied by electrochemical methods, for which it shows interesting redox behaviour with up to nine oxidation states<sup>1</sup>.

The stability in solution of the molecule is due to the capping of each cation by organic *fac*-tridentate ligands. In our group we are using scorpionates ligands like tris-pyrazolylborate (Tp) and tris-pyrazolylmethane (Tpm) which can also act as “linkers” among cubes thanks to their functionalization with electropolymerizable groups (e.g. thiophene derivatives)<sup>2</sup>.

Such connection is made by cyclic voltammetry, a wet chemistry approach, permitting the growth of a film with controlled thickness. CV, AFM, XPS and XAS analysis confirm the stability of the cage after deposition and the preservation of the properties of the bulk. Finally, with the aim of integrating these obtained films into prototypes of two-electrodes devices, a top electrode was deposited to measure the electric activity of the film, which showed memristive-like effect.

**Keywords:** Molecular switches, molecular magnetism, coordination chemistry, thin film, memristor

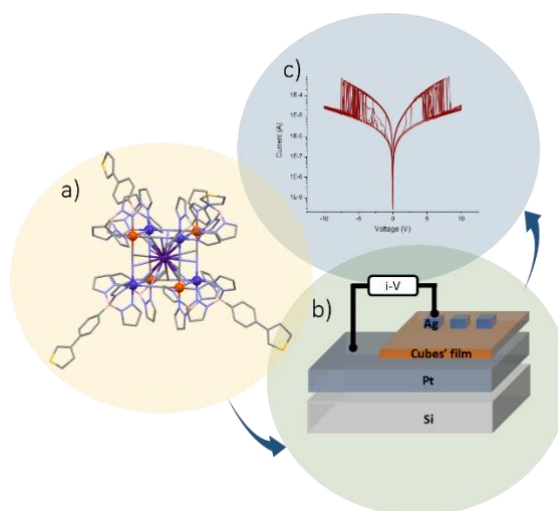


**Figure 1:** (a) Structure of the cube before polymerization. (b) Device configuration. (c) i-V curve response.

## References:

1. J. Jiménez, J. Glatz, A. Benchohra, G. Gontard, L. Chamoreau, J. Meunier, A. Bousseksou, R. Lescouëzec (2020), Electron Transfer in the  $\text{Cs}[\text{Mn}_4\text{Fe}_4]$  Cubic Switch: A Soluble Molecular Model of the MnFe Prussian-Blue Analogues, *Angew. Chem. Int. Ed.*, 59, 8089–8093.
2. A. Benchohra, C. Méthivier, J. Landoulsi, D. Kreher, R. Lescouëzec (2020), Electrospray ionization: an efficient approach to deposit polymetallic molecular switches onto gold surfaces, *Chem. Commun.*, 56, 6587–6589.



# Nanofabrication of large-scale stretchable surface relief diffraction gratings

Yazan Bdour<sup>1</sup>, and Ribal Georges Sabat<sup>1,\*</sup>

<sup>1</sup> Department of Physics and Space Science, Royal Military College of Canada, PO Box 17000, STN Forces, Kingston, Ontario, K7K7B4, Canada

## Abstract:

Holographic optical nanostructures, microstructures and metasurfaces can be inscribed on azobenzene-containing thin films by exposure to an interfering laser pattern at an absorbing wavelength. The primary mechanism invoked in the creation of these surface relief features is a localized mass transport of the azobenzene molecules yielding the formation of a surface profile identical to that of the inscribing laser [1]. A simple sinusoidal interference pattern will yield sinusoidal diffraction gratings. Figure 1 is an atomic force microscope image of a typical sinusoidal surface relief grating inscribed on an azobenzene molecular glass thin film. After inscription, a polydimethylsiloxane (PDMS) layer is deposited over the grating, cured and the grating is transferred to the PDMS. The overall pitch and modulation depth of the transferred grating are nearly identical to the original azobenzene grating. This is done in order to take advantage of the stretchable nature of the PDMS layer. An in-house fixture was built to hold and stretch the PDMS grating while enabling it to be imaged using an atomic force microscope. The PDMS grating was stretched to different strain values and the grating pitch was measured at different steps, as seen in Figure 2. In this figure, the grating was stretched a total of 4 mm from its original shape. This yielded a change in the pitch from 700 nm to 830 nm, or a 19% increase in the pitch value. It was also found that the grating exhibited a strain hysteresis and that it took a few minutes for the PDMS grating to stabilize after the strain has been gradually increased.

**Keywords:** Nanopatterning, stretchable surfaces, diffraction grating, polymer thin films, optical diffraction, adaptive optics.

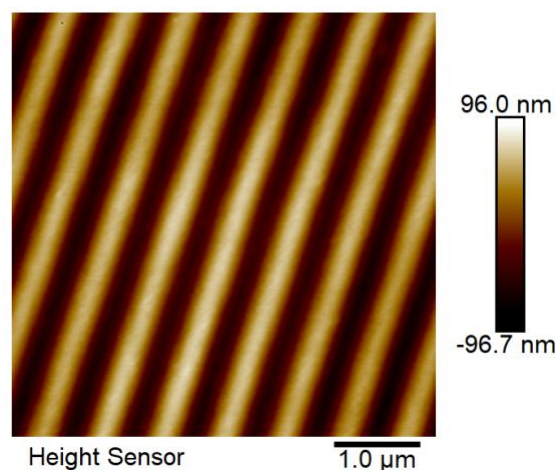


**Figure 1:** Atomic Force Microscope of a surface relief grating on azobenzene molecular glass. The grating has a pitch of 700 nm.

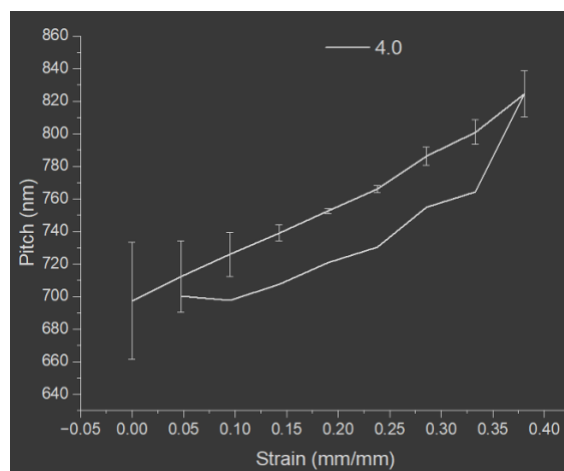


**Figure 2:** Measured grating pitch as a function of strain when the PDMS film is stretched by 4 mm.

## References:

1. Rochon, P., E. Batalla, and A. Natansohn. "Optically induced surface gratings on azoaromatic polymer films." *Applied Physics Letters* 66, no. 2 (1995): 136-138.



# Self-assembling colloids a new route to photonic structures

A. Chiappini<sup>1</sup>, A. Carpentiero<sup>1</sup>, M. Bollani<sup>2</sup>, R. Mudi<sup>3</sup>, B.M. Squeo<sup>4</sup>, M. Pasini<sup>4</sup>, C. Botta<sup>4</sup>, L. Pasquardini<sup>5</sup>, B.N. Shivakiran Bhaktha<sup>6</sup>, K. Debnath<sup>7</sup>, T. Virgili<sup>2</sup>

<sup>1</sup>IFN-CNR CSMFO Lab & FBK Photonics Unit, Via alla Cascata 56/C, 38123 Trento, Italy

<sup>2</sup>IFN-CNR Milano, piazza Leonardo da Vinci 32, 20133 Milano, Italy

<sup>3</sup>Advanced Technology Development Centre, IIT Kharagpur, West Bengal, 721302, India

<sup>4</sup>SCITEC-CNR, Via A. Corti 12, 20133 Milano, Italy

<sup>5</sup>Indivenire Srl, Via alla Cascata 56/C, 38123 Trento, Italy

<sup>6</sup>Department of Physics, IIT Kharagpur, West Bengal, 721302, India

<sup>7</sup>School of Natural and Computing Sciences, University of Aberdeen, AB243UE, Scotland

## Abstract:

Photonic crystals (PCs) and glasses (PGs) are materials with a well-known capability of affecting the propagation and reflection of electromagnetic radiation depending on the structural features, the material's refractive index, and wavelength of light [1,2].

Here we present two complementary confined structures based on identical shape and size elements crystallized under different lattices.

- (a) The first one is based on polystyrene monosize nanoparticles assembled in a disordered structures that is able to tailor the light diffusion due to the establishment of Mie resonances. In particular after the deposited of a thin film of Poly(9,9-dioctylfluorene-altbenzothiadiazole) (F8BT) on top of it. We have observed a modification of the spectroscopic features of the F8BT with an increases its PL quantum efficiency from 25% to 37% due to the cavity effect produced by thesystem [1].
- (b) The second one concerns the existence of optical Tamm states (OTS) in inverse opal (IO) - based three-dimensional photonic crystal on a flat metal substrate [2]. In this case thanks to large surgance area of the inverse opal, it is possible to facilitate the access to the detection volume and therefore reduce the detection limit of organic volents or specific analytes. Here we demonstrate that Tamm-IO can be used as a suitable platform for the detection of low contration of organic solvents. In the specific we have verified the experimentally results obtained are in good agreement with the computationally one. Moreover the sensitivity and repeatability of the Tamm-IO make them a potential platform for the development of integrated optic volatile organic compound sensors.

**Keywords:** photonic crystal, inverse opal, surface plasmon resonance, optical Tamm state, Tamm inverse opal, volatile solvents., photonic glasses, quantum yield; F8BT; photoluminescence properties; optical features.

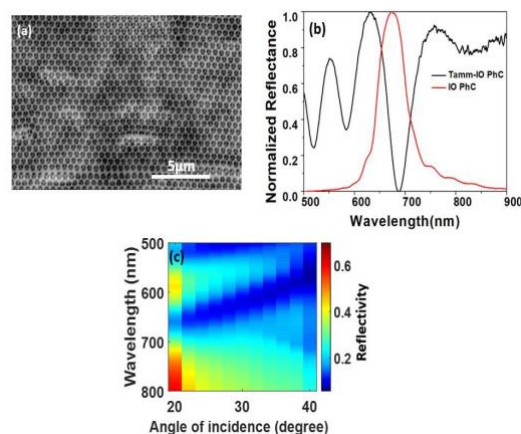


**Figure 1:** (a) SEM image of SiO<sub>2</sub> inverse opal on Pt coated vitreous silica substrate. (b) Experimentally obtained normal incidence reflection spectra from Tamm-IO structure (black curve) and IO structure (red curve). (c) Measured reflection spectra from Tamm-IO at different angles of incidence.

## References:

1. Chiappini, A., Faccialà, D., Novikova, N. I., Sardar, S, D'Andrea, C., Scavia, G., Botta, C., Virgili, T. (2024), Enhancement of Photoluminescence Properties via Polymer Infiltration in a Colloidal Photonic Glass *Molecules* 29, 654-1/654-11
2. Mudi, R., Carpentiero A., Bollani, M., Barozzi, M., Debnath, K., Chiappini, A., Bhaktha, S.B.N (2024), Inverse Opal Optical Tamm State for Sensing Applications *arXiv preprint arXiv:2405.10701*.

# Curminoid-based active surfaces towards the preparation of sensors

Arántzazu González-Campo,<sup>1,\*</sup> Raquel Gimeno-Muñoz,<sup>1</sup> Nuria Aliaga,<sup>1,2</sup>

<sup>1</sup> Institut de Ciència de Materials de Barcelona (ICMAB-CSIC), Campus UAB s/n, 08193 Bellaterra, Spain.

<sup>2</sup> Institució Catalana de Recerca I Estudis Avançats, Passeig Lluís Companys 23, 08010 Barcelona, Spain

e-mail: agonzalez@icmab.es

## Abstract:

The development of new metal detection devices is a subject of growing interest in the scientific community. Many heavy metals are found in chemical or biological species that collaborate in essential processes, and control of their presence and amount is crucial. Their monitoring is necessary to provide insight in their toxicity, their effects on the environment, the development of diseases due to the excess or deficiency of these metals and/or the study of new drugs based on inorganic chemistry. Regarding this matter, the design of fluorophores, for metal fluorometric detection, that can be switched on or off or exhibit a shift in their emission upon reaction with the analyte is a straightforward approach highly desired. Advances in molecular design have involved the preparation of multifunctional molecular materials, including the synthesis of bifunctional probes or heterogeneous sensors [1]. Here, knowing the great chemical versatility of Curcuminoids (CCMoids), new fluorescent CCMoids and their immobilization on surfaces has been explored. CCMoids are derivatives of curcumin exhibiting conjugated features, and fluorescent behavior with the possibility of coordinating both metals and metalloids, affecting this, the electronic/fluorescent performance.[2] Therefore, the shifts in the fluorescence of the surfaces, depending on the metal or metalloid coordinated, together with the possibility of the metal released upon coordination have been analyzed, obtaining an increase, decrease or even a switch of the surface fluorescence depending on the metal/metalloid under study, Figure 1.

**Keywords:** curcuminoids, fluorescence, surface chemistry, sensor, detector, metals, responsive sur-face.

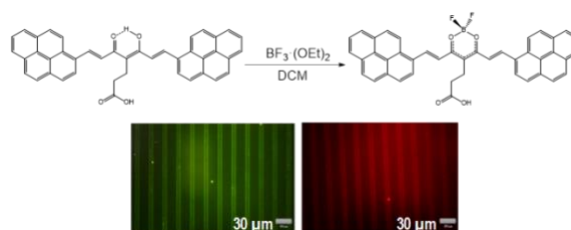


**Figure 1:** On-site coordination of  $\beta$ -diketone with  $\text{BF}_3$  complex in dichlorometane (DCM). The  $\text{BF}_2$  group modifies the fluorescent properties of the system, losing emission in the green region and emitting with greater intensity in the red, near the IR..

**Acknowledgements:** This work was supported by the projects PID2019-108794GB-I00 and ERC 724981 (Tmol4Trans

## References:

1. Pei-Pei, J., Shu-Ting, J., Lin, X. (2019), *Curr. Org. Synth.*, 16, 485.
2. a) Burzurí, E., Island, J.O., Diaz-Torres, R., Fursina, A., González-Campo, A., Roubeau, O., Teat S.J., Aliaga-Alcalde, N., Ruiz, E., van der Zant, H.S.J. (2016), *ACS Nano*, 10, 2521. b) Díaz-Torres, R., Menelaou, M., Roubeau, O., Sorrenti, A., Brandariz-De-Pedro, G., Sañudo, E.C., Teat, S.J., Fraxedas, J., Ruiz E., Aliaga-Alcalde, N. (2016) *Chem. Sci.*, 7, 2793.

# Chemical ‘Click’ sintering of noble nanoparticles for direct fabrication of nanoporous electrodes for (bio)sensing applications

M. Urban<sup>1\*</sup>, G. Rosati<sup>1</sup>, G. Maroli<sup>1</sup>, F. Della Pelle<sup>1,2</sup>, A. Bonini<sup>1,3</sup>, L. Sajti<sup>4</sup>, M. Fedel<sup>4</sup>, R. Blanch Rivera<sup>1</sup>, A. Merkoçi<sup>1,5</sup>

<sup>1</sup>Catalan Institute of Nanoscience and Nanotechnology (ICN2), Bellaterra, Barcelona, Spain

<sup>2</sup>Faculty of Bioscience and Technology for Food, Agriculture, and Environment, University of Teramo, Teramo, Italy

<sup>3</sup>Department of Chemistry and Industrial Chemistry, University of Pisa, Pisa, Italy

<sup>4</sup>RHP Technology GmbH, Austrian Research Center, 2444 Seibersdorf, Austria

<sup>5</sup>Catalan Institution for Research and Advanced Studies (ICREA), Barcelona, Spain

## Abstract:

Noble metals have stood the test of time in electrochemical (bio)sensing, being considered a standard in the field, elaborating ways to use and improve their nanostructured form<sup>1,2</sup>. Nanostructured/nanoporous noble metals have been commonly produced decorating electrodes by drop casting, electroplating of metal salt solutions, or corrosion-based methods, to induce nanostructuration and unlock nanoscale properties<sup>3,4</sup>. All these techniques hold their ground in the field each coming with advantages and disadvantages. Finding new and scalable approaches to produce these materials becomes then highly desirable.

We believe that our chemical sintering approach, which we call “click” sintering, can face this need<sup>5</sup>. The electrode material can be deposited in nanoparticles form (e.g. with inkjet printing) and directly cured into a nanoporous film in a ultrafast way, by triggering the unique features of the nanoscale.

We show how understanding in depth the phenomena occurring in the material can be used as a tool for tuning the fabrication of nanoporous devices. The devices have the potential to be used in a variety of different (bio)sensing applications, taking advantage of the large surface and enhanced electrocatalytic features typical of nanoporous metals.

**Keywords:** inkjet printing, nanoporous metals, metal nanoparticles, chemical sintering, electrochemical biosensing.

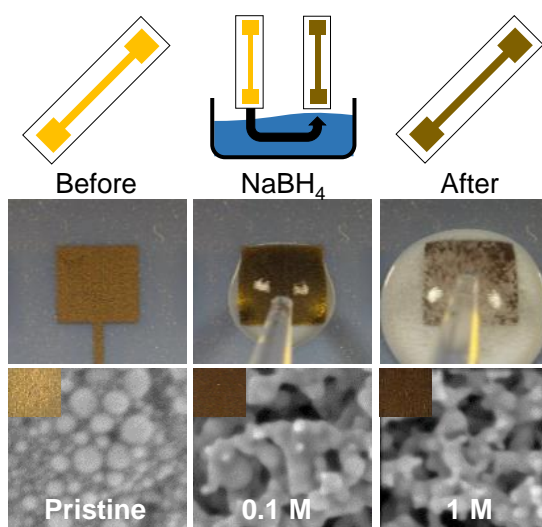


**Figure 1:** Figure illustrating the overall simplicity of the process: a simple immersion into the sintering solution produces directly on the substrate a nanoporous metal film.

## References:

1. Saha, K. et al, (2012) Gold nanoparticles in chemical and biological sensing. *Chem. Rev.* 112, 2739–2779.
2. Koya, A.N. et al., (2021) Nanoporous Metals: From Plasmonic Properties to Applications in Enhanced Spectroscopy and Photocatalysis. *ACS Nano* 15, 6038–6060.
3. Wang, J. (2012) Electrochemical biosensing based on noble metal nanoparticles. *Microchim. Acta* 177, 245–270
4. G. Wittstock et al. (2023) Nanoporous Gold: From Structure Evolution to Functional Properties in Catalysis and Electrochemistry, *Chem. Rev.*, 123, 10, 6716–6792
5. M.Urban et al. (2024) Nanostructure Tuning of Gold Nanoparticles Films via Click Sintering, *Small*, 20, 2306167

# Lanthanide doped up-converting nanoparticles for bioimaging and thermal sensing

L. Mantic<sup>1\*</sup>, I. Dinic<sup>1</sup>, M. Tomic<sup>1</sup>, Marina Vukovic<sup>1</sup>, M.Lazarevic<sup>2</sup>, M. Bukumira<sup>3</sup>, M.Rabasovic<sup>3</sup>

<sup>1</sup>Institute of Technical Sciences of SASA, Belgrade, Serbia

<sup>2</sup>School of Dental Medicine, University of Belgrade, Belgrade, Serbia

<sup>3</sup>Institute of Physics Belgrade, National Institute of the Republic of Serbia, University of Belgrade, Belgrade, Serbia

## Abstract:

Bioimaging and thermal sensing refer to techniques related to the observation of biological structure and function of cells, which are of paramount importance for early diagnostics of diseases. Due to their unique ability to convert NIR to Vis light through a non-linear multiphonon anti-Stokes process, lanthanide doped up-converting nanoparticles (Ln-UCNP) have an important role in this field. The work will present the synthesis procedures applied for the in-situ obtaining of various biocompatible Ln-UCNP and their application for cell labelling (Figure 1), and for temperature sensing in the physiologically relevant range of temperatures. Additional selectivity toward target cancer cell labelling was enabled through their conjugation with the anti-human CD44 antibodies. The Ln-UCNP structural and morphological properties, revealed through XRPD, FTIR, XPS, SEM/TEM-EDS, and HRTEM analysis, are correlated with their up-conversion emission efficiency, and capacity to be used in medicine. For assessing of biological safety of their use, viability of commercially available cell lines, as well as human cells, was additionally evaluated by a colorimetric MTT assay. Laser scanning microscopy imaging under excitation of 976 nm verified their feasibility to be used as new fluorescence imaging probes.

**Keywords:** Up-converting, bioimaging, thermal sensing, luminescence,

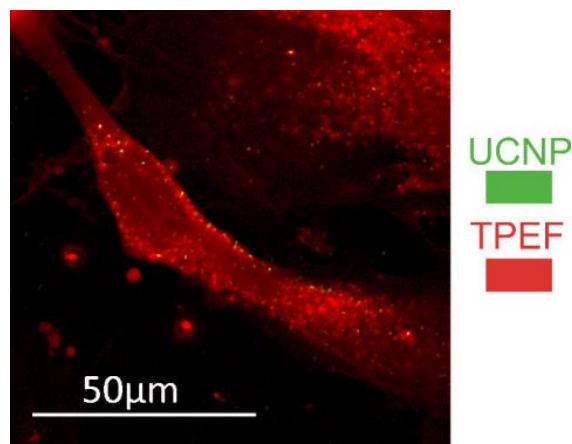


**Figure 1:** Bioimaging of cancer cells by Ln-UCNP (UCNP: UCNP fluorescence in cell at 976 nm; TPEF: cell autofluorescence at two-photon excitation, 730 nm)

## References:

1. Dinić, I., Marina Vuković, M., Rabanal, M.E., Milošević, M., Bukumira, M., Tomić, N., Tomić, M., Mančić L., Ignjatović, N. (2024) Temperature Sensing Properties of Biocompatible Yb/Er-Doped GdF<sub>3</sub> and YF<sub>3</sub> Mesocrystals, *J. Funct. Biomater.* 15(1), 6.
2. Mantic, L., Djukic-Vukovic, A., Dinic, I., Nikolic, M.G., Rabasovic, M.D., Krmpot, A.J., Costa, A.M.L.M., Marinkovic, B.A., Mojovic Lj., Milosevic, O. (2018) One-step synthesis of amino-functionalized up-converting NaYF<sub>4</sub>:Yb,Er nanoparticles for *in vitro* cell imaging, *RSC Advances*, 8, 27429-27437.



# Influence of Electron-Phonon Interaction on Optoelectronic properties of Halide Double Perovskite

Bikash Ranjan Sahoo<sup>1,\*</sup>, P. A. Bhohe<sup>1</sup>

<sup>1</sup> Department of Physics, Indian Institute of Technology Indore, Simrol, Indore, India

## Abstract:

The superior structural stability of halide double perovskites (HDPs) compared to organic-inorganic hybrid perovskites has strengthened their application in photovoltaic research. Halide double perovskites have shown their potency in several applications such as solar cell, LED, photodetectors, laser, photocatalyst and so on. Out of these fascinating properties is the thermochromism, where temperature induced colour change of the material takes place. Moreover, such change is completely reversible over many cycles of iteration. Such a property has potential applications in smart windows, temperature sensors, virtual thermometers, displaying devices, and many more areas.

In HDP semiconductors the charge carriers mainly reside within a narrow energy band near the edges where electron-lattice scattering is primarily governed by long wavelength phonons. Various factors such as random distribution of crystallographic defects, doping and external parameters like temperature and pressure may introduce potential fluctuations into the semiconductor's electronic structure, that can intensify the electron-lattice scattering. As a basic control parameter, temperature primarily introduces lattice thermal expansion and alters the carrier-phonon interactions, which subsequently impact the optoelectronic properties of the material.

Here, we offer both qualitative and quantitative analyses of the fundamental causes of electron-phonon interactions and their impact on the electronic structure of the novel halide double perovskite through comprehensive Raman spectroscopy, X-ray diffraction (XRD), and X-ray absorption fine structure (XAFS) studies. Although no structural phase transition was observed in this material, local octahedral distortion due to charge localization and strong electron-phonon coupling was noted. This distortion alters the electronic landscape of the lattice, which is responsible for the material's remarkable thermochromic behavior. Understanding the structure-property correlation and the potential dynamic mechanism in this lead free halide double perovskite will reinforce the designing of emerging optoelectronic devices.

**Keywords:** X-ray diffraction, band gap, thermochromism, X-ray absorption spectroscopy, Raman spectroscopy.

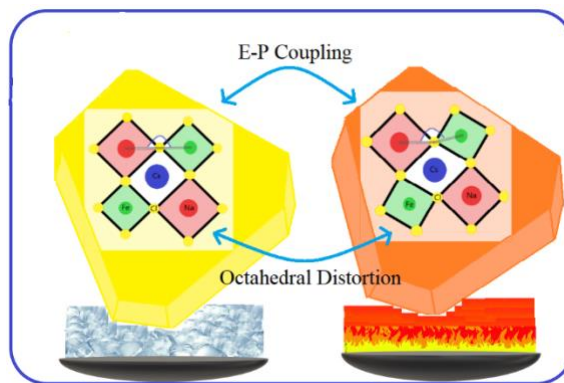


**Figure 1:** Figure illustrating the reversible thermochromism shown by halide double perovskite single crystal due to the electron-phonon coupling arising from octahedral distortion.

## References:

1. Green, M. A.; Ho-Baillie, A.; Snaith, H. J. (2014), The emergence of perovskite solar cells. *Nat. Photon.*, 8, 506–514.
2. Sahoo, B. R.; Joshi, P. U.; Devan, R. S.; Bhohe, P. A. (2024), Unveiling Electron-Phonon Interaction That Influences the Photoluminescence Properties of  $\text{Cs}_2\text{Na}_x\text{Ag}_{1-x}\text{BiCl}_6$  Mixed Halide Double Perovskites. *J. Phys. Chem. C*.
3. Sahoo, B. R.; Devan, R. S.; Bhohe, P. A. Viability of  $\text{Cs}_2\text{AgBiCl}_6$ :  $\text{Cr}^{3+}/\text{Yb}^{3+}$  and  $\text{Cs}_2\text{AgInCl}_6$ :  $\text{Cr}^{3+}/\text{Yb}^{3+}$  as Efficient Photoluminescent Materials and Other Photo-physical Applications. (2024) *ACS Appl. Opt. Mater.*, 2, 617–623.

# Stamping Platinum Electrodes - a new method for modifying the geometry of electrochemical sensors

K. Jedlińska<sup>1\*</sup>, J. Eidenschink<sup>2</sup>, F.-M. Matysik<sup>2</sup>, B. Baś<sup>1</sup>

<sup>1</sup>Department of Analytical Chemistry and Biochemistry, AGH University of Krakow, Kraków, Poland

<sup>2</sup>Institute of Analytical Chemistry, Chemo- and Biosensors, University of Regensburg, Germany

## Abstract:

Electrochemical sensors are widely used in process analytics and medical applications due to their high sensitivity to redox-active molecules, selectivity, and potential for miniaturization. Recent advancements focus on modifying electrode surfaces with nanomaterials to improve conductivity and increase the electrochemically active surface. This study, however, presents a novel approach by modifying the geometry of the electrode surface through selective masking with an insulating material, rather than enhancing the conductive properties.

The proposed method allows for the rapid, cost-effective modification of disk electrodes by masking specific areas with a thin layer of chemically stable insulating material, while leaving other regions exposed and electrochemically active. Desired patterns are achieved by using a laser-engraved stainless steel plate and a stamper to transfer the profiled coating onto the electrode's surface. (Figure 1). Three shapes - microdisk, microband, and ring electrodes - were applied to a platinum disk electrode and validated through optical and scanning electrochemical microscopies (SECM), as well as cyclic voltammetry (CV) (Figure 2). The method is highly flexible, enabling the production of various electrode shapes from a single disk without the need for expensive equipment. It offers a significant advantage over conventional techniques, as it does not require complex manufacturing processes.

This approach is user-friendly, adaptable to different electrode substrates, and aligns with green analytical chemistry principles by minimizing waste and eliminating harmful reagents. Future research will explore the potential for ultramicroelectrode production, further miniaturization, and the creation of electrode arrays for advanced diffusion studies.

This work was supported by the National Science Centre, Poland (Project No. 2022/06/X/ST4/00199).

Research project supported by program "Excellence Initiative-Research University" for the AGH University of Science and Technology.

**Keywords:** Surface geometry, Microelectrode, Microband electrode, Ring electrode, Voltammetry, New method

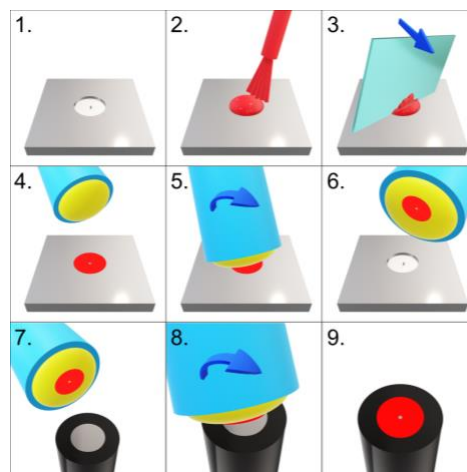


**Figure 1:** Procedure for fabrication of Stamping Platinum Electrodes.

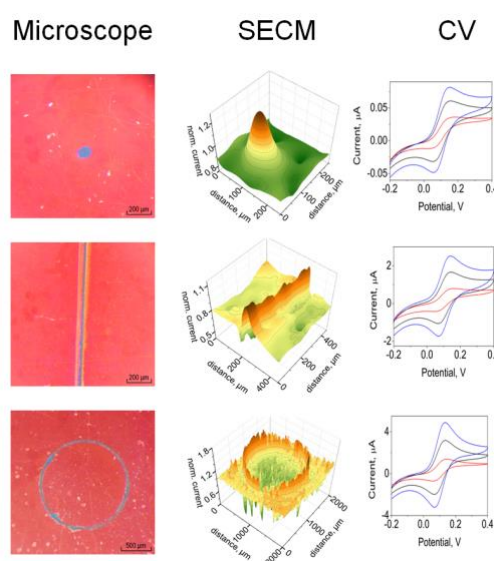


**Figure 2:** Measurement results.

## References:

1. Jedlińska, K., Eidenschink, J., Matysik F.-M., Baś B., (2024) Stamping Platinum Electrodes – Design, Fabrication, and Characterization, *J. Electrochem. Soc.* 171 077502.

# Zinc Oxide Nanotubes doped by Palladium by Combining Electrospinning and Atomic Layer Deposition Techniques for H<sub>2</sub> production

X. Sandua<sup>1,2,\*</sup>, L. Badouric<sup>3</sup>, I. Pellejero<sup>2,4</sup>, P.J. Rivero<sup>1,2</sup>, M. Bechelany<sup>3</sup>, R. Rodríguez<sup>1,2</sup>

<sup>1</sup> Engineering Department, Public University of Navarre, Campus Arrosadía s/n, 31006 Pamplona, Spain

<sup>2</sup> Institute for Advanced Materials and Mathematics (INAMAT<sup>2</sup>), Public University of Navarre, Campus Arrosadía s/n, 31006 Pamplona, Spain

<sup>3</sup> Institut Européen des Membranes, IEM, UMR-5635, Univ Montpellier, ENSCM, CNRS, Place Eugene Bataillon, 34095 Montpellier, France

<sup>4</sup> Science Department, Public University of Navarre, Campus Arrosadía s/n, 31006 Pamplona, Spain

## Abstract:

Photocatalytic methods for hydrogen production offer a sustainable and environmentally friendly approach to meeting energy needs. By harnessing abundant resources like sunlight and water, these methods enable the generation of hydrogen (a clean and renewable energy carrier) without emitting greenhouse gases. This carbon-neutral process not only contributes to mitigating climate change but also reduces air pollution and dependence on finite fossil fuels, promoting environmental conservation and energy security. One of the main photocatalytic precursor in charge of carrying out this phenomenon is ZnO. ZnO is abundant, cost-effective, and environmentally benign, offering advantages in large-scale production and application. Besides, its stability under photocatalytic conditions further enhances its attractiveness for sustained hydrogen production.

The combination of various functional deposition techniques allow the implementation of a more functional precursor. This work has carried out the combination of two widely employed techniques such as electrospinning and atomic layer deposition (ALD) processes, obtaining fiber shaped precursors, which show great area-volume relationship and thus, they are great candidates for hydrogen production applications [1]. Polyacrylic acid (PAA) is used as main polymer for elaborating the electrospinning host matrix, and then a ZnO precursor thin film is deposited by ALD technique over the base polymeric matrix. In addition, Pd is also added by ALD technique in order to dope ZnO fibers, so that these metal nanoparticles can improve photocatalytic efficiency. A controlled calcination process is then carried out in order to eliminate the polymer and obtain the functional fibers. The chemical presence of the precursors and the morphology of the coated surfaces are

analysed by SEM-EDX and XRD characterization tools, along with N<sub>2</sub> adsorption method in order to obtain porosity values of the functional fibers.

With the aim of demonstrating the H<sub>2</sub> production capacity of the obtained precursors, a microreactor based setup is used (Figure 1). This device has an excellent area-volume relationship and permits a good dispersion and immobilization of the photocatalytic precursors on it. Besides, it allows a direct contact between the ZnO precursor and reactive compounds [2].

**Keywords:** photocatalysis, H<sub>2</sub> production, atomic layer deposition, electrospinning, zinc oxide, palladium, microreactor.

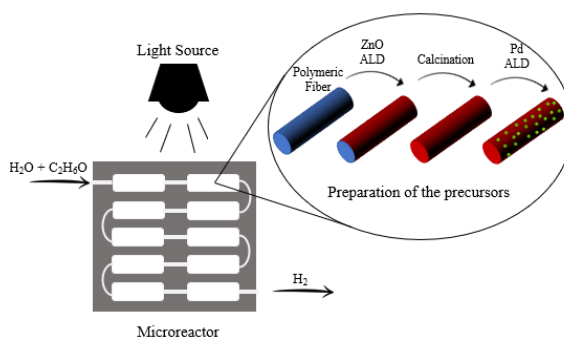


**Figure 1:** Figure illustrating the fundamental scheme of the work.

## References:

1. Vempati, S.; Ranjith, K.S.; Topuz, F.; Biyikli, N.; Uyar, T. (2020). Electrospinning Combined with Atomic Layer Deposition to Generate Applied Nanomaterials: A Review. 3, 6186-6209.
2. Leblebici, M.E.; Stefanidis, G.D.; Gerven, T. Van. (2015). Process Intensification Comparison of Photocatalytic Space-Time Yields of 12 Reactor Designs for Wastewater Treatment. *Chem. Eng. Process. Process Intensif.* 97, 106–111.



**SMS 2024 / NanoMed 2024**  
**Session I. B:**  
**Smart coatings and Surfaces /**  
**Biomaterials/ Bionanomaterials**

# Smart design with graded nanostructures for enhanced wear resistance of surfaces exposed to extreme conditions

Ting Yang<sup>1</sup>, T. A. Venkatesh<sup>2</sup>, Ming Dao<sup>1</sup>

<sup>1</sup>Department of Materials Science and Engineering, Massachusetts Institute of Technology, Cambridge, MA 02139, USA

<sup>2</sup>Department of Materials Science and Chemical Engineering, Stony Brook University, Stony Brook, New York 11794, USA

## Abstract:

The materials used in several applications such as nuclear reactor experience a combination of extreme conditions, i.e., mechanical stresses, radiative conditions and corrosive environments. For example, the pressurized water nuclear reactors typically contain a large number of fuel rods (about 50,000). These fuel rods are cylindrical in shape, contain radioactive material in their cores and are surrounded by a cladding layer. These fuel rods are kept in place with spacer grids such that there is space between the fuel rods for water to flow through and absorb the heat from the fuel rods, which can then be used to produce power. At the regions where the spacers are in contact with the exterior of the fuel rods, (i.e., the surface of the cladding that surrounds the radioactive fuel rod core), vibrational loads caused by turbulence in the water induces fretting damage which can lead to cracking and deterioration of the cladding layer, resulting in serious radioactive leak issues. It has been reported that, of all the causes of such leaks, grid-to-rod contact fatigue damage is the most prominent, accounting for more than 70% of the problems.

In such applications where high cyclic loads are involved [1], surfaces with high yield strength and wear resistance are required. As surfaces with nanograins have been shown experimentally to significantly increase yield strength and enhance surface wear resistance [2], in this work, the potential for graded nanomaterial architectures for extreme environments is systematically investigated. A three-dimensional finite element model is developed to analyze the characteristics of fretting sliding and shakedown behavior, considering different levels of contact friction and gradient layer thicknesses. The results obtained using 304 stainless steel as a representative model material demonstrate that metallic materials with graded nanostructured surfaces exhibit a significant reduction of over 80% in plastically deformed surface areas and volumes. This reduction significantly enhances

the material's resistance to fretting damage when compared to homogeneous coarse-grained metals. It is noteworthy that the graded nanostructured material can exhibit either elastic or plastic shakedown behavior, depending on the contact friction coefficient. By reducing the friction coefficient (e.g., from 0.6 to 0.4 in 304 stainless steel), the graded nanostructured material achieves optimal fretting resistance, resulting in elastic shakedown behavior. This behavior is characterized by the absence of any increment in the accumulated plastic strain in the plastically deformed volume and area during subsequent sliding. These findings, derived from the investigation of graded nanostructured materials using 304 stainless steel as a model system, can be further refined to engineer optimal fretting damage resistance under extreme conditions.

**Keywords:** fretting; frictional sliding; graded nanostructured surfaces; shakedown; finite element.

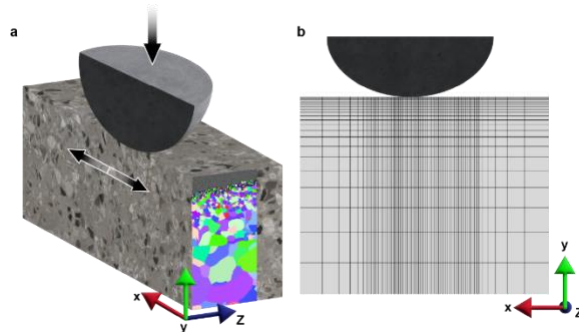


**Figure 1:** Schematic of simulation setup (a) and a close-up view of the finite-element mesh setup near the contact region (b).

## References:

1. Blau PJ. A multi-stage wear model for grid-to-rod fretting of nuclear fuel rods. *Wear* 2014; 313(1):89-96.
2. Singh A, Dao M, Lu L, Suresh S. Deformation, structural changes and damage evolution in nanotwinned copper under repeated frictional contact sliding. *Acta Materialia* 2011; 59(19):7311-7324.

# Development and Characteristics of sub-Stoichiometric High Entropy Carbonitride Coatings for Friction Applications

N. C. Zoita\*, M. Dinu, A. C. Parau

National Institute of Research and Development for Optoelectronics- INOE 2000, Magurele, Romania

## Abstract:

The high-entropy alloys (HEAs) are compositionally complex solid solutions of at least five principal elements in equimolar or near-equimolar ratios. These systems received considerable attention in the last decade due to their special physical, chemical, and mechanical properties in comparison with conventional alloys. In this research we explore the performance of high-entropy  $(\text{TiCrAl}_{0.5}\text{NbCu})\text{C}_x\text{N}_y$  sub-stoichiometric ceramic coatings, designed for friction applications in aerospace, automotive, and machining industries that demand medium-to-high coefficient of friction and high wear-resistant surfaces. The coatings were fabricated via co-sputtering of elemental targets in an  $\text{Ar} + \text{CH}_4 + \text{N}_2$  reactive atmosphere, using a hybrid HiPIMS/DCMS technique. Two distinct sets of coatings were produced: (a)  $(\text{TiCrAl}_{0.5}\text{NbCu})\text{C}_x$  high-entropy carbides (HEC), and (b)  $(\text{TiCrAl}_{0.5}\text{NbCu})\text{C}_x\text{N}_{0.13}$  high-entropy carbonitrides (HECN), with a carbon atomic content ranging  $0 \leq x \leq 0.48$ . There are investigated the structural, mechanical, tribological, and corrosion-resistant properties of these coatings. The metallic samples exhibited a single BCC structure that transitioned to an FCC structure through an intermediary amorphous phase with the addition of small content of carbon or nitrogen. Increasing carbon content enhanced FCC phase crystallinity while reducing film density to  $5.5 \text{ g/cm}^3$  at the highest carbon content ( $x = 0.48$ ). Samples with this carbon concentration demonstrated superior hardness ( $\sim 16.9 \text{ GPa}$ ) and the lowest wear rate ( $\sim 5.5 \times 10^{-6} \text{ mm}^3/\text{Nm}$ ). A strong correlation was observed between the evolution of the resistance to plastic deformation ( $H^3/E^2$  ratio) and the tribological performance. The  $(\text{TiCrAl}_{0.5}\text{NbCu})\text{C}_{0.3}\text{N}_{0.13}$  exhibited the most favorable tribological characteristics for friction applications, with a coefficient of friction of 0.43 and a wear rate of  $\sim 7.7 \times 10^{-6} \text{ mm}^3/\text{Nm}$  (Figure 1).

**Acknowledgments:** This research was funded by the Core Program within the Romanian National Research Development and Innovation Plan 2022-2027, carried out with the support of

MCID, project no. PN 23 05 (id: PN11N-03-01-2023).

**Keywords:** high-entropy carbonitrides; hybrid HiPIMS/DCMS technique; crystallographic structure; surface morphology; tribological properties; mechanical properties; electrochemical properties.

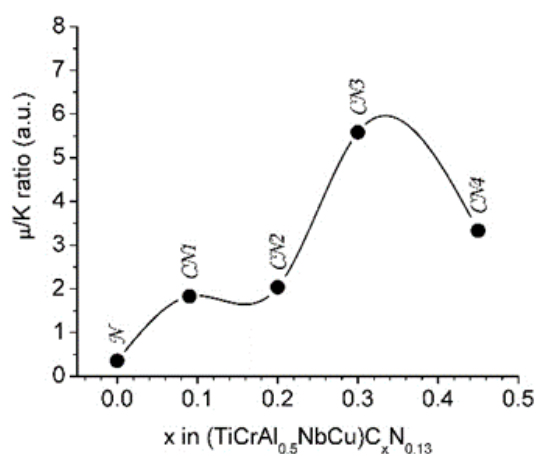


**Figure 1:** The dependence of the  $\mu/k$  ratio (where  $\mu$  is the coefficient of friction and  $k$  is the wear rate) on the carbon concentration,  $x$ .

## References:

1. Akrami, S., Edalati, P., Fuji, M., Edalati, K. (2021) High-entropy ceramics: Review of principles, production and applications, *Mater. Sci. Eng. R Rep.*, 146, 100644.
2. Braic, M.; Braic, V.; Balaceanu, M.; Zoita, N.C.; Vladescu, A.; Grigore, E. (2010) Characteristics of  $(\text{TiAlCrNbY})\text{C}$  Films Deposited by Reactive Magnetron Sputtering. *Surf. Coatings Technol.*, 204, 2010–2014
3. Vasiljević, S., Glišović, J., Stojanović, B., Vencl, A. (2022) Review of the coatings used for brake discs regarding their wear resistance and environmental effect. *Proc. Inst. Mech. Eng. J. Eng. Tribol.*, 236, 1932–1949

# Nanostructured polymer particle coatings for biological studies and sensing

E. Rosqvist<sup>1</sup>, J. Peltonen<sup>1</sup>

<sup>1</sup>Laboratory of Molecular Science and Engineering, Åbo Akademi University, Åbo, Finland

## Abstract:

Polymer particle dispersions, or latices, are colloidal dispersions that are commonly used in paper converting, coatings, paints, and adhesives, among others. Their wide range of tunable properties, such as morphology, functionalisability, and physico-chemical surface properties, as well as their high processability have further led to their use in biotechnological applications.

In this work, blends of latex dispersions, specifically polystyrene (PS, High  $T_g$ ) and acrylonitrile butadiene styrene (ABS, low  $T_g$ ), were used to create nanostructured coatings with a tuneable roughness. These surfaces were used for studying the responses of human dermal fibroblasts (HDF), HeLa cervical cancer cells, and *Staphylococcus aureus* (*S. aureus*) bacteria to nanoscale variations in topography. The latex surfaces were characterised with diverse roughness parameters in order to interpret how the topographical character drives the biological response. By inkjet printing, virtually transparent nanostructured microarrays were produced on borosilicate glass. These hierarchical surfaces were used to study nanostructure-driven differences in focal adhesions of HDF cells attaching to the surfaces. In microbiology studies, the response of *S. aureus* to variations in nanoscale topography was observed even on the surface proteome level – showing roughness correlated levels of virulence-associated proteins. The choice of assay also impacted the response of *S. aureus* to the nanotopography, indicating that study protocols should be chosen with care.

The processability of the coatings was demonstrated by making a low-cost upscalable paper-based screening platform with a tunable surface character, e.g., for the use in drug discovery. The functional coatings were also demonstrated to be suitable for low-cost surface enhanced Raman spectroscopy (SERS).

**Keywords:** Human dermal fibroblast, cervical cancer cells, *Staphylococcus aureus*, nanostructure, latex, surface proteome, viability, surface chemistry, atomic force microscopy, micropatterning, drug discovery, Raman spectroscopy.

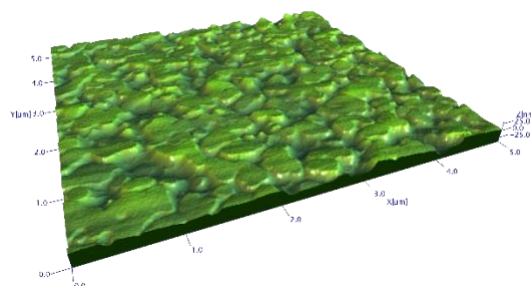


**Figure 1:** A representative 5  $\mu\text{m}$  x 5  $\mu\text{m}$  AFM image of the nanotopography that was obtained with blends of polymer particle dispersion.

## References:

1. Rosqvist, E., Niemelä, E., Venu A.P., Kummala, R., Ihalainen, P., Toivakka, M., Eriksson, J.E., Peltonen, J. (2019) Human dermal fibroblast proliferation controlled by surface roughness of two-component nanostructured latex polymer coatings. *Colloids Surf B Biointerfaces*.
2. San-Martin-Galindo, P. & Rosqvist, E., Tolvanen, S., Miettinen, I., Savijoki, K., Nyman, T. A., Fallarero, A., Peltonen, J. (2021) Modulation of virulence factors of *Staphylococcus aureus* by nanostructured surfaces. *Materials & Design*
3. Rosqvist, E. & Niemelä, E., Venu, A.P., Frisk, J., Koppolu, R., Öhblom, H., Soto-Véliz, D., Mennillo, M., Aubert, M., Sandler, N., Wilén, C. E., Toivakka, M., Eriksson, J. E., Österbacka, R., Peltonen, J., (2020) A low-cost paper-based platform for fast and reliable screening of cellular interactions with materials. *J. Mater. Chem. B*,
4. Rosqvist, E., Böcker, U., Gulin-Sarfraz, T., Afseth, N. K., Tolvanen, S., Peltonen, J., Sarfraz, J. (2023) Low-cost, mass producible nanostructured surface on flexible substrate with ultra-thin gold or silver film for SERS applications. *Nano-Structures & Nano-Objects*.

# Hydrodynamic testing of viscous drag reduction by bio-inspired hybrid coatings

A. Rodríguez-Ortiz<sup>1</sup>, P. Pinilla-Cea<sup>2</sup>, J.C. Suárez-Bermejo<sup>2</sup>

<sup>1</sup> Department of Engineering Design, Universidad Politécnica de Madrid, Madrid, Spain

<sup>2</sup> Department of Naval Architecture, Universidad Politécnica de Madrid, Madrid, Spain

## Abstract:

The main means of transport for goods are large-tonnage ships, so reducing their drag would have a direct impact on fuel savings and the reduction of polluting gases. The hydrodynamic shapes of these ships are at a very advanced stage of study and the improvements achieved are minimal. For this reason we have turned to nature for bio-inspiration, specifically we have focused on sharks to create a coating inspired by their skin. This coating is made up of denticles embedded in a hydrogel substrate that allows them to change their angle of attack. This autonomy of movement allows each denticle to adopt the most beneficial orientation according to the specific contour conditions of each region. In the present work, bio-inspired coatings have been obtained using additive manufacturing, mounted on a soft, flexible substrate, and tested with different sizes, configurations and substrate stiffness (Figure 1). A special testing equipment has been developed to measure the drag force acting on the plate (with and without coating) at different speeds of the fluid. The characteristics of velocity fields around the denticles has been experimentally visualized to assist with the design evolutions of shape and size configuration of the denticles, and also in the distribution pattern of the denticles. The results obtained show that with a specific size, configuration of denticles and substrate stiffness a reduction in viscous drag is achieved with respect to a flat plate, since the main characteristic of this coating is the ability to change the angle of attack of the denticles depending on the changing fluid conditions, which leads to a benefit in the reduction of viscous drag over a large range of velocities.

**Keywords:** bio-inspired coating, viscous drag, hybrid material, hydrogel, turbulent flow.



**Figure 1:** The figure shows one of the specimens used in the viscous drag measurement tests, where can be seen an example of a bio-inspired coating formed by multiple denticles embedded in a hydrogel substrate.

## References:

1. Dean, B. Bhushan, B. (2010) Shark-skin surfaces for fluid-drag reduction in turbulent flow: a review, *Phil. Trans. R. Soc. A* 368, p. 4775–4806.
2. Luo, Y., Wang, J., Sun, G., Li, X., Liu, Y. (2016) Experimental Investigations on Manufacturing Different-Shaped Bio-Inspired Drag-Reducing Morphologies and Hydrodynamic Testing. *Experimental Techniques*, Society for Experimental Mechanics; *Exp Tech* 40, p. 1129–1136.

# Design and Development of Novel Additive Manufactured Structures with Optimised Properties for Biomedical Applications

V. Spinelli<sup>1</sup>, V. Gallicchio<sup>1</sup>, C. Marino<sup>2</sup>, V. D'Antò<sup>1</sup>, G. Spagnuolo<sup>1</sup>, Sandro Rengo<sup>1</sup>

<sup>1</sup>Department of Neurosciences, Reproductive and Odontostomatological Sciences, University of Naples Federico II, Naples, Italy

<sup>2</sup>University of Naples Federico II, Naples, Italy

## Abstract:

Over the past years, several design strategies have been developed with the aim of realising advanced prostheses and scaffolds for tissue engineering. The combined use of micro/nano-composites with additive manufactured structures would seem to be an interesting solution in different biomedical applications [1]. The attention has been focused on a wide range of materials for the repair or regeneration of craniofacial tissues, employing polymeric and composite biomaterials, as well as on the design for additive manufacturing.

Poly( $\epsilon$ -caprolactone) (PCL) (i.e., an aliphatic polyester) is one of the most commonly used biodegradable polymers, as a consequence of its interesting biodegradation rate, processability, and high chemical and thermal stability. On the other hand, with regard to tissue repair/reconstruction, many studies stressed the use of poly(methyl methacrylate) (PMMA)-based bone cements as well as their modifications by embedding copper-doped tricalcium phosphate (Cu-TCP) particles [2].

Accordingly, two different strategies were proposed. First, an optimisation strategy was considered in terms of design for additive manufacturing towards the development of nanocomposite PCL/hydroxyapatite (HA) scaffolds, especially focusing on processes based on extrusion/injection methods (e.g., Fused Deposition Modeling). In particular, the design of experiments was employed to analyse the effect of the process parameters (i.e., deposition velocity, screw rotation velocity, slice thickness, and temperature) on the mechanical, morphological and biological properties.

The best set of parameters for the development of PCL/HA scaffolds with improved functional properties for craniofacial tissue engineering was found.

On the other hand, benefiting from a previous study [2], customised hybrid devices for the repair/reconstruction of craniofacial tissues were also designed and developed. In this case, a hybrid prosthetic device was developed in the

form of a 3D additive manufactured PCL structure with an interconnected pore network. Specific lay-down patterns were designed and the porous network was infiltrated with a modified cement (i.e., PMMA/Cu-TCP). Reverse engineering was combined with Fused Deposition Modeling, in order to develop customised prosthetic devices with improved and tailored morphological, mechanical and functional features. Theoretical and experimental analyses were performed.

**Keywords:** scaffold design, prosthesis design, design of experiments, design for additive manufacturing.

## References:

1. De Santis, R., et al. (2021). Analyzing the Role of Magnetic Features in Additive Manufactured Scaffolds for Enhanced Bone Tissue Regeneration, *Macromolecular Symposia*, 396, 1, 2000314.
2. De Santis, R., Russo, T., Rau, J.V., Papallo, I., Martorelli, M., Gloria, A (2021). Design of 3D Additively Manufactured Hybrid Structures for Cranioplasty, *Materials*, 14(1):181.



# Development of magnetic molecular imprinted polymer systems for biomedical applications

C. Ciarlantini<sup>1,\*</sup>, G. Carnevale<sup>1</sup>, E. Lacolla<sup>1</sup>, I. Francolini<sup>1</sup>, M. Fernández-García<sup>2</sup>,  
C. Muñoz-Núñez<sup>2</sup>, A. Muñoz-Bonilla<sup>2</sup>, A. Piozzi<sup>1</sup>

<sup>1</sup>Department of Chemistry, University of “La Sapienza”, Rome, Italy

<sup>2</sup>Instituto de Ciencia y Tecnología de Polímeros (ICTP-CSIC), Madrid, Spain

## Abstract:

In recent years, molecularly imprinted polymers (MIPs) have received increasing attention due to their unique characteristics such as high stability, simple preparation, robustness, specificity in molecule capture, and low cost of production. The molecular imprinting approach has allowed the development of promising systems to be used both in environmental applications for the capture of pollutants<sup>1</sup>, and in the biomedical field for drug administration, to remove undesirable substances from the body or as diagnostic sensors<sup>2</sup>. Moreover, the functionalization with small molecules can make MIPs a powerful tool for drug delivery. MIPs can also be combined with different nanomaterials such as silica (SiO<sub>2</sub>), iron oxide (Fe<sub>3</sub>O<sub>4</sub>), gold (Au) and silver (Ag) to produce multifunctional composite systems with improved properties<sup>3</sup>. In this work, innovative magnetic MIPs for ciprofloxacin (CPR) delivery were developed. CPR, a fluoroquinolone antibiotic of second-generation, possesses activity against Gram-positive and Gram-negative microorganisms and is frequently used for treating bacterial infections. We developed a nanostructured magnetic composite system consisting of an inorganic core (Fe<sub>3</sub>O<sub>4</sub> nanoparticles) and two polymeric shells, the first composed of chitosan (CS), to avoid nanoparticle aggregation phenomena, and the second one of a molecular imprinted acrylic polymer. CS was chosen for its biocompatibility, good antimicrobial activity, and absorbent capacity<sup>4</sup>.

To obtain the MIP system, an in-situ polymerization of methacrylic acid (MAA) with ethylene glycol dimethacrylate (EGDMA), as a crosslinking agent, and CPR, as a template, was used. Different concentrations of MAA, EGDMA and CPR were investigated. Finally, to evaluate the effectiveness of nanostructured magnetic MIPs, non-imprinted systems (NIPs) were also prepared. The successful coating of Fe<sub>3</sub>O<sub>4</sub> was confirmed by FTIR and elemental analysis. FESEM analysis showed the production of spherical nanoparticles with size of about 10 nm. Following the coating processes with CS,

MMA and EGDMA the particle size increased up to 60 nm. The CPR absorption kinetics highlighted the greater effectiveness of MIP compared to NIP, due to the formation of specific cavities of the target molecule. Finally, antimicrobial tests showed a 100% reduction in bacterial growth in the case of MIPs, due to the higher release rate compared to NIPs.

**Keywords:** biomaterials, molecularly imprinted polymers, hybrid nanomaterials, synthesis of biomaterials, polymer chemistry, drug delivery, release systems, materials characterization methods.

## References:

1. Silvestro, I., Fernández-García M., Ciarlantini C., Francolini I., Girelli A., Piozzi A. (2022) *Int. J. Mol. Sci.*, 23, 1–18.
2. Ayankojo A.G., Boroznjak R., Reut J., Öpik A., Syritski V. (2022) *Sensors Actuators B Chem.*, 353, 1-7.
3. Zaidi S. A. (2017) *Biomater. Sci.*, 5, 388–402.
4. Aranaz I., Alcántara A. R., Civera M. C., Arias C., Elorza B., Caballero A. H., Acosta N. (2021) *Polymers*, 13, 1–27.

# 4D printing of triple-shape memory polymer using a thermal stimulus for biomedical applications

Shubham Shankar Mohol<sup>1</sup>, Pulak Mohan Pandey<sup>1</sup>

<sup>1</sup>Department of Mechanical Engineering, Indian Institute of Technology Delhi, New Delhi, India

## Abstract:

Multi-shape memory polymers (MSMPs), as a class of smart materials, have demonstrated significant potential in the biomedical and soft robotics disciplines. The ability of MSMPs to store more than two shapes extends their applications in several fields. Additionally, 4D printing allows additive manufacturing of complex and precise architectures with controlled shape change. We report the 4D printing of polypropylene carbonate/polycaprolactone (PPC/PCL) blend using a thermal stimulus. Several studies have reported the application of PPC and PCL for biomedical implants, owing to their biocompatible and biodegradable nature. However, their triple-shape memory behavior remains unexplored. The blend was developed by solution blending of PPC and PCL, which was 3D printed using the direct ink writing technique. The morphological observations of the cryogenically fractured PPC/PCL samples showed a phase-segregated morphology, which shows that the blend is immiscible. Subsequently, the immiscibility was characterized by the differential scanning calorimetry, which displayed two distinct transition temperatures, exhibiting a triple-shape memory behaviour. The first transition temperature was attributed to the glass transition of the PPC phase, whereas the second transition temperature was attributed to the melting point of the PCL phase. The shape-memory tests showed that the PPC50/PCL50 composition achieved the most optimum shape-fixing and shape-recovery performance on account of the presence of a co-continuous phase morphology. The triple-shape memory behaviour was demonstrated for the PPC50/PCL50 composition as shown in Figure 1. This study of 4D printing of the triple-SMPs will open new avenues for the technological advancement of biomedical implants.

**Keywords:** 4D printing, triple-shape memory polymer, polypropylene carbonate, polycaprolactone, co-continuous phase morphology, biomedical applications.

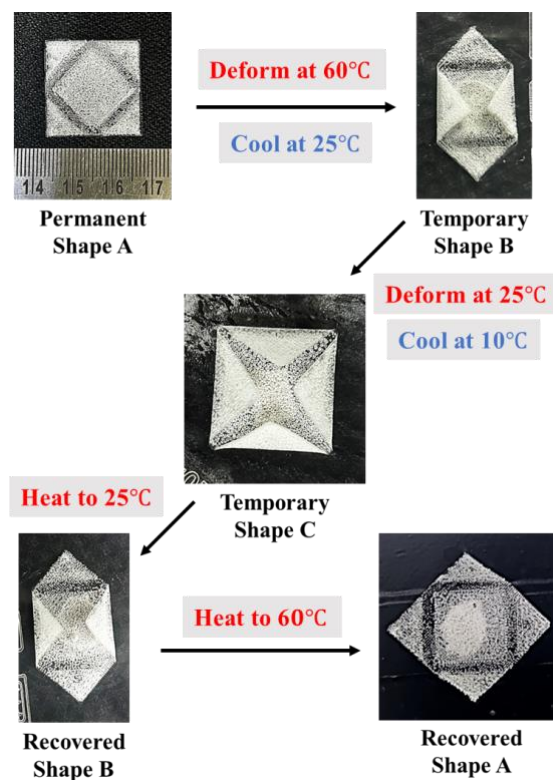


**Figure 1:** Figure illustrating the shape-fixing and shape-recovery phenomena in the triple-shape memory polymer for PPC50/PCL50 composition.

## References:

1. Zheng, Y., Li, Y., Hu, X., Shen, J., & Guo, S. (2017). Biocompatible shape memory blend for self-expandable stents with potential biomedical applications. *ACS applied materials & interfaces*, 9(16), 13988-13998.
2. Li, Y., Cheng, H., Yu, M., Han, C., & Shi, H. (2022). Blends of biodegradable poly ( $\epsilon$ -caprolactone) and sustainable poly (propylene carbonate) with enhanced mechanical and rheological properties. *Colloid and Polymer Science*, 1-10.

# Flexible nanostructured electrodes for neural interfacing including core-shell nanowires including core-shell nanowires

N. Rodríguez-Díez<sup>1\*</sup>, B.L. Rodilla<sup>1,2</sup>, A. Arché-Nuñez<sup>1</sup>, Sandra Ruiz-Gómez<sup>3</sup>, Ana Domínguez-Bajo<sup>4</sup>, Claudia Fernández-González<sup>1</sup>, Clara Guillén-Colomer<sup>1</sup>, Ankor González-Mayorga<sup>5</sup>, Julio Camarero<sup>1,6</sup>, Rodolfo Miranda<sup>1,6</sup>, Elisa López-Dolado<sup>5,7</sup>, María C. Serrano<sup>4</sup>, Pilar Ocón<sup>8</sup>, L. Pérez<sup>1,2</sup>, M.T. González<sup>1</sup>

<sup>1</sup> Fundación IMDEA Nanociencia, Calle Faraday 9, 28049 Madrid, Spain

<sup>2</sup> Departamento de Física de Materiales, Universidad Complutense de Madrid, Plaza de las Ciencias s/n, 28040 Madrid, Spain

<sup>3</sup> Max Planck Institute for Chemical Physics of Solids, Dresden, Germany

<sup>4</sup> Instituto de Ciencia de Materiales de Madrid (ICMM), CSIC, Calle Sor Juana Inés de la Cruz 3, 28049 Madrid, Spain

<sup>5</sup> Hospital Nacional de Paraplégicos, SESCAM, Finca La Peraleda s/n, 45071 Toledo, Spain

<sup>6</sup> Dept. de Física de la Materia Condensada and Instituto "Nicolás Cabrera", Universidad Autónoma de Madrid, 28049 Madrid, Spain

<sup>7</sup> Design and development of biomaterials for neural regeneration, HNP-SESCAM, Associated Unit with CSIC through ICMM, Finca La Peraleda s/n, 45071 Toledo, Spain

<sup>8</sup> Departamento de Química Física Aplicada, Universidad Autónoma de Madrid, 28049 Madrid, Spain

## Abstract:

Neurological disorders are steadily increasing in developed countries, due to evolving lifestyles and the increased longevity. Neural interfaces able to record or stimulate neural activity have become essential tools in their diagnosis and treatment. Yet, present interfaces have several limitations, including larger size than ideal, which can lead to unspecific stimulation and possible secondary effects, and the loss of efficacy, due to the tissue foreign-body response to the interface, which frequently ends up being encapsulated and needs to be replaced. Therefore, advancements in neural implants able to interact with neurons in the less invasive way has emerged as a critical area of research in nanobiomaterials<sup>1,2,3</sup>.

In this context, our research is focused on enhancing the efficiency of neural interfaces intended for implantation by providing nanostructure to the surface of the neural electrodes. These structural modifications lead to improved electrical properties, increase the effective area and decrease the impedance of the electrodes. This, in turn, allows to fabricate electrodes with smaller overall size for a more spatially resolved stimulation, and a reduction of undesirable side effects. In addition, the nanostructure favors the intimate contact neuron-electrode. To reach this aim, we have created flexible electrodes with their surface covered by a network of vertical nanowires (NWs) of 3 types: (1) an ordered hexagonal network of Au NWs<sup>4</sup>, (2) a randomly ordered network of Au NWs<sup>5</sup> and (3) a network of core-shell Au@Ni NWs<sup>6</sup> designed using a combination of template-

assisted electrodeposition and pulsed electrodeposition techniques. With these strategies we can control the morphological and chemical characteristics of the NWs. In particular, Ni NWs coated by an Au shell combine the mechanical properties of Ni, ensuring an improved uniformity and increased length of the NWs in comparison with Au, with the biocompatibility of the Au shell, which will be in contact with the tissue. We characterized the electrodes through electrochemical and morphological analyses using techniques such as scanning electron microscopy (SEM), cyclic voltammetry (CV), and electrochemical impedance spectroscopy (EIS). Finally, the morphology, viability and neuronal differentiation of rat embryonic cortical cells cultured on the NW electrodes were studied, with similar results as for control (glass) substrates, accompanied by a lower glial cell differentiation<sup>4,5,6</sup>.

**Keywords:** Neural Interfaces, Nanomedicine, Nanomaterials, Core-shell, Gold nanowires, Nanostructured electrode, Template-Assisted Electrodeposition, EIS, CV, SEM, Neuronal Differentiation.

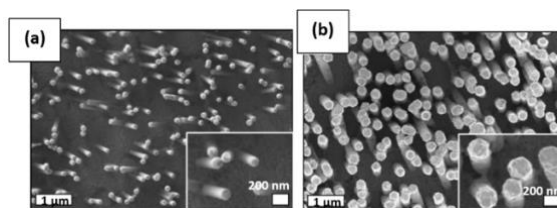


**Figure 1:** Figure (a) electrode coated with Ni NWS, and (b) Ni NWS with an Au Shell grown by electrodeposition.<sup>6</sup>

### References:

1. Patil, A. C. & Thakor, N. V (2016) Implantable neurotechnologies: A review of micro- and nanoelectrodes for neural recording. *Med. Biol. Eng. Comput.* 54, 23–44.
2. Wellman, SM. Eles, JR. Ludwig, KA. et al. (2018) A Materials Roadmap to Functional Neural Interface Design. *Adv Funct Mater* 21;28 (12).
3. Scaini, D. Ballerini, L. (2018) Nanomaterials at the neural interface. *Curr. Opin. Neurol.* 50, 50-55.
4. Domínguez-Bajo, A. Rosa, J.M. et al. (2021) Nanostructured gold electrodes promote neural maturation and network connectivity. *Biomater.* 279, 121186.
5. Domínguez-Bajo, A. Rodilla, B.L. et al. (2020) Interfacing Neurons with Nanostructured Electrodes Modulates Synaptic Circuit Features. *Adv. Biosyst.* 4, 2000117.
6. Rodilla, B.L, Arché-Núñez, A, Ruiz-Gómez, S. et al. (2024) Flexible metallic core-shell nanostructured electrodes for neural interfacing. *Sci Rep* 14, 3729.

# Sol-Gel Synthesis of Silica-based Biomaterials with different weight percentages of Rosmarinic Acid

F. Barrino<sup>1,\*</sup>, F. Giuliano<sup>1</sup>, F. Sedita<sup>1</sup>, C. Dispenza<sup>1</sup>

<sup>1</sup>Department of Engineering, University of Palermo, Viale delle Scienze 6, 90128 Palermo, Italy

## Abstract:

Implanted biomedical devices can induce adverse responses in the human body, which can cause failure of the implant, referred to as implant failure. Early implant failure is induced by numerous factors, especially infections and inflammation. Natural products are today one of the main sources of new pharmaceutical molecules due to the development of infections and inflammations that cause rejection or replacement of the implant. One method used for the synthesis of a wide range of materials, including biomaterials is the Sol-Gel technique<sup>1</sup>. This method involves the formation of a sol (a colloidal dispersion of solid particles in a liquid) which is subsequently transformed into a gel (a cross-linked three-dimensional solid structure) through polymerization or cross-linking processes. In the context of biomaterials, the sol-gel technique has been employed to produce materials with specific characteristics suitable for various biomedical applications, such as tissue regeneration, drug delivery and tissue engineering. The aim of this work is the sol-gel synthesis of biomedical implants with anti-inflammatory properties. Different weight percentages (5, 10, 15, 20 wt%) of rosmarinic acid were incorporated into the silica matrix. Rosmarinic acid is a phenolic compound present in several plants, including rosemary (from which it takes its name), sage and lemon balm. It is known for its antioxidant, anti-inflammatory, antimicrobial and antiviral properties<sup>2</sup>. These properties make it useful in various contexts, such as natural medicine, cosmetics and even the food industry, where it is used as a natural preservative. Rosmarinic acid is the subject of numerous studies to fully understand its beneficial effects on human health. The interactions between different organic and inorganic phases in the hybrid materials were studied using Fourier transform infrared spectroscopy (FTIR)<sup>3</sup>. While the controlled release was monitored at different time intervals with UV-vis spectroscopy.

**Keywords:** Sol-gel glasses, silica-based biomaterials, rosmarinic acid, biomedical applications.

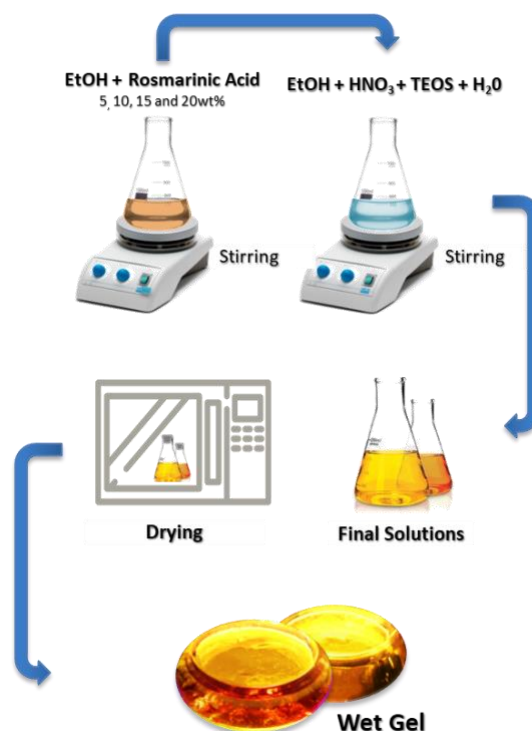


**Figure 1:** Sol-gel procedure used to obtain hybrid materials under study

## References:

1. Barrino, F. (2024). Hybrid Organic–Inorganic Materials Prepared by Sol–Gel and Sol–Gel-Coating Method for Biomedical Use: Study and Synthetic Review of Synthesis and Properties. *Coatings*, 14(4), 425.
2. Noor, S., Mohammad, T., Rub, M. A., Raza, A., Azum, N., Yadav, D. K., ... & Asiri, A. M. (2022). Biomedical features and therapeutic potential of rosmarinic acid. *Archives of Pharmacal Research*, 45(4), 205-228.
3. Catauro, M., Barrino, F., Dal Poggetto, G., Crescente, G., Piccolella, S., & Pacifico, S. (2020). New SiO<sub>2</sub>/caffeic acid hybrid materials: Synthesis, spectroscopic characterization, and bioactivity. *Materials*, 13(2), 394.

# Graphene oxide is biocompatible and strengthens gelatine through non-covalent interactions with its amorphous region

Hak Jin Sim<sup>1,2</sup>, Katarina Marinkovic<sup>1,2</sup>, Ping Xiao<sup>2,3</sup>, and Hui Lu<sup>1\*</sup>

<sup>1</sup>School of Biological Sciences, <sup>2</sup>Department of Materials, <sup>3</sup>Henry Royce Institute, The University of Manchester, UK

## Abstract:

Graphene oxide (GO) has attracted huge attention in biomedical sciences due to its outstanding properties and potential applications. In this study, we synthesized GO using our recently developed 1-pyrenebutyric acid-assisted method [1]; and then assessed how the GO as a filler influences the mechanical properties of GO-gelatine nanocomposite films, and the cytotoxicity of HEK-293 cells grown on the GO-gelatine substrates. We show that the addition of GO (0-2%) improves the mechanical properties of gelatine in a concentration-dependent manner (Figure 1). The presence of 2 wt% GO increased tensile strength, elasticity, ductility, and toughness of the gelatine films about 3.1, 2.5, 2, and 8-fold, respectively. Cell viability, apoptosis and necrosis analyses showed no cytotoxicity from GO. Furthermore, we performed Circular dichroism, X-ray diffraction, Fourier-transform infrared spectroscopy, and X-ray photoelectron spectroscopy analyses to decipher the interactions between GO and gelatine. The results show, for the first time, that GO enhances the mechanical properties of gelatine by forming non-covalent intermolecular interactions with gelatine at its amorphous or disordered regions. We believe that our findings will provide new insight and help pave the way for potential and wide applications of GO in tissue engineering and regenerative biomedicine.

**Keywords:** Graphene Oxide, 2D nanomaterials; gelatine, cytotoxicity, mechanical property, biomaterials, biomedical applications.

films. It shows that GO improves the mechanical properties of gelatin, from tensile strength, and elasticity to ductility and toughness.

## References:

1. Sim, H. J., Xiao, P., Lu, H. (2021) Pyrenebutyric acid-assisted room-temperature synthesis of large-size monolayer graphene oxide with high mechanical strength. *Carbon* 185, 224-233.

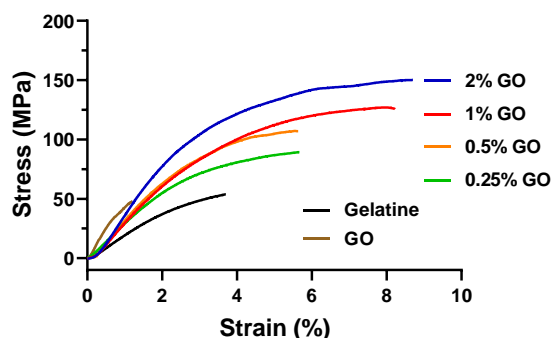


**Figure 1:** Stress-strain tensile behavior profiles of gelatine, GO, and GO-gelatine nanocomposite



# Characterization of lyophilized, extruded histidylated liposome, a versatile platform for mRNA delivery

Albert NGALLE LOTH<sup>1</sup>, Manon MAROQUENNE<sup>2</sup>, Ayoub MEDJMEDI<sup>1</sup>, Chantal PICHON<sup>3,4</sup>,  
Delphine LOGEART-AVRAMOGLU<sup>2</sup>, Federico PERCHE<sup>1</sup>

<sup>1</sup>Centre de Biophysique Moléculaire, CBM, CNRS UPR4301, Orléans, France

<sup>2</sup>Université Paris Cité, CNRS, INSERM, ENVA, B3OA, 75010, Paris, France

<sup>3</sup>Inserm UMS 55 ART ARNm and Université d'Orléans, F-45100 Orléans

<sup>4</sup>Institut Universitaire de France, 1 rue Descartes, F-75035 Paris, France

## Abstract:

The development of mRNA delivery systems, predominantly lipid-based has facilitated recent advances in mRNA-based therapeutics. Liposomes represent the earliest class of mRNA vectors and remain at the forefront of clinical trials. We have previously developed a histidylated liposome that demonstrated efficient nucleic acid delivery. In this study, the liposome preparation process was optimized by freeze-drying followed by extrusion to homogenize size distribution and improve storage stability. A comprehensive characterization of these LYX liposomes was performed, including evaluation in cellular and murine animal models.

LYX liposomes can be stored for up to one year at 4°C, maintaining a stable size ( $150 \pm 10$  nm) and polydispersity index ( $0.10 \pm 0.02$ ), while preserving their transfection efficiency. They exhibit high encapsulation efficiency ( $\sim 95\%$ ) and protect mRNA from RNase degradation. We confirmed their lamellar organization by Small Angle X-ray Scattering and CryoTEM and examined their intracellular trafficking using confocal microscopy. LYX-mRNA lipoplexes can transfect both cell lines and primary cells, albeit with a lower transfection efficiency compared to the commercial Lipofectamine MessengerMAX™ vector. Our data suggest that this could be attributed to slower cell uptake and reduced endosomal escape of LYX. In addition, *in vivo* studies in mice showed that the use of LYX-FLuc mRNA lipoplexes induced the expression of firefly luciferase for up to 5 days when administered intramuscularly and for 48 hours when incorporated into hydrogels and implanted subcutaneously.

Based on these findings, the newly processed histidylated liposomes appear as a promising platform for mRNA delivery, offering versatility for multiple applications.

**Keywords:** mRNA therapeutics, liposome, lipoplexes, SAXS, CryoTEM, confocal microscopy.

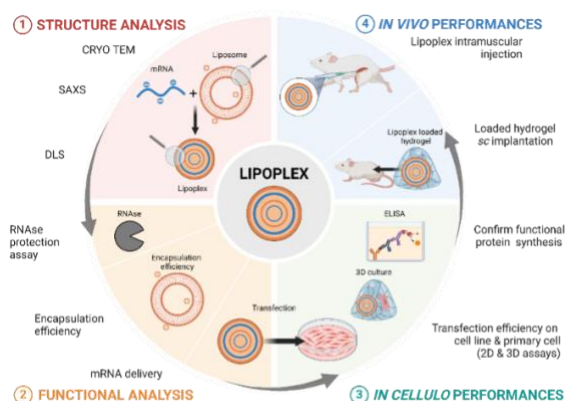


**Figure 1:** Illustration of the main steps of our study.

# Synthesis and Characterization of Cadmium Sulphide Nanoparticles with Antimicrobial Assay

E. U. Ekwujuru <sup>1,\*</sup>, M. G. Peleyeju <sup>1</sup>, C. Ssemakalu <sup>1</sup>, M. E. Monapathi <sup>1</sup> and M. J. Klink <sup>1\*</sup>

<sup>1</sup>Department of Natural Science, Vaal University of Technology, Vanderbijlpark Campus, 1900, S. Africa

\*Corresponding authors: Email addresses: michaelk1@vut.ac.za and ezinneekwujuru@yahoo.com

## Abstract:

Antimicrobial resistance to conventional antibiotics has long been an unsolved problem. The search for a more effective antimicrobial agent has prompted the consideration of nanoparticles due to their small size and potential biocidal activities. Cadmium sulphide nanoparticles (CdS NPs) has been well-considered as a future biocidal material. This study synthesized, characterized and evaluated the antimicrobial behavior of CdS NPs in both dark incubation at 37°C and room temperature (RT) incubation. CdS NPs was synthesized using wet chemical synthesis with cadmium chloride and sodium sulphate as precursors. Characterization was done using Transmission Electron microscopy (TEM), scanning electron microscopy (SEM), Fourier Transform Infrared Spectroscopy (FTIR), X-Ray diffraction analysis (XRD), Energy Dispersive X-ray (EDX), UV-Vis spectroscopy and Raman spectroscopy. Agar well diffusion, minimum inhibitory concentration (MIC) and minimum bactericidal concentration (MBC) were performed to investigate the antimicrobial behavior of the nanoparticles using *E. coli* and *S. aureus* as representative test organisms for gram-negative and positive bacteria respectively. This was done using three concentrations, 50 mg/ml, 25mg/ml and 10 mg/ml. XRD results showed that the synthesized nanoparticles had cubic zinc blende structure. SEM and TEM images confirms that the particles with average size of 8.477 nm were evenly distributed in clusters. Results of FTIR and EDX confirmed that the nanoparticles were pure. The UV-Vis spectroscopy shows the activation of the nanoparticles in the visible light region. The Raman spectroscopy results show peaks at 302.3 cm<sup>-1</sup> and 601 cm<sup>-1</sup> attributed to first and second order longitudinal optical. The antimicrobial assay of CdS NPs shows antimicrobial activity against both *E. coli* and *S. aureus* in a dose-dependent manner, as the zone of inhibition increases with increase in concentration of the nanoparticles. The zone of inhibition was reported to be wider for the RT incubation than the dark incubation but with

similar MIC results. The MBC confirmed that the synthesized nanoparticles was more bactericidal in the dark incubation and more bacteriostatic at RT incubation. The synthesized nanoparticles were generally more effective toward *E. coli*, and the dark incubation was more favorable.

**Keywords:** antimicrobial activity, cadmium sulphide, nanoparticles, bacteriocidal, wet chemical synthesis, room temperature incubation.

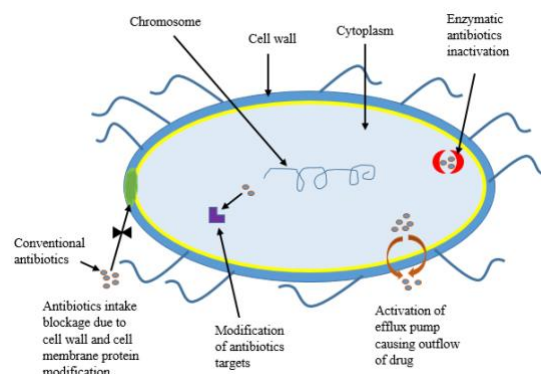


**Figure 1:** Figure illustrating the fundamental question that we are tempting to solve experimentally: How can microbial resistance to conventional antimicrobial agents be curbed using nanotechnology.

## References:

1. Ghasempour, A., Dehghan, H., Ataee, M., Chen, B., Zhao, Z., Sedighi, M., Guo, X., Shahbazi, M.A., (2023). Cadmium sulfide nanoparticles: preparation, characterization, and biomedical applications. *Molecules*, 28(9), p.3857.
2. Adhikari, S., Parajuli, K., Karki, G.B., Khatiwada, S.P. and Adhikari, R., (2023). Structural, optical and antimicrobial properties of carbohydrate-capped cadmium sulfide nanoparticles. *Journal of Nepal Chemical Society*, 43(2), 1-10.

**EGF 2024 - Session I. C:  
Graphene and 2D Materials  
synthesis, characterization, and  
properties**

# Chemistry of 2D Materials for Patterning and Building of Heterostructures

Emilio M. Pérez <sup>1\*</sup>

<sup>1</sup> IMDEA Nanociencia, Faraday 9, 28049, Madrid, Spain

## Abstract:

Patterning of graphene (functionalizing some areas while leaving others intact) is challenging, as all the C atoms in the basal plane are identical, but it is also desirable for a variety of applications, like opening a bandgap in the electronic structure of graphene. Several methods have been reported to pattern graphene, but most of them are very technologically intensive. For example, some groups have explored electron beam lithography,<sup>1</sup> or laser writing.<sup>2,3</sup>

Here, we will present the two approaches developed in our group. First, we describe a method to functionalize graphene covalently under ultra-high vacuum conditions and characterized with scanning tunnelling microscopy.<sup>4,5</sup> We achieve exquisite (>97%) atomic selectivity and yield (92%). The periodic landscape is provided by a single monolayer of graphene grown on Ru(0001) that presents a moiré pattern due to the mismatch between the carbon and ruthenium hexagonal lattices. The moiré contains periodically arranged areas where the graphene–ruthenium interaction is enhanced and shows higher chemical reactivity. Furthermore, we will show how this type of functionalized graphene acts as a catalyst for an unusual and reversible C–C bond forming reaction.<sup>6</sup> Secondly, we will describe easy and scalable protocol for the covalent patterning of graphene based on using microemulsions as templates.<sup>7</sup> This method is technologically trivial and can achieve resolution in the  $\mu\text{m}$  range.

Finally, I will also describe the covalent grafting of 2H-MoS<sub>2</sub> flakes on graphene monolayers embedded in field-effect transistors.<sup>8</sup> A bifunctional molecule was used that features a maleimide and a diazonium functional group, known to connect to sulfide- and carbon-based materials, respectively. MoS<sub>2</sub> flakes were first exfoliated, functionalized by reaction with the maleimide moieties, then anchored to graphene through the diazonium groups. This approach enabled the simultaneous functionalization of several devices. The electronic properties of the resulting heterostructure are shown to be dominated by the MoS<sub>2</sub>–graphene molecular interface.

I will also discuss the journey that has led to these results, including the development of a “click” chemistry reaction for transition metal-dichalcogenides.<sup>9,10</sup>

**Keywords:** graphene, covalent chemistry, MoS<sub>2</sub>, patterning, heterostructures.

## References:

1. Rodríguez González, M. C. *et al.* Multicomponent Covalent Chemical Patterning of Graphene. *ACS Nano* **15**, 10618–10627 (2021). <https://doi.org/10.1021/acsnano.1c03373>
2. Edlthammer, K. F. *et al.* Covalent 2D-Engineering of Graphene by Spatially Resolved Laser Writing/Reading/Erasing. *Angew. Chem., Int. Ed.* **59**, 23329–23334 (2020). <https://doi.org/10.1002/anie.202006874>
3. Wei, T., Al-Fogra, S., Hauke, F. & Hirsch, A. Direct laser writing on graphene with unprecedented efficiency of covalent two-dimensional functionalization. *J. Am. Chem. Soc.* **142**, 21926–21931 (2020). <https://doi.org/10.1021/jacs.0c11153>
4. Navarro, J. J. *et al.* Organic Covalent Patterning of Nanostructured Graphene with Selectivity at the Atomic Level. *Nano Lett.* **16**, 355–361 (2016). <https://doi.org/10.1021/acs.nanolett.5b03928>
5. Navarro, J. J., Calleja, F., Miranda, R., Pérez, E. M. & Parga, A. L. V. d. High yielding and extremely site-selective covalent functionalization of graphene. *Chem. Commun.* **53**, 10418–10421 (2017). <https://doi.org/10.1039/c7cc04458e>
6. Navarro, J. J. *et al.* Graphene catalyzes the reversible formation of a C–C bond between two molecules. *Science Advances* **4**, eaau9366 (2018). <https://doi.org/10.1126/sciadv.aau9366>
7. Naranjo, A., Martín Sabanés, N., Vázquez Sulleiro, M. & Pérez, E. M. Microemulsions for the covalent patterning of graphene. *Chemical Communications* **58**, 7813–7816 (2022). <https://doi.org/10.1039/D2CC01858F>
8. Vázquez Sulleiro, M. *et al.* Fabrication of devices featuring covalently linked MoS<sub>2</sub>–graphene heterostructures. *Nature Chemistry* **14**, 695–700 (2022). <https://doi.org/10.1038/s41557-022-00924-1>
9. Vera-Hidalgo, M., Giovanelli, E., Navio, C. & Perez, E. M. Mild Covalent Functionalization of Transition Metal Dichalcogenides with Maleimides: A “Click” Reaction for 2H-MoS<sub>2</sub> and WS<sub>2</sub>. *J. Am. Chem. Soc.* **141**, 3767–3771 (2019). <https://doi.org/10.1021/jacs.8b10930>
10. Quiros-Ovies, R. *et al.* Controlled Covalent Functionalization of 2 H-MoS<sub>2</sub> with Molecular or Polymeric Adlayers. *Chemistry A European Journal* **26**, 6629–6634 (2020). <https://doi.org/10.1002/chem.202000068>

# Tuning the exchange coupling in graphene-based synthetic antiferromagnets

M. Hsouna<sup>1,2,\*</sup>, C.A. Brondin<sup>3,4</sup>, TO. Menteş<sup>4</sup>, A. Locatelli<sup>4</sup>, N. Stojić<sup>1</sup>

<sup>1</sup>Condensed Matter and Statistical Physics, International Centre for Theoretical Physics, Trieste, Italy

<sup>2</sup>Condensed Matter, The International School for Advanced Studies, Trieste, Italy

<sup>3</sup>Università Ca' Foscari di Venezia, dipartimento di scienze molecolari e nanosistemi, Venice, Italy

<sup>4</sup>Elettra Sincrotrone Trieste S.C.p.A., Basovizza, Trieste, Italy

## Abstract:

Synthetic antiferromagnets are promising building blocks for spintronic devices [1] mostly due to the absence of stray fields and the relatively weak exchange coupling between the constituents. Using graphene as a spacer towards creation of such antiferromagnetic (AFM) stacks has been proven to be a successful approach [2]. Recent experiments at the Nanospectroscopy beamline at Elettra [3] indicate that it is possible to control the type [AFM vs. ferromagnetic (FM)] and strength of Fe-Co magnetic coupling via defects in the graphene (Gr) layer within the Fe/Gr/Co synthetic antiferromagnet. Building on this experimental work, we theoretically investigate the influence of the Fe/Gr interface morphology on the exchange coupling in Fe/Gr/Co. In our density-functional-theory calculations, we consider two models of the Fe/Gr interface; a uniform Fe layer and Fe clusters [4] on graphene. In both cases, we consider ideal graphene as well as a defective one, with the goal of explaining the physical mechanisms underlying the experimentally-observed changes in the magnetic coupling. Modeling Fe as a uniform monolayer, we find the Fe-Co coupling to be purely AFM for the ideal graphene spacer and predominantly AFM for the graphene with vacancies. However, in case of Fe clusters, we obtain an antiferromagnetically coupled heterostack for the ideal graphene and FM coupling for graphene with vacancies. We discuss the interaction of Fe clusters with the underlying Co layer via graphene vacancy defects. The couplings obtained for the cluster configuration fully correspond to the experimental results, revealing the crucial role played by metal clusters and graphene defects in a realistic heterostack. Furthermore, by introducing Ag adatoms at the graphene vacancies, AFM coupling between Co and Fe is restored in our simulations, consistent with the experimental observation. Based on these results and our analysis, we identify the breaking of the superexchange pathway between Co and Fe upon creation of graphene vacancies as

the origin of the switching from AFM to FM coupling.

**Keywords:** synthetic antiferromagnets, graphene spacer, exchange coupling, graphene vacancies.

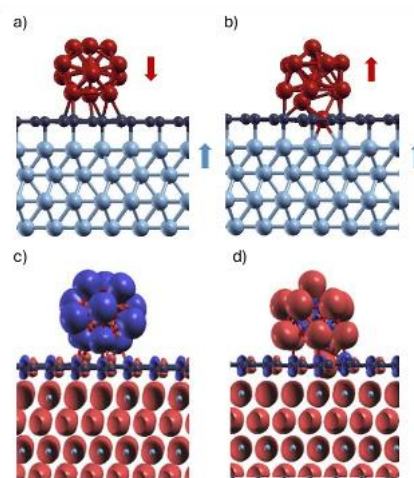


**Figure 1:**

Atomic structure (top row) and spin density plots (bottom row) of Fe<sub>13</sub> cluster on pristine graphene/Co in (a) and (c), Fe<sub>13</sub> cluster on graphene with a triple vacancy defect/Co in (b) and (d). Red, dark blue, and light blue spheres denote Fe, C, and Co atoms, respectively. The arrows indicate the direction of the magnetization in Fe and Co, where parallel (antiparallel) arrows show FM (AFM) coupling. The spin densities are plotted using the isovalue of 0.005 e/Bohr<sup>3</sup>, where red (blue) color denotes positive (negative) spin density.

## References:

1. Duine et al., Nat. Phys. 14, 217, 2018;
2. Gargiani et al., Nat. Commun. 8,699, 2017;
3. Brondin, Hsouna et al., submitted 2024;
4. Binz et al., Phys. Rev. Lett. 109, 026103, 2012.



# Band Gaps Engineering in the 2D $\text{Mo}(\text{S}_{1-x},\text{Te}_x)_2$ -Alloy Adsorbed on Graphite, or Sandwiched Between Layers of Graphene

B. P. Burton

<sup>2</sup>NIST, 1 Bureau Drive, Gaithersburg, MD, USA

## Abstract:

First principles VASP<sup>1</sup> formation-energy calculations were performed for: (1) a  $\text{Mo}_9(\text{S}_{18-m},\text{Te}_m)$ -2D-alloy ( $m=0,1,\dots,18$ ) adsorbed (van der Waals bonded<sup>2</sup> to four layers of Graphite (a  $4\times 4\times 2$  155-atom supercell); and (2) a  $\text{Mo}_8(\text{S}_{16-m},\text{Te}_m)$ -2D-alloy ( $m=0,1,\dots,16$ ) between two relaxed layers of (**G**); (3) between two relaxed **G**-layers and one **G**-layer on each side. Atomic positions and cell dimensions were fully relaxed, and band gaps (BG) were calculated with a perl script, from VTSTscripts<sup>3</sup>.

Calculated BGs for the supercells shown as insets in Figures (a), (b) and (c), and for the various 2D-alloy (chemical) configurations in vacuum. All predicted BG are direct. The trends predicted for 2D alloys in vacuum (blue diamonds) are as one would expect given the difference in electronegativities: **S**-rich configurations correlate with larger BGs than **Te** because **S** has a larger electronegativity (holds e- more tightly than **Te**). But when van der Waals bonded to **G** the trend is reversed; evidently, **G** is an e- source for **S** and an e- sink for **Te**.

These results suggest that for BG-engineering materials such as  $\text{Mo}(\text{S},\text{Se})_2$ ,  $\text{Mo}(\text{Se},\text{Te})_2$ , and  $\text{Mo}(\text{S},\text{Te})_2$ , using a conductive substrate, or heterostructure, such as Graphene strongly influences the BG, relative to vacuum.

In addition, aspects of phase stability and phase transitions will be discussed: e.g. in bulk  $\text{Mo}(\text{S}_{1-x},\text{Te}_x)_2$  alloys are predicted to phase separate, whereas, they are predicted to order when they are adsorbed on Sapphire, or Graphite, or sandwiched between **G** layers.

**Keywords:** 2D  $\text{Mo}(\text{S},\text{Te})_2$  alloy; TMD; Band Gaps; First Principles; Graphite; Graphene.

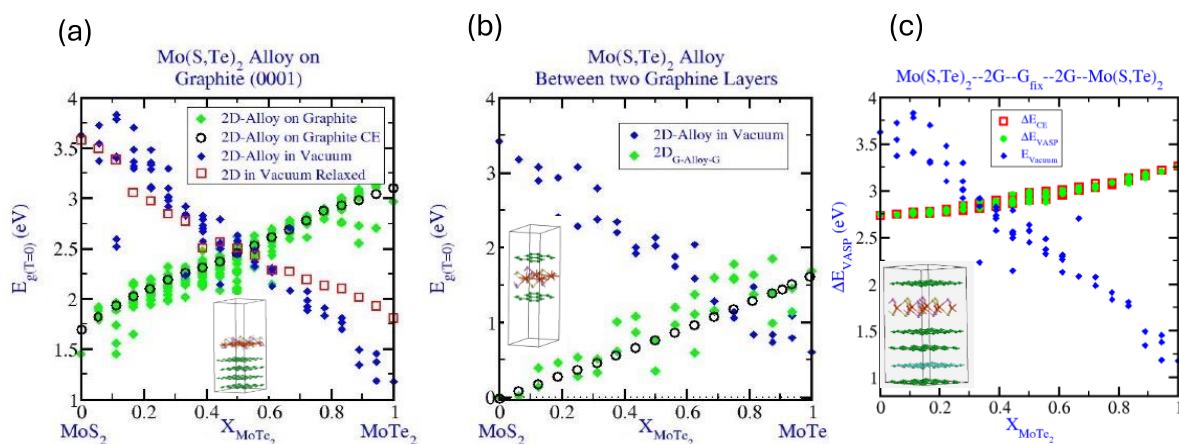


**Figure:** Calculated BGs for the  $\text{Mo}_9(\text{S}_{1-x},\text{Te}_x)$ -2D-alloy: (a) adsorbed on four **G**-layers (green), and in vacuum (blue); relaxed in vacuum (red); Black circles (CE) were calculated via cluster expansion; (b) Calculated band gaps for the  $\text{Mo}_9(\text{S}_{1-x},\text{Te}_x)$ -2D-alloy sandwiched between two relaxed layers of **G** (green) and in vacuum (blue); (c) alloy sandwiched between two relaxed and one fixed **G**-layer.

## References:

1. G. Kresse and J. Hafner, PRB 47, 558- (1993)
2. J. Klimes et al. PRB 83, 195131 (2011).
3. G. Henkelman, et. Al. J. Chem. Phys. 113, 9901 (2000)



# Emergent cavity junction around metal-on-graphene contacts

Yuhao Zhao<sup>1,\*</sup>, Maëlle Kapfer<sup>2,\*</sup>, Kenji Watanabe<sup>3</sup>, Takshi Taniguchi<sup>3</sup>, Oded Zilberberg<sup>4</sup>, Bjarke S. Jessen<sup>5</sup>

<sup>1</sup>Institute for Theoretical Physics, ETH Zurich, 8093 Zurich, Switzerland

<sup>2</sup>Department of Physics, Columbia University, New York, NY, USA

<sup>3</sup>National Institute for Materials Science, 1-1 Namiki, Tsukuba, 305-0044, Japan

<sup>4</sup>Department of Physics, University of Konstanz, 78464 Konstanz, Germany

<sup>5</sup>Department of Physics, Technical University of Denmark, 2800 Copenhagen, Denmark

## Abstract:

Harnessing graphene devices for applications relies on a comprehensive understanding of how to interact with them. Specifically, scattering processes at the interface with metallic contacts can induce reproducible abnormalities in measurements. Here, we report on emergent transport signatures appearing when contacting sub-micrometer high-quality metallic top contacts to graphene. Using electrostatic simulations and first-principle calculations, we reveal their origin: the contact induces an n-doped radial cavity around it, which is cooperatively defined by the metal-induced electrostatic potential and Klein tunneling. This intricate mechanism leads to a secondary resistance peak as a function of graphene doping that decreases with increasing contact size. Interestingly, in the presence of a perpendicular magnetic field, the cavity spawns a distinct set of Landau levels that interfere with the Landau fan emanating from the graphene bulk. Essentially, an emergent 'second bulk' forms around the contact, as a result of the interplay between the magnetic field and the contact-induced electrostatic potential. The interplay between the intrinsic and emergent bulks leads to direct observation of bulk-boundary correspondence in our experiments. Our work unveils the microscopic mechanisms manifesting at metal-graphene interfaces, opening new avenues for understanding and devising graphene-based electronic devices.

**Keywords:** metal-graphene heterostructure, top contact, metal-graphene interface, cavity modes, Klein tunneling

## References:

1. Y. Zhao, M. Kapfer, K. Watanabe, T. Taniguchi, O. Zilberberg, B. S. Jessen, arxiv 2408.10973 (2024).

# The Effects of Drying Method and Gelation Time on Reduced Graphene Oxide Aerogels

S. Mallia<sup>1</sup>, A. Agius Anastasi<sup>1</sup>, D. A. Vella<sup>1</sup>

<sup>1</sup>Department of Metallurgy and Materials Engineering, University of Malta, Msida, Malta

**Abstract:** Graphene has proven itself to be an interesting and novel nanomaterial. Graphene's practical adoption has however been limited to various thin films and coatings due to the nanomaterial's atomically thin 2D structure [1]. Application of the nanomaterial into 3D structures is therefore an essential step for graphene's widespread adoption. To this end, 2D graphene can be assembled into 3D aerogels. Aerogels are synthetic 3D mesoporous materials, formed through the drying of a gelled colloid and composed of structure with a low density, and high surface-to-volume ratio. The production and application of graphene and its derivatives into aerogel structures is recently gaining interest, however a robust understanding of the aerogel synthesis procedure on the resulting graphene aerogel is still lacking, resulting in unpredictable and unrepeatable aerogel properties. In this work we report on the influence of two critical and underexplored parameters for aerogel production - the gelation time and the drying method applied.

Reduced graphene oxide (rGO) aerogels were synthesised from graphene oxide (GO) and ascorbic acid via thermochemical reduction. The GO was allowed to gel at 90 °C for two different gelation times, 40 minutes (the point at which the sol solidifies into a manageable gel), and 12 hours. The resultant hydrogels were then either freeze dried or supercritically dried using CO<sub>2</sub>. Finally, the dried aerogels were pyrolyzed at 750 °C for 3 h under a N<sub>2</sub> atmosphere. The GO precursor, intermediate hydrogels, un-pyrolyzed aerogels, and the final pyrolyzed rGO aerogels were characterized by scanning electron microscopy coupled with energy dispersive spectroscopy and micro-Raman spectroscopy. The mechanical properties of the aerogels were assessed through uniaxial quasi-static compression testing. The aerogels were also subjected to a water uptake and stability test. The results from these tests were used then to describe and understand the effects of gelation time and drying method on the final rGO aerogels.

A short gelation time gave rise to larger rGO aerogels, consisting of orderly and cellular pores of around 300 μm as shown in Figure 1, and were characterised by significant elastic strain, a low compressive modulus, and poor water stability.

With a longer gelation time, the rGO aerogel pore size decreased to around 3 μm, forming a denser microstructure with less elastic properties and better water stability. With supercritical drying, the randomly oriented microstructure of the GO hydrogel was retained, however the macrostructure of the gels shrunk, creating dense rGO aerogels with nanometrically-wide pores, high compressive moduli, smaller elastic strains, auxetic behaviour, and improved water stability. The gelation time did not have a significant effect on the resultant rGO aerogel when supercritically dried, with only minor differences being observed.

The results obtained suggest that the gelation time of a rGO gel directly impacts the inter-sheet bond strength, in turn, affecting the behaviour of the gel when subjected to either of the two drying methods. A weaker inter-sheet bond strength results in a gel structure that is more pliable, providing less resistance to the growth ice crystals during freeze drying, and to shrinkage of pores during supercritical drying (likely induced by unwanted capillary stresses). With longer gelation times, the ice crystal growth during freeze drying and the shrinkage during supercritical drying are impeded by the stiffer inter-sheet bonds of the gel.

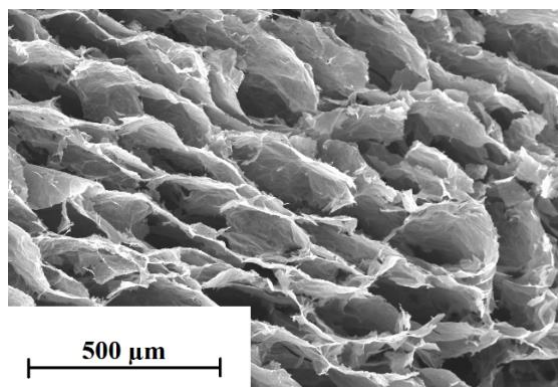


**Figure 1:** A scanning electron micrograph of a rGO aerogel that was gelled at 40 minutes and dried via freeze drying.

**Keywords:** Reduced graphene oxide aerogel, freeze drying, supercritical drying, gelation time.

## References:

[1] E. L. Wolf, Applications of Graphene – An Overview, *Springer Chemistry*, 2014

# The Chemistry of Graphene Oxide and its derivatives, a multi-purpose nanolaboratory

F. Amato <sup>1\*</sup>, A. Motta <sup>1</sup>, L. Giaccari <sup>1</sup>, P. Altimari <sup>1</sup>, A. G. Marrani <sup>1</sup>  
<sup>1</sup> Department of Chemistry, University “La Sapienza”, Rome, Italy

## Abstract:

The large-scale production of graphene is of great importance owing to its unique physical-chemical properties. However, the employment of graphene on a large scale is still limited owing to its yield of production and low water-dispersibility. To overcome these problems, graphene-like materials can be obtained starting from the oxidized form of graphene, known as graphene oxide (GO). This water-dispersible 2D nanomaterial ideally consists of a single graphitic layer with atomic thickness, lateral dimension up to micrometer-scale, and plenty of oxygen-based functional groups such as hydroxyl and epoxide groups, in addition to the less abundant carboxyl moieties. In the presence of reducing reagents, the purified GO is converted to reduced graphene oxide (RGO), the most similar material to graphene (Figure 1). As a result of these redox processes, in the structure of RGO, a large portion of oxygen-based functional groups are removed, the extended conjugation is partially restored and many structural defects are formed. However, as in the case of graphene, the layers of RGO are prone to aggregate in water by restricting its employment in many fields, especially biological ones. Herein, the sustainable preparation of highly water-dispersible RGO is presented. In particular, the GO obtained from graphite and widely characterized through both morphological and spectroscopic techniques was first enriched with carboxyl functional groups and after chemically reduced in water and at room temperature. The obtained dispersion shows good colloidal stability in water in a wide range of pH, ensured by the ionizable carboxyl groups. In addition to this type of covalent functionalization, non-covalent with azamacrocycles (e.g. porphyrins) was also successfully explored, as proved by spectroscopic investigations. Overall, the understanding of the aforementioned types of reactivity has paved the way for biological application and in the preparation of GO-based nanosponges for wastewater remediation.

**Keywords:** graphene, graphene oxide, functionalization, Raman spectroscopy, atomic force microscopy, nanosponges, wastewater remediation.

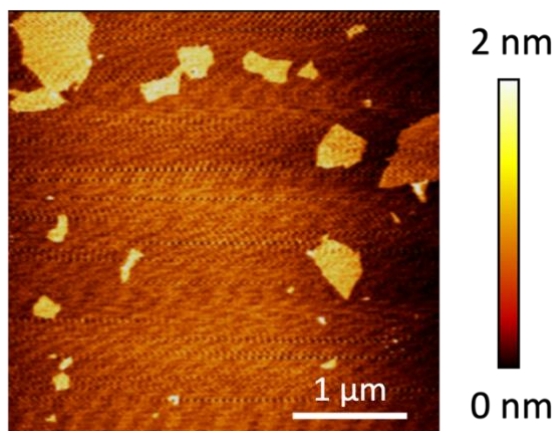


**Figure 1:** AFM image of single layers of RGO of different lateral sizes.

## References:

1. Eigler, S., Hirsch, A. (2014), Chemistry with Graphene and Graphene Oxide-Challenges for Synthetic Chemists, *Angew. Chem. Int. Ed.*, 53, 7720-7738.
2. Amato, F., Motta, A., Giaccari, L., Di Pasquale, R., Scaramuzzo, F. A., Zanoni, R., Marrani, A. G. (2023), One-pot carboxyl enrichment fosters water-dispersibility of reduced graphene oxide: a combined experimental and theoretical assessment, *Nanoscale Adv.*, 5, 893-906.
3. Amato, F., Perini, G., Friggeri, G., Augello, A., Motta A., Giaccari, L., Zanoni, R., De Spirito, M., Palmieri, V., Marrani, A. G., Papi, M. (2023), Unlocking the Stability of Reduced Graphene Oxide Nanosheets in Biological Media via Use of Sodium Ascorbate, *Adv. Mater. Interfaces*, 10, 2300105.

**Acknowledgments:** The research was financially supported by the European Union – NextGenerationEU under the National Recovery and Resilience Plan (NRRP), Mission 4, Component 2 Investment 1.3 - Call for tender No. 1561 of 11.10.2022 of Ministero dell’Università e della Ricerca (MUR); Project code PE0000021, Concession Decree No. 1561 of 11.10.2022 adopted by Ministero dell’Università e della Ricerca (MUR), CUP B53C22004070006; Project title “Network 4 Energy Sustainable Transition – NEST”.

# A continuous approach to developing new pathways for the synthesis of graphene derived materials

S. Kellici

<sup>1</sup> School of Engineering, London South Bank University, London, SE1 0AA

## Abstract:

The economic viability of graphene-derived materials is intrinsically linked to the synthesis routes that can reduce costs, increase performance, and enhance durability.<sup>1</sup> The presentation will highlight the application of the Continuous Hydrothermal Flow Synthesis (CHFS) process for the synthesis of a variety of 2D-related derivatives of graphene and MXene.

The CHFS process, is an environmentally benign, single-step process that involves mixing a flow of superheated water with a flow of water-soluble precursor(s) to give controlled, continuous, and rapid synthesis of nanomaterials. This system offers a variety of instant controls, including temperature, pressure, residence time, and reactant concentration, that allows a high degree of tailoring or functionalisation of the materials in their design to be fit for purpose

We will also explore how these materials have been applied in target oriented applications including energy, communication and environmental (photocatalysis).

## References:

1. Alli, U., Hettiarachchi, S.J. and Kellici, S., 2020. Chemical functionalisation of 2D materials by batch and continuous hydrothermal flow synthesis. *Chemistry–A European Journal*, 26(29), pp.6447-6460.
2. Baragau, I.A., Buckeridge, J., Nguyen, K.G., Heil, T., Sajjad, M.T., Thomson, S.A., Rennie, A., Morgan, D.J., Power, N.P., Nicolae, S.A. and Titirici, M.M., 2023. Outstanding visible light photocatalysis using nano-TiO<sub>2</sub> hybrids with nitrogen-doped carbon quantum dots and/or reduced graphene oxide. *Journal of Materials Chemistry A*, 11(18), pp.9791-9806.
3. Alli, U., McCarthy, K., Baragau, I.A., Power, N.P., Morgan, D.J., Dunn, S., Killian, S., Kennedy, T. and Kellici, S., 2022. In-situ continuous hydrothermal synthesis of TiO<sub>2</sub> nanoparticles on conductive N-doped MXene nanosheets for binder-free Li-ion battery anodes. *Chemical Engineering Journal*, 430, p.132976.

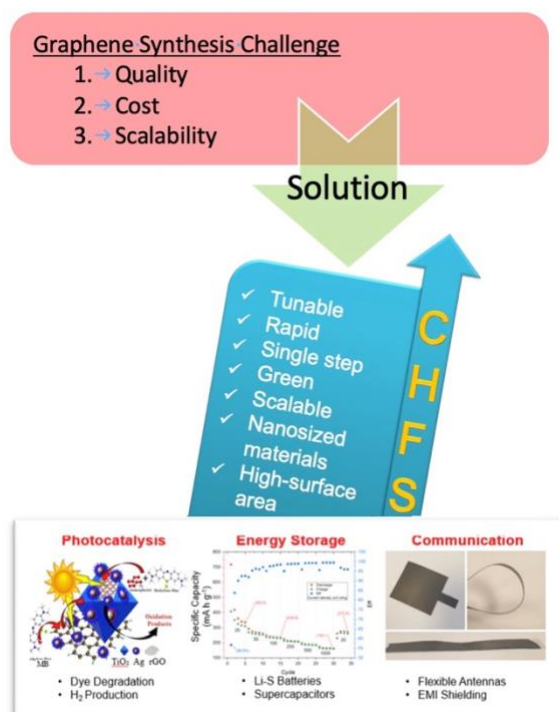


**Figure 1:** Target-oriented spectrum of applications



# Nonionic, Cationic and Anionic Surfactants-Assisted Liquid Exfoliation of Graphite into Few-Layer Graphene: Impact of Ultrasound, Solvents and Surfactants

M. Saeed <sup>1,\*</sup>, A. Ismail <sup>1</sup>, M. AlSaeedi <sup>1</sup>, Sh. Ahmad <sup>1</sup>

<sup>1</sup> Nanotechnology and Advanced Materials Program, Kuwait Institute for Scientific Research, Kuwait

## Abstract:

In this Research, the different ionic and non-ionic surfactants has been used to study its effect on the chemical exfoliation of graphene concentration with respect to the surfactant concentration utilization liquid phase exfoliation (LPE). The novel comparison between the three types of surfactants, in addition to the conventional ones, and their effect on the graphene dispersion were demonstrated. However, no studies have yet shown the effect of such surfactants on the quality of the exfoliated graphene, the number of layers produced, or defect density. Graphite powder was used as the raw material for the LPE process and N-methyl-pyrrolidone (NMP), dimethylformamide (DMF) and H<sub>2</sub>O were used as the exfoliation solvents medium through tip and bath sonication. A cationic surfactant cetyltrimethylammonium bromide (CTAB), a nonionic surfactant triblock copolymers (P123) and (F-127); and sodium dodecyl sulfate (SDS) as an anionic surfactant were used. The DMF solvent is much better than NMP solvent in the presence or absence of surfactants. Non-ionic surfactants P123 and F-127 showed better behavior, providing better colliding in the graphene dispersions than ionic ones, while the cationic showed the lowest potential. The graphene concentration showed that F-127 has the best results. Raman spectra confirmed that using aqueous-based dispersions directly affected the defect density but with thicker graphene flakes, while thinner flakes and higher defect densities were obtained using solvent-based solutions. Tip sonication showed a varying quality and yield and it was shown to reach the optimum condition at 60% amplitude. The findings suggest a compromise route to reach thinner flakes with high graphene concentration, yet stable colliding with low defect density, by fundamentally gaining knowledge of the LPE process to offer a low-cost and high-quality graphene dispersion.

**Keywords:** Graphene, dispersion, liquid-phase-exfoliation, sonication, solvent, surfactants

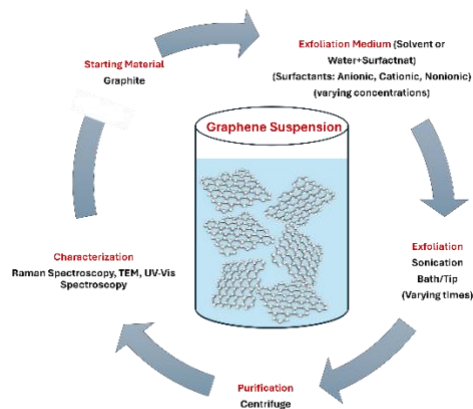


**Figure 1:** Figure illustrating the main process and factors studied in this study of graphene synthesis via liquid phase exfoliation.



# Effect of Graphene Reinforcement on the Tribological and Fracture Behaviours of Silicon-Based Nanocomposites

H. Abo El-Einein<sup>1\*</sup>, A. Berrais<sup>2</sup>, A. Weibel<sup>2</sup>, C. Laurent<sup>2</sup>, B. Berthel<sup>1</sup>, M.I. De Barros Bouchet<sup>1</sup>

<sup>1</sup>Ecole Centrale de Lyon, CNRS, ENTPE, LTDS, UMR5513, 69130 Ecully, France

<sup>2</sup>CIRIMAT, UMR UPS-CNRS-INP 5085, Institut Carnot Université Toulouse 3 Paul-Sabatier, 31062 Toulouse cedex 9, France

## Abstract:

There is a strongly growing demand for highly wear-resistant and reliable ceramic-based materials that can be used for a wide range of industrial applications. For this reason, the development of ceramic-based, high-performance materials with superior tribological and high mechanical properties is of utmost interest. The aim of this work is to investigate the friction, wear and mechanical properties of novel graphene reinforced ceramic matrix nanocomposites (GCMC), more particularly silicon nitride ( $\text{Si}_3\text{N}_4$ ) composite, that can be used for technical applications such as bearings and rotary seals. The quality of graphene and the homogeneity of its dispersion at the nanoscale significantly affect the mechanical properties and tribological behavior of the final composite<sup>1,2</sup>. Therefore, Few-Layered-Graphene-reinforced (FLG) sheets are deposited by chemical vapor deposition (CVD) directly on the silicon nitride grains, then they are sintered by spark plasma sintering (SPS). The special feature of this deposition process<sup>3</sup> is to produce a composite material whose silicon grains are perfectly enveloped by FLG controlling the covering rate and the number of graphene sheets. Different FLG-reinforced and non-reinforced  $\text{Si}_3\text{N}_4$  samples were selected to investigate the effect of the graphene covering rate and sheets number on the mechanical properties, friction and wear behaviors. The tribological behavior is investigated under severe contact pressure in dry and water-based lubricated conditions using three different counterpart materials, tungsten carbide (WC), silicon nitride ( $\text{Si}_3\text{N}_4$ ) and aluminum oxide ( $\text{Al}_2\text{O}_3$ ). Furthermore, the mechanical properties of these materials were determined by means of a diametrical compression test (Brazilian test). The ultimate strength can be measured directly while the elastic properties were obtained by coupling displacement field measurements by the Digital Image Correlation technique (DIC) and a classical Levenberg-Marquardt algorithm. Then, the mechanisms of fatigue crack initiation and

propagation are studied by analyzing the fracture surfaces using the scanning electron microscope. By increasing the graphene content in the GCMC, a significant decrease in friction was observed whether in dry or water-based lubricated conditions, more particularly against WC and  $\text{Al}_2\text{O}_3$  counterparts. On the other hand, wear does not only decrease with the variation of the graphene content in the ceramic matrix, but it is also strictly dependent on the lubrication conditions.

Results show that graphene reinforcement significantly improves the tribological performance even under severe contact pressure. On the other hand, it has an influence on the mechanical properties, which has to be taken into consideration for the industrial application. By investigating the tribological performance and mechanical properties of the new FLG-nanocomposites should make it possible to clarify the relationship between properties and structure and to optimize the deposition process.

**Keywords:** Graphene reinforcement, nanocomposites, friction, wear, tribochemistry, Brazilian disc test, fracture.

## References:

1. P. Miranzo et al., From bulk to cellular structures: A review on ceramic/graphene filler composites, *J. Eur. Ceram. Soc.* 37. 10.1016/j.jeurceramsoc.2017.03.016.
2. J. Balko et al., Wear damage of  $\text{Si}_3\text{N}_4$ -graphene nanocomposites at room and elevated temperatures, *J. Eur. Ceram. Soc.* 10.1016/j.jeurceramsoc.2014.02.025.
3. A. Weibel et al., Fast and easy preparation of few-layered-graphene/magnesia powders for strong, hard and electrically conducting composites, *Carbon* 136 (2018) 270-279. doi: 10.1016/j.carbon.2018.04.085 <https://oatao.univ-toulouse.fr/20140>.

# Multi-Probe Evaluation of the Mechanical Response of Monolayer Graphene [1]

Javier Varillas<sup>1,2</sup>, Jaroslav Lukeš<sup>3</sup>, Anastasios Manikas<sup>4</sup>, Jan Maňák<sup>5</sup>, Jíří Dluhoš<sup>6</sup>,  
Zuzana Melníková<sup>1</sup>, Costas Galiotis, Otakar Frank<sup>1</sup>, and Martin Kalbáč<sup>1</sup>

<sup>1</sup> J. Heyrovský Institute of Physical Chemistry, Czech Academy of Sciences, Prague, Czech Republic

<sup>2</sup> Institute of Thermomechanics, Czech Academy of Sciences, Prague, Czech Republic

<sup>3</sup> Bruker Nano Surfaces and Metrology, Prague, Czech Republic

<sup>4</sup> Department of Chemical Engineering, University of Patras, Patras, Greece

<sup>5</sup> TESCAN Group, a.s., Brno, Czech Republic

<sup>6</sup> Institute of Physics, Czech Academy of Sciences, Prague, Czech Republic

## Abstract:

We employ push-to-pull (PTP) mechanical testing to probe the uniaxial tensile response of freestanding monolayer graphene. The experimental analysis includes different analytical roads to estimate the elastic modulus of end-clamped graphene samples, combining in-situ Raman spectroscopy and scanning electronic microscope (SEM) measurements. We find that spatially resolved Raman measurements of the strain values through 2D-mode shift evaluations provide a sensible reading of the local and average strains in our PTP-loaded graphene samples. This is justified by our proof-of-concept method, which uses the Raman-derived strains to assess the elastic modulus of monolayer graphene. Our outcomes agree with previous experimental and theoretical elastic modulus values (approximately 1 TPa [2, 3]). To support our experimental results, we run large-scale molecular dynamics (MD) simulations that perform uniaxial tensile loading to (pristine and defective) freestanding graphene sheets under varying clamping conditions. Our MD results indicate that the mechanical properties extracted from the uniaxial stress-strain responses of the sheets highly depend on both the type and the spatial profile of the clamping between the graphene and the pulling agent. Also, when the uniaxial pulling of end-clamped graphene is performed by a substrate that adheres to the graphene sheet through van der Waals forces (as in the case of PTP testing), the measured values of the elastic modulus can be underestimated up to approximately 30%. Overall, our study highlights the limitations of conventional analyses of PTP experiments (using indentation readouts and in-situ SEM imaging) and proposes new potential avenues (involving Raman measurements) for future research on the elastic properties of 2D materials.

**Keywords:** graphene, Raman spectroscopy, scanning electron microscopy, push-to-pull, molecular dynamics, elastic properties, defects.

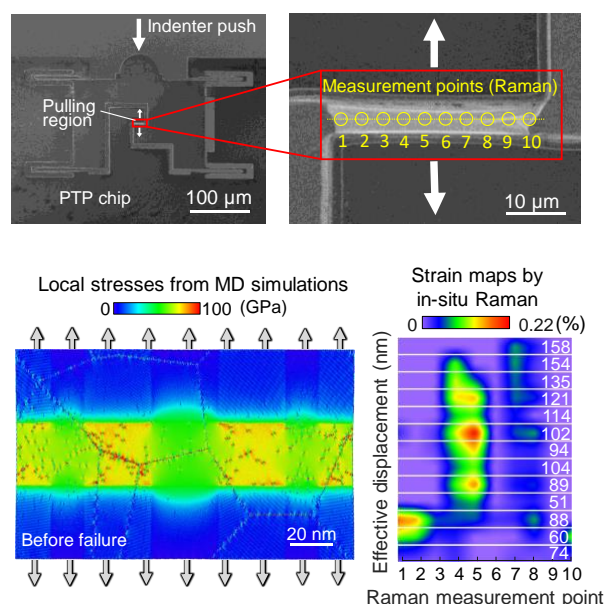


**Figure 1:** Top: PTP test device and Raman measurement points across the monolayer graphene sample. Bottom: Spatially resolved stresses (left, MD) and strains (right, Raman) during uniaxial loading of end-clamped monolayer graphene.

## References:

1. Varillas et al., *Mechanical response of monolayer graphene via a multi-probe approach*, Int. J. Mech. Sci., 273, (2024). doi: 10.1016/j.ijmecsci.2024.109208
2. Lee et al., *Measurement of the elastic properties and intrinsic strength of monolayer graphene*. Science, 18 (2008). doi: 10.1126/science.1157996.
3. Cao et al., *Elastic straining of free-standing monolayer graphene*. Nat. Commun. 11, 284 (2020). doi: 10.1038/s41467-019-14130-0

# Laser-induced graphene on biocompatible polymers

T. Vićentić<sup>1</sup>, M. V. Pergal<sup>1</sup>, M. Rašljić Rafajilović<sup>1</sup>, A. Gavran<sup>1</sup>, S. D. Ilić, and M. Spasenović<sup>1</sup>

<sup>1</sup>Center for Microelectronic Technologies, Institute of Chemistry, Technology and Metallurgy, University of Belgrade, Belgrade, Serbia

## Abstract:

Laser-induced graphene (LIG) possesses desirable properties for numerous applications, including wearable sensors, because it is electrically conductive, flexible, ecologically acceptable, and comparatively easier to manufacture than graphene obtained by other techniques<sup>1</sup>. LIG has been successfully produced on various precursor materials<sup>2</sup>. However, it is essential to produce LIG on substrates that are biocompatible to enhance the incorporation of LIG-based technologies into nanobiotechnology. We demonstrate the production of LIG on different types of cross-linked biocompatible polymer precursors, such as sodium alginate<sup>3</sup>, poly(dimethylsiloxane)/Triton (PDMS/Triton) and poly(dimethylsiloxane)/poly(ethylene glycol) (PDMS/PEG) materials. The produced LIG is systematically investigated, providing a comprehensive understanding of the physicochemical characteristics of the material on the different substrates. Raman spectroscopy, Fourier-transform infrared spectroscopy, scanning electron microscopy with energy-dispersive X-ray analysis, X-ray diffraction, and transmission electron microscopy confirm the successful generation of graphene. To optimize the manufacturing process of high-quality LIG, we also examined the influence of the operating parameters of the laser on the quality of the graphene. We found that there is an optimum laser power and dwell time for each polymer substrate. These findings could play a guiding role in LIG formation on other biocompatible substrates. Moreover, we investigated the potential applications of LIG as a sensing component in wearable sensors for physiological parameter monitoring.

**Keywords:** laser-induced graphene, nanotechnology, graphene synthesis, biocompatible materials, graphene

characterization, wearable sensors, alginate, PDMS

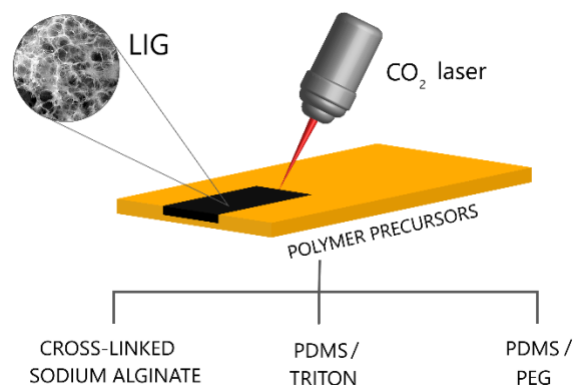


**Figure 1:** Illustration of the production process of LIG on biocompatible polymers.

## References:

1. Lin, J. *et al.* Laser-induced porous graphene films from commercial polymers. *Nature Communications* 2014 5:1 5, 1–8 (2014).
2. Ye, R., James, D. K. & Tour, J. M. Laser-Induced Graphene: From Discovery to Translation. *Advanced Materials* 31, 1803621 (2019).
3. Vićentić, T. *et al.* Laser-induced graphene on cross-linked sodium alginate. *Nanotechnology* (2023) doi:10.1088/1361-6528/AD143A.

## Acknowledgment:

This research was supported by the Science Fund of the Republic of Serbia, #4950, Polymer/graphene heterostructures for physiological sensors – Polygraph

# Development of new substrates for super-resolution studies of supported Lipic Bilayers (slb) by graphene induced energy transfer

Mgr. Hüseyin Evci

J. Heyrovsky Institute of Physical Chemistry, U Slovanky 1388/5, Czech Republic

## Abstract

Fluorescence microscopy is a widely used technique in biological research. Intrinsically it suffers from low spatial resolution on the order of hundreds of nanometers in lateral plane and several microns in the axial direction. A recent rapid development of novel techniques achieved nano-metric resolution in lateral dimension.<sup>1</sup> In contrast, there still exists a high demand for robust techniques shrinking the axial resolution to the desired nanometer scale. One of the most promising approaches is Graphene Induced Energy Transfer (GIET) developed by Prof. Enderlein group.<sup>2</sup> In brief, fluorescence is quenched in a distance-dependent manner by the atomically thin graphene sheet. As the range of the energy transfer occurs up to ~ 30 nm, for instance lipid bilayers with the thickness of 5 nm can be resolved with the GIET technique in detail. Here, I attempt to fabricate the graphene-based supports for the formation of lipid bilayers, which would enable to study glycosylation, vesicle formation, or receptor desensitization by GIET. Specifically, the graphene supports are cushioned with Pyrene-PEG polymer, where pyrene interacts with the graphene and PEG helps to minimize the effect of the graphene on the bilayer behavior. The experiments were focused on the formation of the supported lipid bilayers (SLB) containing negatively charged lipids on these newly prepared substrates and the lateral mobility in SLBs were characterized.

## References:

1. Huang B, Bates M, Zhuang X. *Annu Rev Biochem.* **2009**, 78, 993-1016.
2. Ghosh, A. et al. *Nat. Photonics* **2019**, 13, 860–865.

**EGF 2024 / SMS 2024 Session II. A:  
Graphene properties and  
applications  
Functional / Multifunctional, Hybrid,  
Composites and Responsive  
Materials**

# Thermal properties of Xenes measured by optothermal Raman spectroscopy.

E. Bonaventura,<sup>1,2</sup> D. S. Dhungana,<sup>2</sup> C. Massetti,<sup>2</sup> J. Pedrini,<sup>1</sup> C. Grazianetti,<sup>2</sup> C. Martella,<sup>2</sup> F. Pezzoli,<sup>1</sup> A. Molle,<sup>2</sup> E. Bonera<sup>1,\*</sup>

<sup>1</sup>Department of Material Science, Università degli Studi di Milano-Bicocca, Milan, Italy

<sup>2</sup>CNR-IMM Unit of Agrate Brianza, Agrate Brianza, Italy

## Abstract:

After the outcomes on graphene, Xenes like phosphorene, silicene, and stanene layers, as well as their epitaxial heterostructures, introduced novel advancements in two-dimensional (2D) materials science and nanotechnology.[1] With all these materials being promising for application to electronics and optoelectronics, an issue remains as to how heat diffusion is managed when they are subjected to thermal dissipation of heat. The problem is also related to the dissipation from Xenes towards the substrate or to metal contacts.

Here, using an optothermal method based on Raman spectroscopy as non-destructive probe, we explore the effective thermal conductivity of phosphorene and silicene on different substrates.[2-3] The so-proposed approach discloses a viable route for the assessment of the thermal properties of silicene and other supported 2D materials. The management of power dissipation at the nanoscale could eventually be exploited in fields like thermoelectrics. We believe that our work provides a new perspective on an unresolved nanoscale issue such as the thermal response of classes of 2D materials, enabling significant advances in the field of the heat management. [MUR-Prin Photo]

**Keywords:** 2D materials, Raman spectroscopy, silicene, thermal properties, thermoelectrics, xenes

## References:

1. D. S. Dhungana, C. Grazianetti, C. Martella, S. Achilli, G. Fratesi, and A. Molle, *Adv. Funct. Mat.* 31 (30), 2102797, 2021
2. E. Bonera and A. Molle, *Nanomaterials* 2022, 12, 1410.
3. E. Bonaventura, D. S. Dhungana, C. Martella, C. Grazianetti, S. Macis, S. Lupi, E. Bonera, and A. Molle, *Nanoscale Horiz.*, 2022, 7, 924.



# Interfacial Ferroelectricity in van der Waals semiconductors and their heterostructures

Vladimir Fal'ko

National Graphene Institute, University of Manchester

## Abstract

Over the recent years, several studies have established ferroelectric properties of rhombohedral transition-metal dichalcogenides (TMD), both grown as bulk crystals and assembled into twisted bilayers and multilayers [1-5]. For bilayers assembled from monolayer TMD crystals with parallel orientation of unit cells, lattice reconstruction (characteristic for small-angle twisted bilayers [6,7]) results in the out-of-plane polarised ferroelectric domains and networks of domain walls, switchable by mutual sliding of the monolayers promoted by an out-of-plane electric field [3] and manifested in the hysteretic field-effect transistor [4] and tunneling FET operations [8], and readable optically by the linear Stark shift of the interlayer excitons [9].

In bulk 3R-TMD crystals, groups of layers with the same stacking order appear as three-dimensional twins separated by planes of twin boundaries. Here, we propose [10] the formation of two-dimensional (2D) electron/hole gases at twin boundaries, analyse their stable density in photo-doped structures, which appears to be in the range of  $n^* \sim 8 \times 10^{12} \text{ cm}^{-2}$  for electrons at both intrinsic mirror twin boundaries in bulk crystals and twisted twin boundaries in structures assembled from two thin mono-domain films. We also predict the values of 'magic' twist angles between the assembled twins, for which the commensurability between the accumulated carrier density,  $n^*$ , and moiré pattern would promote the formation of a strongly correlated state of electrons, such as Wigner crystal.

## References

1. F. Ferreira, et al, Scientific Reports 11, 13422 (2021)
2. F. Ferreira, et al, Phys Rev B 106, 125408 (2022)
3. V. Enaldiev, et al, Nano Letters 22, 1534 (2022)
4. A. Weston, et al, Nature Nanotechnology 17, 390 (2022)
5. L. Molino et al, Advanced Materials 35, 2370273 (2023)
6. V. Enaldiev, et al, Phys Rev Lett 124, 206101 (2020)
7. A. Weston, et al, Nature Nanotechnology 15, 592 (2020)
8. Y. Gao, et al, Nature Communications 15, 4449 (2024)
9. J. Sung, et al, Nature Nanotechnology 15, 750 (2020)
10. J. McHugh, et al, Nature Communications 15, 6838 (2024)

# Low resistance laser-reduced graphene oxide: electrical and mechanical characterization for flexible electronic applications

M. G. Bonando<sup>1</sup>, N. M. M. Fernandes<sup>1</sup>, S. S. Piva<sup>1</sup>, R. J. E. Andrade<sup>1</sup>, C. C. C. Silva<sup>1</sup>, L. A. M. Saito<sup>1\*</sup>

<sup>1</sup>MackGraphe - Institute for Research in Graphene and Nanotechnologies  
Mackenzie Presbyterian University, São Paulo - SP, Brazil

## Abstract:

There is growing innovation in electronics and sensors and an increasing need for methods that are easy to produce, contribute to point-of-care monitoring, are flexible, miniaturized, and can replace the rigid silicon electronics found in current devices [1]. This is due to the implementation of new emerging materials, including graphene. Graphene stands out due to its electrical, chemical, and optical properties [2], but its handling, large-scale production, and transfer process are still a current challenge. Graphene oxide has been gaining increasing prominence to overcome these challenges due to its reduction methods. Among the various methods of reduction of graphene oxide (GO), laser-induced reduction (LrGO) emerges as an efficient and controlled technique, which allows local modification of the electronic and structural properties of the material without the need for chemical agents. This process offers significant advantages, such as the possibility of micrometer-scale patterning and selective reduction of GO, which can be exploited to fabricate flexible electronic circuits [3].

We report through an optimized study of the photothermal reduction of GO [4], the analysis and characterization of the electrical and mechanical properties of the rGO with the lowest reported electrical resistance at ambient conditions of  $32 \pm 3 \text{ } \Omega/\text{sq}$  on nylon filtration membrane before and after a fatigue test of 1000 cycles. Figure 1 shows the bending process with the sample with different radii, varying between 0.05 and 5 mm. There was no significant change in the electrical resistance of the rGO samples.

We will present the topographic characterization (roughness, thickness, homogeneity) through images obtained through scanning electron microscope, confocal microscopy, and Raman spectroscopy. Also, the study of Raman spectroscopy on different layers of rGO allows us to observe the degree of reduction through the thin films.

The mechanical properties were analyzed by studying the rGO thin film under compression, bending, tension, twisting, and a fatigue test of

1000 cycles. This study contributes to developing flexible and stable electronics using graphene oxide reduced in an ambient condition on green chemistry for the reduction process.

**Keywords:** graphene, graphene oxide, graphene oxide reduction, laser reduction, photothermal reduction, laser-scribing, flexible electronics

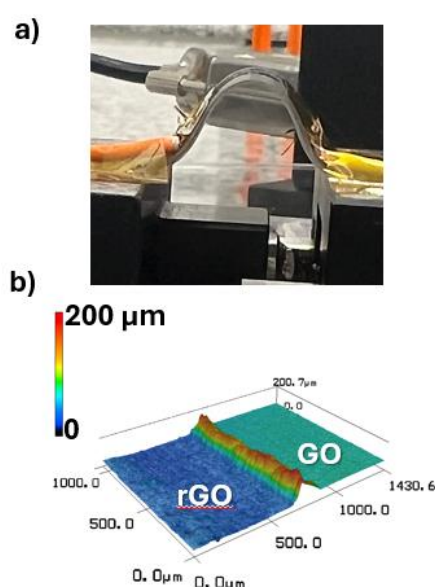


**Figure 1:** - a) Setup of a controlled bending of reduced graphene oxide. b) Surface characterization of GO and rGO interface.

## References:

1. MCMANUS, Daryl et al. Water-based and biocompatible 2D crystal inks for all-inkjet-printed heterostructures. *Nature nanotechnology*, v. 12, n. 4, p. 343-350, 2017.
2. NOVOSELOV, Kostya S. et al. Electric field effect in atomically thin carbon films. *science*, v. 306, n. 5696, p. 666-669, 2004.
3. LI, Guijun. Direct laser writing of graphene electrodes. *Journal of applied physics*, v. 127, n. 1, 2020.
4. BONANDO, Matheus Guitti et al. The impact of different flexible substrates on the photothermal reduction quality of graphene oxide. *Nanoscale Advances*, 2024.

# On the origin of cyclic instability of SMA actuators

P. Šittner<sup>1\*</sup>, O. Tyc<sup>1</sup>, E. Iaparova<sup>1</sup>, O. Molnarová<sup>1</sup>, L. Heller<sup>1</sup>

<sup>1</sup> Institute of Physics of the Czech Academy of Sciences, Prague, Czech Republic

## Abstract:

The functional stress-strain-temperature of NiTi shape memory alloy (SMA) actuators due to B2 cubic to B19' monoclinic martensitic transformation (MT) should be ideally phase and strain reversible in closed loop thermomechanical load cycles, provided that the austenite and martensite phases do not deform plastically. In reality, whenever the MT takes place under external stress (Fig. 1a,b), incremental plastic strains are generated. These plastic strains, along with consequently generated internal stresses and permanent lattice defects, accumulate over cyclic thermomechanical loading and cause functional fatigue which prevents many promising engineering applications of NiTi SMAs from realization.

To shed light on the mechanism by which these plastic strains are generated, we have performed special closed-loop thermomechanical loading tests to evaluate recoverable and plastic strains generated separately by the forward and reverse MTs under wide range of external stress.

The experiments revealed that both forward and reverse MTs, if they occur above certain stress thresholds, generate well-defined characteristic incremental plastic strains. Specifically, the forward MT upon cooling under stresses up to 500 MPa does not produce plastic strain or lattice defects, whereas the reverse MT upon heating generates plastic strains even under stress as low as 100 MPa. The plastic deformation generated by MT under low stresses takes place by [100](001) dislocation slip and while under high stresses it occurs via kinking deformation in stress induced martensite.

The characteristic thresholds and magnitudes of plastic strains generated separately by the forward and reverse MTs (Fig. 1c) define the functional fatigue limits for NiTi. Specifically, the cyclic stress-strain-temperature responses remain stable if both forward and reverse MTs occur below the characteristic thresholds. Conversely, they become unstable and exhibit predictable ratcheting if the one or both MTs exceed these thresholds. Given that the reverse MT generates larger plastic strains in thermal cycles under external stress than the forward MT, it is proposed to be largely responsible for functional fatigue of NiTi actuators.

**Keywords:** actuation, shape memory alloy, NiTi, martensitic transformation

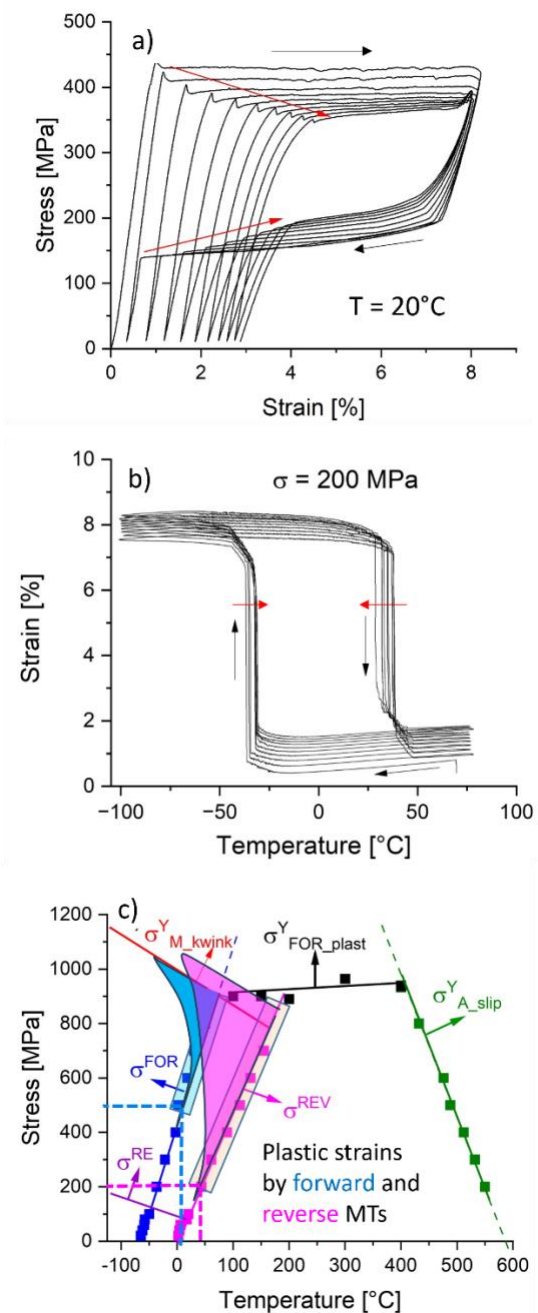


**Figure 1:** Instability of cyclic superelastic (a) and actuation (b) response of NiTi wire originates from accumulation of characteristic incremental plastic strains generated by forward and reverse MTs taking place under external stress. The temperature, stress thresholds for generation of plastic strains are marked by dashed lines and the characteristic magnitudes of plastic strains are plotted in stress-temperature diagram of the used NiTi wire (c).

# Hybridization of Materials and Processes by means of Additive Manufacturing Technologies

T. Moritz \*, U. Scheithauer, A. Günther, L. Gottlieb, E. Schwarzer-Fischer, J. Abel  
Processes/Components, Fraunhofer Institute for Ceramic Technologies and Systems, Dresden,  
Germany

## Abstract:

Property combinations in advanced ceramic components like electrical conductivity and insulation, porosity and density or simply black and white color offer a variety of attractive applications in almost all branches, especially under harsh conditions. Moreover, hybridization of shaping processes, i.e. the combination of either conventional shaping methods with Additive Manufacturing (AM) or the combination of different AM methods provides highly efficient production methods for individualized or personalized components. At IKTS especially AM methods like Fused Filament Fabrication, Vat Photopolymerization, and Multi Material Jetting [1] are used for both, material and process hybridization. Together with ceramic injection molding or extrusion, innovative process solutions are gone for combining zirconia or cermets with stainless steel, black and white zirconia, electrical conductive and insulating silicon nitride or differently colored sintered glasses to attain geometrically complex, multifunctional parts.

The contribution will show several approaches to combine materials via powder technological routes and subsequent co-sintering. The most important prerequisites for the production of durable material composites are highlighted. The Multi Material Jetting will be introduced as an opportunity to build up functionally graded components dropwise. Furthermore, a technique implementing a metallic non-woven as anchoring structure between a ceramic part and a lower melting metallic phase will be explained.

As practical examples a full ceramic ignitor, a spike engine [2], a plasma electrode, a watch bezel, and afterglowing sintered glass components will be introduced.

**Keywords:** Ceramic Additive Manufacturing, Multi Material Jetting, Hybridization, Co-Sintering

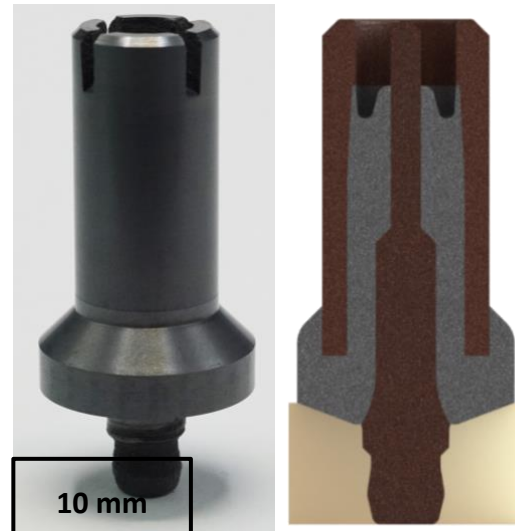


**Figure 1:** Left: Full ceramic ignitor consisting of  $\text{Si}_3\text{N}_4/\text{MoSi}_2$  compositions for attaining an electrically conductive/insulating phase made by Multi Material Jetting. Right: schematic cross-section of the additively built component consisting of the two ceramic compositions plus a sacrificial supporting material at the bottom.

## References:

1. Weingarten, S. et al.: Additive manufacturing of ceramic-based multi-material components using CerAM MMJ. *Keramische Zeitschrift* Vol. 73, 6, 38 – 43, 2021, doi: 10.1007/s42410-021-0523-y
2. U. Scheithauer et al.: Additive manufacturing of ceramic single and multi-material components—A groundbreaking innovation for space applications too? *Acta Astronautica* Vol. 221, 155 – 162, 2024, doi: 10.1016/j.actaastro.2024.05.003



# Manufacturing and Thermal Simulation of Graphene Doped Carbon Fiber Reinforced Composites for Through Thickness Heat Transfer

J. M. J. Gugliuzza <sup>1\*</sup>, S. Carosella <sup>1</sup>, P. Middendorf <sup>1</sup>

<sup>1</sup>Institute of Aircraft Design, University of Stuttgart, Stuttgart, Germany

## Abstract:

Modern electrified aircraft generate a lot of heat through electric motors and fuel cells. Whereby lightweight manufacturing with carbon fiber reinforced polymers (CFRPs) poses the challenge of effective heat management, as polymers are typically thermal insulators. Studies have shown that the thermal conductivity of polymers can be increased by doping them with graphene platelets [1]. Manufacturing techniques of CFRPs with these nanocomposites are to be investigated in this research. Two different nanocomposites will be produced and tested with pitch- and PAN-based carbon fibers and different fiber architectures. The resulting doped CFRPs will be analyzed for their specific heat capacity and thermal diffusivity using laser flash analysis (LFA) to determine the heat conductivity. There are a variety of different graphene raw materials with different geometrical and thermal properties, that are also affected by the surface interface between the graphene and the polymer or the fiber molecules [2], two different raw materials will be characterized in a previous step. Subsequently, the macroscopic effects on the doped CFRP characterized by the LFA will be measured and a thermal microscale simulation (Figure 1) will be fine-tuned to match the experimental results. Therefore, the microscopic structure of the produced CFRPs will also be analyzed using microscopy. This research aims to establish a working mesoscale material model for thermal simulations of doped CFRPs on a larger scale.

**Keywords:** graphene-doped polymer, carbon fiber reinforced nanocomposite, laser flash analysis, heat transfer simulation.

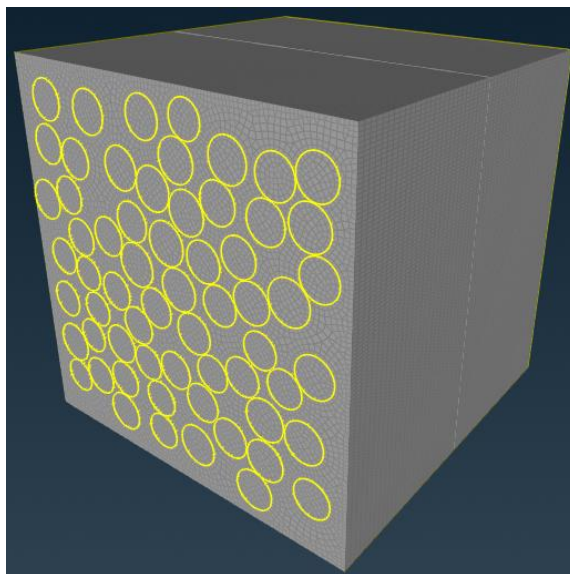


**Figure 1:** Figure showing the microscopic finite element model for a numeric thermal simulation of a graphene-doped CFRP.

## References:

1. A. C. Ackermann *u. a.*, „Mechanical, thermal, and electrical properties of amine- and non-functionalized reduced graphene oxide/epoxy carbon fiber-reinforced polymers“, *Polymer Composites*, Bd. 44, Nr. 8, S. 4937–4954, Aug. 2023, doi: 10.1002/pc.27461.
2. E. Pop, V. Varshney, und A. K. Roy, „Thermal properties of graphene: Fundamentals and applications“, *MRS Bull.*, Bd. 37, Nr. 12, S. 1273–1281, Dez. 2012, doi: 10.1557/mrs.2012.203.

# Moiré Engineering in Twisted WTe<sub>2</sub> Structures

Sharieh Jamalzadeh Kheirabadi<sup>1\*</sup>, Farzan Gity<sup>1</sup>, Paul K. Hurley<sup>1,2</sup>, and Lida Ansari<sup>1</sup>

<sup>1</sup> MicroNano systems, Tyndall National Institute, University College Cork, Cork, T12 R5CP, Ireland

<sup>2</sup> School of Chemistry, University College Cork, Cork, Ireland

## Abstract

Twisted graphene-based structures with specific rotation angle ( $\theta$ ), have emerged as promising structures with insightful superconducting and magnetism properties in experimental and theoretical observations [1, 2]. Small twist angles generate giant moiré patterns with the moiré periodicity scaling inversely with  $\theta$ , and a reduced mini-Brillouin zone [3]. Moreover, the ferroelectricity properties in the moiré heterostructures such as bilayer graphene/hexagonal boron nitride is a promising approach for neuromorphic device potential applications [4].

Beyond graphene, some experimental studies have reported twisted structures of transition metal dichalcogenides (TMDs) nanosheets, with primarily focus on group-VI homo- or hetero-bilayers of MoS<sub>2</sub>/MoSe<sub>2</sub> or WS<sub>2</sub>/WSe<sub>2</sub> [5]. A series of two-dimensional (2D) twisted bilayer TMDs with commensurate angles and are investigated theoretically as well [6]. The results of TMD-based twisted structures exhibit the appearance of flat bands and even ultra-flat bands by decreasing twist angle (or increasing the system size or number of atoms in the relevant supercells) which provide suitable candidates for studying the correlation effects at large twist angles [6].

In this research, we have investigated twisted bilayer WTe<sub>2</sub> and their resulting angle-dependent magnetic properties using first principles calculations. The results show that twisting one layer with different angles significantly impacts the electronic and magnetic engineering of such twisted structures. Moreover, they reveal the unique potential of twisted structures with van der Waals interactions, paving the way for investigating novel physical phenomena in 2D materials through symmetry control.

**Keywords:** Twistronics, Moiré engineering, 2D materials, TMDs, van der Waals interaction, first principles calculations, density functional theory.

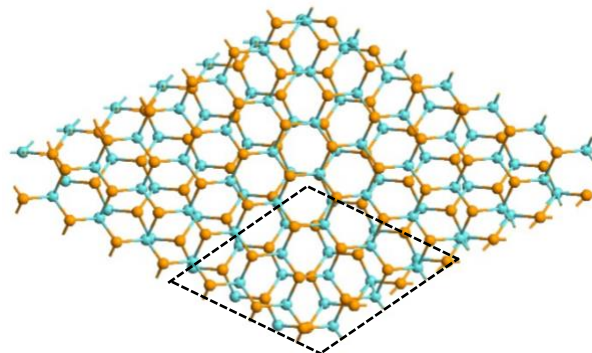


**Figure 1:** Atomic structure of WTe<sub>2</sub> with twist angle  $\theta = 9.43^\circ$ . The cyan and orange circles indicate Tungsten and Tellurium, respectively.

## Acknowledgement

Support from the Science Foundation Ireland through AMBER Research Centre (SFI-12/RC/2278\_P2) and the SFI/HEA Irish Centre for High-End Computing (ICHEC) are acknowledged.

## References

1. Cao, Y., et al. (2018), Unconventional superconductivity in magic-angle graphene superlattices, *Nature (London)*, 556, 43.
2. He, M., et al. (2021) Competing correlated states and abundant orbital magnetism in twisted monolayer-bilayer graphene, *Nature Communications*, 12, 4727.
3. Lopes dos Santos, J. M. B., Peres, N. M. R., and Castro Neto, A. H. (2007) Graphene bilayer with a twist: Electronic structure, *Phys. Rev. Lett.*, 99, 256802.
4. Zheng, Z. et al. (2020) Unconventional ferroelectricity in moiré heterostructures, *Nature*, 588, 71–76.
5. Wang, L. et al. (2020) Correlated electronic phases in twisted bilayer transition metal dichalcogenides, *Nat. Mater.*, 19 861–6.
6. Qiaoling, Xu., Yuzheng, G., Lede, X. (2022) Moire flat bands in twisted 2D hexagonal vdW materials, *2D Mater.*, 9 014005.



**SMS / Sensors 2024 Session II. B:  
New Materials for sensors and  
actuators: Sensing the Future with  
New Materials**

# Conducting research on the use of curcuminoid-based surfaces as sensors

N. Aliaga-Alcalde<sup>1,2,\*</sup>, Raquel Gimeno-Muñoz<sup>2</sup>, Raúl Díaz-Torres<sup>2</sup>, Olivier Roubeau<sup>3</sup>, José Manuel Díaz-Cruz<sup>4</sup>, Rossella Zaffino<sup>2</sup>, Daniel Herrera<sup>2</sup>, Arántzazu González-Campo<sup>2</sup>

<sup>1</sup>ICREA (Institució Catalana de Recerca i Estudis Avançats), Passeig Lluís Companys 23, 08010 Barcelona, Spain

<sup>2</sup>Institut de Ciència de Materials de Barcelona (ICMAB-CSIC), 08193 Barcelona, Spain

<sup>3</sup>Instituto de Ciencia de Materiales de Aragón (ICMA), CSIC and Universidad de Zaragoza, Plaza San Francisco s/n, 50009 Zaragoza, Spain

<sup>4</sup>Departament de Química Inorgànica and Institut de Recerca de Química Teòrica i Computacional, Universitat de Barcelona, Diagonal 645, 08028 Barcelona, Spain

## Abstract:

Curcuminoids (CCMoids) are linear and conjugated molecules with a high incidence in biomedical topics.[1] These systems are dyes with a dierylheptanoid skeleton coordinated to aromatic units that can be synthesized by simple steps and include a number of different functions, making them ideal as molecular platforms.[2] Among others, such multifunctionality can include changes in colour by coordination, as well as in their luminescent properties. In solution, some CCMoids, particularly curcumin, have been used as colorimetric and optical sensors.

Our FunNanoSurf group designs CCMoid systems that can be immobilized on various substrates (e.g., inorganics, functionalized surfaces, NPs, FETs, etc.) in a covalent and/or supramolecular manner for the creation of hybrid materials (CCMoid+substrate) and their application in molecular electronics and/or as sensors.[3]

This work describes our efforts in the creation of functionalized surfaces based on sensitive CCMoids after exposure to metal salts. Our results show that such surfaces can also be used as BF<sub>3</sub> sensors both in solution (organic or aqueous) and in the gaseous state.[4] The talk aims to expose the synthetic potential in the creation of new CCMoid systems, as well as possible future applications.

**Keywords:** curcuminoids, curcumin derivatives, molecular platforms, luminescence, coordination chemistry, micro-contact printing, immobilization, functionalized surfaces, sensor.

## References:

1. Aliaga-Alcalde, N., Marqués-Gallego, P., Kraaijkamp, M., Herranz-Lancho, C., den Dulk, H., Görner, H., Roubeau, O., Teat, S., J. Weyhermüller, T., Reedijk J. (2010), Copper curcuminoids containing anthracene

groups: fluorescent molecules with cytotoxic activity. *Inorg. Chem.*, 49, 9655.

2. Riba-Lopez, D., Zaffino, R., Herrera, D., Matheu, R., Silvestri, F., Ferreira da Silva, J., Sanudo, E. C., Mas-Torrent, M., Barrena, E., Pfattner, R., Ruiz, E., Gonzalez-Campo, A. Aliaga-Alcalde, N. (2022) Dielectric behavior of curcuminoid polymorphs on different substrates by direct soft vacuum deposition. *iScience*, 25(12),105686(1-29).
3. Cardona-Lamarca, T., Y. Baum, T., Zaffino, R., Herrera, D., Pfattner, R., Gómez-Coca, S., Ruiz, E., González-Campo, A., Aliaga-Alcalde, N. (2024) Experimental and theoretical studies of the electronic transport of an extended curcuminoid in graphene nano-junctions. *Chem. Sci.*, DOI: 10.1039/d4sc04969a.
4. Gimeno-Muñoz, R., Díaz-Torres, R., Gómez-Coca, S., Roubeau, O., Díaz-Cruz, J. M., Aliaga-Alcarea, N., González-Campo A. (2024) Curcuminoid-based responsive surfaces for fluorescent BF<sub>3</sub> detection, a fast and reversible approach. *Sensors and Actuators B: Chemical*, manuscript sent.

# Engineering Porosity for Tuning Electromechanical Properties in Piezoelectric Systems

K. S. Challagulla<sup>1</sup>, T. A. Venkatesh<sup>2</sup>

<sup>1</sup>Department of Mechanical Engineering, Laurentian University,  
Sudbury, Ontario, P3E 2C6, Canada

<sup>2</sup>Department of Materials Science and Chemical Engineering, Stony Brook University,  
Stony Brook, New York 11794, USA

## Abstract:

Porous piezoelectric materials with their unique electromechanical properties are desirable in certain practical applications such as hydrophones. However, a comprehensive understanding of the effect of foam shape, porosity aspect ratio, porosity volume fraction and simultaneously piezoelectric material properties in a range of piezoelectric material systems such as barium sodium niobate (BNN), barium titanate ( $\text{BaTiO}_3$ ) and relaxor ferroelectric (RL) materials, especially, in the ultra-low-density domain, on the overall electromechanical response of 3-3 type piezoelectric foam structures is not yet available. Hence, in this study, three-dimensional finite element models are developed to accurately predict the electromechanical response of 3-3 type piezoelectric foam structures made of several classes of piezoelectric materials such as barium sodium niobate (BNN), barium titanate ( $\text{BaTiO}_3$ ) and relaxor (PMN-PT based) ferroelectrics (RL). Nine different types of foam structures are identified based on microstructural features and their electromechanical response is characterized as a function of foam shape, porosity aspect ratio, porosity volume fraction and simultaneously material properties (Figure 1). Based on the three-dimensional finite element simulations, the following principal conclusions are obtained: (i) Microstructural features and material properties found to have significant effect on various elastic, dielectric and piezoelectric constants of the foam structures and their corresponding figures of merit; (ii) For ultra-low density foams (at about 97% porosity volume fraction) for equiaxed ( $L_1=L_2=L_3$ ) foam structure (Class II) with cuboidal porosity shape (i.e.  $b=a$ ), relaxor ferroelectrics foams exhibit highest piezoelectric coupling constant ( $K_r \sim 0.954$ ), barium sodium niobate foams exhibits lowest piezoelectric constant ( $K_r \sim 0.240$ ) and barium titanate foams showed intermediate behaviour with  $K_r \sim 0.442$ ; (iii) All piezoelectric materials showed enhanced piezoelectric figures of merit by modifying the shape of the porosity. For example, at 30% porosity volume fraction, hydrostatic strain coefficients ( $d_h$ ), hydrostatic voltage coefficient ( $g_h$ ),

the hydrostatic figure of merit ( $d_h g_h$ ) are, respectively, increased by 21%, 360%, 457% for barium sodium niobate foams, 75%, 548%, 1037% for barium titanate foams and 12%, 221% and 259% for relaxor ferroelectrics foams by changing shape of the porosity for equiaxed foam ( $L_1=L_2=L_3$ ) structure (Class II) from a cuboidal shape (with  $b=a$ ) to a flat-cuboidal (with  $b=0.25a$ ).

**Keywords:** Barium Sodium Niobate (BNN), Barium Titanate ( $\text{BaTiO}_3$ ), Relaxor Ferroelectrics (RL), Piezoelectric properties, Foams, Porous structures.

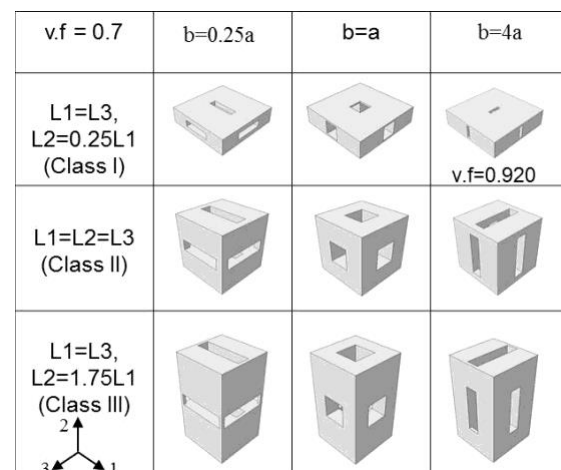


**Figure 1:** Schematic illustrating nine piezoelectric foam structures based on structural aspect ratio and porosity aspect ratio for three different classes (Class I, Class II and Class III).

## References:

1. C.R. Bowen and H. Kara, "Pore Anisotropy in 3-3 Piezoelectric Composites," *Mater. Chem. Phys.*, **75**, 45-9 (2002).
2. K.S. Challagulla and T.A. Venkatesh, "Electromechanical Response of Piezoelectric Foams," *Acta Mater.*, **60**, 2111-27 (2012).

# Combined optical and conductivity properties of ZnO for gas sensor devices

Zhigang Shao<sup>1</sup>, Kane Jacob<sup>1</sup>, Martin Jakooobi,<sup>1</sup> Vincent Collière,<sup>1</sup> Laure Vendier,<sup>1</sup> Yannick Coppel,<sup>1</sup> Katia Fajerberg,<sup>1</sup> Jean-Daniel Marty,<sup>2</sup> Andrey Ryzhikov,<sup>3</sup> Christophe Mingotaud,<sup>2</sup> Myrtil L. Kahn<sup>1</sup>

<sup>1</sup>Laboratoire de Chimie de Coordination, CNRS UPR 8241, University of Toulouse, 205 route de Narbonne, 31077 Toulouse, France. e-mail: myrtil.kahn@lcc-toulouse.fr.

<sup>2</sup>Laboratoire SOFTMAT, CNRS UMR 5623, Université de Toulouse, Université Paul Sabatier, 118 route de Narbonne 31062 Toulouse

<sup>3</sup>Institut de Science des Matériaux de Mulhouse (IS2M), UMR CNRS 7361, Université de Haute Alsace (UHA), ENSCMu, 3 rue Alfred Werner, 68093 Mulhouse

## Abstract:

Zinc oxide (ZnO) exhibits a high exciton binding energy (60 meV) and a wide band gap (3.37 eV), rendering it an excellent candidate for use in optical and electronic devices.<sup>[1]</sup> In this regard, a ZnO hybrid fibre with a core-shell structure was obtained by taking advantage of a gel made of dicyclohexyl zinc organometallic precursor, Zn(Cy)<sub>2</sub>, and dodecylamine (DDA) at room temperature.<sup>[2]</sup> This shaping allows the majority of ZnO to be distributed within the core, while the organics derived from the DDA ligand are primarily located in the shell of the prepared fibre. The diameter of the fibre can be modified by the use of extrusion needles of varying diameter. Characterization by X-ray diffraction (XRD), transmission and scanning electron microscopy (TEM&SEM), gas sorption (BET) evidenced that the diameter of the fibre has an impact on the ZnO nanoparticles prior to and following annealing of the fibres, which has a strong impact on the the gas sensor response when such ZnO is used as sensitive layer of gas sensor devices. Gas sensors were fabricated by depositing ZnO on substrates with electrodes using a spin coating apparatus from ground fibres with pristine diameters of 0.5, 1.0, and 1.5 mm. The simultaneous optical and electrical performance of the sensors was evaluated by exposing them to acetone at various temperatures. A real-time variation of resistance and optical RGB (red, green and blue) intensity of the sensor exposed to different concentrations of acetone (from 5 to 20 standard cm<sup>3</sup>/min, sccm) is shown in Figure 1. While the electronic sensitivity is greater, it is more susceptible to saturation and exhibits a slower recovery rate compared to optical measurements. Smaller ZnO nanoparticles exhibited enhanced optical sensitivity. Notably, upon exposure to acetone, the sensing layer displayed a reversible change in colour, transitioning from yellowish to dark. Overall, the synthesis of ZnO nanoparticles with precise control over size resulted in the production of

materials with distinct optical and electronic properties of interest for gas-sensing applications. Our approach is now to make the mechanistic correlation between these two properties in order to achieve operational devices.

**Keywords:** gel, fiber, ZnO NPs, optical, electronic, surface reaction, gas sensor.

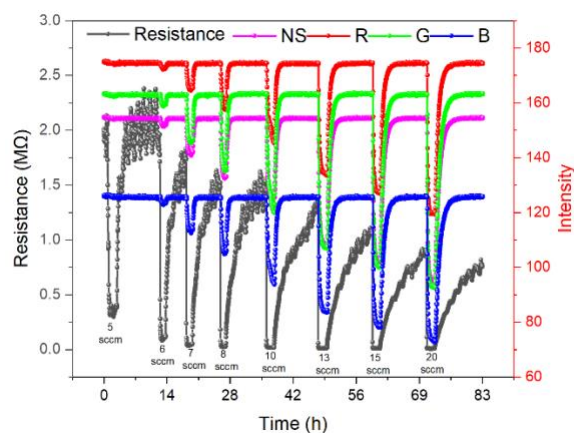


**Figure 1.** Example of a real-time optical (RGB) and electronic response to acetone for concentration from 5 to 20 sccm at 350 °C.

## References:

1. Shen, Yang, Zhihao Yuan, Zhen Cui, Deming Ma, Kunqi Yang, Yanbo Dong, Fangping Wang, Ai Du, and Enling Li. "Electronic, Magnetic, and Optical Properties of Metal Adsorbed G-Zno Systems." *Frontiers in Chemistry* 10 (2022): 943902.
2. Wang, Yiping, Yannick Coppel, Juliette Fitremann, Stéphane Massou, Christophe Mingotaud, and Myrtil L Kahn. "Gelation Mechanism Revealed in Organometallic Gels: Prevalence of Van Der Waals Interactions on Oligomerization by Coordination Chemistry." *Chemphyschem* 24, no. 14 (2023): e202300077.

# Toward Highly Sensitive Biosensing Systems Based on Perovskite Fluorescent Labels

W. Teixeira <sup>1\*</sup>, C. Collantes <sup>1</sup>, P. Martínez <sup>1</sup>, J. Carrascosa <sup>1</sup>, V. González-Pedro <sup>1,2</sup>, M-J. Bañuls <sup>1,2</sup>, A. Maquieira <sup>1,2</sup>

<sup>1</sup> Instituto Interuniversitario de Investigación de Reconocimiento Molecular y Desarrollo Tecnológico (IDM), Universitat Politècnica de València (UPV), València, Spain

<sup>2</sup> Departamento de Química, Universitat Politècnica de València, València, Spain

## Abstract:

Metal halide perovskite nanocrystals (MHP NCs) exhibit narrow emission bands, broad absorption spectrum, high photoluminescence quantum yields, multiphoton absorption cross-sections, and an easily tunable emission spectrum. Given their appealing optical properties, this material would be an excellent candidate for fluorescent labels in biosensing approaches, as long as their high instability against humidity and poor colloidal stability, which limits its application in biological environments<sup>1</sup>, were addressed.

In this communication, we present three strategies (A, B, and C) for obtaining water-stable perovskite-based labels, and their application as fluorescent reporters in biosensing. Strategy A is based on the intercalation of MHP NCs inside mesoporous silica nanoparticles<sup>2</sup>, assisted by high-pressure packed columns, and followed by a heat treatment, which confers high stability in aqueous media and preserves their optical and morphological features. In strategy B, core-shell perovskite-silica structures are synthesised utilising water-induced phase transformation combined with sol-gel methods, and stabilised through thermal annealing<sup>3</sup>. Finally, strategy C is devoted to obtaining water-stable polymer nanobeads incrustated with NCs, employing coprecipitation methodologies<sup>4</sup>. The green- to red-emitting particles obtained following these strategies were characterised, and the stabilised composites were successfully probed as fluorescent agents for staining cell cultures and fluorescent labels for detecting specific biorecognition events through their conjugation to biomolecules (Figure 1). For immunoassay biosensing approaches, carried out in fluorescent-linked immunosorbent assay (FLISA) and lateral-flow immunoassay (LFIA) platforms, limits of detection as low as 70 and 60 picomolar were achieved for LDH protein and HlgG antibody, respectively. These results point toward the development of highly sensitive biosensing systems based on perovskite fluorescent labels.

**Keywords:** metal halide perovskite nanocrystals, fluorescent labels, immunoassays, bioimaging.

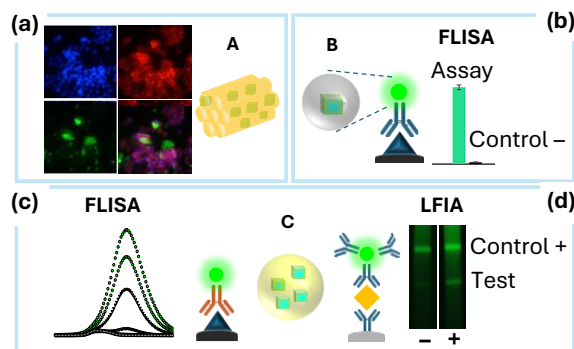


**Figure 1:** Water-stable fluorescent labels A, B, and C applied to (a) cell staining, (b,c) FLISA, and (d) LFIA immunoassays.

## References:

1. Collantes, C., Teixeira, W. *et al.* (2023) Designing stable lead halide perovskite nanocrystals: From a single particle to nanocomposites, *Appl. Mater. Today*, 31, 101775.
2. Collantes, C.; Teixeira, W. *et al.* (2023) Water-assisted synthesis of stable and multicolored CsPbX<sub>3</sub>@SiO<sub>2</sub> core-shell nanoparticles as fluorescent probes for biosensing. *Dalton Trans.*, 52, 18464.
3. Malgras, V. *et al.* (2016) Observation of quantum confinement in monodisperse methylammonium lead halide perovskite nanocrystals embedded in mesoporous silica, *J. Am. Chem. Soc.*, 138(42), 13874-13881.
4. Avugadda, S. *et al.* (2022) Highly emitting perovskite nanocrystals with 2-year stability in water through an automated polymer encapsulation for bioimaging, *ACS Nano*, 16, 13657-13666.

## Acknowledgements

This work was supported by the Spanish State Research Agency (“WEAROPSENS”-PID2022-14 0653OB-I00), the Spanish Ministry of Economy (FPI-2017 PhD grant), the European Union (NextGenerationEU, INVESTIGO Program), and the UPV (PAID-01-19-06 PhD grant). The Group of Science and (Bio)Analytical Technologies from the Spanish Royal Society of Chemistry supported the attendance at this congress.



# Printing technologies at the forefront of analytical tools and sensors innovation

Franc Paré<sup>1,3</sup>, Gemma Gabriel<sup>2</sup>, Mireia Baeza<sup>1,3</sup>

<sup>1</sup> Department of Chemistry, Faculty of Science, Edifici C Nord, Universitat Autònoma de Barcelona, Carrer dels Til·lers, 08193 Cerdanyola del Vallès (Bellaterra), Barcelona, Spain

<sup>2</sup> Instituto de Microelectrónica de Barcelona, IMB CNM (CSIC), 08193 Cerdanyola del Vallès (Bellaterra), Barcelona, Spain

<sup>3</sup> GENOCOV Research Group, Universitat Autònoma de Barcelona, 08193 Cerdanyola del Vallès (Bellaterra), Barcelona, Spain

## Abstract:

Printing technologies, which have been on the rise for years, allow for a whole new range of possibilities in the fabrication of analytical devices. On the one hand, 3D-printing has seen two main paths of innovation. Being able to employ a wide range of polymeric materials, with solvent-resistant, electric conductor, elastic or transparent properties, they can be turned into newly designed analytical platforms which can integrate all stages of the analytical procedure: from sample pre-treatment to analyte detection. Firstly with microfluidic platforms, which have become the staple for dynamic analytical tools. These have the advantages of low sample consumption, compactness, low-cost, better process control, waste reduction, and overall monitoring [1]. The second path is the fabrication of miniaturized electrodes. They are not only low-cost, but thanks to 3D-printing's accessibility to tools for device design, prototyping and fabrication, it is possible to perform easy modifications to electrodes. This grants it the capacity of great adaptability by merely changing their geometry, adapting into. On the other hand, inkjet printing technology focuses mainly on electronic instruments fabrication. It has the capacity to produce low-cost, highly reproducible, scaled down electrodes in a short time due to the lack of need of masks. This allows for easier optimization and testing of electroanalytical sensors. With the ability of working with combinations of metallic, polymeric, and carbonaceous materials it can tackle a broad range of problems and applications [2]. Its great versatility has led to the production of both potentiometric and amperometric sensors.

**Keywords:** 3D-printing, inkjet-printing, pH sensor, device-miniaturization, microfluidic platform.

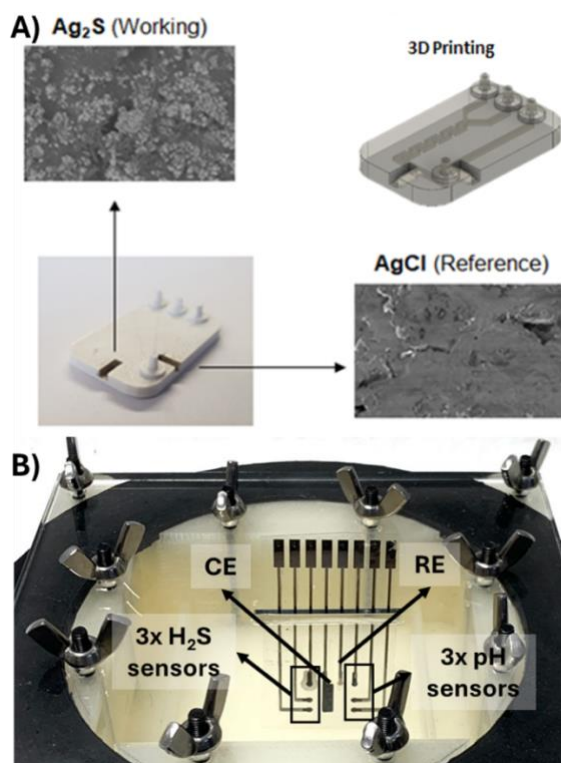


**Figure 1:** Sensing devices fabricated using different printing technologies: A) a 3D-printed microfluidic platform with screen-printed electrodes and B) an array of H<sub>2</sub>S and pH sensors by means of inkjet printing implemented into one face of a miniaturized bioscrubber.

## References:

1. Pol, R.; Céspedes, F.; Gabriel, D.; Baeza, M. Fully Integrated Screen-Printed Sulfide-Selective Sensor on a 3D-Printed Potentiometric Microfluidic Platform. *Sensors Actuators, B Chem.* **2019**, *290*, 364–370, doi:10.1016/j.snb.2019.03.132.
2. Paré, F.; Castro, R.; Gabriel, D.; Guimerà, X.; Gabriel, G.; Baeza, M. Feasible H<sub>2</sub>S Sensing in Water with a Printed Amperometric Microsensor. *ACS ES&T Water* **2023**, *3*, 1116–1125, doi:10.1021/acsestwater.2c00589.

# Wearable Textile-based Chemiresistive pH Sensors with MXene-Chitosan Composite

P. Kumar<sup>1,\*</sup>, G. M. Stojanović<sup>1</sup>, M. Gupta<sup>2</sup>, H. F. Hawari<sup>3</sup>

<sup>1</sup> Faculty of Technical Sciences, University of Novi Sad, Trg Dositeja Obradovića 6, 21000 Novi Sad, Serbia

<sup>2</sup> Naturality R&D, Calle Sant Leopold 101, Terrassa, Barcelona, Spain

<sup>3</sup> Department of Electrical and Electronic Engineering, Universiti Teknologi PETRONAS, 32610 Seri Iskandar, Perak, Malaysia

## Abstract:

pH monitoring is very essential for analyzing human health. Any deviations from standard pH range can cause some medical conditions such as metabolic disorders and wound healing complications. Thus its monitoring is very crucial. Recently, some wearable electrochemical and colorimetric sensors utilizing different nanomaterials have been reported for monitoring the pH noninvasively [1-2]. However, they are limited by complex fabrication processes. In this work, we proposed textile-based chemiresistive pH sensors and examined MXene-chitosan (MX-CS) as a sensing material.  $Ti_3C_2T_x$  MXene and chitosan solutions were initially synthesized. Afterward, MXene and MX-CS sensors (Figure 1a) were fabricated by depositing these sensing materials onto interdigitated textile electrodes (IDEs), followed by drying them at 40 °C in open air. Before that, IDE electrodes were prepared by cutting the thin conductive fabric using a cutter plotter machine and transferring them onto the adhesive tape. Morphological study revealed the presence of MXene-chitosan material covering the textile. The average electrical resistance (dry condition) of MXene and MX-CS were measured to be 1.17 M $\Omega$  and 0.765 M $\Omega$ , respectively. The chemiresistive response of textile sensors with MX-CS was investigated in buffers with a pH range of 4–8 (Figure 1b). The sensor's response was found to be linear with a coefficient of correlation  $R^2 \sim 0.934$  whereas, MXene-based sensor showed  $R^2 \sim 0.732$ . The sensitivity of MXene-chitosan-based sensor was found to be 210.5  $\Omega$ /pH, revealing a higher value than that of MXene only (136.8  $\Omega$ /pH). Such wearable and biocompatible pH sensors are highly suitable for continuous monitoring of pH variations in the body.

**Keywords:** pH sensing, MXene, chitosan, wearable, textile sensors, chemiresistive, biosensors, health-care, biomedical applications.

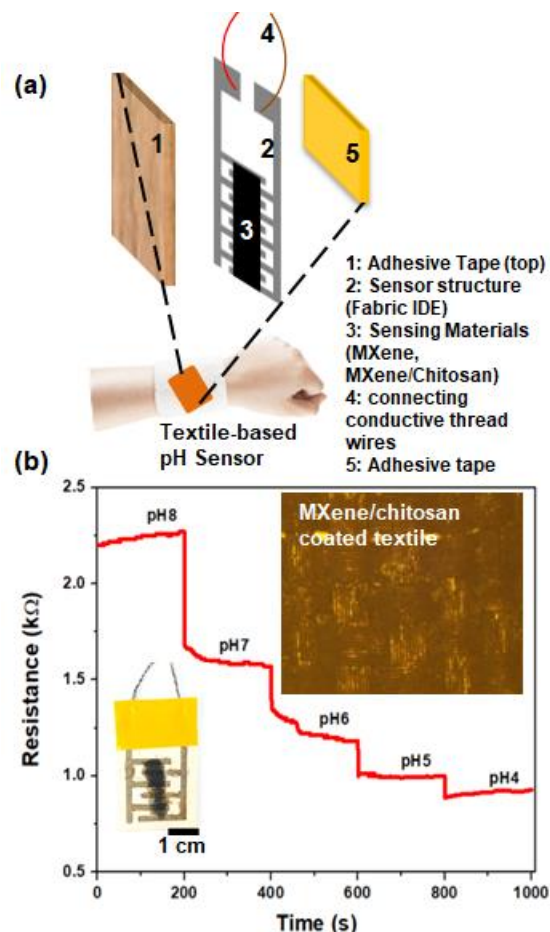


**Figure 1:** (a) Illustration of components of textile-based pH sensor with MX-CS sensing layer. (b) Sensing response of MX-CS-based pH sensor. The insets show the photograph of the sensing device (left) and the optical microscopic image of MX-CS coated fabric (right).

## References:

1. Manjakkal, L., et al. (2019), Textile-Based potentiometric electrochemical pH Sensor for Wearable Applications, *Biosensors*, 9, 14.
2. Huang, Y., et al. (2023) A wearable colorimetric sweat pH sensor-based smart textile for health state diagnosis, *Mater. Horiz.*, 10, 4163-4171.

# Smart Patch for Continuous Monitoring and Stretchable Electronics in Enhancing Patient Outcomes

A. Ben-Aissa<sup>1\*</sup>, M. Moreno<sup>1</sup>, B. Molina<sup>1</sup>, M. Alique<sup>1</sup>, A. Moya<sup>1</sup>

<sup>1</sup>Eurecat, Centre Tecnològic de Catalunya, Functional Printing and Embedded Devices Unit, Mataró, Spain

## Abstract:

The management of critically ill patients within Intensive Care Units (ICUs) represents a great challenge to global healthcare and requires a paradigm shift towards vigilant and continuous monitoring to optimize clinical decision-making and improve outcomes[1]. Due to the dynamic nature of patients' conditions in these settings, the limitations of intermittent monitoring systems are highlighted. The potential consequences of inadequate monitoring, including delayed recognition of deteriorating conditions and suboptimal utilization of healthcare resources emphasize the need for real-time, comprehensive data to guide timely interventions and prevent adverse events.

The integration of advanced sensors, wearable devices, and data analytics empower healthcare professionals with the ability to continuously track vital signs, physiological parameters, and other critical metrics. This constant stream of data facilitates early detection of subtle changes in a patient's condition, enabling proactive interventions and personalized care plans tailored to individual needs.

The development of these recent wearable devices has been influenced by printed electronics (PE), known for its ability to create flexible devices on diverse stretchable substrates using innovative printable materials [2]. These wearables can be made on materials like thermoplastic polyurethanes (TPU), enabling integration into textiles and facilitating human-skin interaction [3].

Herein, in this study, we harness the potential of PE for medical applications, specifically displaying a fully integrated non-invasive wearable designed for the early detection of sepsis in ICU patients. Our approach includes electrochemical biosensors for the continuous monitoring of IL-6, glucose and lactate concentrations in sweat, which provide real-time data on the patient's energy metabolism reflecting cellular dysfunction and its monitorization might prevent or revert the fatal metabolic dysregulation in septic patients.

This research underscores the transformative potential of stretchable electronics and innovative materials, offering a flexible biosensor platform that transcends traditional medical applications allowing personalized interventions for optimal management.



**Figure 1:** Printed sensor integrated on the smart patch to measure the concentrations of glucose and lactate

## References:

1. Bailly, S., Meyfroidt, G., Timsit, J. F. (2020). What's new in ICU in 2020: Critical care for today and tomorrow. *Intensive Care Medicine*, 46(10), 1882-1890
2. M. J. Nunes, et al., "Screen-Printed Electrodes Testing for Detection of Potential Stress Biomarkers in Sweat", *Electrocatalysis*, vol. 13, 2022, doi: 10.1007/s12678-022-00709-7
3. M. Alique, et al., "Multiplex Sensing Electronic Skin Based on Seamless Fully Printed Stretchable Piezoelectric Devices", *Adv. Sensor Res.*, vol. 2, doi: 10.1002/adsr.202200016

**SMS / NanoMed / Sensors 2024**  
**Joint Session II. C:**  
**Biosensors and sensors for medical**  
**applications**



# MOF-based sensors with enhanced electroconductivity: application for vascular endothelial growth factor (VEGF) detection

R. Antiochia\*<sup>1</sup>, M.C. di Gregorio<sup>2</sup>, V. Gigli<sup>3</sup>, T. Gentili<sup>2</sup>, C. Tortolini<sup>3</sup>, A.M. Isidori<sup>3</sup>, M. Nuti<sup>3</sup>

<sup>1</sup>Department of Chemistry and Drug Technologies, Sapienza University of Rome, Italy

<sup>2</sup>Department of Chemistry, Sapienza University of Rome, Italy

<sup>3</sup>Department of Experimental Medicine, Sapienza University of Rome, Italy

## Abstract:

Metal-organic frameworks (MOFs) are a newly developing important class of multifunction crystalline porous materials that consist of connecting metal ions and organic linkers. MOFs exhibit high porosity, high surface areas, and tunable physical and chemical properties, demonstrating promise in a large-number of applications, such as gas storage, drug delivery, catalysis and sensing. However, their poor electro-conductivity may affect their extensive use in electrochemical (bio)sensing. Therefore, various strategies have been employed in order to overcome this limitation, when they are used as electrode surface modifiers for electrochemical platforms development. In our work, we used as starting material MIL-100(Fe), a cheap, highly stable and bio-compatible MOF composed by trimesic acid and Fe<sup>3+</sup>.

In order to tune the electroconductivity of the MOF-based electrochemical platform, the following aspects have been investigated:

- 1) use of screen-printed electrodes (SPEs) modified with different nanomaterials, such as MWCNTs and graphene;
- 2) MOF synthesis reaction time (2-48h);
- 3) effect of AuNPs on MOF crystallization.

The electrochemical platforms were characterized by spectroscopy, microscopy and electrochemical techniques (Powder X-ray diffraction, Raman spectroscopy, Scanning Electron Microscopy, Transmission Electron Microscopy, Energy-dispersive X-ray, Cyclic Voltammetry and Electrochemical Impedance Spectroscopy).

The platform which showed the best electrochemical performances was used for the development of a novel MOF-based voltammetric immunosensor for a sensitive and rapid detection of the vascular endothelial growth factor (VEGF) in human serum at the point of care (POC).

A high level of VEGF can be regarded as a predictor of different cancers, such as brain, lung, breast, lymphoma, and gastrointestinal tumors. Therefore, VEGF has been recently emerged as a promising biomarker of tumor cells.

Therefore, MOF-based electrochemical biosensors with enhanced electroconductivity could provide a unique alternative for a non-invasive and *in-situ* detection of VEGF with high sensitivity and selectivity.

**Keywords:** MOF-based sensors, voltammetric immunosensor, VEGF detection, POC device, biomedical applications.

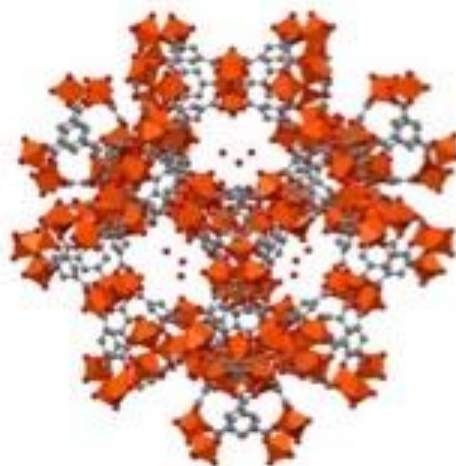


**Figure 1:** Figure illustrating the structure of MIL(100)-Fe.

## References:

1. Qian K, Deng Q, Fang G, Wang J, Pan M, Wang S, et al. Metal-organic frameworks supported surface-imprinted nanoparticles for the sensitive detection of metolcarb. *Biosens Bioelectron.* 2016;79: 359–63. <https://doi.org/10.1016/j.bios.2015.12.071>.
2. Kreno LE, Leong K, Farha OK, Allendorf M, Van Duyne RP, Hupp JT. Metal-organic framework materials as chemical sensors. *Chem Rev.* 2012;112(2):1105–25. <https://doi.org/10.1021/cr200324t>
3. Horcajada P, Surblé S, Serre C, Hong D-Y, Seo Y-K, Chang J-S, et al. Synthesis and catalytic properties of MIL-100(Fe), an iron(III) carboxylate with large pores. *Chem Comm* 2007, 2820–2822.



# Non-invasive, minimalistic, and self-operated glucose sensor for point-of-care testing in saliva

E. Guerrero San Vicente, D. Martin Prats, X. Palmer, R. Grinyte, J. M. Cabot  
LEITAT Technological Centre, Barcelona, Spain

## Abstract:

Glucose sensors available in the market require painful and invasive extraction (i.e. blood or interstitial fluid). Consequently, there is a need to explore non-invasive diagnostic methods for frequent monitoring of glucose levels in the body without causing discomfort to the patient. Saliva is the perfect biofluid for non-invasive measurements, however, it presents very low biomarkers concentrations and lots of interferents. Present studies clearly depict a correlation between fasting plasma glucose and fasting saliva glucose of diabetics.<sup>1</sup> Glucose range in saliva goes from 0.12mM in a healthy person and starts from 0.48mM in a prediabetic person.<sup>2</sup> This brings several challenges to non-invasive, saliva-based glucometers. In this work, we developed a miniaturized, wireless, and low power printed organic electronic device with high sensitivity, that is able to quantify low glucose levels in saliva samples.

The glucometer incorporates the saliva sampling kit, the biofunctionalized screen-printed electrodes, the operative printed circuit board (PCB) and the smartphone app to collect and process the data. This saliva glucometer has the following characteristics:

- Saliva sampling kits allows non-invasive and comfortable saliva sample intake.
- Electrodes were screen printed into Kapton substrate with carbon ink for the working and counter electrodes and silver ink for the reference electrode.
- Biofunctionalization of the working electrode was done by the drop casting of enzymes: glucose oxidase and horseradish oxidase, and an electro active compound: ferrocyanide. The obtained analytical signal is the current intensity due to the electrochemical reduction of the enzymatically generated ferricyanide in the present of glucose.
- The PCB development: circuitry and NFC antenna were printed on a PCB board and microchip with power and energy management were integrated. The current measurements are operated by the smart phone app (Chemister) developed by the same company.

Several calibrations have been done with the whole system in buffer solutions where very low detection limits were achieved (LOD: 0,00719 mM and LOQ: 0,021788 mM). Real samples were measured to ensure the validation of the fully operative glucometer.

Therefore, this system provides a highly sensitive, self-operated, and non-invasive tool for glucose detection in undiluted saliva for non-invasive, self-operated point-of-care analysis.

**Keywords:** glucometer, saliva samples, biosensors, non-invasive, wireless, point-of-care device.



**Figure 1:** Digital, wireless, minimalistic, self-operated saliva glucometer developed.

## References:

1. Agrawal RP, Sharma N, Rathore MS, Gupta VB, Jain S, et al. "Noninvasive Method for Glucose Level Estimation by Saliva. J Diabetes", Metab. Vol. 4, pp 266
2. Gupta S, Nayak MT, Sunitha JD, Dawar G, Sinha N, Rallan NS. "Correlation of salivary glucose level with blood glucose level in diabetes mellitus", J Oral Maxillofac Pathol. Vol.21 (3), pp 334-339, 2017.

# A miniaturized, wireless and implantable sensory system to screen bone healing.

E. Guerrero SanVicente <sup>1</sup>, C. Hennemann <sup>2</sup>, J. Disser <sup>2</sup>, R. Grinyte <sup>1</sup>, N. Marjanovi <sup>2</sup>, J. M. Cabot <sup>1</sup>

<sup>1</sup> Diagnostic Devices, LEITAT, Barcelona, Spain

<sup>2</sup> Electronics, CSEM, Neuchatel, Switzerland

## Abstract:

The monitoring of bone regeneration after large bone fractures is still a challenge that needs to be addressed. Therefore, in this project a novel solution was proposed in order to help and screen bone healing. This goal was accomplished by a combination of a bone scaffold and an implantable sensory system (Figure 1) entitling the following challenges:

- Sensors to monitor the most significant parameters of bone regeneration and infection presence: pH, Temperature (T), strain-gauge and biosensors for Transforming Growth Factor (TGF $\beta$ 1).
- Biocompatible and implantable, a feature that was ensured by conducting in-vitro cytotoxicity in cells and in-vivo tests in animal models.
- Flexible for implantation (Kapton as base material) at the same time as cost-effective.
- Wireless so it incorporated a battery, and the biosensors used the Differential Pulse Electrochemical technique that is label and reagent free for being inside the body.
- Continuous and real-time measurement which was done via Bluetooth and smartphone readout.

Each sensor was developed individually in the laboratory environment, and then integrated in a full system divided into a hard PCB (microcontrollers, battery, bluetooth, transceiver) and flex PCB (biosensors and sensors). The whole system was coated with Parylene-F, then moulded into a medical grade silicon and sterilized with hydrogen peroxide plasma. Furthermore, all the necessary in-vitro cytotoxicity tests were done in cell before the *in vivo* biocompatibility and performance studies in sheep models were conducted.

**Keywords:** implantable sensors, pH sensor, temperature sensor, strain gauge sensor, biosensors, smart wireless system, bone regeneration.

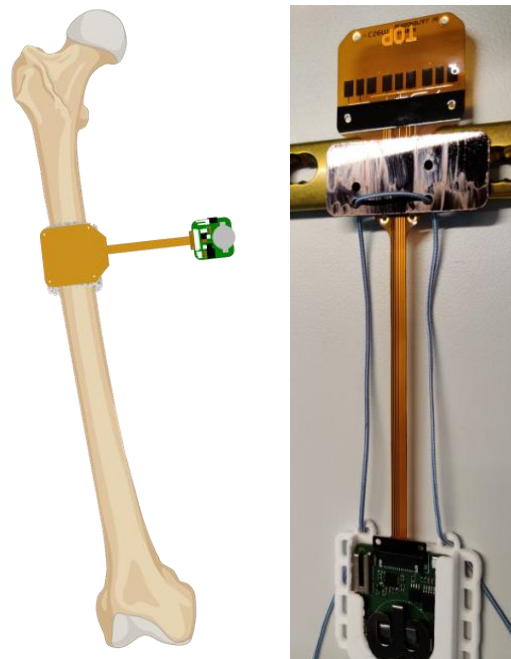


**Figure 1:** Illustration of the concept idea for wireless monitoring of bone regeneration with a scaffold in the bone defect and a sensor on top (left) and a picture of the integrated system built with pH, T, strain-gauge sensors and biosensors for its application (right).

## References:

1. K. C. McGilvray, E. Unal, K. L. Troyer, B. G. Santoni, R. H. Palmer, J. T. Easley, H. V. Demir, C. M. Puttlitz, "Implantable Microelectromechanical Sensors for Diagnostic Monitoring and Post-Surgical Prediction of Bone Fracture Healing" *Journal Of Orthopaedic Research* October, pp. 1439-1446, 2015.
2. M. Graya, J. Meehanb, C. Warda, S.P. Langdonb, I.H. Kunklerb, A. Murrayd, D. Argylea, "Implantable biosensors and their contribution to the future of precision medicine," *The Veterinary Journal*, vol. 239, pp. 21–29, 2018..

# Introducing all-inkjet-printed microneedles for in-vivo biosensing

G. Rosati<sup>1,\*</sup>, P.B. Deroco<sup>1,2,3+</sup>, M.G. Bonando<sup>1,4,5+</sup>, G.G. Dalkiranis<sup>1,6</sup>, K. Cordero-Edwards<sup>1</sup>, G. Maroli<sup>1,7</sup>, L.T Kubota<sup>2,3</sup>, O.N. Oliveira Jr.<sup>6</sup>, L.A. Miyazato Saito<sup>4,5</sup>, C.C.C. Silva<sup>4,5</sup>, A. Merkoçi<sup>1,8,\*</sup>

<sup>1</sup>Catalan Institute of Nanoscience and Nanotechnology (ICN2), CSIC and BIST, Campus UAB, Bellaterra, 08193 Barcelona, Spain

<sup>2</sup>Institute of Chemistry, University of Campinas – UNICAMP, Campinas, 13083-970, Brazil

<sup>3</sup>National Institute of Science and Technology in Bioanalytic (INCTBio), Brazil

<sup>4</sup>School of Engineering, Mackenzie Presbyterian University, Rua da Consolação, 930 Sao Paulo, 01302-907, Brazil

<sup>5</sup>MackGraphe – Mackenzie Institute for Research in Graphene and Nanotechnologies, Rua da Consolação, 930 – Sao Paulo, SP, 01302-907, Brazil

<sup>6</sup>São Carlos Institute of Physics, P.O. Box 369, 13560-970 São Carlos, SP, Brazil.

<sup>7</sup>Instituto de Investigaciones en Ingeniería Eléctrica Alfredo Desages (IIIE), Universidad Nacional del Sur, Avenida Colón 80 Bahía Blanca, Buenos Aires, CONICET, Argentina

<sup>8</sup>ICREA, Passeig Lluís Companys 23 08010 Barcelona, Spain

## Abstract:

Microneedles proved helpful for minimally invasive sampling, diagnostics and biosensing, monitoring, and drug delivery. They hold great potential not only in medicine but also in agronomy for precision farming [1,2]. They are still not pervasive because of their cumbersome and difficult-to-scale-up fabrication. In principle, mass production could be viable with inkjet printing already employed in flexible electronics and biosensing owing to its features, such as non-contact mask-less deposition of nanofunctional inks and ultrafast concept-to-prototype time. In fact, microstructures in the low-micrometer range have been produced with 3D inkjet metal nanoparticles. However, this has been possible only with very advanced equipment [3-6]. In this work, we propose a new approach for the fabrication of microneedles using 3D inkjet-printed silver nanoparticles with commercial ink and a widespread inkjet printer as a proof-of-concept of the feasibility of this approach for the scalable fabrication of devices with applications in healthcare and agronomy.

Inkjet printing of metal nanoparticles-based inks is used routinely to fabricate thin-film flexible electronics and biosensors on plastics and other substrates. Standard inkjet printing methods are based on the drop-on-demand method, so picoliter drops are jetted from the printhead onto the substrate, defined by the layout. If the substrate is absorbent (e.g., paper or mesoporous-coated plastics), the droplets spread on its surface and dries faster, thanks to the higher surface-to-volume ratio of the substrate structure. If the substrate is impermeable (e.g., normal plastics), the droplets accumulate in one or multiple drops depending on the surface energy of the substrate

and eventual priming procedures performed on it. For nanofunctional inks based on metal nanoparticles, the thickness of the deposited metal nanoparticles layer depends on the droplets' volume, the type of substrate, the nanoparticle content of the ink, and the number of printed layers. However, there is a lower limit in the x-y dimension of the printable “vertical” structures due to the formation of large drops when the jetted droplets accumulate onto the substrate. There is also a limit for the height that can be reached due to the x-y dispersion of the ink in liquid form on the substrate when multiple layers are printed. That is why these structures cannot be defined as 3D or vertical, and we call them 2.5D. A useful example comes from extrusion polymer filament 3D printing. With this widespread method, polymer filaments are taken close to their melting temperature and extruded through a nozzle over a plate following a 2D design. The polymer solidifies very rapidly out of the nozzle and the process is repeated for multiple layers with slightly different designs. Each 2D design is obtained by segmenting a 3D one into layers as thick as the extruded filament to obtain the 3D object, with each layer being printed and sticking over the previous one. If the polymer had been taken and kept to a higher temperature, it would have completely melted and spread onto the plate, and the layers would have just formed a big drop onto the same plate. This is what we call 2.5D printing on a magnified scale.

To inkjet-print a 3D metal nanoparticles object, thus having vertical dimensions comparable with the horizontal ones, we have taken the core characteristic of standard 3D printing into a research-grade inkjet printer. We have added a

thin heater element under our printing substrate to immediately cure the ink picoliter droplets once reaching the substrate, and we have programmed the inkjet printer to print multiple 2D designs and create vertical structures of different shapes (Fig. 1). As in standard 3D printing, temperature control is crucial. In general, if the temperature is too low, the droplets will remain liquid, limiting or completely hindering the structure's verticality. In contrast, the ink would dry inside the printhead nozzle at too high temperatures, clogging them definitely. Furthermore, we tried to avoid high temperatures to keep the method open for sensitive substrates such as plastic and paper.

**Keywords:** microneedles, inkjet printing, silver nanoparticles, plants, precision agriculture, EIS.

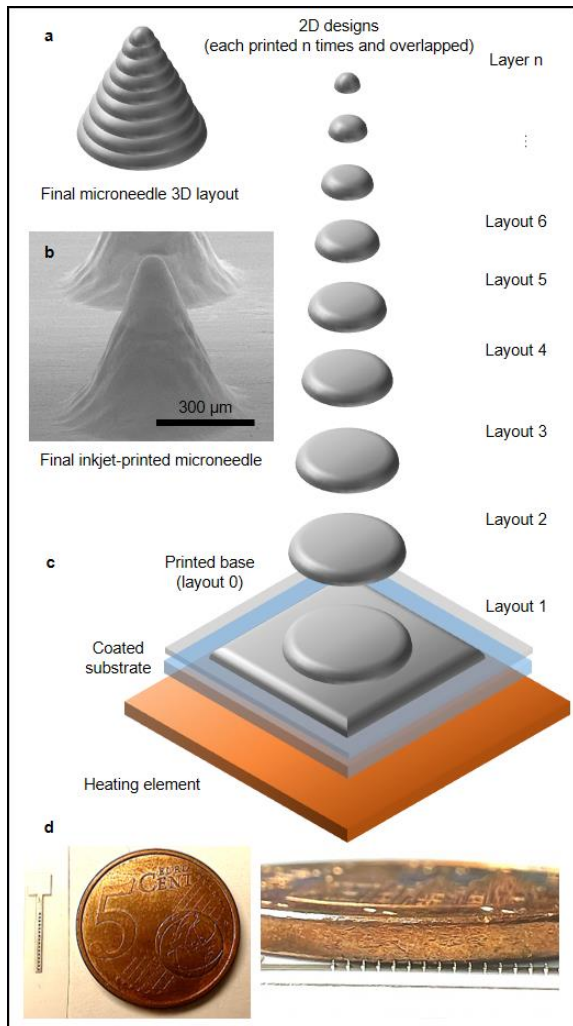


**Figure 1:** Figure illustrating the microneedles fabrication method and SEM and optical pictures showing the resulting structures.

## References:

1. A. Bukhamsin et al. (2021) Robust, Long-Term, and Exceptionally Sensitive Microneedle-Based Bioimpedance Sensor for Precision Farming. *Advanced Science*, 8, 2101261.
2. A. Merkoçi (2021) Smart nanobiosensors in agriculture. *Nature Food*, 2-12, 920 - 921.
3. J.U. Park et al. (2007) High-resolution electrohydrodynamic jet printing. *Nature Materials* 6,782-789.
4. S.H. Ko et al. (2010) Metal nanoparticle direct inkjet printing for low-temperature 3D micro metal structure fabrication. *Journal of Micromechanics and Microengineering* 20, 125010.
5. B. Wan An et al. (2015) High-Resolution Printing of 3D Structures Using an Electrohydrodynamic Inkjet with Multiple Functional Inks. *Advanced Materials* 27, 4322-4328.
6. J. Vaithilingam et al. (2018) 3-Dimensional inkjet printing of macro structures from silver nanoparticles. *Materials and Design*, 139, 81-88.

**NanoMed / Sensors 2024 joint  
Session II. D:  
Bioinspired, Biomimetic bioactive  
biomaterials Intelligent drug  
delivery and release system**



# HOW TO GET A SURFACE STRUCTURATION THROUGH A SIMPLE PROCESS OF POLYMER MANUFACTURING?

Jannick DUCHET-RUMEAU, Amélie TEISSONIERE, Guillaume ESPY, Sébastien LIVI,  
Jean-François GERARD

*Universite Claude Bernard Lyon 1, INSA Lyon, Université Jean Monnet, CNRS  
UMR 5223, Ingénierie des Matériaux Polymères F-69621 Villeurbanne Cédex, France*

## Abstract:

Superhydrophobicity has been a very rich field of research in recent years and has resulted in an impressive number of scientific publications<sup>1</sup>. These studies, both experimental and theoretical, are often guided by the observation of Nature where many examples of superhydrophobic surfaces can be found. For example, the lotus leaf and the rose petal are superhydrophobic with different adhesion properties, as well as the cuticle of some insects. From these studies, biomimetic approaches for the design of superhydrophobic surfaces that are of great interest in many applications are derived, such as for self-cleaning, oil-water separation, drag-reduction for ships, anti-corrosion, etc.

In a first part, a simple model will be argued and will give geometrical guidelines to obtain a superhydrophobic surface<sup>2</sup>. In a second part, Using guidelines established thanks to this model, simple texturing ways will be described : texturing using fillers, from immiscible polymer blends, foaming using supercritical CO<sub>2</sub>, or foaming in extrusion. Despite generating rough surfaces, none of these approaches led to superhydrophobicity. However, exposing thermoplastics to solvent at a high temperature permitted to generate rough superhydrophobic surfaces. This process has been developed and its mechanisms studied in order to have at the end an in-line polyolefin film texturing process by an exposition to low-toxicity and low-volatility solvents<sup>3</sup>.

In a last part, another strategy will be described through the design of a photocurable coating deposited by spray<sup>4</sup>. By combining increase of viscosity, fillers content and hydrophobic additives, superhydrophobic and mechanically resistant coating were generated.

**Keywords:** polymer, superhydrophobicity, roughness, texturing, wetting model, coating

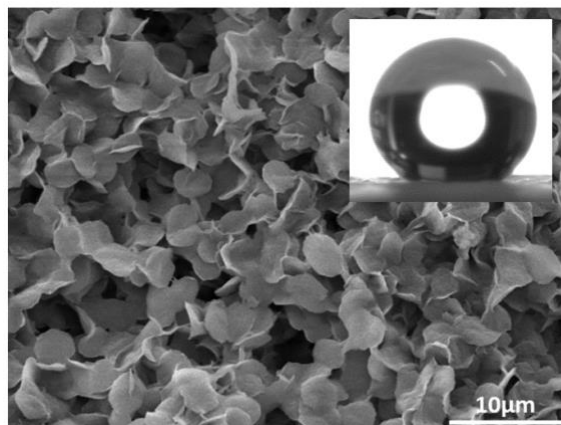


**Figure 1:** Figure illustrating the surface texturation generated from a polyolefin film after a dissolution-recrystallisation solvent assisted process.

## References:

1. Yan, Y. Y.; Gao, N.; Barthlott, W. Mimicking Natural Superhydrophobic Surfaces and Grasping the Wetting Process: A Review on Recent Progress in Preparing Superhydrophobic Surfaces. *Adv. Colloid Interface Sci.* 2011, 169 (2), 80–105. <https://doi.org/10.1016/j.cis.2011.08.005>.
2. « What if designing superhydrophobic polymer surfaces turned out to be very simple ? » Espy, G., Duchet-Rumeau, J., Livi, S., Lhost, O., Gérard, JF. *Surfaces and Interfaces* 41 (2023) 103072 <https://doi.org/10.1016/j.surfin.2023.103072>
3. G. Espy, S. Livi, J. Duchet-Rumeau, O. Lhost, JF Gérard European patent application N°EP21315240.8 (2023)
4. Fourmentin, A.; Galy, J.; Charlot, A.; Gérard, J.-F. Bioinspired Silica-Containing Polyurethane-Acrylate Films: Towards Superhydrophobicity with Tunable Water Adhesion. *Polymer* 2018, 155, 1–12. <https://doi.org/10.1016/j.polymer.2018.09.016>.

# Design of Nanomaterials for Radiation Therapy

Gerard Tobías-Rossell

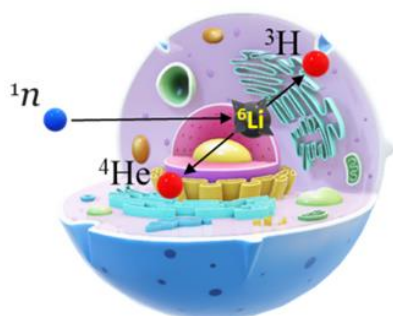
Institut de Ciència de Materials de Barcelona (ICMAB-CSIC), Bellaterra, Spain

## Abstract:

The application of nanotechnology to medicine (nanomedicine) has become one of the most promising routes for the targeted diagnosis and treatment of diseases. The small size of nanomaterials, large surface area and high reactivity impart unique physicochemical properties to these materials, in such a way that several therapeutics based on nanomaterials (liposomes, nanoparticles, polymers) have been approved for clinical use in the past few years. However, there are still several limitations that need to be overcome to obtain novel and efficient nanocarriers. Among the different types of nanomaterials, one advantage of using hollow nanomaterials, such as carbon nanotubes and carbon nanohorns is that their inner cavity can be filled with a chosen payload while the outer surface can be modified with selected moieties. For instance, following this approach we have shown that by filling radioactive isotopes it is possible to achieve ultra-sensitive imaging and the delivery of an unprecedented amount of radiodose density thus allowing their use for cancer therapy.<sup>1-3</sup> Furthermore, we have recently expanded this approach to the encapsulation of  $^6\text{Li}$  for their use as neutron capture therapy agents, for LiNCT (Fig. 2).<sup>4,5</sup>

**Keywords:** carbon nanotubes, cancer, carbon nanohorns, radiation therapy, BNCT, neutron capture therapy.

2. Wang JT-W, et al. Neutron-irradiated antibody-functionalised carbon nanocapsules for targeted cancer radiotherapy. *Carbon* 2020;162:410.
3. Gajewska A, Wang JT-W, Klippstein R, Martincic M, et al. Functionalization of filled radioactive multi-walled carbon nanocapsules by arylation reaction for in vivo delivery of radio-therapy. *J Mater Chem B*. 2022;10:47.
4. Gonçalves G, et al. Lithium halide filled carbon nanocapsules: Paving the way towards lithium neutron capture therapy (LiNCT). *Carbon* 2023;208:148.
5. Tobias et al., Lithium filled nanocapsules and use thereof. Patent WO2023180615



## LiNCT

**Figure 1:** Schematic representation of lithium neutron capture therapy (LiNCT) to kill cells.

## References:

1. Wang J.T-W, et al. Neutron Activated  $^{153}\text{Sm}$  Sealed in Carbon Nanocapsules for in Vivo Imaging and Tumor Radiotherapy. *ACS Nano*. 2020;14:129.

# Bioinspired nanovesicles as bioengineered hybrid tools against cancer cells

V. Cauda <sup>1,\*</sup>

<sup>1</sup>Department of Applied Science and Technology, Politecnico di Torino, Corso Duca degli Abruzzi 24, 10129 Turin Italy, \*e-mail valentina.cauda@polito.it

## Abstract:

Extracellular Vesicles (EVs) are nowadays of utmost interest in the nanomedicine field, being responsible for the delivery of key biomolecules and signaling moieties throughout the body with incredibly high efficiency and in vivo site-selectivity. For this reason, pristine, engineered EVs or other EV by-products are employed as nano-sized particles to build drug delivery and even theranostic tools. However, the large-scale production of EVs at standardized and suitable clinical grade levels is very expensive and time-consuming and this hinders the EV translation to clinics. Here we propose an innovative approach to design fully artificial EV-mimicking nanoparticles (EV-mimics) for theranostic scopes; in particular, we decided to mimic EVs produced by metastatic cancer cell line (in particular prostate and colon rectum), which have been demonstrated to have a strong tropism towards other tissues, like bone, liver and lung. Different lipidic compositions were conceived with increasing complexity, starting from a consolidated liposomal formulation and getting gradually closer to the natural reference composition. This was achieved through a bottom-up approach, employing commercial lipids as building blocks, to obtain artificial lipid bilayers with controllable size, which can be further decorated with key molecules such as peptides to resemble their natural counterparts in terms of cargo delivery efficacy. Furthermore, to enable these EV-mimics with full therapeutic potential, solid state nanoparticles were incorporated into the lipidic bilayer. In particular lipid-coated metal oxide nanoparticles are here proposed as effective EV-mimics for site-selective drug delivery or stimuli responsive nanotools producing selective damages to cancer cells while sparing healthy ones. Our EV-mimics are produced, experimentally characterized in vitro in both 2D and 3D models and in vivo.

The proposed approach holds great promise in research and industrial fields. Indeed, EV-mimics can become a cost-effective, very powerful off-the-shelf theranostic product, with high reproducibility of morphological and in vivo functional properties, in compliance with regulatory standards.

**Keywords:** lipid bilayers, extracellular vesicles, liposomes, lipid nanoparticles, zinc oxide, porous organosilica, theranostics, drug delivery, ultrasound-responsive nanoparticles, sonodynamics, biomedical applications.

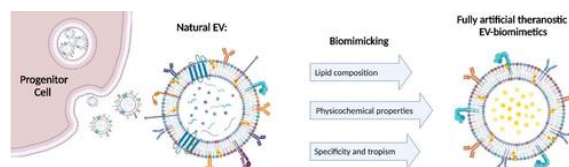


**Figure 1:** Figure illustrating the fundamental approach here proposed:

How to understand how natural Extracellular Vesicles are made and select their key biomolecular component to then rationally design EV-mimicking nanoparticles for diagnosis and therapy. Reproduced under licensing CC-BY 4.0. Copyright © 2022 The Authors. Published by American Chemical Society [1].

## Acknowledgment

This project has received funding from the European Union's Horizon 2020 research and innovation programme under grant agreement No 964386.

## References:

1. G. Rosso, V. Cauda *ACS Biomater. Sci. Eng.*, 2023, 9 (11), 5924-5932
2. M. Sancho, G. Rosso, L. DeCola, V. Cauda et al. *Nanoscale* 2023, 15, 14628-14640
3. B. Dumontel, F. Susa, T. Limongi, V. Vighetto, V. Cauda et al. *Cell&Bioscience*, 2022, Vol 12 (61), 1-18
4. N. M. Percivalle, M. Carofiglio, M. Conte, V. Cauda et al. *IJMS*, 2022, 23, 15815
5. V. Vighetto, V. Cauda, *Discover Nano* 2024, 19, 28, 1-20
6. S. Barui, N. M. Percivalle, V. Cauda et al. *Cancer Nanotechnol.*, 2022, 13(37) 1-24
7. M. Carofiglio, V. Cauda et al. *ACS Applied Nano Materials*, 2022, 5 (11), 17212
8. L. Racca, G. Rosso, V. Cauda et al. *Cancer Nanotechnol.* 2023, 14, 37
9. G. Rosso, M. Conte, G. Mesiano, V. Cauda *Cancer Nanotechnol.* 2024, Vol. 15, article n. 42, pp. 1-23

# Emerging nanotechnologies for targeting pathogenic bacterial biofilms

Vesselin N. Paunov

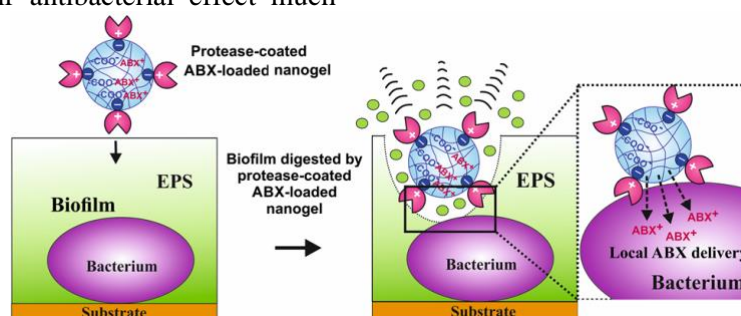
Department of Chemistry, Nazarbayev University, Astana, 010000, Kazakhstan

Research group: [paunovgroup.org](http://paunovgroup.org)

## Abstract:

Biofilms are prevalent in chronic wounds and once formed are very hard to remove, which is associated with poor outcomes and high mortality rates. Biofilms are comprised of surface-attached bacteria embedded in an extracellular polymeric substance (EPS) matrix, which confers increased antibiotic resistance and host immune evasion. Disruption of this matrix is essential to tackle the biofilm-embedded bacteria. Here, we propose several novel nanotechnologies [1,2] to do this, based on protease-functionalized nanogel carriers of antibiotics. Such active antibiotic nanocarriers, surface coated with the EPS degrading enzymes, “digest” their way through the biofilm EPS matrix, reach the buried bacteria and deliver a high dose of antibiotic directly on their cell walls, which overwhelms their defenses. We demonstrated their effectiveness against six wound biofilm-forming bacteria, *S. aureus*, *P. aeruginosa*, *S. epidermidis*, *K. pneumoniae*, *E. coli* and *E. faecalis*. We confirmed a 6-fold decrease in the biofilm mass and a substantial reduction in bacterial cell density. We showed that co-treatments of ciprofloxacin and Alcalase-coated Carbopol nanogels led to a 3-log reduction in viable biofilm-forming cells when compared to ciprofloxacin treatments alone. Encapsulating an equivalent concentration of ciprofloxacin into the Alcalase-coated nanogel particles boosted their antibacterial effect much

further, reducing the bacterial cell viability to below detectable amounts [4,5]. The Alcalase-coated nanogel particles showed very low cytotoxicity to human adult keratinocyte cells, inducing a very low apoptotic response in these cells. Overall, we demonstrated that the Alcalase-coated nanogels loaded with a cationic antibiotic elicit very strong biofilm-clearing effects against wound-associated biofilm-forming pathogenic bacteria [6]. We also demonstrate that beta-lactamase inhibitor-loaded nanocarriers in co-treatments with either free or nanocarrier-loaded beta-lactam antibiotics can enhance their effectiveness further than when used alone. Recently, we also used surface functionalized shellac/Pluronic 407-stabilized antibiotic nanocarriers [7] on *P. aeruginosa*, which is susceptible to ticarcillin but is resistant to amoxicillin. We show an amplification of the antibiotic effect of amoxicillin and ticarcillin-loaded in surface functionalized shellac nanoparticles, both alone and as a co-treatment with free or nanocarrier-loaded clavulanic acid [8]. This approach may breathe new life into a wide variety of existing antibiotics, helping to overcome antibiotic resistance. It has the potential to become a very powerful treatment of chronically infected wounds with biofilm forming bacteria.



## References

1. Weldrick, P.J., Iveson, S., Hardman, M.J., Paunov, V.N., *Nanoscale*, 2019, 11, 10472.
2. Weldrick, P.J., Hardman, M.J., Paunov, V.N., *ACS Appl. Mater. Interf.*, 2019, 11, 43902.
3. Weldrick, P.J., San, S., Paunov, V.N., *ACS Appl. Nano Mater.* 2021, 4, 1187.
4. Weldrick, P.J., Hardman, M.J., Paunov, V.N., *Mater. Chem. Front.*, 2021, 5, 961.
5. Weldrick, P.J., Wang, A., Halbus, A.F., Paunov, V.N., *Nanoscale* 2022, 14, 4018.
6. Asare, E.O., Mun, E.A., Marsili, E., Paunov, V.N., *J. Mater. Chem. B*, 2022, 14, 5129 – 5153.
7. S.S.M, Al-Obaidy, G.M. Greenway and V.N. Paunov, *Nanoscale Adv.*, 2019, 1, 858.
8. B.W. Filby, P.J. Weldrick, V.N. Paunov, *ACS Applied Bio Materials*, 2022, 1, 3826.



# Using Label-Free Single Particle Tracking to Characterise the Effect of Cell Layers on Nanoparticle Diffusion in Experimental Models

Schleyer, G.\*<sup>1</sup>, Patterson, E.A.<sup>2</sup> and Curran, J.M<sup>1</sup>

<sup>1</sup>Department of Materials, Design & Manufacturing Engineering, University of Liverpool  
Brownlow Hill, Liverpool, UK

<sup>2</sup>Department of Mechanical and Aerospace Engineering, University of Liverpool  
Brownlow Hill, Liverpool, UK

## Abstract:

Quantifying the effect of cell layers on nanoparticle behaviour can contribute to an understanding of the forces and mechanisms that govern nano-entity dynamics in biological environments, and consequently aid in the design and optimization of therapeutic nanoparticles. A highly accessible label-free microscopy technique is described that has the potential to quantify and characterise the influence of cellular activity and biological interaction on the dynamics of nanoparticles in a solution. Fluorescence microscopy techniques are one of the most widespread tools to monitor and track biological interactions at the nano scale; however, among other issues, the influence of fluorescent tags on diffusion and biological activity is still unclear. Theoretical models of diffusion cannot encompass highly variable phenomena such as cellular interaction or protein corona formation highlighting the need for the development of experimental regimes. The aim of this study is to develop a model for the diffusion of nano-entities through biological media in the presence of a cell monolayer with a view to developing a technology platform for *in-vitro* test systems to monitor living organisms interacting with cells on the micro and nano scale. Using a standard inverted optical microscope adjusted to produce near-coherent light to generate optical signatures of nanoparticles, or caustics, as described by Patterson and Whelan [1], positively- and negatively-charged gold nanoparticles as small as 50nm in diameter have been visualized and tracked above a cell layer. 100nm diameter gold nanoparticles were tracked diffusing at different heights above a human mesenchymal stem cell monolayer over time (Figure 1). The influence of nanoparticle charge and media composition on nanoparticle dynamics in biological environments was also investigated. Analysis of the values of the diffusion coefficients of the particles and the size of the convex hull enveloping their motion has shown that the local

extracellular microenvironment of nanoparticles influences their diffusion. Significant changes in nanoparticle diffusion rate have been observed one hour after exposure to a cell layer and factors such as the presence of serum proteins, nanoparticle surface charge and cellular activity could potentially influence nanoparticle dynamics.

**Keywords:** Nanoparticle, label free, microscopy, optical, diffusion, dynamics, cellular interaction, extracellular environment, experimental model

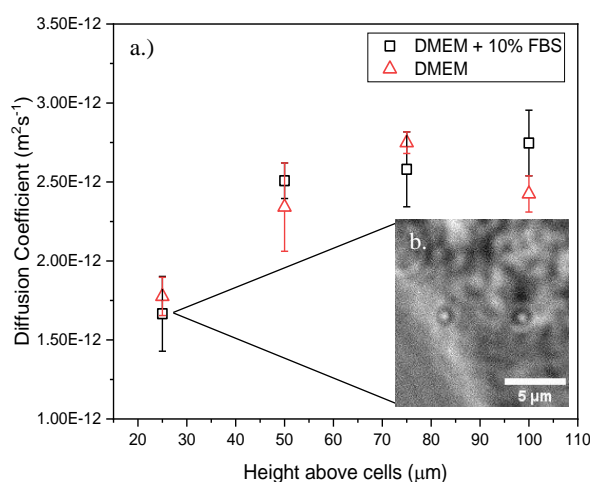


**Figure 1:** a.) Diffusion coefficient of gold citrate nanoparticles with a diameter of 100nm, measured 15 minutes after exposure to a cell monolayer, as a function of their height above the cell monolayer with error bars of  $\pm 1$  standard deviation and b.) Caustic signatures of 100nm citrate nanoparticles.

## References:

1. Patterson, E. A. & Whelan, M. P. (2008) Optical signatures of small nanoparticles in a conventional microscope. *Small* **4** **10**, 1703-1706

# Platinum nanozymes against central nervous system dysfunctions

L. Boselli<sup>1\*</sup>, G. Tarricone<sup>1,2</sup>, G. Mirra<sup>1,2</sup>, L. Cursi<sup>1</sup>, V. Castagnola<sup>3</sup>, F. Benfenati<sup>3</sup>, P.P. Pompa<sup>1</sup>

<sup>1</sup> Nanobiointeractions & Nanodiagnostics, Istituto Italiano di Tecnologia (IIT), Genova, Italy

<sup>2</sup> Department of Chemistry and Industrial Chemistry, University of Genova, Genova, Italy

<sup>3</sup> Center for Synaptic Neuroscience and Technology, Istituto Italiano di Tecnologia, Genova, Italy

## Abstract:

Abnormal levels of reactive oxygen species (ROS) are involved in several central nervous system (CNS) dysfunctions, including stroke, Alzheimer's and Parkinson's disease, and age-related macular degeneration (AMD).<sup>1</sup> The impairments coming from these disorders are devastating, and in some cases, the neurodegeneration progression eventually leads to death. Pharmacological approaches using antioxidant molecular drugs were attempted but were ineffective in stopping the disease's progression. CNS dysfunctions are associated with antioxidant enzymes depletion/dysregulation. In this context, nanozymes (enzyme-mimicking nanoparticles) have recently attracted increasing attention as potential future therapeutics.<sup>2</sup> Indeed, nanozymes can act similarly to superoxide dismutase and catalase enzymes but are associated with lower production costs, easy large-scale production, and higher stability/durability.<sup>2</sup>

Nanozyme metrology is a crucial aspect to understand the potential of these new nanodrugs. In this framework, we developed a characterization platform and analyzed the antioxidant catalytic activities of a series of different nanozymes (platinum, palladium, gold, ceria, and iron-oxide NPs).<sup>3</sup> The best-performing nanozyme was investigated *in vitro* to validate its ROS-scavenging therapeutic potential in the neurovascular unit (primary neurons, primary astrocytes, and endothelial cells). We showed how the nanozyme catalytic activities could change during their journey from the bloodstream up the cell lysosome. Biomolecular corona (a layer of proteins adsorbing onto the NPs surface in biological fluids) and pH modulate the NPs enzyme-like behavior.<sup>4</sup> We obtained on-demand platinum nanozyme-mediated ROS-scavenging, able to maintain physiological homeostasis during oxidative stress in the neurovascular unit cellular components. In addition, *in vivo* experiments confirmed the therapeutic potential of nanozymes in an AMD mouse model,

highlighting intriguing anti-inflammatory properties.<sup>5</sup>

**Keywords:** nanozymes, ROS scavenging, biomolecular corona, neurodegenerative diseases

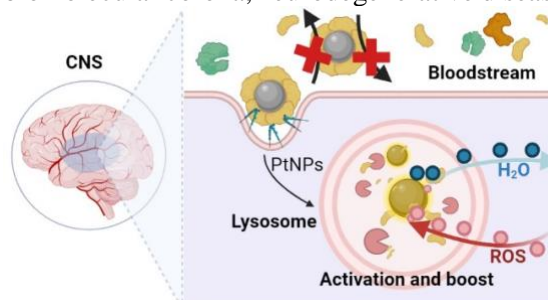


**Figure 1:** Schematics illustrating the platinum nanozyme bio-switch process: the biomolecular corona inhibits its catalytic activity in the extracellular environment while the lysosomal environment reactivates and boosts the nanozyme functionalities.

## References:

1. Salim, S. (2017), Oxidative stress and the central nervous system, JPET, 360(1), 201-205.
2. Chen, K. et al. (2021), Catalytic nanozymes for central nervous system disease, Coord. Chem. Rev., 432, 213751.
3. Cursi, L., et al. (2024) Metrology of Platinum Nanozymes: Mechanistic Insights and Analytical Issues, Adv. Funct. Mater., 2315587.
4. Tarricone, G. et al. (2023), Catalytic Bioswitch of Platinum Nanozymes: Mechanistic Insights of Reactive Oxygen Species Scavenging in the Neurovascular Unit, Nano Letters, 23(10), 4660-4668.
5. Cupini, S. et al. (2023), Platinum nanozymes counteract photoreceptor degeneration and retina inflammation in a light-damage model of age-related macular degeneration, ACS Nano, 17(22), 22800-22820.



**SMS / NanoMed / Sensors 2024  
joint Session II. E:  
Biomaterials / NanoBioMaterials /  
Bioimaging / Biosensors**

# Integrin-Targeting Peptides for the Design of Cell-Eager Nanostructured Biomaterials

L. Gentilucci<sup>1,2,\*</sup>, T. He<sup>1</sup>

<sup>1</sup>Department of Chemistry “G. Ciamician”, University of Bologna, via Selmi 2, Bologna 40126, Italy.

<sup>2</sup>Health Sciences & Technologies CIRI, University of Bologna, Via Tolara di Sopra 41/E, Ozzano Emilia, Bologna 40064, Italy

## Abstract:

Integrins are adhesion receptors expressed on many cell types that mediate cell-cell and cell-ECM interactions, and regulate fundamental functions, such as adhesion, signaling, and viability. Integrins are deeply involved in a variety of diseases, including the initiation and progression of cancer, coronary diseases, inflammatory, and autoimmune pathologies.

In this context, we designed peptidic/peptidomimetic integrin ligands equipped with linkers for expedient conjugation with NPs, drugs, or drug-carrier systems, for specific recognition or delivery to cells overexpressing the targeted integrins. Peptide-functionalized surfaces are important for studying integrin-mediated cell adhesion, growth, spreading and differentiation, and in biomedicine, for implant materials and tissue engineering. In particular, the functionalization and microfabrication of nanostructured surfaces consent to control spatial distance and peptide arrangement because ordered structures happen in the native ECM.

The rapid and exact identification and quantification of specific biomarkers is a key technology for always achieving more efficient diagnostic methodologies. We developed the first diagnostic application of a nanostructured device constituted of patterned monolayers of disk-shaped zeolite crystals, coated with  $\alpha_5\beta_1/\alpha_v\beta_3$  integrin ligands via isocyanate linker, to the rapid detection of cancer cells.

On the other hand, electrospun mats of nanofibers resemble the morphology and structure of the ECM and are, therefore, excellent candidates as cell-adhesive scaffolds. The fiber surface was used for the direct solid-phase synthesis of  $\alpha_5\beta_1/\alpha_v\beta_3$  integrin-binding peptides, a method with potential applications in combinatorial chemistry.

In contrast, a device for the identification and quantification of leucocytes expressing active  $\alpha_4\beta_1/\alpha_4\beta_7$  integrins can be utilized for monitoring ongoing inflammatory activity.

**Keywords:** peptidomimetics, electrospun mats, zeolite crystals, monolayers, nanopatterning,

integrins, cell adhesion, crowding effects, biomedical applications, cancer, inflammation.

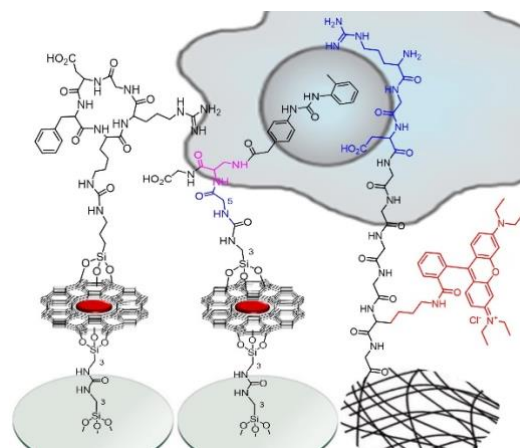


**Figure:** Peptide ligands of diverse integrins are anchored onto nanostructured surfaces (e.g. zeolite crystal monolayers, electrospun mats) to promote adhesion of specific integrin-expressing cells.

## References:

1. Anselmi, M. et al. (2023) Design and pharmacological characterization of  $\alpha_4\beta_1$  integrin cyclopeptide agonists: computational investigation of ligand determinants for agonism versus antagonism, *J. Med. Chem.* 66, 5021-5040.
2. Liguori, A. et al. (2024) Peptide direct growth on poly(acrylic acid)/poly(vinyl alcohol) electrospun fibers coated with branched poly(ethylenimine): a solid-phase approach for scaffolds biofunctionalization, *Colloids Surf B Biointerfaces*, 241, 114052.
3. Anselmi, M. et al. (2021) Design of  $\alpha/\beta$ -hybrid peptide ligands of  $\alpha_4\beta_1$  integrin equipped with a linkable side chain for chemoselective biofunctionalization of microstructured materials, *Biomedicines*, 9, 1737.
4. Greco, A. et al (2015) Diagnostic implementation of fast and selective integrin-mediated adhesion of cancer cells on functionalized zeolite L monolayers, *Bioconj. Chem.* 26, 1873-1878.

# Destination brain: trans- and paracellular strategies to overcome the blood-brain barrier

V.Castagnola<sup>1,2,\*</sup>, M. Trevisani<sup>1</sup>, S. Vercellino<sup>1,2</sup>, L. Boselli<sup>3</sup>, L. Pappagallo<sup>1,4</sup>, F. De Chirico<sup>1</sup>, A. Danielli<sup>4</sup>, A. Berselli<sup>1</sup>, G. Alberini<sup>1</sup>, L. Maragliano<sup>1,5</sup>, F. Benfenati<sup>1,2</sup>

<sup>1</sup>Center for Synaptic Neuroscience and Technology, Istituto Italiano di Tecnologia, Genova, Italy

<sup>2</sup>IRCCS Ospedale Policlinico San Martino, Genova, Italy

<sup>3</sup>Nanobiointeractions & Nanodiagnosics, Istituto Italiano di Tecnologia, Genova, Italy

<sup>4</sup>Dipartimento di Farmacia e Biotecnologie, Università di Bologna, Bologna, Italy

<sup>5</sup>Department of Life and Environmental Sciences, Polytechnic University of Marche, Ancona, Italy

## Abstract:

Reaching the brain for non-invasive therapeutic interventions still represents a formidable challenge for our society. One of the main difficulties is related to the presence of the blood-brain barrier (BBB), an essential protection mechanism that selectively limits the passage of molecules and pathogens into the delicate neuronal environment but, on the other hand, significantly hinders the effective delivery of therapeutic formulations administered *via* the bloodstream.[1] Nanomaterials, given their propensity to engage with the biological machinery actively, open up opportunities to exploit transcellular routes to overcome the BBB. However, for a nanoformulation traveling in the bloodstream, the formation of a biomolecular corona masking the engineered materials' identity significantly limits this approach.[2]

In our work, we explore strategies to exploit the natural protein corona of nanomaterials or totally avoid it with the help of biomimetic approaches to enhance the BBB crossing ability. For this second option, we selected M13 bacteriophages, harmless bacteria-specific viruses largely present in our gut virome and oral cavity, as a safe and effective vehicle. Phages offer facile genetic manipulation, enabling the expression of targeting moieties on their capsids, and are produced through an easily scalable process. Here, we show how these flexible nanocarriers can transport molecules and nanomaterials across BBB *in vitro* models of increasing complexity, eluding the protein corona and keeping their integrity and engineered tropism.

In a complementary strategy, we studied the role of Claudin-5, the major tight-junction protein found in the brain endothelium, in paracellular sealing. Using competitive binding peptides designed with an *in silico* approach,[3] we were able to loosen the binding of adjacent claudins, making the paracellular space more permeable to small molecules.

Altogether, our approaches offer exciting prospects for advancing therapeutic interventions in neurological disorders.

**Keywords:** Blood-brain barrier, tight junctions, Claudin-5, biomimetic nanomaterials, M13 bacteriophages, peptidomimetics.

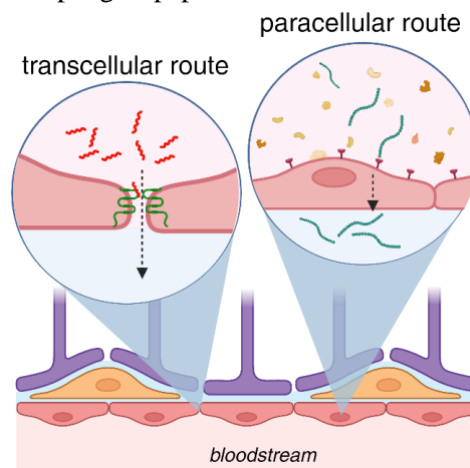


**Figure 1:** Two complementary approaches to overcome the BBB: the paracellular route exploiting competing binding peptides to Claudin-5 and the transcellular route adopted by the M13-phages nanocarrier.

## References:

1. Moschetta, M., Trevisani, M., Castagnola, V. & Bramini, M. in *New Insights Into Glioblastoma* 435-475 (Elsevier, 2023).
2. Boselli, L., Castagnola, V., Armirotti, A., Benfenati, F. & Pompa, P. P. (2023) Biomolecular Corona of Gold Nanoparticles: The Urgent Need for Strong Roots to Grow Strong Branches. *Small*, 2306474.
3. Berselli, A., Alberini, G., Benfenati, F. & Maragliano, L. (2022) Computational assessment of different structural models for claudin-5 complexes in blood-brain barrier tight junctions. *ACS Chemical Neuroscience* **13**, 2140-2153.

# Control of protein adsorption, cell adhesion and growth on polysaccharide based multilayer films by incorporation of graphene oxide

Tonya Andreeva<sup>1,\*</sup>, Rumen Krastev<sup>1,2</sup>

<sup>1</sup> Reutlingen University, Reutlingen, Germany

<sup>2</sup> NMI Natural and Medical Sciences Institute at the University of Tübingen, Reutlingen, Germany

## Abstract:

Controlling protein adsorption, as well as cell adhesion, viability, and proliferation on solid surfaces is critical for the successful implantation and proper functioning of temporary and permanent medical implants.

This work was motivated by the growing interest in construction of biocompatible coatings for functionalization of medical devices. Here, a straightforward approach to improve the biocompatibility of biomaterials by controlling cellular response to their surface is presented. It is based on surface modification by self-assembly of polyelectrolytes (PEs) and graphene oxide (GO) into ultra-thin composite polyelectrolyte multilayer (PEM) films. PEMs were based on the two most attractive natural polysaccharides, hyaluronic acid (HA) and chitosan (Ch), which build films that are distinguished by their non-toxicity, biodegradability and biofilm repulsion, but at the same time are completely resistant to cell adhesion [1]. The insertion of a non-polymeric component into the polymer matrix is the strategy used here to alter the properties of these PEMs and thereby regulate the interaction between the cells and the surface of the implants. Due to its unique physicochemical properties (mechanical, electrical, optical and thermal) GO and its polymer nanocomposites are intensively studied, especially with regard to their potential biomedical applications such as drug delivery, cancer therapy and imaging (theragnostics), and biosensing [2].

Analysis of the structure of the HA/Ch/GO films by atomic force microscopy revealed generally smooth surfaces with nano-roughness increasing in parallel with the number of embedded GO-layers. All coatings were hydrophilic and incorporation of GO exerted only a weak effect on water contact angle. Terminating the HA/Ch multilayer with a single GO-monolayer or embedding different number of GO-layers into the polymer matrix provided the opportunity to modify the adhesion and proliferation of fibroblasts and endothelial cells over the entire

range of zero (for the control HA/Ch coating without GO) up to 100%, equal to the gold standard for cellular response (for the composite HA/Ch/GO film with GO-top layer). Regardless of the number and localization of GO-layer(s), their incorporation had a positive effect in terms of cell adhesion, proliferation and viability, compared to HA/Ch multilayer without GO, without compromising the cytotoxicity at all. Tunable protein adsorption onto HA/Ch polysaccharide films was also demonstrated by quantitative evaluation of the extent of adsorption of the most abundant serum protein, human serum albumin.



**Figure 1:** GO-layer promotes adhesion and proliferation of 3T3 fibroblasts and HUVEC endothelial cells on PEM-based coatings.

**Keywords:** biofunctionalization, polyelectrolyte multilayer coatings, thin hybrid films, cell adhesion, cell proliferation, protein adsorption, surface properties, hydrophilicity

## Acknowledgements:

The authors gratefully acknowledge the funding by the German Research Foundation (Deutsche Forschungsgemeinschaft, DFG) for the subproject 2 within the Research Unit FOR5250 “Permanent and bioresorbable implants with tailored functionality” (No. 449916462).

## References:

1. Schneider, A., Richert, L., Francius, G., Voegel, J.-C., Picart, C. (2007) Elasticity, biodegradability and cell adhesive properties of chitosan/hyaluronan multilayer films, *Biomed. Mater.*, 2, S45.
2. Feng, L., Liu, Zh. (2011) Graphene in biomedicine: opportunities and challenges, *Nanomedicine*, 6(2), 317–324.

# Exploring the Protein Surface Interactions of a Protein Inspired by a Natural Glue

D. Ayed<sup>1,2\*</sup>, Z. Khalil<sup>1,3</sup>, C. R. Picot<sup>3</sup>, M. Weidenhaupt<sup>1</sup>, F. Bruckert<sup>1</sup>, R. Mathey<sup>2</sup>, Y. Hou-BROUTIN<sup>2</sup>, C. Vendrely<sup>1</sup>

<sup>1</sup> CNRS, Grenoble-INP, LMGP, University Grenoble Alpes, 38000 Grenoble, France

<sup>2</sup> CEA, CNRS, Grenoble INP, IRIG-SYMMES, University Grenoble Alpes, 38000 Grenoble, France

<sup>3</sup> ERRMECe (EA 1391), Institute of Materials, CY Cergy Paris University, 95000 Neuville sur Oise, France

## Abstract:

Wet adhesion technology plays a significant role in different areas, especially for biomedical applications. Aquatic organisms such as sandcastle worms, mussels, and barnacles have developed to become wet adhesion specialists, showing excellent underwater adhesion abilities<sup>1</sup>. Barnacle cement adhesive proteins and their related recombinant proteins have emerged as promising candidates for developing environmentally friendly adhesive materials<sup>2</sup>, thanks to their unique structural properties, chemical composition, and adhesion mechanism. The adhesion mechanism appears to be linked to the self-assembly of proteins forming an architecture network of fibers on the surface of materials. Thus, revealing the original barnacle cement adhesive molecular mechanism involves deciphering the interactions between the cement proteins and different surfaces. More generally, it would enhance the fundamental understanding of protein-surface interactions. In this study, M19-2, a recombinant protein inspired by *Megabalanus rosa* barnacle cement was expressed in *Escherichia coli* and purified to yield a high level of pure target protein. To investigate M19-2 adsorption behavior on various surfaces with different physicochemical properties, surface plasmon resonance imaging (SPRi) was employed. SPRi allows for precise and real-time determination of protein adsorption onto a range of model surfaces (hydrophobic, hydrophilic, positively charged, negatively charged) under varied conditions, such as temperature, pH, and ionic strength. Moreover, the adsorption and desorption kinetics of M19-2 under different conditions were performed to understand the molecular aspects of protein interactions with the surfaces.

Depending on the surface physicochemical properties, M19-2 proteins' behavior can undergo modifications. A thorough examination of protein interactions, both with diverse surfaces and between proteins themselves, offers insight

into the formation of adhesive architectural networks. This understanding enables us to propose mechanisms that could explain the natural adhesion of barnacle cement.

**Keywords:** Barnacle, adhesion, proteins, surface

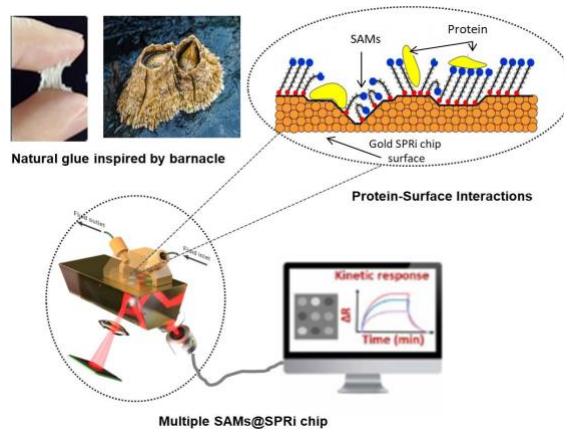


**Figure 1:** Schema illustrating the investigation of protein-surface interactions using SPRi.

## References:

1. Gan K, Liang C, Bi X et al. (2022) *Front Bioeng Biotechnol.* 25;10:870445
2. Ye L, Liu X, Li K, et al. (2023) *Int J Biol Macromol.* 253(Pt 5):1



# Locally Selective Immobilisation of DNA Origami for Raman Spectroscopy based Biosensors

J. Hann<sup>1,\*</sup>, M. Janssen<sup>1</sup>, C. Meinecke<sup>1,2</sup>, S. Hartmann<sup>1</sup>, A. Heerwig<sup>3</sup>, D. Reuter<sup>1,2</sup>, Michael Mertig<sup>3</sup>

<sup>1</sup>Center of Micro- and Nanotechnology, University of Technology Chemnitz, Chemnitz, Germany

<sup>2</sup>Fraunhofer Institute for Electronic Nanosystems (ENAS), Chemnitz, Germany

<sup>3</sup>Kurt-Schwabe-Institut für Mess- und Sensortechnik Meinsberg e.V., Meinsberg, Germany

## Abstract:

Novel biosensors are increasingly utilising nanoobjects such as metallic nanoparticles in combination with biological recognition elements (e.g. DNA aptamers or antibodies) to achieve higher selectivity or sensitivity through optical/plasmonic enhancement effects. In our approach we arrange two metallic nanoparticles around a biological recognition element in order to form an innovative biosensor platform for e.g. bio-marker molecules (see Fig. 1). To enable the precise, heterogeneous arrangement with only a few nanometers distance for detection by surface-enhanced Raman spectroscopy, we use the DNA origami method as a kind of nano-board with a resolution of 2-5 nm [1]. Nanoobjects can be deposited on a DNA origami in exact distance to each other [2,3] by the use of complementary functional groups. However, in order to detect even low concentrations of the analyte, signal accumulation through a regular plasmonic structure by template-based surface deposition in a locally selective and aligned manner is desirable. In this work, we present a new immobilization system based on lithographically structured thin films for selective deposition of DNA origami, used for the integration of our DNA origami-based biosensor elements. We used SiO<sub>2</sub> as a binding active (BA) layer, which enables electrostatic binding of the negatively charged DNA origami through the negatively charged silanol groups via a magnesium bridge. As a binding resistant (BR) layer, we used Parylene C as well as Parylene F. To optimize the selectivity of the system, different surface activation steps (e.g. atmospheric plasma treatments) as well as surface modifications were investigated and compared in their effect on the system performance (selectivity and coverage BA layer). For example, SiO<sub>2</sub> was modified with poly-L-lysine to create a positive surface charge that allowed direct binding of the DNA origami without magnesium. In addition, Pluronic F-127 was investigated with respect to its effect on the BR layer (see Fig. 2).

**Keywords:** DNA origami, surface immobilization, nanotechnology, surface modification

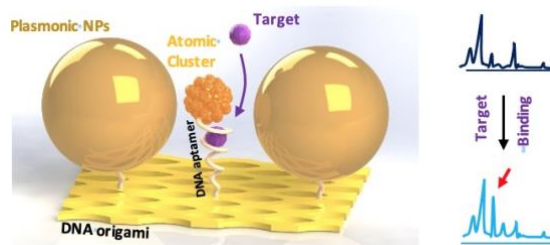


**Figure 1:** Schematic sketch of the DNA origami-based biosensor element. When the target is attached to the bio-RE (ssDNA), a change in the Raman signal is detected by SERS.

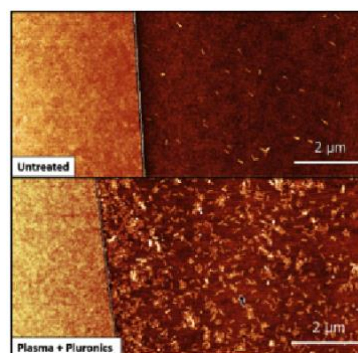


**Figure 2:** AFM topography image after DNA origami immobilization on SiO<sub>2</sub> (right) with Parylene F (left) - untreated (top) and after plasma and Pluronic treatment (bottom).

**Acknowledgment:** This work was supported by funding from the European project DeDNAed under grant agreement No 964248.

## References:

1. Strauss, M. T., Schueder, F., Haas, D., Nickels, P. C., Jungmann, R. (2018), Quantifying absolute addressability in DNA origami with molecular resolution, *Nat Commun*, 9, 1600.
2. Kuzyk, A., Jungmann, R., Acuna, G. P., Liu, N. (2018), DNA Origami Route for Nanophotonics, *ACS Photonics*, 5, 1151-1163.
3. J. Zessin, F. Fischer, A. Heerwig, A. Kick, S. Boye, M. Stamm, A. Kiriy, M. Mertig, (2017), Tunable Fluorescence of a Semiconductor Polythiophene Positioned on DNA Origami, *Nano Lett.*, 17, 5163–5170.

# Multi-scale nanoimprinted nanopillar structures within a microfluidic device fabrication with surface functionalization

HO. M. Chu<sup>1,2,\*</sup>, P. Goldberg Oppenheimer<sup>1,2</sup>, L. M. Grover<sup>1,2</sup>

<sup>1</sup>School of Chemical Engineering, University of Birmingham, Birmingham, UK

<sup>2</sup>Healthcare Technologies Institute, University of Birmingham, Birmingham, UK

## Abstract:

Trace-level sensing is an important requirement in diagnosing health conditions, where in optical approaches water can be a significant background that Raman spectroscopy has advantages over other spectroscopy methods. Raman scattering is a weak effect, therefore, to achieve up to single-molecule sensitivities, advanced approaches such as surface enhanced Raman spectroscopy (SERS) are applied. This requires the utilisation of metallic nanostructures near biomarkers (~10s of nanometres), which results in Raman signal enhancements by orders of magnitude. However, the process to fabricate nanomaterials in a scalable and reliable manner with high resolution is an expensive process, typically limited to semiconductor-related applications. This study presents bioinspired moth-eye nanostructures within a microfluidic device produced in one nanoimprint lithography process (Figure 1). Additionally, the issue of selectivity and specificity of SERS is addressed with a surface molecular imprinted surface, leading to enhancement factors of  $10^6$ . Through COMSOL® modelling, this is consistent to the experimentally observed enhancement for 1,2-Di(4-pyridyl) ethylene. For human serum albumin, which is a model protein is found to have a limit of detection of 7 ng/ml which is significantly lower than the lower limit for urine where any values above 30 ng/ml is considered a health issue. These results show promising a method for multiscale fabrication process, capable of nano and micro fabrication validated for plasmonic biosensing.

**Keywords:** nanoimprint lithography, Surface-Enhanced Raman Spectroscopy, microfluidics, surface hydration, crowding effects, micropatterning, biomedical applications.

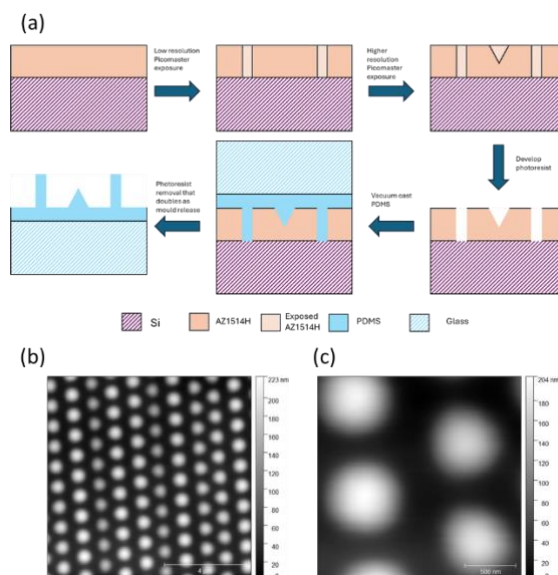


**Figure 1:** (a) scheme of the nanoimprint lithography process, showing how utilizing different direct laser writing focus depths can produce a mold for both micro and nanostructures. (b) – (c) Atomic force microscopy images of the nanopillar arrays produced from the nanoimprint process.

## References:

1. Zhang, J.R.; Yan, Y.D.; Miao, P.; Cai, J.X. (2017) Fabrication of Gold-Coated PDMS Surfaces with Arrayed Triangular Micro/Nanopyramids for Use as SERS Substrates. *BEILSTEIN J. Nanotechnol.* 8, 2271–2282, doi:10.3762/bjnano.8.227
2. Montesi, S.B.; Bajwa, E.K.; Malhotra, A. (2012) Biomarkers of Sleep Apnea. *Chest*, 142, 239–245, doi:10.1378/CHEST.11-2322.

# Advanced Integrated Multipurpose Spectroscopic Lab-on-a-chip for Timely Detection of Extracellular Vesicles as Key-Markers of Inflammatory Bowel Disease

**E.Buchan**<sup>1</sup>, J.J.S.Rickard<sup>1</sup>, M.R.Thomas<sup>2</sup>, P.Goldberg Oppenheimer<sup>1,3</sup>

<sup>1</sup> School of Chemical Engineering, University of Birmingham, Birmingham, UK

<sup>2</sup> Institute of Cardiovascular Sciences, University of Birmingham, Birmingham, UK

<sup>3</sup> Healthcare Technologies Institute, Institute of Translational Medicine, Birmingham, UK

**Abstract:** Inflammatory bowel diseases (IBD), predominantly represented by ulcerative colitis and Crohn's disease, are chronic inflammatory conditions affecting around 2.5-3 million individuals in Europe with the incidence continuing to rise worldwide. Currently, there is no simple method for identifying early disease in individuals at the point-of-care or in the community, with no portable technology available for quantitative assessment of early-stage IBDs with sufficient timeliness and sensitivity to support rapid and early-diagnosis. Therefore, the development of a quick, simple and low-cost bedside, point-of-care technique to detect biomarkers indicative of diseases, from readily available biofluids such as saliva, are of vital importance. Lipid membrane extracellular vesicles (EVs), varying in size and conformation, are known to play a role in numerous processes including intercellular communication, immune modulation and cellular proliferation. EVs can act as a biomarker, specifying the progression of the diseased state of the cells in which they originate. Herein, we have developed a portable advanced integrated multipurpose spectroscopic lab-on-a-chip (AIMSpec-LoC) for timely and rapid detection of IBDs *via* specific fingerprinting for low-cost, non-invasive, early-stage diagnosis. The hybrid on-chip isolation and Raman spectroscopic analysis, with our advanced AI discrimination provides simultaneous analysis of multiple EV subtypes indicative of disease, demonstrating classification accuracy of >97% in the diagnosis of IBD with discernible Raman spectral differences for each class stemming primarily from protein, lipid and amino acid changes. AIMSpec-LoC is subsequently validated, uniquely capturing and detecting EVs while delivering molecular fingerprint specificity with sensitivity of >96%, yielding an attractive tool for sensing target biomarker molecules, such as the identified cytokines, for timely diagnosis and rapid monitoring. Convenient and effective, it can reduce the time spent waiting for a definitive diagnosis and potentially improve patient prognosis. Overall, AIMSpec-LoC development lays the platform towards a *real-time* diagnostic technology addressing an unmet need for improved clinical

interventions in a variety of diseases as well as further potential use within the wider material science and engineering communities.

**Keywords:** Inflammatory bowel disease, lab-on-a-chip, Raman spectroscopy, artificial neural network classification, extracellular vesicles, candidate biomarkers

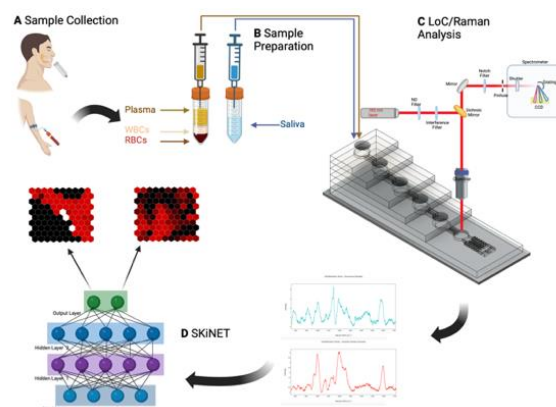


**Figure 1:** Schematics of LoC methodology including the sample collection from biofluids *e.g.*, saliva, followed by sample preparation to dilute saliva, followed-by on-chip isolation, separation and the subsequent Raman detection of EVs obtained from saliva and rapid analysis *via* artificial neural network algorithm, SKiNET, acting as a decision support tool in the classification of acquired data, output in both the diseased state as well as subgroup of isolated EVs.

## References:

1. Davies, R.T., Kim, J., Jang, S.C., Choi, E., Gho, Y.S., Park, J. (2012), Microfluidic filtration system to isolate extracellular vesicles from blood, *Lab on a chip*, 24, 5202-5210.
2. Buchan, E., Rickard, J.J.R., Goldberg Oppenheimer, P. (2023), Raman spectroscopic molecular fingerprinting of biomarkers for inflammatory bowel disease, *Clinical and Translational Medicine*, 11, 1-6.



# Multifunctional Stimuli-Responsive Systems for Sensing

Loretta L. del Mercato

Nanotechnology Institute of National Research Council of Italy (Nanotec-Cnr), Via Monteroni, c/o  
Campus Ecotekne, Lecce, 73100, IT  
e-mail: [loretta.delmercato@cnr.it](mailto:loretta.delmercato@cnr.it)

## Abstract:

The microenvironment in degenerative pathologies or post-traumatic injuries is highly heterogeneous and dynamic, characterized by the establishment of pH and oxygen gradients due to altered cellular metabolic activity and impaired tissue perfusion. [1] This significant heterogeneity greatly influences the effectiveness of therapeutic interventions aimed at tissue repair and regeneration.[2] Dynamic mapping of key parameters, such as pH and oxygen levels, is essential for understanding their role in cellular processes and tissue regeneration, providing insights into how pH/oxygen distribution affects cell morphology, function, and recovery. Various imaging and sensing techniques have been developed and applied in research and clinical settings to visualize and monitor cellular responses in these microenvironments.[3] Among these, ratiometric fluorescence-based sensors have proven to be powerful tools for non-invasive tracking of dynamic changes. This talk discusses the synthesis and application of nanostructured materials (Fig 1), with an emphasis on their potential in regenerative medicine and microenvironment sensing. Examples include the use of extracellular matrix-like nanofibers [4-5] and hydrogels [6-7] for the spatiotemporal mapping of pH and oxygen changes in 3D in vitro models of tissue injury, underscoring the possibility of using these systems for personalized therapeutic development in the context of tissue degeneration and trauma recovery.

**Keywords:** Ratiometric optical pH-sensors; silica microparticles; hydrogels; fluorescence; pH sensing; microparticle tracking; cancer; cell metabolism; data compression, automated cluster analysis.

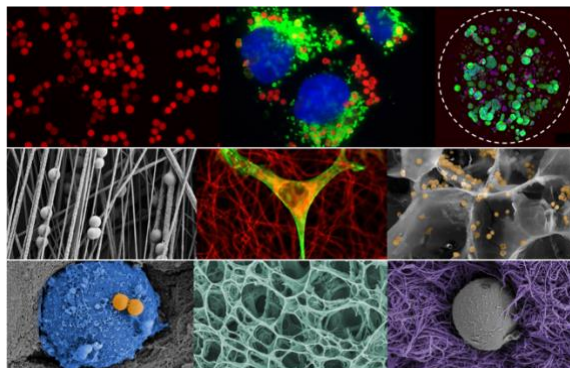


**Figure 1:** Optical pH and oxygen-sensing systems for complex cell systems, utilizing fluorescent ratiometric microparticles, hydrogels, electrospun nanofibers, and additive-manufactured scaffolds.

## References:

1. G. Grasso et al., *Nanoscale Advances*, 5 (2023) 4311-4336.
2. O. Tredan et al., *J. Natl. Cancer Inst.*, 99 (2007) 1441-1454.
3. G. Rong et al., *Annu Rev Anal Chem* 12 (2019) 109-128.
4. V. Onesto et al., *ACS Nano*, 17 (2023) 3313-3323.
5. G. Grasso et al., *Bio-Design and Manufacturing* (2024) 1-15.
6. R. Rizzo et al., *Materials Today Bio*, 20 (2023) 100655.
7. Siciliano A.C. et al., *Advanced Healthcare Materials* 2024, 2401138.

**Acknowledgment:** The research leading to these results was supported from the Italian Ministry of Research, under the complementary actions to the NRRP “Fit4MedRob - Fit for Medical Robotics” Grant (# PNC0000007), the European Research Council (ERC) under the European Union's Horizon 2020 research and innovation programme (grant agreement No 759959, ERC-StG “INTERCELLMED”).

# Validation of an Intracranial Raman Spectroscopic Probe for *In-Situ* Monitoring of Traumatic Brain Injury

C. A. Stickland<sup>1</sup>, Z. Sztranyovszky<sup>1</sup>, J. J. S. Rickard<sup>1,2</sup>, P. Goldberg Oppenheimer<sup>1,3,\*</sup>

<sup>1</sup> School of Chemical Engineering, College of Engineering and Physical Science, University of Birmingham, B15 2TT, UK

<sup>2</sup> Department of Physics, Cavendish Laboratory, University of Cambridge, JJ Thomson Avenue, Cambridge, CB3 0HE, UK

<sup>3</sup> Institute of Healthcare Technologies, Mindelsohn Way, Birmingham, B15 2TH, UK

## Abstract:

The development of an optical interface to directly distinguish the brain tissue's biochemistry is the next step in understanding traumatic brain injury (TBI) pathophysiology and provide the best and most appropriate treatment in cases where in-hospital intracranial access is required. Despite TBI being a globally leading cause of morbidity and mortality, there is still a lack of objective diagnostic tools available. Further, given its pathophysiological complexity the majority of treatments provided are purely symptomatic without standardized therapeutic targets.

Our tailor-engineered prototype of the intracranial Raman spectroscopy probe (Intra-RSP) is designed to bridge the gap and provide real-time spectroscopic insights to monitor TBI and its evolution as well as identify patient-specific molecular targets for timely intervention.

In combination with our in-house developed software, using machine learning algorithms for multivariate analysis, the Intra-RSP is shown to accurately differentiate simulated TBI conditions in rat brains from the healthy controls, directly from the brain surface as well as through the rat's skull. Using clinically pre-established methods of cranial entry, the Intra-RSP can be inserted into a 2-piece optimized cranial bolt with integrated focussing and correctly identify rat brains mildly damaged from inflicted spinal cord injury were found to be correctly classified with 94.5% accuracy. Through optimization and rigorous *in-vivo* validation, the Intra-RSP prototype is envisioned to seamlessly integrate into existing standards of neurological care, serving as a minimally invasive, *in-situ* neuromonitoring tool. This transformative approach has the potential to revolutionize the landscape of neurological care by providing clinicians with unprecedented insights into the nature of brain injuries and fostering targeted, timely and effective therapeutic interventions.

**Keywords:** Raman Spectroscopy, Traumatic Brain Injury, Neurodiagnostics, Biomarker Detections.

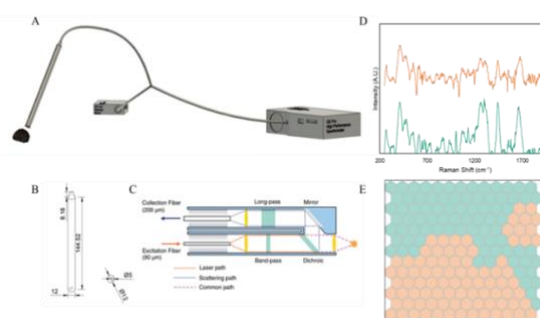


**Figure 1:** Illustration of the portable Intra-RSP device, including probe head dimensions and internal structure of co-axially aligned fibres. The Intra-RSP collects sufficiently specific data to separate in the self-organised maps to accuracy of 94.5%.

## References:

1. Mowbray M, Banbury C, Rickard JJ, Davies DJ, Goldberg Oppenheimer P. Development and Characterization of a Probe Device toward Intracranial Spectroscopy of Traumatic Brain Injury. *ACS biomaterials science & engineering*. 2021;7(3):1252-62.
2. Banbury C, Mason R, Styles I, Eisenstein N, Clancy M, Belli A, et al. Development of the self optimising Kohonen index network (SKiNET) for Raman spectroscopy based detection of anatomical eye tissue. *Scientific reports*. 2019;9(1):10812.



# CMOS-Compatible Electrochemical ELISA Platform for Semi-continuous Cytokine Monitoring in Organ-on-Chip Systems

S. J. Zapiain-Merino <sup>1,2</sup>, A. Torosyan <sup>2</sup>, K. Jans <sup>1</sup>, R. Vos <sup>1</sup>, L. Lagae <sup>1,2</sup>, O. Henry <sup>1</sup>

<sup>1</sup> Life Science Technologies (LST), Interuniversitair Micro-Electronica Centrum (IMEC), Leuven, BE

<sup>2</sup> Department of Physics and Astronomy, Katholieke Universiteit Leuven (KUL), Leuven, BE

## Abstract:

The rapid advancement in the field of microphysiological systems (MPS) necessitates the development of biosensor platforms capable of continuously monitoring the viability of the biological entities on these systems. A marker for MPS viability is the variation in the concentration of cytokines, which correlates with the health of the tissue. These molecules are typically present at low concentrations (~pg-ng/mL) requiring continuous and precise assessment.

Current methods for evaluating cytokines related to MPS viability predominantly rely on offline measurements or semi-autonomous external microfluidic systems, which often involve bulky setups which are difficult to fit into incubators used for cell growth. One of the primary objectives is to facilitate measurements as close to the MPS as possible to obtain real-time information on cellular functionality and behaviour. [1] A crucial step towards achieving this goal is the combination of the sensing platform with integrated CMOS systems. However, this integration poses significant challenges due to the necessity of using CMOS-compatible materials as transducers.

In response to this challenge, we have developed a biosensing platform using CMOS-compatible materials. The platform consists of a multichannel microfluidic cartridge with an integrated on-chip pump connected to a multielectrode chip. The multielectrode chips are functionalized with a bifunctional layer that anchors antibodies and prevents non-specific binding.

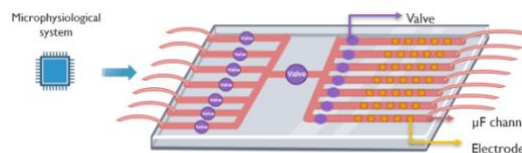


**Figure 1.** Schematic of the developed microfluidic platform for semi-continuous measurement of cytokines

As a proof of concept, we validated the platform by quantifying IL-6, a cytokine associated with cellular stress, under various media conditions for a fibrosis MPS. This validation demonstrates the platform's potential for continuous cytokine monitoring in MPS applications, providing a powerful tool for real-time assessment of secreted biomarkers.

**Keywords:** Cytokines, Microfluidic, Electrochemical ELISA, Biomarkers, CMOS Microfabrication, Organ-on-Chip.

## References

1. Zhu, Y., et al (2021). *Current Opinion in Biomedical Engineering*, 19, 100309

**NanoMed 2024 Session II. F:  
Nanomaterials for Biomedical /  
Tissue engineering, drug, and gene  
delivery**

# Production and Characterization of Deformable Vesicles for Transdermal Application

L. Baldino <sup>1\*</sup>, S. Sarnelli <sup>1</sup>, E. Reverchon <sup>1</sup>

<sup>1</sup> Department of Industrial Engineering, University of Salerno, Via Giovanni Paolo II, 132, 84084 Fisciano (SA), Italy

## Abstract:

Transdermal drug delivery systems received a great interest thanks to their advantages over traditional oral and parenteral delivery systems. However, the barrier effect of the skin inhibits and/or reduces the transdermal transport of active pharmaceutical ingredients to the target site [1]. To overcome this limitation, an advanced kind of vesicles, called transfersomes or “deformable liposomes”, has been developed. Transfersomes are formed by phospholipids and edge activators that provide deformability properties to the nanocarrier (Figure 1) [2,3]. In this work, transfersomes were produced by SuperSomes, a continuous and innovative process assisted by supercritical CO<sub>2</sub>, operated at 100 bar and 40 °C [4]. The experiments were performed by setting phosphatidylcholine/Span<sup>®</sup> 80 weight ratio at 80:20 and changing the amount of phosphatidylcholine from 500 to 2000 mg. Formulations prepared using 1000 mg of phosphatidylcholine resulted in stable transfersomes characterized by a mean diameter of 128 ± 30 nm and a Zeta-potential of -14.00 ± 3.43 mV. Deformability tests were carried out at different deformation rates (from 0.035 to 0.6 mL/min) and using 100 nm pore size filters. Operating at 0.1 mL/min flow rate, it was possible to avoid the rupture of transfersomes since, after deformation, they recovered up to 75% of their initial size, thus, confirming an elastic behaviour.

**Keywords:** transfersomes, nanovesicles, transdermal drug delivery, deformability, supercritical CO<sub>2</sub> process, controlled release.

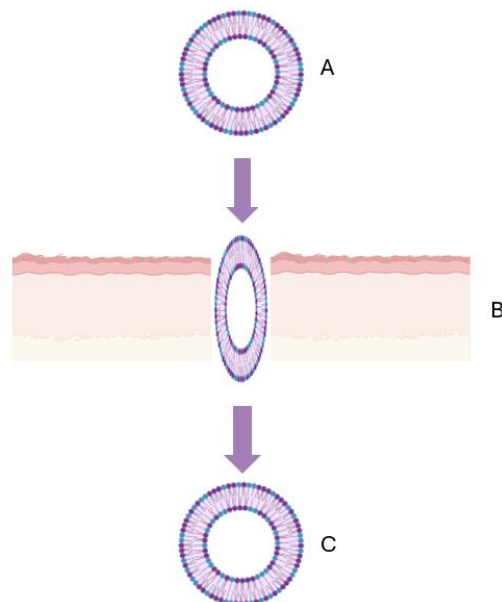


**Figure 1:** Schematic illustration on transfersomes penetration through the skin layer. (A) shows the transfersome before deformation; (B) is referred to the penetration through the skin layer; (C) shows the transfersome after deformation.

## References:

1. Opatha, S.A.T., Titapiwatanakun, V., Chutoprapat, R. (2020), Transfersomes: A promising nanoencapsulation technique for transdermal drug delivery, *Pharmaceutics*, 12, 855.
2. Akram, M.W., Jamshaid, H., Rehman, F.U., Zaeem, M., Khan, J.Z., Zeb, A. (2022), Transfersomes: a revolutionary nanosystem for efficient transdermal drug delivery, *AAPS PharmSciTech*, 23, 1-18.
3. Riccardi, D., Baldino, L., Reverchon, E. (2024), Liposomes, transfersomes and niosomes: production methods and their applications in the vaccinal field, *J. Transl. Med.*, 22, 339.
4. Squittieri, R., Baldino, L., Reverchon, E. (2023), Production of antioxidant transfersomes by a supercritical CO<sub>2</sub> assisted process for transdermal delivery applications, *Nanomaterials*, 13, 1812.

# Potential neuroprotective effects of intranasally delivered multi-walled carbon nanotubes

S.Fiorito<sup>1,\*</sup>, M.Soligo<sup>1</sup>, D.Uccelletti<sup>2</sup>

<sup>1</sup> Institute of Translational Pharmacology, National Research Council (CNR), Rome, Italy

<sup>2</sup> Department of Biology “C. Darwin”, Sapienza University, Rome, Italy

## Abstract:

Carbon nanotubes (CNTs) are currently under active investigation for their use in several biomedical applications, especially in neurological diseases and nervous system injury due to their electrochemical properties. Nowadays, no CNTs-based therapeutic products for internal use appear to be close to the market, due to the still limited knowledge on their fate after delivery to living organisms and, in particular, on their toxicological profile. We explored the capacity of CNTs *in vivo* to reach the rat brain through inhalation and to address the distribution in the brain parenchyma of two intranasally delivered Multi Walled Carbon Nanotubes (MWCNTs 1 and a-MWCNTs 2), the first being non electroconductive while the second results in being electroconductive. Inhaled MWCNTs were demonstrated to affect the function of Central Nervous System (CNS) in rats. Modification of some neural cell activation markers was demonstrated in rat brain 4 days after CNT inhalation. We also verified the neuroprotective potential of the two types of CNTs, as already demonstrated *in vitro*<sup>1</sup>, delivering them in rats affected by early diabetic encephalopathy and analysing the modulation of nerve growth factor metabolism and the effects of CNTs on the neuronal and glial phenotypes<sup>2</sup>. We observed that both CNT types, intranasally delivered, reached numerous brain areas and, in particular, the limbic area that plays a crucial role in the development and progression of major neurodegenerative diseases. Furthermore, we observed that electroconductive MWCNTs were able to exert neuroprotective effects through the modulation of a key neurotrophic factor, mature Nerve Growth Factor (mNGF) and probably the improvement of neurodegeneration-related gliosis. Our results showed that only the a-MWCNTs 2 treatment induced a significant increase in the mNGF/proNGF ratio in the hippocampus of diabetic rats, suggesting the triggering of neuroprotective effects by these CNTs. Moreover, we assessed the cytotoxic effect of these CNTs *in vivo* in a simple animal model: the *Caenorhabditis elegans* that, due to its

biological characteristics, is used as a biological model in toxicological assessments. No toxicity was observed. For both the MWCNTs examined. We demonstrated that MWCNTs are able to reach the CNS through inhalation and, that is more important, to exert their effects on brain tissues, without being cytotoxic. To the best of our knowledge, this is the first study showing that MWCNTs delivered via the intranasal route are able to reach numerous brain areas and in particular the limbic area that plays a crucial role in the development and progression of major neurodegenerative diseases. Furthermore, most important from a translational standpoint, electroconductive a-MWCNTs 2 were demonstrated to be potentially able to exert a neuroprotective effect through the modulation of a key neurotrophic factor.

**Keywords:** carbon nnotubes, multi walled carbon nanotubes, neuroprotective effect, mature Nerve Growth Factor, neurodegenerative diseases, medical applications.

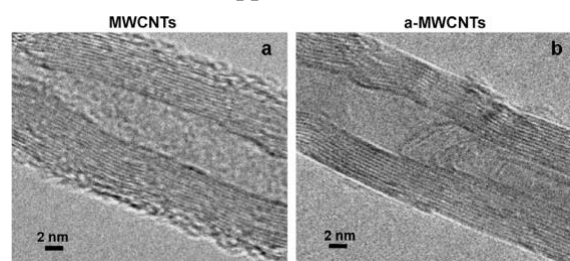


**Fig. 1** TEM details of as-prepared MWCNTs (a) and of electroconductive annealed MWCNTs (b), Scale bars: 2 nm.

## References:

1. Fiorito S., Roussier J. (2018), Switching on microglia with electroconductive multi-walled carbon nanotubes, *Carbon*. 129, 572-584
2. Soligo M., Felsani F.M., (2021), Distribution in the brain and possible neuroprotective effects of intranasally delivered multi-walled carbon nanotubes, *Nanoscale Adv.*, 3, 418-431.

# PIC micelles encapsulating medical Cu-64 as a Drug Delivery System for Cancer Therapy

Mary Alfonse George Mikhail<sup>1</sup>, Nobuya Hayashi<sup>1,2</sup>, Taisei Eto<sup>1</sup>, Kazuaki Tsukada<sup>3</sup>, Akihiro Kishimura<sup>4,5</sup>, and Hiroshi Kamizawa<sup>6</sup>

<sup>1</sup> Kyushu University, Interdisciplinary Graduate School of Engineering Sciences, Fukuoka, Japan

<sup>2</sup> Kyushu University, International Research Center for Space and Planetary Environmental Science, Fukuoka, Japan

<sup>3</sup> Japan Atomic Energy Agency, Ibaraki, Japan

<sup>4</sup> Kyushu University, Department of Applied Chemistry, Fukuoka, Japan

<sup>5</sup> Kyushu University, Center for Future Chemistry, Fukuoka, Japan

<sup>6</sup> Kyushu University, Graduate School of Systems Life Sciences, Fukuoka, Japan

## Abstract:

Copper-64 (<sup>64</sup>Cu) is a promising theranostic candidate utilized for both positron emission tomography (PET) in cancer diagnosis and as a potential therapeutic candidate. This radioisotope emits widely used therapeutic particles,  $\beta^+$  and  $\beta^-$  but Auger electrons, known to have lethal effects on cancer cells. Selecting an appropriate Drug Delivery System (DDS) is crucial to studying the impact of <sup>64</sup>Cu on cancer cells. Polyion complexes (PICs) are up-and-coming DDS designed to effectively deliver genes, small nucleic acids, proteins, and charged macromolecular drugs. PIC formation can occur in aqueous media without organic solvent, and the preparation process is remarkably straightforward. Typically, PICs are obtained by simply mixing oppositely charged macromolecules (Figure 1). Therefore, it is a simple and versatile technique to encapsulate CuCl<sub>2</sub> ions to target cancer cells. In this study, <sup>64</sup>CuCl<sub>2</sub>, free and chelated with DOTA, was successfully encapsulated within the PIC micelles. TLC results indicated that the chelated <sup>64</sup>CuCl<sub>2</sub> had a higher affinity for PIC micelles. Furthermore, in-vitro experiments were conducted to evaluate the impact of the encapsulated copper on both a normal cell line (HaCaT) and a cancerous cell line (HSC-3). The results showed that the proliferation of normal cells remained unaffected by adding PIC micelles, CuCl<sub>2</sub>, or encapsulated CuCl<sub>2</sub> micelles, indicating no toxicity. Conversely, cancer cells exhibited high mortality rates when exposed to free CuCl<sub>2</sub> or encapsulated CuCl<sub>2</sub> micelles, which confirmed the effective delivery of CuCl<sub>2</sub> to cancer cells (Figure 2). Cancer cell apoptosis occurs due to the external stress from ROS (Reactive Oxygen Species) produced by CuCl<sub>2</sub>.

**Keywords:** Copper-64, Poly Ion Complex (PIC) micelles, Drug Delivery System (DDS), Cancer, Theranostics.

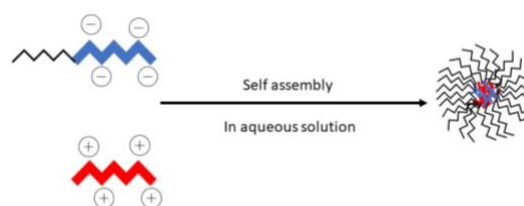


**Figure 1:** A schematic diagram illustrating the PIC micelle formation.

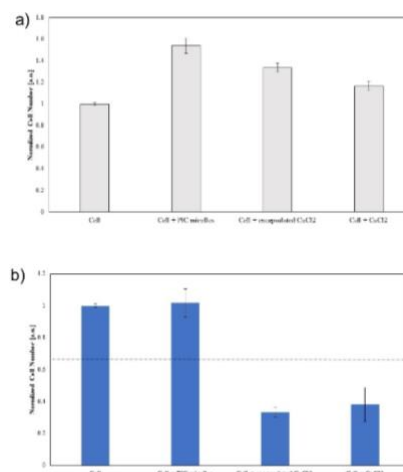


**Figure 2:** Panel (a) shows the effect of the encapsulated CuCl<sub>2</sub> on the HaCaT cell. Panel b. illustrates the HSC 3 cell line toxicity of the encapsulated CuCl<sub>2</sub>

## References:

1. Akihiro Kishimura, Development of polyion complex vesicles (PICsomes) from block copolymers for biomedical applications, *Polymer Journal* 45, 892–897, 2013.
2. Nobuya Hayashi et al., Activation of p53-Mediated Apoptosis Pathway in HSC3 Cancer Cell Irradiated by Atmospheric DBD Oxygen Plasma, *IEEE Transactions on Plasma Science*, Vol. 47, NO. 2, 2019.



# Release of indocyanine green from nanostructured absorbable patch manufactured by bio-printer

A. de Nigris<sup>1,\*</sup>, G. Quero<sup>2</sup>, G. P. Vanoli<sup>1</sup>, L. Ambrosone<sup>1</sup>

<sup>1</sup>Department of Medicine "V. Tiberio" (DiMeS), University of Molise, 86100, Campobasso, Italy

<sup>2</sup>Department of Biosciences and Territory (DiBT), University of Molise, 86090, Pesche, Italy

## Abstract:

Implantable delivery systems have the potential for maximizing efficacy while minimizing dose frequency and toxicity. Reservoir delivery systems provide potential advantages over matrix systems because filling a preformed reservoir eliminates exposure to heat, organic solvents, or shear stresses that cause inactivation of unstable molecules in matrix ones. In this research, a hydrogel based on sodium alginate and porcine gelatin was nanostructured using liposomes and fabricated using a 3D bio-printer.

The developed system constitutes the initial state of a bioresorbable implantable device that could deliver both hydrophobic and hydrophilic drugs. This study focuses on the kinetics and mechanism of release. The drug investigated is indocyanine green and the release kinetics is monitored by diffusion measurements from the solid matrix to the release bath (Fig. 1). Further investigations are conducted to understand how drug delivery is tuned by the presence of liposomes.

The surface morphology of the patch is evaluated through atomic force microscopy (Fig. 2). Finally, the experimental results will provide the basis for a predictive model useful for the *in vivo* release of the proposed nanostructured systems.

**Keywords:** liposomes, drug delivery, release kinetics, biopolymers, indocyanine green, bioprinting, model.

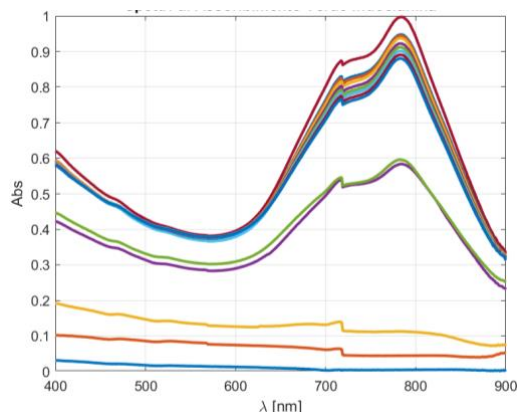


**Figure 1:** Spectrophotometric measurements of the free dye release kinetic in water from the polymeric patch.

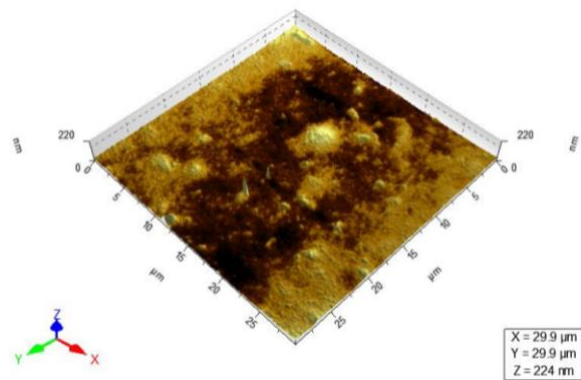


**Figure 2:** Atomic force microscopy image giving a graphical representation of the topology measurement acquired on the dried bio-printed samples containing the free drug.

## References:

1. Di Nezza F., Guerra G., et al. "Thermodynamic properties and photodegradation kinetics of indocyanine green in aqueous solution." *Dyes and Pigments* 134 (2016): 342-347.
2. Di Nezza F., Zeppa L., et al. "A physicochemical study of ophthalmology vital dyes: From dimerization equilibrium in buffer solution to their liposomal dispersions." *Dyes and Pigments* 162 (2019): 680-687.
3. Passaro F., Testa G., et al. "Nanotechnology-Based Cardiac Targeting and Direct Cardiac Reprogramming: The Betrothed". *Stem Cells Int* (2017) doi:10.1155/2017/4940397

# Developing Experimental Models to Characterise the Diffusion of Nanoparticles Through Complex Environments using a Novel Real-Time Label-Free Tracking Platform

M. Lorenzo López<sup>1,2,\*</sup>, V.R. Kearns<sup>2</sup>, E.A. Patterson<sup>1</sup>, J.M. Curran<sup>1</sup>

<sup>1</sup> School of Engineering, University of Liverpool, Liverpool, UK

<sup>2</sup> Department of Eye and Vision Science, University of Liverpool, Liverpool, UK

## Abstract:

Nanomedicine has the potential to increase the stability and bioavailability of drugs in the vitreous humour to treat retinal diseases. Thus, reducing the number of intravitreal injections needed and therefore their side effects. However, the pharmacokinetics of these novel therapeutics in the vitreous humour and how they reach the retina still need to be elucidated; *in vitro* models are necessary to understand the motion of nanocarriers in the posterior segment of the eye. Existing nanoparticle tracking techniques require fluorescent labels, which can affect nanoparticle motion, protein interactions, cell internalization, and impact cytotoxicity. In this study, a real-time label-free non-invasive tracking technology, for single nanoparticles in an optical inverted microscope based on the optical phenomena of caustics<sup>1</sup>, was used to characterise the diffusion of nanoparticles in agar-hyaluronic acid hydrogels, previously validated as vitreous humour substitutes for *in vitro* models<sup>2</sup>.

Three hydrogels with low, medium and high viscosity were synthesized using different concentrations of agar and hyaluronic acid in PBS. Gold nanoparticles (AuNP) were used to understand the effect of nanoparticle surface charge (100 nm AuNPs positively and negatively charged) and nanoparticle size (50 nm, 100 nm, and 200 nm AuNPs) on their diffusion and distribution in the synthetic hydrogels.

The results demonstrated that the diffusion of nanoparticles through these hydrogels was heterogeneous and representative of the local environment; in particular distinct diffusion profiles were associated with gel and liquid phases within the hydrogel (Fig 1). Nanoparticle size was a key factor in determining the behaviour, and distribution, of nanoparticles in the different phases. These findings suggest that nanoparticle diameter is a critical parameter for designing novel therapeutics for retinal diseases. Moreover, the surface charge of the nanoparticle did not affect their diffusion or distribution in these synthetic hydrogels. This label-free nanoparticle tracking technique is a powerful tool to characterise the diffusion and transport of nanoparticles in heterogeneous hydrogels. Hence, this technique has

the potential to become an indispensable method in the development of *in vitro* pre-clinical models to optimise nanoparticle-based drug delivery systems for the treatment of retinal diseases.

**Keywords:** Label-free, nanoparticle tracking, *in vitro* models, retinal diseases, drug delivery, nanomedicine, hydrogels.

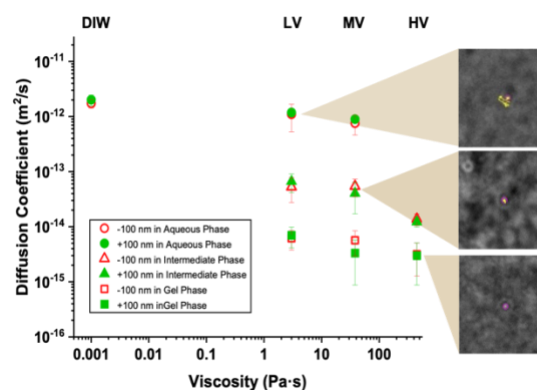


**Figure 1:** Diffusion coefficient values of 100 nm diameter AuNPs positively charged (green) and negatively charged (red) in deionized water (DIW) and in low (LV), medium (MV) and high viscous (HV) agar hyaluronic acid hydrogels at the physiological mid-eye temperature of 34°C. Showing the diffusion values for each hydrogel phase: aqueous phase (circles), intermediate phase (triangles), and gel phase (squares). Error bars correspond to  $\pm 1$  standard deviation. Images represent the AuNPs trails of motion in the three different hydrogel phases: aqueous, intermediate and gel (from top to bottom); in the three hydrogels: LV, MV, and HV (from top to bottom).

## References:

1. Patterson, E. A., & Whelan, M. P. (2008). Tracking nanoparticles in an optical microscope using caustics. *Nanotechnology*, 19(10), 105502.
2. Thakur, S. S., Shenoy, S. K., Suk, J. S., Hanes, J. S., & Rupenthal, I. D. (2020). Validation of hyaluronic acid-agar-based hydrogels as vitreous humor mimetics for *in vitro* drug and particle migration evaluations. *European journal of pharmaceuticals and biopharmaceutics*, 148, 118–125.

# Gold Nanoparticles and endothelial progenitor cells: a win-win alliance for targeting tumors

C. Anceschi<sup>1\*</sup>, E. Frediani<sup>1</sup>, J. Ruzzolini<sup>1</sup>, F. Margheri<sup>1</sup>, A. Chillà<sup>1</sup>, F. Ratto<sup>2</sup>, P. Armanetti<sup>3</sup>, L. Menichetti<sup>3</sup>, M. Del Rosso<sup>1</sup>, G. Fibbi<sup>1</sup>, A. Laurenzana<sup>1</sup>.

<sup>1</sup> Department of Experimental and Clinical Biomedical Sciences, University of Florence, Firenze

<sup>2</sup> Institute of Applied Physics “N. Carrara”, National Research Council Sesto Fiorentino, Italy

<sup>3</sup> Institute of Clinical Physiology (IFC) National Research Council, Pisa, Italy

## Abstract:

Plasmonic photothermal therapy utilizes biologically inert Near Infrared (NIR) gold nanoparticles (AuNPs) that convert light into heat capable of eliminating cancerous tissue. This approach has lower morbidity than surgical resection and can potentially synergize with other treatment modalities including chemotherapy and immunotherapy. In this work, we propose tumor tropic cellular vectors, called Endothelial Colony Forming Cells (ECFCs), enriched with gold chitosan-coated nanorods (AuNRs)<sup>1</sup>. ECFCs display a great capability to intake AuNRs without losing viability and exerting an *in vitro* and *in vivo* antitumor activity per se<sup>2</sup>. Conventional optical and Transmission electron microscopes (TEM), Photoacoustic imaging (PA) were used to evaluate AuNRs intracellular uptake in Melanoma cells (M6) and ECFCs. Melanoma spheroids were employed to investigate the behavior of AuNRs-ECFC in 3D-culture. The tumor tropic properties of AuNRs-ECFC were confirmed *in vivo*, using a human melanoma xenograft rat model. The PA signal provided from ECFC loaded with AuNRs exhibited a stronger enhancement compared to AuNRs-M6. As expected, ECFCs loaded with AuNRs, thanks to their ability to enter the spheroid, exert their antitumor activity by reducing the volume of the sphere, compared to control spheroids plated with unloaded ECFCs. Besides, the PA signal provided from AuNR-ECFCs inside spheroids exhibited a strong enhancement compared to M6-AuNRs ones. Histological analyses of explanted tumor mass demonstrate that gold is still retained after 1 week from injection and organs including liver, spleen, kidney, and lung did not show any morphological alteration compared to control rats treated with unloaded ECFCs. We demonstrated *in vitro* that AuNRs-loaded ECFCs are able to generate higher photoacoustic signals than AuNRs loaded in M6 cells. 3D cultures confirm the cytostatic effect of AuNRs-ECFC on tumor. *In vivo*, we show, via immunohistochemical analysis, a great

tumor-homing efficiency of AuNRs-ECFCs after a bolus intravenous administration and their permanence inside the tumor masses 1 week after administration. These important AuNRs properties will be exploited in the so called “Trojan Horse Strategy” to perform NIR-infrared photothermal ablation and re-sensitize melanoma cells to radiotherapy.

**Keywords:** Endothelial colony forming cells (ECFCs), near Infrared Light (NIR), Gold Nanorods (AuNRs), Melanoma cells, Photothermal ablation, Radiotherapy.

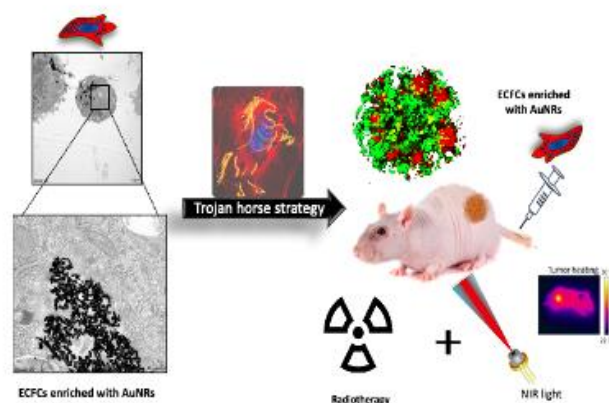


**Figure 1:** Endothelial Colony Forming Cells loaded with AuNRs exploit the “Trojan Horse Strategy” in order to reach the tumor mass and perform NIR-light photothermal ablation and radiotherapy.

## References:

1. Chillà A, et al. (Jul 20) “Cell-Mediated Release of Nanoparticles as a Preferential Option for Future Treatment of Melanoma.” *Cancers* vol. 12,7 1771. 2, doi:10.3390/cancers12071771
2. Armanetti P, et al. (Dec 20) Enhanced Antitumoral Activity and Photoacoustic Imaging Properties of AuNP-Enriched Endothelial Colony Forming Cells on Melanoma, *Adv Sci (Weinh)*. 2020;8(4): doi:10.1002/advs.202001175

# Yin/Yang effectiveness of gold nanoparticles in controlling tumor progression and promoting vascularization in vasculopathies

Anna Laurenzana<sup>1</sup>, Cecilia Anceschi<sup>1</sup>, Francesca Scavone<sup>1</sup>, Anastasia Chillà<sup>1</sup>, Elena Frediani<sup>1</sup>, Francesca Margheri<sup>1</sup>, Fulvio Ratto<sup>2</sup>, Claudia Borri<sup>2</sup>, Mario Del Rosso<sup>1</sup>, Tommaso del Rosso<sup>3</sup>, Gabriella Fibbi<sup>1</sup>

<sup>1</sup> Department of Experimental and Clinical Biomedical Sciences University of Florence Florence 50134 Italy. <sup>2</sup>

Institute of Applied Physics "N. Carrara" National Research Council Sesto Fiorentino 50019 Italy

<sup>3</sup> Department of Physics Pontifícia Universidade Católica do Rio de Janeiro Rio de Janeiro 22451-900 Brazil

## Abstract

The application of nanomaterials in the fields of medicine and biotechnology is of enormous interest, particularly in the areas where traditional solutions have failed. Nanoparticles can offer clear advantages compared to traditional therapies: i) fewer side effects of delivered drugs; ii) increased versatility in formulation; and iii) display of optical or magnetic properties that can be tuned to detect early disease (diagnosis) or to cause damage to cancer cells (therapy). Certainly, the biological activity of NPs depends on chemical and physical factors such as size and shape, surface area, agglomeration state, chemical composition, surface chemistry (charge and hydrophilicity), surface activity, solubility, dose, and so on. In particular, gold nanoparticles, due to the chemically inert nature of gold and the relative ease surface chemistry manipulation for downstream applications, have received much attention.

The present work describes the effects and biological interaction of two different types of gold nanoparticles on Endothelial Colony Forming Cells (ECFCs), a subtype of Progenitor Endothelial Cells (EPCs). We demonstrated that ECFCs can be heavily loaded with Near Infrared Gold Nanoparticles (NIR AuNPs) and be used as theranostic vector in two different cancer models. Indeed, NIR AuNP -loaded ECFCs enhanced AuNP optical properties and exhibited excellent thermotransductive property when exposed to Near infrared light. Moreover, NIR AuNPs are able to reach hypoxic areas of a 3D tumor model and could possibly re-sensitize tumors to radiotherapy.

Since ECFCs are considered as the most appropriate Endothelial cell (EC) type for therapeutic angiogenesis, we have shown that ECFCs loaded with a different type of Au-NPs (Au-carbinoids) having a peak of absorbance at 510nm and obtained by Pulsed Laser Ablation, trigger a cascade of events that stimulate neo-angiogenesis *in vitro* and *in vivo*.

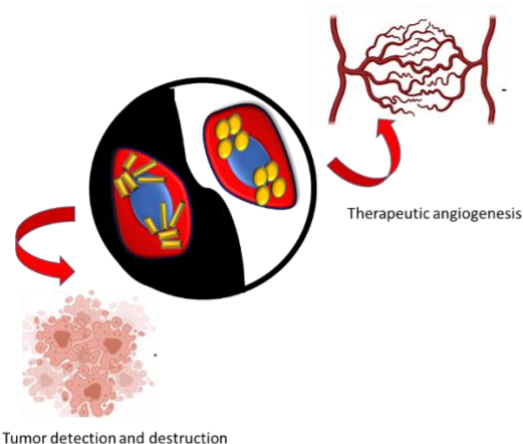


**Figure Caption:** Endothelial Colony Forming Cells loaded with gold nanoparticles can be used for photothermal treatment of tumors or to induce angiogenesis in vessel defective pathologies

**Keywords:** Near Infrared Gold Nanoparticle (NIR AuNPs); Pulsed-laser-ablated gold-nanoparticles (Au-Carbinoids), Endothelial Colony Forming Cells (ECFCs); Cancer cells; Angiogenesis; Vasculopathies

## Acknowledgment

This work was supported by Tuscany Region (Call on Health Bando Ricerca Salute 2018) through Project "THERMINATOR" and by Associazione Italiana Ricerca sul Cancro (AIRC) grant IG 2020 N. 24381.

## Conclusions

NIR-AuNP doped ECFCs appear to be a powerful theranostic tool for tailored early disease detection and innovative cancer treatment.

Au-carbinoids might represent a differential therapeutic option for patients with diseases associated with progressive loss of microvasculature



# Synthesis of nanostructured polymer systems for quantification of circulating biomarkers

P. Mastella <sup>1,2,\*</sup>, S. Luin <sup>2</sup>, F. Beltram <sup>1,2</sup>

<sup>1</sup>Fondazione Pisana per la Scienza, San Giuliano Terme, PI, Italy

<sup>2</sup>NEST Laboratories, Scuola Normale Superiore and CNR-NANO, Pisa, Italy

## Abstract:

Cancer pathologies can be monitored by measuring the concentration in biological fluids (e.g. blood or urine) of so-called tumour biomarkers: hormones, proteins or other biomolecules released by the cancerous tissue or by the body in response to certain types of neoplasia. This allows detecting the occurrence or recurrence of a tumour, or serves as an early indicator in monitoring treatments. The main obstacle currently limiting the application of this approach is the difficulty of common bioanalytical techniques in quantifying sub-picomolar concentrations. In this field, nanotechnology can offer important advantages over conventional techniques. The use of biodegradable and biocompatible polymer-based systems guarantees a high degree of flexibility in functionalisation and characterisation, while allowing possible future clinical uses. This work focuses on the synthesis of a polymer/oligonucleotide-based nanostructure for the recognition and quantification of proteins *in vivo*. The system studied is based on the use of polymeric nanoparticles of PVA (polyvinyl alcohol) or polyglutamic acid cross-linked by oligonucleotide sequences and loaded with releasable reporters. The experimental work involved the development of protocols for functionalising the polymer with oligomeric sequences using maleimide linkers. With this protocol, polymers were obtained derived with two different oligonucleotide sequences (linker A and linker B), designed to act as the reverse complement of a third oligonucleotide sequence containing an aptamer (Figure 1). The cross-link exploits the hybridisation of the three oligonucleotides, resulting in triggerable nanogels that disassemble upon recognition of the desired target by the specific aptamer. All the systems were characterised using appropriate analytical techniques to assess key parameters such as degree of functionalisation, size, polydispersity and component concentration.

**Keywords:** cancer, proteins, nanoparticles, polymers, oligonucleotides

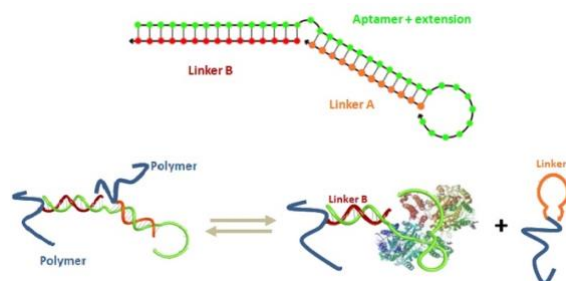


**Figure 1:** Schematic representation of the aptameric priming mechanism. Aptameric priming consists of two oligonucleotide sequences (A and B) that are partially complementary to the extended aptameric sequence, with linker A complementary to part of the original aptamer. The recognition of the target molecule (e.g. serum prostate antigen, PSA) alters the melting temperature of the oligonucleotides, leading to the nanostructure disassembly.

## References:

1. Matteoli, Giulia et al. "Aptamer-based gold nanoparticle aggregates for ultrasensitive amplification-free detection of PSMA." *Scientific reports* vol. 13,1 19926. 15 Nov. 2023. doi:10.1038/s41598-023-46974-4
2. Yang, Huanghao et al. "Engineering target-responsive hydrogels based on aptamer-target interactions." *Journal of the American Chemical Society* vol. 130,20 (2008): 6320-1. doi:10.1021/ja801339w



# Perfluorocarbon-PLGA particle ultrastructure affects pH sensitivity in $^{19}\text{F}$ NMR and MRI

Alvja Mali<sup>1,2</sup>, Mariah Daal<sup>1</sup>, Natalia Ziólkowska<sup>3</sup>, Nicolas Stumpe<sup>4</sup>, Naiara Larreina Vicente<sup>1,2</sup>, N. Koen van Riessen<sup>1</sup>, Visakh V. S. Pillai<sup>5</sup>, Francesco Simone Ruggeri<sup>5,6</sup>, Cyril Cadiou<sup>7</sup>, Françoise Chuburu<sup>7</sup>, Daniel Jirak<sup>3,8</sup>, Paul B. White<sup>9</sup>, Mangala Srinivas<sup>1,10</sup>

<sup>1</sup>Department of Cell Biology and Immunology, Wageningen University and Research, Wageningen, The Netherlands.

<sup>2</sup>Leiden University Medical Center, Leiden, The Netherlands.

<sup>3</sup>Institute for Clinical and Experimental Medicine, Vídeňská 1958/9, Prague, 140 21 Czech Republic.

<sup>4</sup>Institute for Molecular Cardiology, Heinrich Heine University, Düsseldorf, Germany (N.S., T.G.-S., U.F.).

<sup>5</sup>Physical Chemistry and Soft Matter, Wageningen University and Research, Wageningen, The Netherlands.

<sup>6</sup>Laboratory of Organic Chemistry, Wageningen University and Research, Wageningen, The Netherlands.

<sup>7</sup>ICMR Equipe e de Coordination, Université de Reims.

<sup>8</sup>Faculty of Health Studies, Technical University of Liberec, Studentská 1402/2, Liberec, 461 17 Czech Republic.

<sup>9</sup>Institute for Molecules and Materials, Radboud University, Nijmegen, The Netherlands.

<sup>10</sup>Cenya Imaging B.V., Amsterdam, The Netherlands.

## Abstract:

Magnetic resonance imaging (MRI) offers excellent tissue penetration and resolution, with  $^{19}\text{F}$  MRI showing great promise in biomedical research. The combination of fluorine-19 and paramagnetic chelates is widely used to exploit Paramagnetic Relaxation Enhancement (PRE) mostly for modulating  $^{19}\text{F}$  MRI signals in response to stimuli like acidity. Unlike traditional probes that rely on sensitive linkers, our approach leverages nanoparticle (NP) ultrastructure to trigger an “on-off” signal mechanism [1].

We developed a novel pH-sensitive “smart” probe using PLGA (Poly(D,L-lactide-co-glycolide)) NPs co-encapsulating hydrophobic gadolinium (Gd) chelate and PFCE (Perfluoro-15-crown-5-ether) with single-core and multi-core ultrastructures [2]. Multi-core NPs demonstrated substantial pH sensitivity, showing a 15-fold increase in  $^{19}\text{F}$   $T_2$  relaxation times and signal intensity from neutral to acidic pH, while single-core and control NPs maintained stable  $^{19}\text{F}$   $T_2$  and signal intensity [3]. Atomic Force Microscopy (AFM) detected a slight, statistically insignificant increase in NP diameter at acidic pH, which could influence the PRE effect due to its distance dependence.  $^{19}\text{F}$  NMR confirmed reversible pH sensitivity, with the signal returning to baseline upon neutralization.

In-cell  $^{19}\text{F}$  NMR revealed significant increases in  $^{19}\text{F}$  signal intensity and  $T_2$  values in response to intracellular acidity after 12 hours. Confocal microscopy confirmed NP localization in lysosomes, and proof-of-concept in vivo mouse

study validated pH responsiveness, with strong  $^{19}\text{F}$  signals observed within tumors. This research highlights the potential of multi-core PLGA NPs for advanced pH-sensitive diagnostics and therapeutic monitoring, demonstrating their utility in applications involving pH variations.

**Keywords:** PLGA NPs,  $^{19}\text{F}$  MRI, Paramagnetic relaxation enhancement, Perfluorocarbons, multi-core NPs, pH-sensitivity.

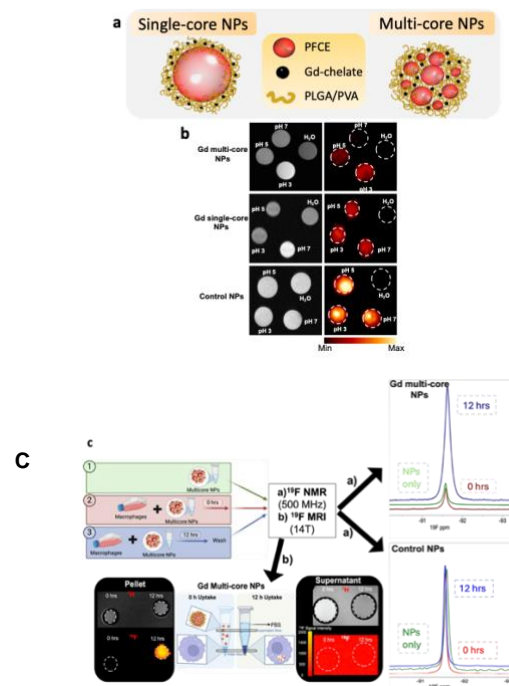


**Figure 1:** Figure (a) Schematic representation of single-core and multi-core PLGA NPs. (b)  $^{19}\text{F}$  and  $^1\text{H}$  MRI (14T) of Gd multi-core and

single-core NPs, along with control NPs, at pH 7, 5, and 3, highlighting the pH-sensitive signal enhancement of multi-core NPs. (c) In-cell  $^{19}\text{F}$  NMR and MRI showing cellular uptake and signal changes in response to intracellular acidity. "Time zero" represents the premix of NPs and cells, simulating NPs outside of the cells.

#### References:

1. Zhu, X., et al., *Stimuli-responsive  $^{19}\text{F}$  MRI probes: From materials design to in vitro detection and in vivo diagnosis*. *TrAC Trends in Analytical Chemistry*, 2024. **172**: p. 117607.
2. Koshkina, O., et al., *Multicore Liquid Perfluorocarbon-Loaded Multimodal Nanoparticles for Stable Ultrasound and  $^{19}\text{F}$  MRI Applied to In Vivo Cell Tracking*. *Advanced Functional Materials*, 2019. **29**(19): p. 1806485.
3. Mali, A., et al., *The internal structure of gadolinium and perfluorocarbon-loaded polymer nanoparticles affects  $^{19}\text{F}$  MRI relaxation times*. *Nanoscale*, 2023. **15**(44): p. 18068-18079.

# **SMS / EGF 2024 Session III. A: Applications for energy and environment**

# Anaerobic Biodegradation of Pharmaceutical Herbal Waste Using Batch Test Study

A. Hussain<sup>1</sup>, M. Priyadarshi<sup>1</sup>, P. Das<sup>1</sup>

<sup>1</sup> Civil Engineering Department, Netaji Subhas University of Technology, West Campus, Jaffarpur, New Delhi-110073, India

## **Abstract:**

The pharmaceutical industry generates a massive amount of herbal solid waste daily in India. For developing countries like India, the management of such waste is a challenging problem. However, anaerobic biodegradation of municipal solid waste and sewage sludges has emerged as the best alternative and promising technique in the management of such wastes around the globe. Given the above facts, the present study was carried out to assess the biochemical methane potential of herbal waste emanating from the pharmaceutical industry. The experimental batch test study was carried out using the wastes originating from four commonly used herbs, viz., Ashwagandha, Amla, Draksha, and Yavani as food and anaerobic digester sludge as inoculum along with required nutrients using a serum bottle technique. The batch tests were conducted under controlled mesophilic temperature conditions at 35°C with food to inoculum ratio of 0.75. The maximum biomethane potential and sludge activity were exhibited by the waste derived from the Ashwagandha herb owing to its higher organic content and better solubilization potential of its organic matter for biogas yield. On the other hand, albeit with higher organic matter present in the waste derived from the herb Yavani, it exhibited the least biogas yield due to the possible hindrance of waste solubilization by the presence of lignin and cellulose. The waste derived from Draksha and Amla showed intermediate biomethane potential and sludge activity. Overall, anaerobic digestion proves to be the best alternative, innovative option, and treatment method that can be a milestone for the proper management of industrial wastes and can be implemented on real-scale systems successfully.

**Keywords:** herbal waste, biochemical methane potential, anaerobic digestion, sludge activity, cellulose

# Ca(OH)<sub>2</sub> pellets with mesoporous alumina as a binder for thermochemical energy storage

David Castro<sup>1\*</sup>, E. S. Sanz-Pérez<sup>1</sup>, Laura Briones<sup>1</sup>, José María Escola<sup>1</sup>

<sup>1</sup>Chemical and Environmental Engineering Group, Rey Juan Carlos University, C/Tulipán s/n, 28933, Móstoles, Madrid, Spain, david.castro@urjc.es

## Abstract:

Renewable sources have emerged as a kind of clean energy to displace fossil fuels averting climate change. However, the main drawback is the intermittence of this energy, which can be overcome by thermal energy storage (TES) systems integrated in concentrated solar power (CSP) plants. The high energy density (178 kJ/mol) at elevated temperatures (> 600 °C) places the CaO+CO<sub>2</sub>↔CaCO<sub>3</sub> system as a promising TES system in CSP (1). Nevertheless, CaO powder used in fluidized beds produces attrition and sintering, resulting in a decay of the energy charge/discharge along cycles. CaO pellets are too soft, and cracking and agglomeration occur, hampering their commercial application. To solve this problem, pellets of Ca(OH)<sub>2</sub>/γ-Al<sub>2</sub>O<sub>3</sub> were synthesized with mesoporous γ-Al<sub>2</sub>O<sub>3</sub> as a binder in different concentrations (0-40 wt %) to increase the resistance to thermal stress and hinder the sintering, improving the energy storage ability (2). The samples were analyzed in a thermo-microbalance with 15 or 50 decarbonation/carbonation cycles. The CAA 20-20 pellet (60 wt % Ca(OH)<sub>2</sub>/20 wt % γ-Al<sub>2</sub>O<sub>3</sub>/20 wt % mesoporous γ-Al<sub>2</sub>O<sub>3</sub>) (Figure 1) showed the highest energy storage density (1030 kJ/kg pellet) with a remarkable crushing strength (~29 N), due to the formation of the calcium aluminate Mayenite (Ca<sub>12</sub>Al<sub>14</sub>O<sub>33</sub>) caused by the interaction between mesoporous γ-Al<sub>2</sub>O<sub>3</sub> and CaO. Additionally, Al-MCM-41 silica was used to coat the CAA 20-20 pellet to increase the crushing strength up to 37 N, taking a slight decay in the energy storage density after 50 cycles (824 kJ/kg pellet). Both CAA 20-20 pellets, coated and uncoated, are promising materials to be harnessed in calcium looping system in CSP plants.

**Keywords:** Thermochemical energy storage, CSP, CaO/CaCO<sub>3</sub> cycle, calcium looping, mesoporous alumina

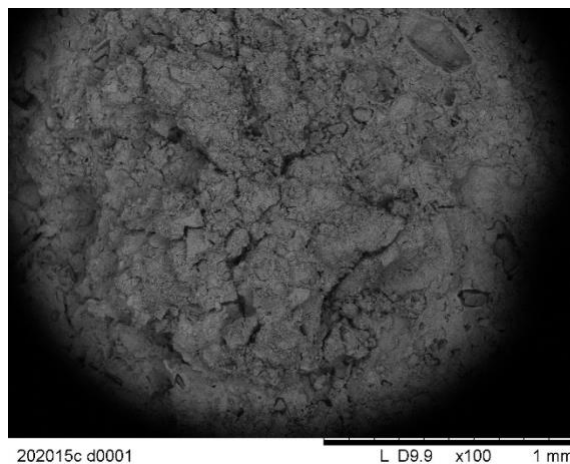


**Figure 1:** SEM images of the CAA 20-20 pellet (60 wt % Ca(OH)<sub>2</sub>/20 wt % γ-Al<sub>2</sub>O<sub>3</sub>/20 wt % mesoporous γ-Al<sub>2</sub>O<sub>3</sub>) after 50 decarbonation/carbonation cycles, wherein it can be observed that the pellet holds its integrity with only a few cracks over its surface despite the continuous expansion/contraction during the carbonation/decarbonation cycles.

## References:

1. Benítez-Guerrero, M., Valverde, J.M., Sanchez-Jimenez, P.E., Perejon, A., Perez-Maqueda, L.A. (2018). Calcium-Looping performance of mechanically modified Al<sub>2</sub>O<sub>3</sub>-CaO composites for energy storage and CO<sub>2</sub> capture. *Chem. Eng. J.*, 334, 2343-2355.
2. Castro-Yáñez D., Erans M., Peral A., Sanz R., González-Aguilar J., Romero M., Briones L., Sanz-Pérez E.S., Escola J.M. (2024). The key role played by mesoporous alumina as binder for obtaining ultra-hard CaO based pellets for thermochemical heat storage leveraging the CaO/CaCO<sub>3</sub> cycle. *J. Cleaner Prod.*, 448, 141702.



# Ecological enhancement of PVDF electroactive phase with plant-sourced ZnO for sustainable energy harvesting

Hajar Rejdali<sup>a,b</sup>, Imane Salhi<sup>a</sup>, Mhamed Boutaous<sup>b</sup>, Jacques Jay<sup>b</sup>, Abdelowahed Hajjaji<sup>a</sup>, Fouad Belhora<sup>a</sup>

<sup>a</sup>Laboratory of Engineering Sciences for Energy (LabSIPE), National School of Applied Sciences, El Jadida, 24002, Morocco

<sup>b</sup>Energy and Thermal of Lyon (CETHIL), INSA Lyon, Villeurbanne Cedex, 69621, France

## Abstract:

Amidst the dwindling resources of fossil fuels and growing concerns about the environmental impact of chemical batteries, the surge in demand for portable electronic devices and IoT technologies underscores the pressing need for advanced, lightweight, and sustainable energy conversion and power supply solutions. In this context, flexible piezoelectric nanogenerators emerge as highly promising contenders. They offer seamless integration with personal electronics and wireless sensors, providing a renewable energy source capable of sustained operation over extended periods. Poly(vinylidene fluoride) (PVDF) and its copolymers have captured significant attention in this field. Renowned for their flexibility, strength, ease of processing, and cost-effectiveness. Our current study focuses on doping the PVDF matrix with ZnO nanoparticles (0, 5, 10, and 15 wt%) using the solution casting method. Our approach stands out due to the selection of environmentally friendly materials. Unlike other doping composites often used with PVDF, such as lead zirconate titanate (PZT) (containing lead) and cadmium sulfide (CdS) (containing cadmium), known for their toxicity, our study utilizes ZnO nanoparticles derived from natural sources, which are environmentally friendly and cost-effective. The effect of these nanoparticles on the crystallization of the electroactive phase in PVDF films was then investigated using X-ray diffraction (Figure 1), scanning electron microscopy, FT-IR spectroscopy, and Raman spectroscopy. The composite film containing 10% by weight of ZnO exhibits a maximum  $\beta$  phase fraction of 86% compared to other films. This improvement can be attributed to the interfacial interactions occurring between the nanoparticle surface and the CH<sub>2</sub>/CF<sub>2</sub> dipoles of PVDF, thereby inducing the electroactive phases. Additionally, the differential scanning calorimetry technique used to analyze the thermal properties of the samples also shows an increase in the

$\beta$  phase fraction in PVDF. These findings offer promising prospects for enhancing the piezoelectric performance of the films, which can be subsequently utilized for vibrational and/or mechanical energy harvesting.

**Keywords:** Poly(vinylidene fluoride), piezoelectric, green ZnO, energy harvesting

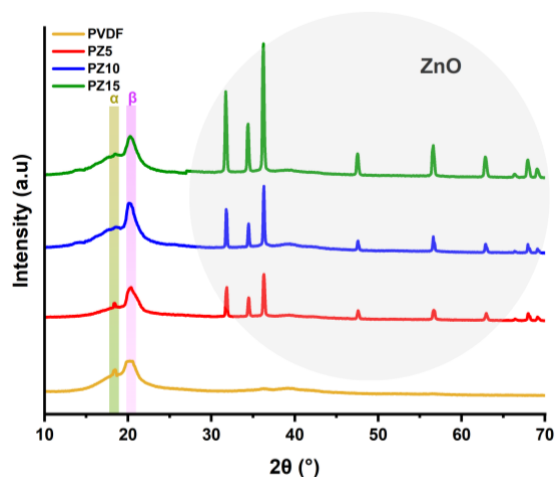


**Figure 1:** XRD spectra of PVDF pure, PZ5, PZ10, and PZ15.

## References:

1. K. Oumghar et al., "PVDF-HFP/PZT nanocomposite thin films: Preparation, structure and piezoelectric properties," *EPJ Applied Physics*, vol. 97, 2022
2. E. Kar, N. Bose, B. Dutta, S. Banerjee, N. Mukherjee, and S. Mukherjee, "2D SnO<sub>2</sub> nanosheet/PVDF composite based flexible, self-cleaning piezoelectric energy harvester," *Energy Convers Manag*, vol. 184, pp. 600–608, Mar. 2019.

# Covalent immobilization of EDTA onto graphene oxide and its application for heavy metal removal

Ahlam Al-Shammakhi, El-Said I. El-Shafey\*, Bushra Al-Wahaibi, Syeda N.F. Ali  
Chemistry department, Sultan Qaboos University, Muscat, Oman

## Abstract:

A novel method is introduced in this research. Graphene oxide (GO) was prepared from graphite via an oxidative exfoliation method. GO was surface functionalized using ethylene diamine and GO-NH<sub>2</sub> was produced. EDTA (H-form) was immobilized onto GO-NH<sub>2</sub> via an amide coupling process to produce GO-EDTA. Nitrogen content, FTIR, and TGA showed evidences of successful functionalization process. Pb(II), Cu(II) and Zn(II) solutions were tested for their sorption onto GO-EDTA (Na-form) in terms of sorbent mass, initial pH, contact time, metal concentration, and temperature. pH 6.0 was found optimum for metal sorption that took place via chelation. The kinetic sorption data were found to fit well pseudo second order model with better performance at a higher temperature. The activation energy (E<sub>a</sub>) of metal adsorption was less than 40 kJ/mol indicating the occurrence of physisorption. Equilibrium sorption data followed well the Langmuir isotherm with metal uptake following the order of Pb(II) > Cu(II) > Zn(II) with better performance at a higher temperature. Adsorption capacity was 72.4, 46.5 and 28.0 mg/g at 25 °C while it was 86.2, 56.8 and 31.95 mg/g at 35 °C for Pb(II), Cu(II) and Zn(II), respectively. Metal sorption followed the order: GO-EDTA > GO-NH<sub>2</sub> > GO. Metal sorption was found to be endothermic and spontaneous. GO-EDTA proved from this study that it is an effective sorbent for heavy metals and can be reused efficiently.

**Keywords:** graphene oxide, EDTA, immobilization, heavy metals, chelating ion exchanger.

## References

1. Chen, C. H., Hu, S., Shih, J. F., Yang, C. Y., Luo, Y. W., Jhang, R. H. & Hung Jr, Y. (2017). Effective synthesis of highly oxidized graphene oxide that enables wafer-scale nanopatterning: preformed acidic oxidizing medium approach. *Scientific reports*, 7(1), 1-10.
2. Al-Shamakhi, A., Al-Wahaibi, B., Ali, S. N. F., & El-Shafey, E. S. I. (2024). Covalently Immobilized EDTA onto Graphene Oxide Using Ethylene Diamine as a Crosslinker for Cu (II), Pb (II), and Zn (II) Sorption. *Solvent Extraction and Ion Exchange*, 1-23..

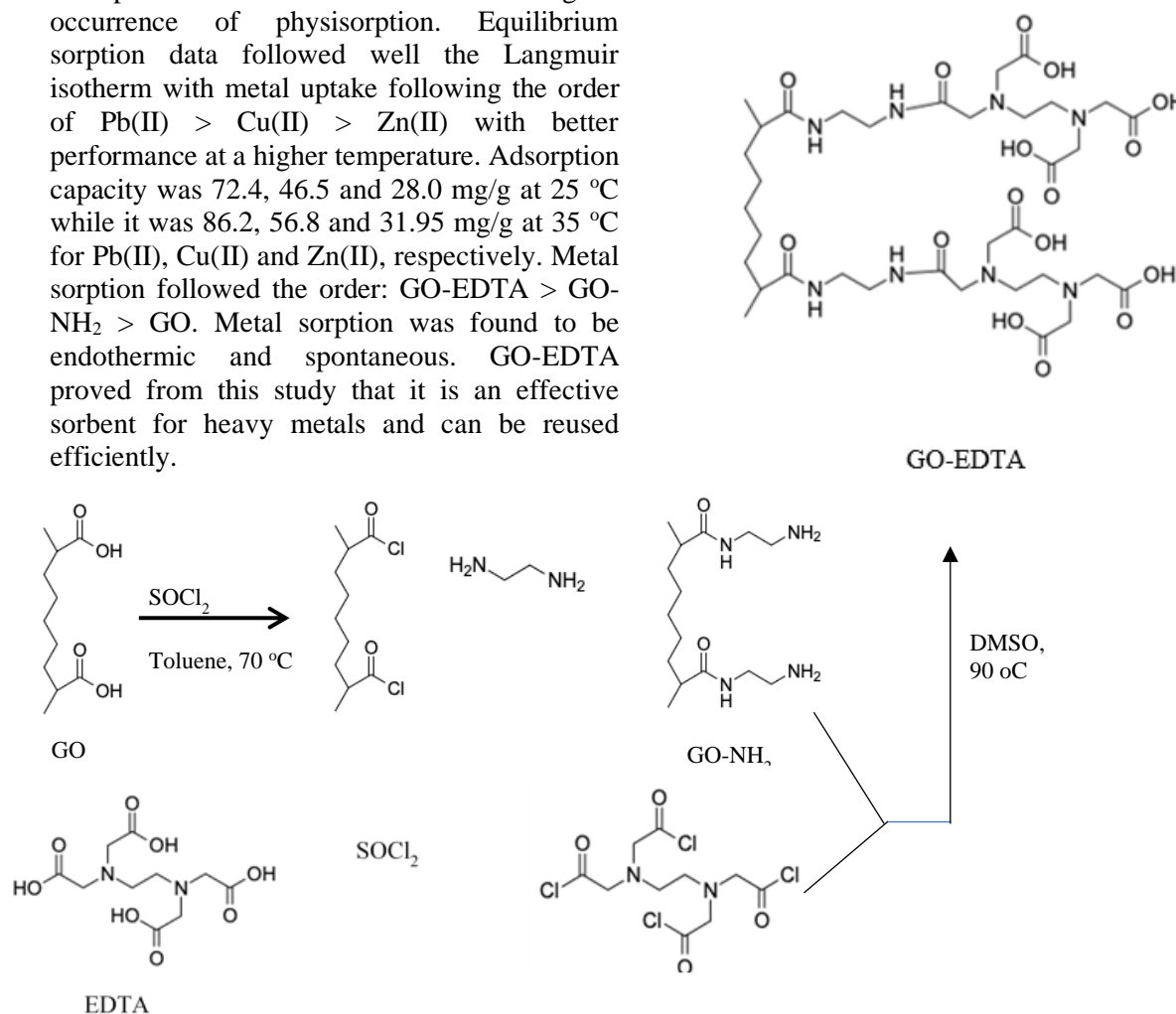


Figure 1. Preparation scheme of GO-EDTA

# PEO coatings for photocatalytic remediation of water

D. Czekanowska<sup>1,2,\*</sup>, C. Blawert<sup>3</sup>, M. Serdechnova<sup>3</sup>, A. Bamburov<sup>4</sup>, R. Vasilic<sup>5</sup>, P. Gluchowski<sup>1,2</sup>

<sup>1</sup> Graphene Energy Ltd, Wrocław, Poland

<sup>2</sup> Institute of Low Temperature and Structure Research, Polish Academy of Sciences, Wrocław, Poland

<sup>3</sup> Institute of Surface Science, Helmholtz-Zentrum Hereon, Geesthacht, Germany

<sup>4</sup> University of Aveiro, Aveiro, Portugal

<sup>5</sup> Faculty of Physics, University of Belgrade, Belgrade, Serbia

## Abstract:

Plasma electrolytic oxidation (PEO) is a high-voltage anodizing process that offers a prosperous technique for the manufacture of functional coatings. In short, it consists of passing high voltages through an aqueous electrolyte containing additional materials, which creates plasma discharge on the surface of the substrate. The main effect of this discharge is to produce a thick, hard and dense ceramic coating on substrates made of light alloys. Various materials with characteristic properties can be added to the aqueous electrolyte in the process and consequently to form layers for different applications. In the present case, we are employing thin films that show promise in the field of water treatment, taking advantage of their strong photocatalytic properties. The photocatalytic process for the above applications is one highly effective way of dealing with the growing problem of water pollution as evidenced by the extensive development of this topic in the environmental field. During the photocatalytic process, the photocatalyst, under exposure to UV-Vis radiation, is capable of degrading organic contaminants in water such as drugs, pesticides, and dyes. This is due to the photogeneration of electrons and holes in the electronic structure of the photocatalyst, which is capable of reacting on the surface of the material with dissolved oxygen and hydroxyl ions in water or with the water molecules themselves. This results in the formation of so-called reactive oxygen species (ROS) such as superoxide radicals ( $O_2^-$ ), and hydroxyl radicals (OH), which effectively lead to the breakdown of organic pollutants through chemical reactions. Significantly, the materials that make up our layers enable the formation of highly porous coatings that enhance the absorption of contaminants into their surface, translating into an enhanced photocatalytic reaction. For the creation of the layers, we used popular photocatalysts such as  $TiO_2$ -graphene,  $WO_3$ ,  $MoO_3$ ,  $Bi_2WO_6$  with different porosities and different configurations in terms of the arrangement of the individual photocatalyst layers in their hybrids. Importantly, the synthesized materials used to form the layers are characterized by appropriate energy gap sizes for the generation of ROS upon exposure to light in the

blue-green light range as confirmed by diffuse reflection spectroscopy, translating into their high photocatalytic activity, which has been tested on selected drugs and pesticides. Our materials have been extensively studied in terms of their structure, morphology, and photocatalytic activity. XRD studies on the photocatalyst powders as well as on the prepared coatings, showed that the crystal structure remains the same for layers as for bulk powders. SEM imaging of layers with EDS mapping in cross-section and without revealed the high porosity of our layers and the presence of individual elements derived from the photocatalyst in the layer structure. Thin films prepared in the form of convenient plates employing the PEO technique are therefore an extremely promising proposal in the strategy of eliminating hazardous pollutants in wastewater creating a real applied impact on environmental improvement.

**Keywords:** plasma electrolytic oxidation (PEO), water remediation, photocatalysis, hybrid photocatalysts.

## References:

1. Stojadinović, S., Radić, N., Vasilčić, R., Petković, M., Stefanov, P., Zeković, Lj., Grbić, B. (2012), Photocatalytic properties of  $TiO_2/WO_3$  coatings formed by plasma electrolytic oxidation of titanium in 12-tungstosilicic acid, *Applied Catalysis B: Environmental*, 126, 334-341.
2. Sikdar, S., Menezes, P.V., Maccione, R., Jacob, T., Menezes, P.L. (2021), Plasma Electrolytic Oxidation (PEO) Process-Processing, Properties, and Applications. *Nanomaterials*, 11(6), 1375.
3. Al-Nuaim, M.A., Alwasiti, A.A., Shnain, Z.Y. (2023), The photocatalytic process in the treatment of polluted water. *Chem. Pap.* 77, 677-701.

# Biodegradation of 2-Chlorophenol by anaerobic reduction on graphene oxide membranes supported on tubular ceramic filtration elements.

D. Guevara <sup>1\*</sup>, J. Font <sup>1</sup>, F. Stüber<sup>1</sup>

<sup>1</sup> Universitat Rovira i Virgili, Departament d'Enginyeria Química, Tarragona, Spain

\*[daniela.guevara@urv.cat](mailto:daniela.guevara@urv.cat)

## Abstract:

An ultrafiltration tubular ceramic membrane ( $ZrO_2-TiO_2$ , MWCO: 50 kg/mol, id: 3 mm, L: 250 mm, TAMI industries) was used as support for depositing a graphene oxide (GO) layer. The porous graphene oxide layer was formed by in-out vacuum-assisted filtration of a homogeneous GO solution through the tubular ceramic support (TCS). Graphene oxide powder was synthesized by a modified Hummer method starting from pristine graphite and it was characterized by different techniques such as XRD, Raman, and FTIR.

Once obtained the GO coated TCS, anaerobic biodegradation of model compounds was carried out. A synthetic wastewater solution (feed solution) was prepared and placed into a 1 L glass bottle (feed tank). For preparing this synthetic wastewater, 2-chlorophenol was selected as the model compound. Nitrogen gas was employed to pressurize the feed tank, allowing manual control of the flux through the tubular membrane by setting the transmembrane pressure (TMP), and simultaneously purging oxygen, thus maintaining anaerobic conditions. A small sample of anaerobic sludge from a municipal WWTP was inoculated onto the coated membrane surface to promote microbial strain growth capable of biodegrading 2-chlorophenol. Then the membrane was placed within a MEMBRALOX® filtration cell, serving as a compact bioreactor. Temperature control belongs to a refrigerator (1 °C for feed solution) and an incubator (37 °C for the bioreactor). An HPLC method was applied to quantify the 2-Chlorophenol removal. The schematic biodegradation system is shown in Figure 1.

The results showed the effective removal of 2-chlorophenol (negligible over non-GO coated membranes), even when it is present at a high inlet concentration (40 mg/L). Notably, while the concentration of 2-chlorophenol increased, the system exhibited high stability, achieving near 100 % removal efficiency for long time periods.

**Keywords:** 2-chlorophenol, anaerobic reduction, filtration cell, sludge.

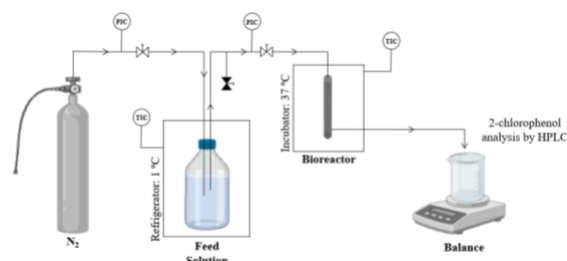


**Figure 1:** Schematic biodegradation system. The synthetic wastewater was continuously fed to the bioreactor at a constant flux of  $0.20 \text{ L} \cdot \text{m}^{-2} \cdot \text{h}^{-1}$ .

## References:

1. Amin, M. S. A. *et al.* Compact Carbon-Based membrane reactors for the intensified anaerobic decolorization of dye effluents. *Membranes* **12**, 174 (2022).
2. Giménez-Pérez, A. *et al.* Synthesis of N-doped and non-doped partially oxidized graphene membranes supported over ceramic materials. *Journal of Materials Science* **51**, 8346–8360 (2016).

# Efficient CoZnCr@MXene based electrocatalyst for High-Current-Density Alkaline Water Splitting at Industrial Temperature

P. Chauhan <sup>1,\*</sup>, Z. Sofer <sup>1</sup>

<sup>1</sup> Department of Inorganic Chemistry, University of Chemistry and Technology, Prague, Czech Republic

## Abstract:

The implementation of catalyst that can achieve high current densities under industrial conditions is essential for closing the gap between fundamental knowledge and practical applications. Designing rational surfaces is crucial for electrocatalysts to drive hydrogen economy forward. In this study, we designed CoZnCr LDH@Mo<sub>2</sub>TiC<sub>2</sub> MXene electrocatalyst with excellent catalytic activity in alkaline and seawater. The electrode demonstrates the excellent durability with very negligible potential decrement over 65 hr. The resulting electrode required 1.56 V to deliver 100 mA cm<sup>-2</sup> for overall water splitting. Furthermore, the catalyst retain high catalytic stability with an overpotential increase of less than 50 mV at 10 mA cm<sup>-2</sup> from 0 M to Sat. NaCl in electrolyte. Moreover, the electrode required only 1.47 V and 1.52 V to reach 10 mA cm<sup>-2</sup> under 1M KOH+Seawater and Natural seawater with excellent durability under 1M KOH+seawater over 52 hr. The results outlines strategies for creating high-performance electrocatalysts for industrial water splitting at high current densities.

**Keywords:** Hydrogen evolution, Oxygen Evolution, Overallwater splitting, Salinity, Seawater splitting



## **Sensors 2024 Session III.B: gas sensors, physical sensors, etc**

# Enhancement of Sensing Properties of Semiconductor Resistive Gas Sensors by Surface Treatment

Hyoun Woo Kim<sup>1</sup>, Sang Sub Kim<sup>2,\*</sup>

<sup>1</sup> Division of Materials Science and Engineering, Hanyang University, Seoul, Republic of Korea

<sup>2</sup> Department of Materials Science and Engineering, Inha University, Incheon, Republic of Korea

## Abstract:

The repeatable, reliable and ultra-high sensitive, humidity tolerant, selective, initial-stage detection of toxic and hazardous gaseous species has become increasingly important in modern industries and normal living places as well. The unique purpose of gas sensors include safety both in industry and at home, health care, defense of terror and chemical warfare, and environment monitoring. There are a variety types of gas sensors including chemiresistive-type, electrochemical type, optical type, and catalytic type, etc. They have their own advantages and disadvantages, and can be classified in terms of materials used, sensing principles, etc. Chemiresistive-type gas sensors have been extensively investigated for the purpose of exploiting its merits such as easy fabrication, low cost, adaptability to nanostructures, and potential possibility of attaining extremely high sensing performances. However, for practical application of the chemiresistive-type gas sensors, several sensing properties need to be further improved: higher selectivity to a target gas, long time stability, humidity tolerance, minimized temperature dependency, and specific detection, etc. In order to enhance such sensing capabilities, considerable efforts have been made so far [Figure 1]. Various techniques have been employed to improve the sensing capabilities of metal oxide chemiresistive-type gas sensors. In particular surface modification techniques are most widely used. Here, recent advancement and experimental results on surface modifications are discussed. Beam irradiation and surface decoration lead to great enhancement in sensing properties and will be discussed in detail.

**Keywords:** Gas sensors, Surface treatment, Resistive gas sensors, Surface decoration, Beam treatment, Semiconducting oxide gas sensors.

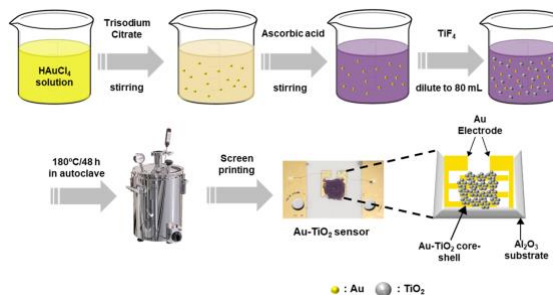


**Figure 1:** Schematics of the synthesis of Au-TiO<sub>2</sub> core-shell nanoparticles and the fabrication of the sensing device

## References:

1. Kim, J.H.; Mirzaei, A.; Bang, J.H.; Kim, H.W.; Kim, S.S. Achievement of Self-Heated Sensing of Hazardous Gases by WS<sub>2</sub> (core)-SnO<sub>2</sub> (shell) Nanosheets. *J. Hazard. Mater.* 2021, *412*, 125196.
2. Kim, J.H.; Mirzaei, A.; Sakaguchi, I.; Hishita, S.; Ohsawa, T.; Suzuki, T.T.; Kim, S.S.; Saito, N. Decoration of Pt/Pd Bimetallic Nanoparticles on Ru-Implanted WS<sub>2</sub> Nano-sheets for Acetone Sensing Studies. *Appl. Surf. Sci.* 2023, *641*, 158478.

# Development of an electrochemical oxygen micro sensor for industrial application

Amira Benayache<sup>1</sup>, Virginie Martini<sup>1</sup>, Caroline Marlot<sup>2</sup>, Khalifa Aguir<sup>1</sup>

<sup>1</sup> Aix Marseille Univ, CNRS, IM2NP, Marseille, France,

<sup>2</sup> SETNAG, Marseille, France

## Abstract:

Oxygen sensors are widely used in many sectors such as automobile, health, and process control in addition of food industry. SETNAG company would like to develop a new market by miniaturize its oxygen probe. The MicroPoas is a handmade probe, which is the main part of SETNAG's oxygen analyzers. This probe works under electrochemical principle [1]. An equilibrium is created between a reference atmosphere and the analyzed atmosphere. The measured value is a difference of potential. These phenomena are governed by Nernst law. The material of the active part is yttria stabilized zirconia (YSZ) well known for oxygen detection [2]. After manufacturing the probe is inserted in a tubular furnace to reach temperatures around 600°C. Moving on a miniaturized sensor device using microelectronic technique will allow us to reduce power consumption and fabrication delay. The design of our microsensor includes a platinum micro heater to reach the chosen work temperature, a reference layer (not uncluded for now) and a sensitive YSZ thin layer. Firstly, we studied the sensitive layer which is deposited by reactive magnetron sputtering using an industrial target (8% mol). We determined the well-adapted deposition parameters presented in table 1. The YSZ thin film has been deposited on Si/SiO<sub>2</sub> substrate and an interdigitated platinum electrode for planar first electrical tests. Then a sandwich configuration has been realized to obtain transversal measurements like into the integrated device (Figure 1). The measurements have been carried on obtaining resistance variation of the sensitive YSZ layer under different exposition concentrations of oxygen (5% O<sub>2</sub>, 8% O<sub>2</sub>, 15% O<sub>2</sub>, and 20% O<sub>2</sub>). Additional analyses included SEM and EDX for chemical and structural assessments will be discussed. After several electrical tests of YSZ layer under different concentrations of oxygen, resistance response changes are relevant ((Figure 2) depending on the layer thickness and the working temperature of the sensor. EDX analysis confirmed the uniformity and the amount of deposited YSZ of 6.4 ± 0.3% mol.

**Keywords:** Oxygen microsensor, Electrochemical sensor, Ytria Stabilized Zirconia, MicroPoas

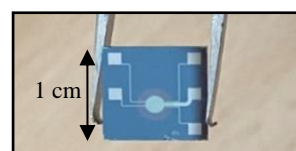


**Figure 1:** Photograph of the realized sensor (ship size 8x8 mm). The chip includes a Pt sensor to measure the temperature, as well as two other Pt electrodes to measure the gas response of the sensitive layer. The active layer, shaped like a circle, appears in a purple color.

Pressure (mbar)	Flow Ar/O <sub>2</sub> (sccm)	Power (Watt)	Thickness (nm)
30*10 <sup>-3</sup>	30/10	100	200

**Table 1:** Parameters of a deposited layer of YSZ by reactive magnetron sputtering.

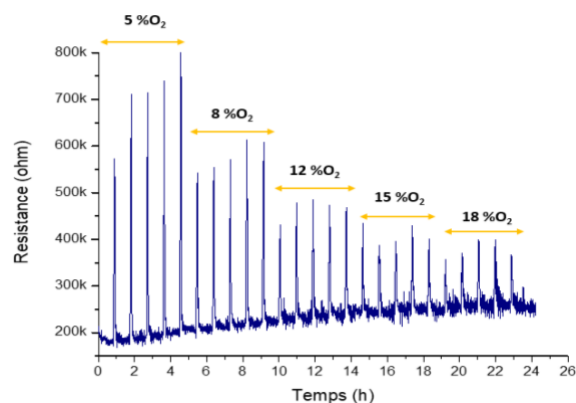


**Figure 2:** YSZ sensitive layer resistance measurement under two different O<sub>2</sub> concentrations at 600°C (exposure time 5 min), sandwich polarization (-0.4V) and planar polarization (0.2V).

## References:

1. Zirconia Probe with Internal Metal Reference, CNRS/ANVAR/University of Grenoble Patent filed in September (1973).
2. Halley, S., Ramaiyan, K. P., Tsui, L.-k., & Garzon, F. (2022). A review of zirconia oxygen, NO<sub>x</sub>, and mixed potential gas sensors – History and current trends. *Sensors and Actuators B: Chemical*, 370, 132363. [DOI: 10.1016/j.snb.2022.13236]

# Optimizing Gas Sensing Response: High-Temperature Gradient Laser Annealing of Block Copolymer-Templated Metal Oxide Nanowires

P. Pula <sup>1\*</sup>, P.W. Majewski <sup>1</sup>

<sup>1</sup> Chemistry Department, University of Warsaw, Warsaw, Poland

## Abstract:

Gas sensors play a critical role in detecting volatile compounds in the environment, with high response being one of critical parameters of sensor efficacy. To enhance it, nanostructures, among them nanowires, provide a highly developed surface that provides reactive interface for sensed molecules. Recently, we introduced a rapid and efficient Solvent Evaporation Annealing (SEA) protocol for the selective deposition of metal oxide nanowires within a self-assembled organic block copolymer template. Our study demonstrated the ethanol sensing capabilities of such nanowire stacks.[1] However, the performance of gas sensors utilizing metal oxide nanowires is heavily dependent on the degree of crystallinity within the nanostructure. Optimal crystallinity enhances nanowire conductivity and continuity, thereby improving sensor characteristics. To expedite the determination of the optimal annealing temperature for oxide nanowire mesh obtained through SEA, we propose a novel approach. In this method, a high-power infrared laser beam formed in a line-shape, incident on a silicon substrate with the nanowires deposited, generates a localized high 1D thermal gradient along the substrate. This controlled thermal environment enables precise determination of the optimal temperature in a single-step process, significantly reducing experimentation time and resource usage. Additionally, the technique eliminates polymer residues known to hinder sensor responsivity and electrical performance. A sample can be photothermally annealed in a closed vacuum chamber with a transparent lid and under oxidizing/reducing conditions. For the demonstration of utility of such setup we have tested iron oxide multilayered mesh response and selected annealing temperature providing highest investigated response. This innovative approach offers accelerated establishment of the optimum annealing temperature, promising enhanced gas sensing capabilities.

**Keywords:** block copolymers, metal oxide nanowires, gas sensors, high-temperature annealing.

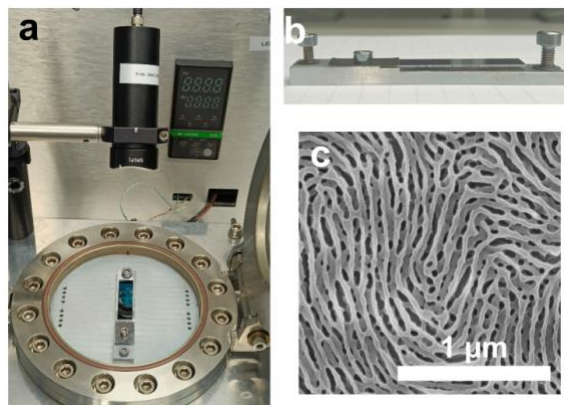


**Figure 1:** a) a picture of an experimental setup with a laser head on top and a steel bar with a silicon substrate mounted in the chamber bottom, b) the steel bar with a silicon substrate magnified, c) morphology of an iron oxide replica after high-temperature annealing in air atmosphere.

## References:

1. Pula, P., Leniart, A. A., Krol, J., Gorzkowski, M. T., Suster, M. C., Wrobel, P., Lewera, A., Majewski, P. W. (2023). Block Copolymer-Templated, Single-Step Synthesis of Transition Metal Oxide Nanostructures for Sensing Applications, *ACS Appl. Mater. Interfaces*, 15(50), 57970-57980.

# Experimental Investigation of Thermal Tuning for Laterally Excited Bulk Acoustic Wave MEMS Resonators using SOI Bulk Heating

M. Bengashier\*, O. Casha, I. Grech, R. Farrugia, J. Micallef and E. Gatt  
Department of Microelectronics and Nanoelectronics, University of Malta, Msida, Malta

## Abstract:

Lateral-mode MEMS resonators employing piezoelectric actuation, have been successfully implemented within applications including filters and clock generators, as a replacement of the quartz crystal component. The shift in the resonant frequency due to environmental conditions such as temperature and pressure variations, or fabrication process tolerances, such as those due to geometrical dimensions and material properties variations, is still considered to be a drawback for MEMS resonators. Therefore, the ability to fine tuning the frequency of a resonator is critical in several high precision applications. This paper presents the experimental investigation of electrothermal fine frequency tuning for a 60 MHz laterally excited contour mode bulk acoustic wave (LBAW) MEMS resonator, fabricated using the PiezoMUMPs multi-process wafer process, which consists of a  $0.5\ \mu\text{m}$  Aluminium Nitride (AlN) layer over a silicon-on-insulator (SOI) structure having a thickness of  $10\ \mu\text{m}$  (Figure 1). Tuning is achieved via electrothermal SOI bulk heating of the resonator, so that its resonant frequency is shifted by inducing additional stresses in the device, as well as varying its elastic properties via a temperature change. While this paper focuses on the application of SOI bulk heating to MEMS resonators, the same heating principle can be employed in other applications, such as the calibration or resetting of MEMS gas sensors based on resonators coated with a functionalized layer. Figure 1(b) presents a micrograph of the fabricated five element electrode LBAW PiezoMUMPs resonator. It includes two additional metal heating electrodes positioned directly over the SOI layer on both sides of the resonator, enabling a closed-loop current to be applied through bonding wires. This setup generates electrothermal power, heating the SOI layer and transferring the heat to the resonator body through the tethers. Additionally, two sensing metal electrodes with an oxide layer beneath them are used to measure the scattering parameter  $S_{21}$  via a vector network analyzer. To vary the heating current, a voltage source of 9 V and a 15 k $\Omega$  variable resistor connected in series with the heating electrodes was used. The measured transmission magnitude plots for different heating currents are shown in Figure 2. These experimental results show that the resonant frequency decreases

with an increase in the electrical heating power applied to the resonator SOI bulk via the two heating electrodes. For a 50 mW heating power swing, the resonator frequency varies from 61.368 MHz to 61.418 MHz, as shown in Figure 2. Measured results show that the SOI bulk resistance remains approximately constant over this tuning range, with a value of around 31  $\Omega$ .

**Keywords:** Thermal Tuning, SOI Bulk Heating, LBAW Resonators, PiezoMUMPs, MEMS.

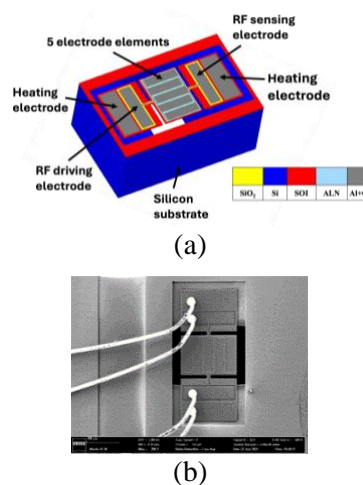


**Figure 1:** (a) Simplified diagram of the LBAW rectangular resonator including the pads used for electrothermal tuning (b) Micrograph of the fabricated LBAW PiezoMUMPs resonator including two electrothermal heating electrodes.

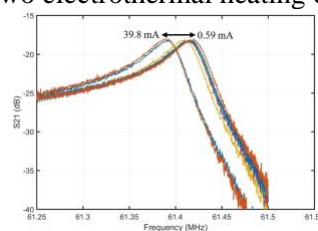


**Figure 2:** Measured variation of the frequency response of the resonator transmission gain  $|S_{21}|$  with the heating element current.

## References:

1. Sviličića, B. (2016) Tunability of Piezoelectric MEMS Ring Resonator Based Filter, *Procedia Engineering*, 168, 1517-1520.
2. Zhang, W., Hu, K., Peng, Z., Meng, G. (2015) Tunable micro- and nanomechanical resonators, *Sensors*, 15 (10), pp. 26478-26566.



# Impact of Optical Fiber Design on the Performance of Interferometric Temperature Sensors at Elevated Temperatures

S. Pevec<sup>1\*</sup>, M. Njegovec<sup>1</sup>, V. Budinski<sup>1</sup>, V. Žužek<sup>2</sup>, J. Bojkovski<sup>2</sup>, D. Donlagic<sup>1</sup>  
<sup>1</sup>Faculty of Electrical Engineering and Computer Science, University of Maribor, Slovenia  
<sup>2</sup>Faculty of Electrical Engineering, University of Ljubljana, 1000 Ljubljana, Slovenia

## Abstract:

Investigation of the impact of the optical fiber core design and composition on the performance of fiber-based interferometric temperature sensors at elevated temperatures is presented. A collection of commercially available single-mode fibers with different core designs and compositions were configured into otherwise nearly identical Fabry-Perot temperature sensors, which were then systemically tested for drift at a range of elevated temperatures between 200 and 800 °C. Results indicate that sensor drifts correlate to core doping levels and fiber designs. In some fibers, significant drifts were observed even at temperatures below 400 °C, while all sensors exhibited significant drifts at temperatures above 600 °C. The latter partially agrees with various but also inconclusive reports available in the literature. The further investigation utilized annealing of sensors at a maximum temperature that did not cause significant fiber devitrification. All annealed sensors demonstrated substantial improvement in their stability at elevated temperatures, even if they were submitted to relatively fast cooling cycles. However, even with this aggressive annealing procedure, while it reduced drifts and thus potentially extended applicable operating temperature ranges, it did not completely eliminate issues with the drifts at the high end of the attainable operating temperature range. A clear correlation of the sensor drifts to fiber core compositions, however, points towards potential opportunities where specialty optical fibers with modified core composition might further improve the performance of interference sensors (and FBGs) performance at the highest operating temperature.

**Keywords:** Optical fibers, temperature sensors, Fabry-Perot interferometer, core-dopant composition, fiber design.

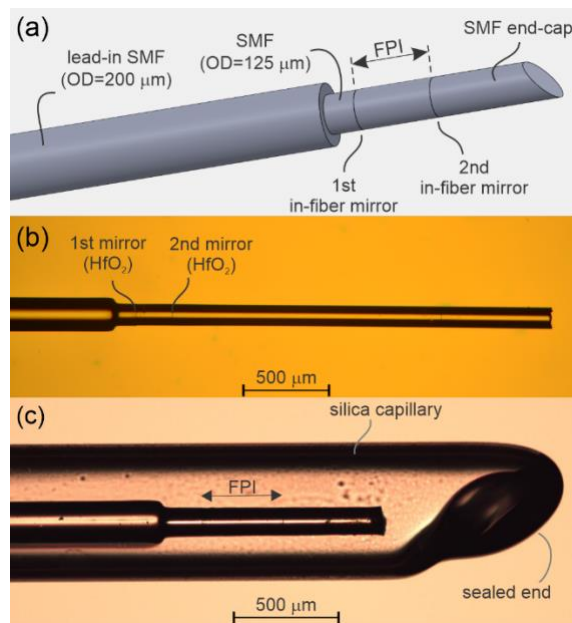


**Figure 1:** Temperature sensor: (a) sensor design, (b) optical image of typical fabricated sensor, (c) sensor packaged in quartz capillary.

## Funding:

This research was funded by EURAMET, INFOTherm (Grant No. 22IEM07) and Slovenian Research Agency (ARIS) under grant no. P2-0368.

## References:

1. Grobnic, D.; Hnatovsky, C.; Dedyulin, S.; Walker, R. B.; Ding, H. M.; Mihailov, S. J. (2021), Fiber Bragg Grating Wavelength Drift in Long-Term High Temperature Annealing. *Sensors-Basel* 21, 1-28.
2. Chen, Z. S.; Xiong, S. S.; Gao, S. C.; Zhang, H.; Wan, L.; Huang, X. C.; Huang, B. S.; Feng, Y. H.; Liu, W. P.; Li, Z. H. (2018), High-Temperature Sensor Based on Fabry-Perot Interferometer in Microfiber Tip. *Sensors-Basel* 18, 1-7.
3. Paek, U. C.; Kurkjian, C. R. (1975), Calculation of Cooling Rate and Induced Stresses in Drawing of Optical Fibers. *J Am Ceram Soc* 58, 330-335.

# A modular gamma-ray scanner consisting of two linear CsI+SiPM arrays for radioactive waste sorting

Gaetano Elio Poma<sup>1\*</sup>, Chiara Rita Failla<sup>1</sup>, Luigi Giovanni Cosentino<sup>1</sup>, Fabio Longhitano<sup>2</sup>,  
Gianfranco Vecchio<sup>1</sup>, Paolo Finocchiaro<sup>1</sup>

<sup>1</sup>INFN-LNS, Via S. Sofia 62, 95125, Catania, Italy

<sup>2</sup>INFN-Sezione di Catania, Via S. Sofia 64, 95123, Catania, Italy

## Abstract:

A significant advancement in radiation detection and localization is represented by the PI3SO (Proximity Imaging System for Sort and Segregate Operations) project. The system employs a double-array scanner equipped with CsI(Tl) scintillators and Silicon Photo-Multipliers (SiPMs) to identify and localize radioactive materials. Our evaluation highlights its capability to detect and quantify radioactive sources even in the presence of shielding materials.

Comprising of 128 CsI(Tl)+SiPM detectors arranged in a double-array configuration, the PI3SO system offers extensive coverage and redundancy. Initial characterization tests of individual detector elements provided a robust foundation for understanding the system's overall performance. These detectors were calibrated with known radioactive sources, and their performance was assessed based on energy resolution and peak detection capabilities.

During experimental trials, the system was tested with three distinct radioactive sources (<sup>137</sup>Cs, <sup>60</sup>Co, and <sup>22</sup>Na) placed at predetermined positions. The system effectively identified gamma sources, with results visually represented through imaging, indicating the presence and intensity of radioactive materials. A notable achievement was the system's ability to detect and localize a shielded <sup>137</sup>Cs source covered with a lead slab, underscoring its robustness in scenarios where materials may be partially or fully obscured.

Further validation of the PI3SO system was achieved by evaluating its energy resolution and detection efficiency. The system achieved an energy resolution of approximately 9% FWHM at 662 keV (for <sup>137</sup>Cs), aligning with benchmark values for similar detectors. The capabilities of the PI3SO system, even in the presence of shielding, make it a valuable tool for nuclear decommissioning and radioactive waste (radwaste) sort and segregate operations. Our findings indicate that the PI3SO system not only enhances safety and efficiency in handling

radioactive materials but also provides a robust solution for both routine monitoring and emergency response scenarios. Future research will focus on refining the system's capabilities, placing it at the forefront of radiation detection technology.

**Keywords:** radiation detection, CsI(Tl) scintillators, Silicon Photo-Multipliers (SiPMs), energy resolution, radioactive sources, gamma-ray spectra, shielding materials, nuclear decommissioning.

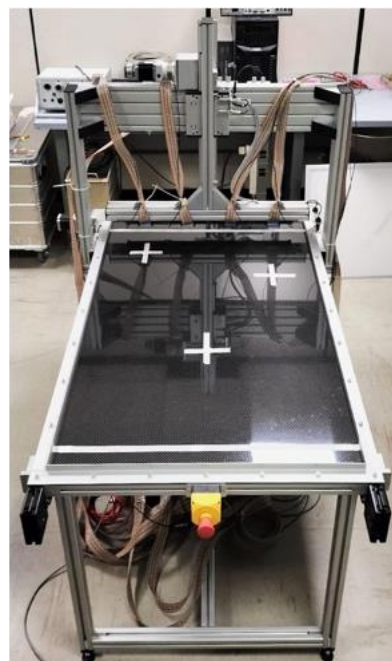


**Figure 1:** Top view of the PI3SO gamma-ray scanner table. 4+4 ribbon cables for the signals from the 128 detectors are visible, along with the data acquisition and power supply electronics installed under the table.

## References:

1. G. E. Poma et al., "Hot-spots finding with modular gamma-ray system for sort and segregate activities," in EPJ Web of Conferences, vol. 288, p. 06007, EDP Sciences, 2023.

# Posters Abstracts

# Sol gel microencapsulated additives for auto-healing coatings of galvanized stainless steel

L. Florentino<sup>1,2\*</sup>, O. Conejero<sup>1,2</sup>, R. B. de la Rua<sup>1,2</sup>

<sup>1</sup> Surface Department. Idonial Foundation, C/ Calafates, 33417 Avilés, Spain

<sup>2</sup> Research funded by the Ministry of Science and Innovation through the Center for Industrial Technological Development (CDTI), CER-20231008.

## Abstract:

The microencapsulation of active substances for inclusion in smart surface coatings is currently proposed as a novel technique to protect their integrity and functionality, so that their activity does not take place until the capsule shell is opened upon receipt of a stimulus. Metallic corrosion continues to be a current problem in the industry as it is a degradation process that occurs naturally and inevitably. Among the methods available to prevent this phenomenon, the application of coatings is the most convenient alternative due to its low cost, simplicity, flexibility and availability of starting materials. However, their use entails other problems such as cracking or degradation, so they must be repaired or replaced, since any crack or defect in them would cause corrosive substances to reach the metal surface. For this reason, the use of self-healing coatings is considered in recent times as the most innovative option. This type of coatings are based on the use of additives capable of repairing the defects in the damaged areas. Direct doping with these additives has been widely studied but has some disadvantages, such as easy leaching from the matrix or reaction with some of its components and consequent loss of efficiency. In this work, isolation of these self-repairing agents was carried out efficiently by microencapsulation (Figure 1). The most commonly used methods for their microencapsulation are in-situ or interfacial polymerization [1]. Isocyanates are the most promising self-healing reagents as they do not require a catalyst, however, their encapsulation is hampered by their high reactivity [2]. Most examples in the literature are based on the introduction of these capsules in epoxy resins but few and very recent are the examples where they are introduced in sol gel matrix for self-healing coating of a galvanized steel [3]. Here we describe the encapsulation technique of interesting additives by sol gel technology, synthesizing “microcontainers” of these compounds to achieve a more prolonged effect and isolate the inhibitor from the coating matrix. In addition, these microcapsules are dispersed in

a new sol gel coating formulation specially designed for galvanized steel to increase its corrosion resistance and provide it with self-repairing capabilities.

**Keywords:** sol-gel technology, smart coating, microencapsulation, corrosion, auto-healing, self-healing, stimulus-response, microcontainers, anti-corrosion additives.

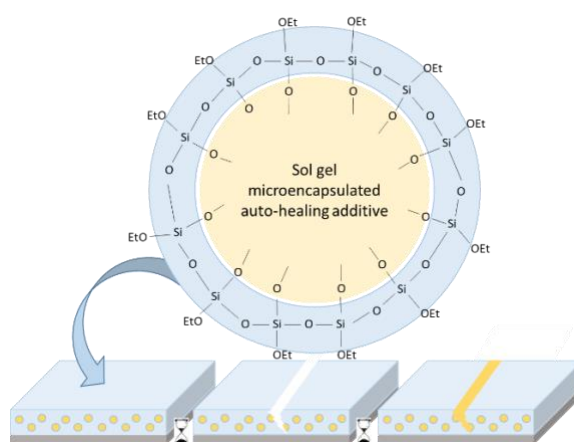


**Figure 1:** Scheme of self-healing additive protected by sol-gel shell and its mode of action when it is part of a functional coating, also designed by the sol-gel technique. The drawing illustrates how these self-healing additives allow to fill cracks or small pinholes automatically and autonomously acting in response to a stimulus.

## References

1. Guo Liang Li et al. Synthesis of Polyurethane/Poly(urea-formaldehyde) Double-shelled Microcapsules for Self-healing Anticorrosion Coatings. *Chinese Journal of Polymer Science*, 2020, 38, 45–52.
2. Santos et al. Microencapsulation of reactive isocyanates for application in self-healing materials: a review, *Journal of Microencapsulation*, 2021, 38, 5, 338–356.
3. Huang, Y. et al. Enhanced corrosion resistance and self-healing effect of sol-gel coating incorporating one-pot-synthesized corrosion inhibitor-encapsulated silica nanocontainers. *J Sol-Gel Sci Technol*, 2022, 104, 78–90.

# Development of hybrid sol-gel coatings with improved anticorrosion properties for Cr-free passivation of galvanized steel

M. Prado <sup>1\*</sup>, P. Sánchez <sup>1</sup>, O. Conejero <sup>1</sup>  
<sup>1</sup> Idonial Technology Centre, Avilés, Spain

## Abstract:

Chromium (VI)-based conversion coatings have been widely used in the post-treatment of galvanized steel and other metals due to their high corrosion resistance and self-healing capability. However, due to its high toxicity and carcinogenicity, the use of hexavalent chromium has been limited in many countries. Silane technology appear to be a viable alternative for the replacement of chromium(VI)-based coatings. This technology is based on a group of silicon-based organic-inorganic chemicals that offer corrosion protection for metals and stable adhesion to a wide range of paints. Among all of them, sol-gel coatings have proven to be useful for improving corrosion resistance when applied on metallic materials. This sol-gel technology involves the creation of a network of oxides by hydrolysis and condensation reactions from different precursors in a liquid medium

The synthesis of coatings via sol-gel can be done from inorganic or organic precursors, each of them with different characteristics. For that reason and in order to take advantage of the different characteristics of both precursors, hybrid coatings have been investigated, where the organic component is incorporated into the inorganic matrix to give the coating unique properties in terms of morphology, size and multifunctional properties associated with the interaction between the two components.

In this work hybrid sol-gel coatings were prepared under different experimental conditions by hydrolysis of 3-(Glycidoxy propyl) methyl diethoxy silane (GPTMS) and tetra-ethyl-ortosilicate (TEOS). Polyvinylpirrolidone (PVP) and polyethylene glycol (PEG-6000) were employed in order to improve coating thickness and minimise stresses in the curing stage.

In addition, different inhibiting agents such as ZnO and ZrO nanoparticles, lanthanum and zirconil nitrate, were added in different percentages to the sol-gel matrix in order to improve the anti-corrosion properties and thus extend the life of the coating. The sol-gel film was deposited on galvanized steel plates by dip coating.

**Keywords:** Hybrid sol-gel coating, anticorrosión, Cr(VI) replacement

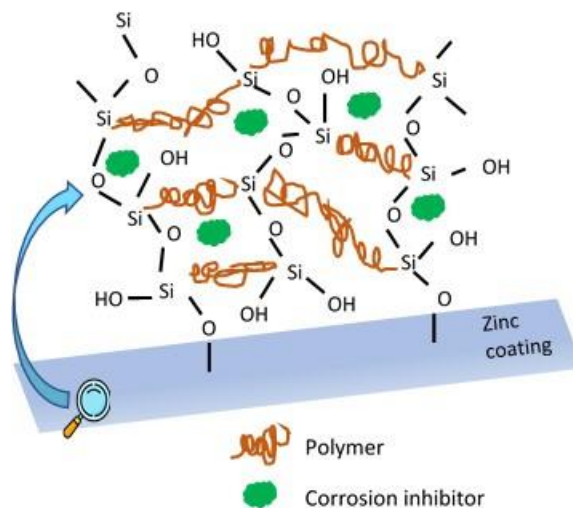


**Figure 1:** Hybrid sol-gel coating matrix with corrosion inhibitors

## References:

1. Suarez Vega, A. et al. (2020) Effect of lanthanum 4-hydroxy cinnamate on the polymerisation, condensation and thermal stability of hybrid sol-gel formulations, *Journal of Sol-gel science and technology*, published on line: <https://doi.org/10.1007/s10971-020-05315-x>
2. Contreras, G et al. (2015) Síntesis y evaluación de recubrimientos híbridos sol-gel base TEOS:GPTMS:APTES para la protección contra la corrosión de la aleación AA2124-T4 y su material compuesto AA2124-T4/25%SiCp, *Rev. LatinAm. Metal. Mat*, 35 (2), 222-236
3. Armentia, S. et al. (2018) Development of silane-based coatings with zirconia nanoparticles combining wetting, tribological and aesthetical properties, *Coatings*, 8, 368



# Short Electrospun Cellulose Acetate Nanofibers as Seed Coating Applications

P.A.M. Chagas<sup>1\*</sup>, G. B. Medeiros<sup>1</sup>, W. P. Oliveira<sup>2</sup>, M.L. Aguiar<sup>1</sup>

<sup>1</sup> Department of Chemical Engineering, Federal University of São Carlos, São Carlos, Brazil

<sup>2</sup> Faculty of Pharmaceutical Sciences of Ribeirão Preto, University of São Paulo, Ribeirão Preto, Brazil

## Abstract:

The agricultural sector faces significant challenges, including the inefficient delivery of agrochemicals such as fertilizers and pesticides, and the effects of abiotic and biotic stress on seed germination and plant development. The inefficient delivery results in substantial losses, with up to 90% of applied chemicals wasted due to evaporation, degradation, and improper targeting. Consequently, agricultural productivity is compromised, and environmental contamination increases. Moreover, soybean seeds, like many other crops, are susceptible to various stressors that negatively impact their germination and growth. Hence, the development of innovative strategies to deliver bioactives is a relevant research subject. Short electrospun cellulose acetate nanofibers represent a novel and scalable solution for addressing critical challenges in agriculture. These short nanofibers can be uniformly dispersed in water and applied as a coating to soybean seeds using spray techniques, as shown in **Figure 1**. This method ensures effective application of beneficial compounds directly to the seed surface, promoting enhanced germination and growth. The short nanofibers can encapsulate various agrochemicals, including zinc oxide nanoparticles, providing a controlled release mechanism that addresses issues of rapid degradation and inefficient delivery. In conclusion, the use of short electrospun cellulose acetate nanofibers for seed coating represents a significant advancement in agricultural technology. This innovative approach addresses the inefficiencies of traditional agrochemical applications and offers a scalable and sustainable solution to the challenges of agrochemical delivery. Successful implementation of this technology could lead to widespread benefits in crop production and environmental conservation, setting the stage for future advancements in agricultural nanotechnology and significantly improving global food security.

**Keywords:** nanotechnology, nanofibers, cellulose acetate, soybean seed, agriculture, electrospinning, coating.

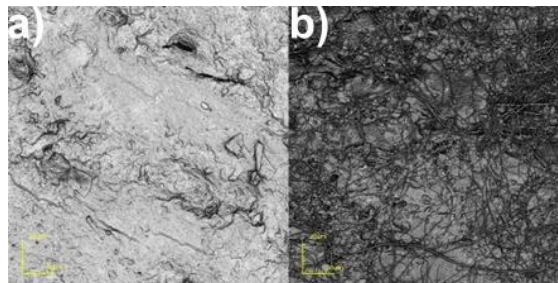


**Figure 1:** Optical microscopy images of the a) uncoated soybean seed surface and b) soybean seed surface coated with short cellulose acetate nanofibers. Both images were captured using the Olympus LEXT OLS 4000 confocal optical microscope.

## References:

1. Abdul Hameed, M. M., Mohamed Khan, S. A. P., Thamer, B. M., Rajkumar, N., El-Hamshary, H., & El-Newehy, M. (2023). Electrospun nanofibers for drug delivery applications: Methods and mechanism. *Polymers for Advanced Technologies*, 34(1), 6-23.
2. Xu, T., Ma, C., Aytac, Z., Hu, X., Ng, K. W., White, J. C., & Demokritou, P. (2020). Enhancing agrichemical delivery and seedling development with biodegradable, tunable, biopolymer-based nanofiber seed coatings. *ACS Sustainable Chemistry & Engineering*, 8(25), 9537-9548.

# Structural, mechanical, wear and anticorrosive properties of protective multilayeres based on TiSi carbo-nitrides used for the development of cutting tools

Lidia R. Constantin<sup>1</sup>, Anca C. Parau<sup>1</sup>, Mihaela Dinu<sup>1</sup>, Iulian Pana<sup>1</sup>, Catalin Vitelaru<sup>1</sup>, Diana Maria Vranceanu<sup>2,3</sup>, Alina Vladescu (Dragomir)<sup>1</sup>

<sup>1</sup>National Institute of Research and Development for Optoelectronics - INOE 2000, Department for Advanced Surface Processing and Analysis by Vacuum Technologies, 409 Atomistilor St., Magurele, RO77125, Romania

<sup>2</sup>Drugon International SRL, 2 Tractorului, Constanta, Romania

<sup>3</sup>University Politehnica of Bucharest, Faculty of Materials Science and Engineering, 313 Spl. Independentei, RO60042, Bucharest, Romania

## Abstract:

Woodworking applications represents a fast-growing area for the creation of advanced coatings with excellent wear resistance, reduced friction, and robust corrosion protection [1]. The current demands placed on improved products and optimized production processes are driving the development of cutting technology [2]. Technological innovations, such as the application of advanced machining material concepts, together with the need for pollution-free machining processes, increased flexibility, and improved cost-effectiveness, encourage the application of high-performance processes and impose higher stresses on tools [3].

Titanium silicon carbonitride coatings (TiSiCN) have emerged as a promising solution that offers an unique combination of properties ideal for various industrial applications. This research aims to reveal new insights on TiSiCN coatings, enhancing their application in environments that require durability, efficiency, and longevity.

In this work, cathodic arc evaporation technique was employed to obtain Ti/TiSi/TiSiN/TiSiCN multilayered coatings. Coatings with different C/N ratios were deposited using the reactive gas mixture as a control parameter, with N<sub>2</sub> mass flow rates ranging in the 80 to 110 sccm interval, while the C<sub>2</sub>H<sub>2</sub> mass flow rates varied between 110 and 20 sccm. All the other process parameters used for each deposition run were kept identical (2x 10<sup>-3</sup> Pa residual pressure, 6 x10<sup>-2</sup> Pa working pressure, -200 V substrate bias, 90 A arc current), to obtain final thickness of ~ 2 μm for all investigated layers. The deposited samples were characterized from morphological, microstructural and mechanical point of view. Elemental composition, surface morphology and phase composition by X-ray diffraction were assessed and compared before and after corrosion and tribocorrosion process evaluation. The

presence of corrosion products was observed by microscopical evaluation and compared as a function of steel substrates and film composition, evidencing the deterioration amplitude and mechanisms in each case.

## Acknowledgement:

This research was funded by a grant of the Romanian National Authority for Scientific Research and Innovation, CCCDI – UEFISCDI, project number COFUND-M-ERANET-3-HardCoat-1, no. 311/2022 (INOE) and COFUND-M-ERANET-3-HardCoat-2, no. 312/2022 (Drugon), within PNCDI III, and by the Romanian Ministry of Research, Innovation and Digitalization through the National Plan of Research, Development and Innovation 2022-2027, Core Program, Project no: PN 23 05, Contract no: PN11N-03-01-2023.

**Keywords** corrosion resistance, protective coatings, carbonitrides, cathodic arc evaporation

## References:

1. F. Klocke, T. Krieg (1999) Coated tools for metal cutting - features and applications CIRP Ann. - Manuf. Technol., 48
2. Bobzin, K., (2017) High-performance coatings for cutting tools, CIRP J. of Manufact.Sci.Technol., 18, 1.
3. Faga M. G., Settineri L., (2006) Innovative anti-wear coatings on cutting tools for wood machining, Surface and Coatings Technology, 201, 3002-3007.

# The Impact of Plasma Treatment on Magnesium's Corrosion Resistance and Biocompatibility

A. Kocijan <sup>1,\*</sup>, J. Kovač <sup>2</sup>, I. Junkar <sup>2</sup>, Matic Resnik <sup>2</sup>, V. Kononenko <sup>3</sup> and M. Conradi <sup>1</sup>

<sup>1</sup> Institute of Metals and Technology, Ljubljana, Slovenia

<sup>2</sup> Jozef Stefan Institute, Jamova 39, 1000 Ljubljana, Slovenia

<sup>3</sup> Biotechnical Faculty, University of Ljubljana, Večna Pot 111, 1000 Ljubljana, Slovenia

## Abstract:

Magnesium is considered non-toxic because it is an essential element in the human body. However, it corrodes rapidly under physiological conditions, causing local hydrogen evolution and alkalization. The oxide layer that forms, mainly composed of Mg(OH)<sub>2</sub>, is porous and exhibits poor barrier properties, leading to severe corrosion propagation. This porous corrosion layer is a primary reason for the poor corrosion resistance of magnesium alloys. The high biodegradability also compromises mechanical stability before sufficient tissue recovery can occur. To address these issues, various strategies have been proposed to enhance the mechanical and corrosion properties of magnesium: alloying with different elements, tailoring the microstructure, and applying surface modifications through physico-chemical methods or coatings. Plasma surface modification is a well-established technique for improving surface properties without affecting the bulk material.

In our study, plasma surface modification was utilized to tailor the surface properties of magnesium, focusing on surface chemistry, topography, and wettability. Two sets of samples underwent a two-step plasma treatment using different gases (hydrogen and oxygen), while one set received a single-step treatment using only oxygen. X-ray photoelectron spectroscopy (XPS) was employed to determine the surface composition, the oxidation states of the elements, and the thickness of the surface oxide layer on the magnesium samples after various plasma treatments. Surface morphology was characterized using atomic force microscopy (AFM) and scanning electron microscopy (SEM). Wettability was assessed by measuring static water contact angles, and corrosion resistance was evaluated through potentiodynamic measurements.

The interaction of live cells with the modified magnesium surfaces was assessed for biocompatibility using MG-63 cells (human bone osteosarcoma cells). Our findings demonstrated that plasma surface treatment significantly

reduced carbon content and facilitated the formation of a 15–20 nm thick MgO layer, enhancing corrosion resistance while maintaining biocompatibility compared to untreated magnesium. Therefore, plasma surface treatment is a crucial step in developing novel magnesium surfaces with improved corrosion resistance for biomedical applications.

**Keywords** magnesium, plasma treatment, surface chemistry, topography, wetting, corrosion, biocompatibility

## References:

1. Kocijan, A., Kovač, J., Junkar, I., Resnik, M., Kononenko, V., Conradi, M. (2022), The Influence of Plasma Treatment on the Corrosion and Biocompatibility of Magnesium. *Materials*, 15, 7405.
2. Luo, Y., Sun, Y., Lv, J., Wang, X., Li, J., Wang, F. (2015), Transition of interface oxide layer from porous Mg(OH)<sub>2</sub> to dense MgO induced by polyaniline and corrosion resistance of Mg alloy therefrom. *Appl. Surf. Sci.*, 328, 247–254.
3. Song, G.L., Atrens, A., Wu, X.L., Zhang, B. (1998), Corrosion behaviour of AZ21, AZ501 and AZ91 in sodium chloride. *Corros. Sci.*, 40, 1769–1791.
4. Kim, S.R., Lee, K.M., Kim, J.H., Choi, Y.J., Park, H.I., Jung, H.C., Roh, H.J., Han, J.H.L., Kim, J.R., Lee, B.-K. (2022), Biocompatibility evaluation of peo-treated magnesium alloy implants placed in rabbit femur condyle notches and paravertebral muscles. *Biomater. Res.*, 26, 29.

# Tribological properties of laser-textured Ti6Al4V alloy upon addition of MoS<sub>2</sub> nanotubes under water and oil lubrication: introducing the concept of green tribology

M. Conradi<sup>1\*</sup>, B. Podgornik<sup>1</sup>, A. Kocijan<sup>1</sup>, M. Remškar<sup>2</sup>, D. Klobčar<sup>3</sup>

<sup>1</sup>Institute of metals and technology, Lepi pot 11, 1000 Ljubljana, Slovenia

<sup>2</sup>Jozef Stefan Institute, Jamova 39, 1000 Ljubljana

<sup>3</sup>Faculty of Mechanical Engineering, University of Ljubljana, Aškerčeva 6, 1000 Ljubljana, Slovenia

## Abstract:

A Nd-YAG laser was employed to texture the Ti6Al4V surface with dimples of 50 and 100 μm in diameter and center-to-center distances of 100, 200, and 400 μm, defining the surface texture density. Tribological evaluations were performed to compare the behavior of untextured and laser-textured samples under water and PAO6 oil lubrication, with and without the addition of MoS<sub>2</sub> nanotubes. The incorporation of MoS<sub>2</sub> nanotubes positively affected friction reduction in both media for laser-textured Ti6Al4V. The optimal results for friction and wear were observed on the 100-200 (diameter-center-to-center distance) surface lubricated with PAO6 oil containing 2 wt. % MoS<sub>2</sub>, which maintained the low wear rates of the untextured surface while reducing friction by over 30%. For water lubrication, the best tribological outcomes were achieved with the 100-400 pattern for wear and the 50-100 pattern for friction when 2 wt. % MoS<sub>2</sub> was added.

This research confirms that water lubrication can be competitive with oil lubrication for specific laser-textured configurations of the Ti6Al4V surface, especially when MoS<sub>2</sub> nanotubes are used as a solid lubricant. This suggests that laser-textured Ti6Al4V alloy can be effectively utilized in tribologically challenging environments with water as a lubricant. The application of water-based lubrication with MoS<sub>2</sub> nanotubes aligns with the principles of green tribology, emphasizing a balance between tribological performance and ecological sustainability, with minimal environmental and biological impact. Consequently, this approach offers the potential to implement Ti6Al4V alloy in more demanding tribological applications.

**Keywords:** green tribology; surface texturing; MoS<sub>2</sub> nanotubes; lubrication; Ti6Al4V alloy.

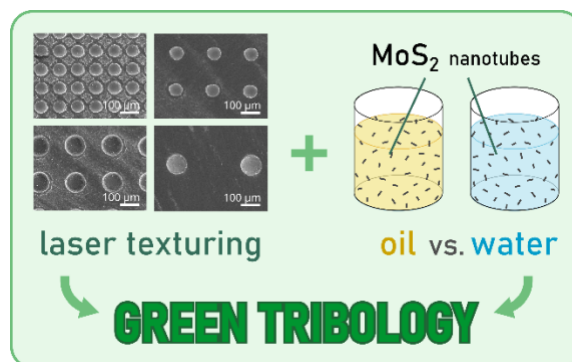


**Figure 1:** Laser-textured surfaces towards green tribology: Oil vs. water lubrication with the addition of MoS<sub>2</sub> nanotubes.

## References:

1. Conradi, M., Podgornik, B., Kocijan, A., Remškar, M., Klobčar, D. (2022) Water versus oil lubrication of laser-textured Ti6Al4V alloy upon addition of MoS<sub>2</sub> nanotubes for green tribology, *Materials*, 15, 1-12.
2. Nosonovsky M, Bhushan B. (2010), Green tribology: principles, research areas and challenges, *Trans R Soc A*, 368, 4677–4694.

# Bipolar Current Collectors of Carbon Fiber Reinforced Polymer for Laminates of Energy Storage Structural Composites

Byeong Jun So, Gilyong Shin, Yuseung Choi, Hoyeon Lee, and Tae June Kang\*  
Department of Mechanical Engineering, Inha University, Incheon, South Korea

## Abstract:

A bipolar current collector (CC) is an electrode with active materials of opposite polarity on each side that are used to collect electrons in the cell stack. Compared to the monopolar electrode configuration, the use of cell stacking with bipolar CCs reduces the weight and volume of the stacked device by reducing the number of CCs required [1].

The bipolar configuration allows direct electron transfer between the cathode and anode through a common bipolar CC, eliminating the need for external wiring of the CCs. This simplifies the interconnected components of the stacked cell while maintaining device integrity. The low series resistance and internal polarization achieved by the bipolar configuration can minimize ohmic losses during electron transport within the stacked device, resulting in higher areal power and energy densities.

A CC designed for efficient cell stacking should have high mechanical strength, high electrical conductivity, and impermeability to ions in the electrolyte used in the cell. Furthermore, it should demonstrate electrochemical stability across a wide range of working potentials and various electrolyte environments, including acidic and alkaline conditions. These attributes not only enhance the energy storage capacity but also increase the versatility and safety of the CC when utilized in different electrolyte environments.

In this work, a bipolar CC fabricated using a carbon textile, which is widely used as an electrode material in energy storage structural composites, is introduced. The carbon fiber reinforced plastic-based bipolar CCs were fabricated by attaching thermoplastic films to both sides of the carbon fabric and injecting resin into the carbon fabric using resin transfer molding. During the resin-curing process, pressure was applied to the sample surface to enhance the properties of the CCs. The mechanical and electrical properties and electrochemical stability of the fabricated CCs were evaluated. To demonstrate the applicability of the CCs, structural power composites and stacked zinc-ion battery devices were fabricated,

and its performance scalability was evaluated in terms of voltage, power, and energy density.

**Keywords:** bipolar electrode, structural battery, structural power composites.

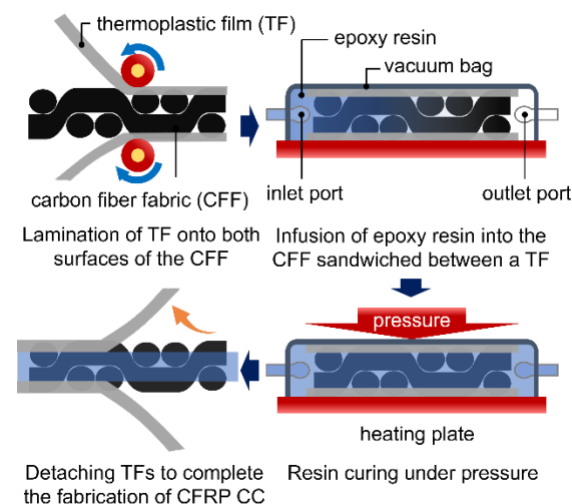


**Figure 1:** Illustration of fabrication process of bipolar CFRP CCs.

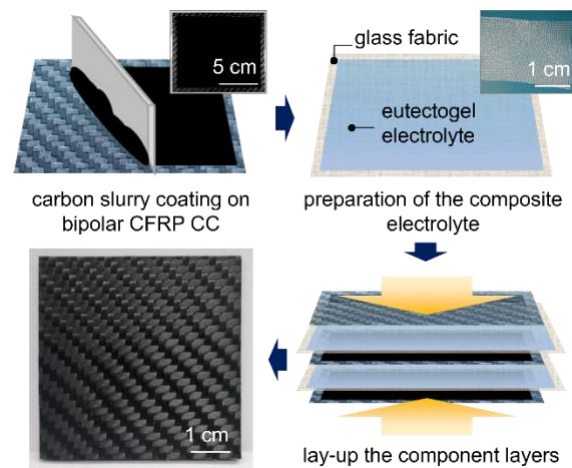


**Figure 2:** Fabrication procedure of the laminates of energy storage structural composites.

## References:

1. Yusu Han et. al. (2024) Current collectors of carbon fiber reinforced polymer for stackable energy storage composites, *Energy Storage Mater.*, 64, 103070.



# Containment of Heavy Metal Diffusion from River Yamuna to the Surrounding Geology using Bentonite Based Nanomaterial

M. Priyadarshi<sup>1</sup>, P. Das<sup>1</sup>, A. Hussain<sup>1</sup>

<sup>1</sup> Civil Engineering Department, Netaji Subhas University of Technology, West Campus, Jaffarpur, New Delhi-110073, India

## Abstract:

River Yamuna in India while passing through the Delhi stretch receives an enormous amount of unprecedented and untreated industrial effluents and sewage. These massive and untreated discharges contain high concentrations of heavy metals, thereby increasing the river's severe contamination. The agricultural land across the river bank when irrigated with river water generally results in heavy metal contamination of soil and crops of the area through diffusion at a critical level that poses long-term environmental problems. Heavy metals may also be absorbed and accumulate in edible and non-edible parts of vegetables in such a concentration that can cause adverse health effects in humans. The present study was conducted to assess the heavy metal diffusion rates and their subsequent impact on human health owing to the possible contamination of soils and crops. Also, the design of a barrier system for attenuating the heavy metals at the source is a part of the study. In this work, the health hazards associated with the heavy metal diffusion from the river to the crops and groundwater table have been assessed for the first time. The diffusion coefficient before and after providing the bentonite-based barrier for controlling heavy metals has also been computed. The maximum apparent diffusion coefficient value of  $9.8 \times 10^{-10} \text{ m}^2/\text{s}$  at the depth of 3m with 30 years of time duration was assessed. The study reveals the hazardous effects of heavy metals on crops and groundwater. Subsequently, the diffusion rates using bentonite-based barrier material was also determined. It was observed that bentonite-based nanomaterials are helpful in the eradication of heavy metals and significantly reduce the diffusion that ultimately protects the entire surroundings and geology.

**Keywords:** heavy metals, bentonite, contamination, adsorption, health hazards.

# CoPt alloys catalysts for Methanol Oxidation Reaction (MOR): influence of material shape onto their catalytic properties

O.G. Dragos-Pinzaru <sup>1,\*</sup>, G. Buema <sup>1</sup>, M. Tibu <sup>1</sup>, F. Borza <sup>1</sup>, G. Ababei <sup>1</sup>, G. Stoian <sup>1</sup>, C. Hlenschi <sup>1</sup>, I. Tabakovic <sup>2</sup>, N. Lupu <sup>1</sup>

<sup>1</sup> National Institute of R&D for Technical Physics, Iasi, Romania

<sup>2</sup> ECE Department, University of Minnesota, Minneapolis, Minnesota 55435, USA

## Abstract:

Nowadays, the environmental pollution issues are among the most important challenges of humanity in general and of research community in particular. One of the main air pollutants are exhaust gases resulting from the combustion of the conventional fuels (diesel or gasoline). One of the possibilities to reduce the consumption of conventional fuels is to replace it with methanol. In the recent years, the research community have focused more on methanol as a significant hydrogen-rich fuel, being able to release energy by methanol oxidation reaction (MOR) process. However, the MOR is a catalytic process and the lack of efficient catalysts is one of the main problems preventing the use of methanol as an energy source. The most used catalysts for MOR are noble metals, such as Pt and Pd, but the expensive cost of these catalysts along with their scarcity, prevents their widespread commercial use. In these conditions, the development of new catalyst able to drive MOR is necessary.

CoPt alloys is one of the newest developed classes of catalyst [1], which have drawn a lot of attention, being able to efficiently oxidize the methanol, due to its easy active site generation based on the electrochemical-chemical oxidation mechanisms.

In the present work, we study the influence of the material shape onto the electrocatalytic properties of CoPt alloys for the MOR. Three different samples in shape of thin films, nanowires and nanoparticles have been prepared by electrodeposition. The synthesis, was carried out at pH 5.5 from an aqueous solution of hexachloroplatinate containing 0.4 M H<sub>3</sub>BO<sub>3</sub>, 0.3 M NH<sub>4</sub>Cl, 0.1 M CoSO<sub>4</sub>·7H<sub>2</sub>O, 0.00386 M H<sub>2</sub>PtCl<sub>6</sub>, and 0.00389 M saccharine as Na-salts. The as prepared catalyst materials microstructure was analyzed by Scanning Electron Microscopy (SEM) and Transmission Electron Microscopy (TEM). The chemical composition was determined by Energy Dispersive X-Ray Spectroscopy (EDS), facility, attached to the SEM microscope, while the catalytic activity was studied by using cyclic voltammetry (CV) technique. Figure 1 shows the CV results of the

CoPt alloys in shape of thin films (blue curve), nanoparticles (black curve) and nanowires (red curve), prepared at -0.8V/SCE. The CV curves were traced in aqueous solution of 2.0M CH<sub>3</sub>-OH and 0.1M H<sub>2</sub>SO<sub>4</sub> at scan rates of 100 mV/s.

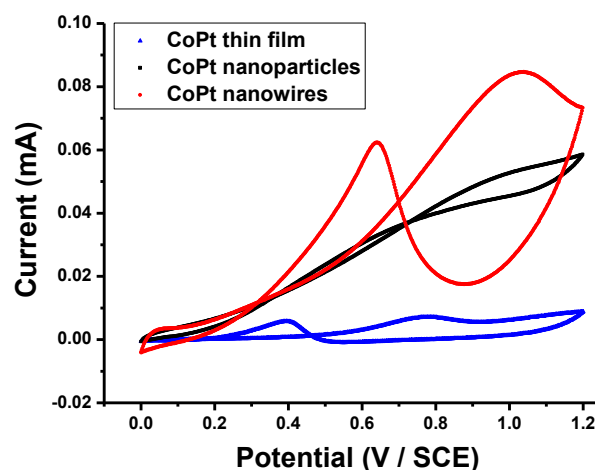


**Figure 1:** CV results of the CoPt alloys in shape of thin films (blue curve), nanoparticles (black curve) and nanowires (red curve).

As it can be observed from Figure 1, the material shape strongly influences the catalytic efficiency. Thus, the smaller efficiency was obtained for the CoPt alloys electrodeposited in shape of thin films, while the highest catalytic efficiency was obtained for the CoPt electrodeposited in shape of nanowires.

**Keywords:** CoPt alloys, catalysts for MOR, electrodeposition, thin films, nanowires, nanoparticles.

## References:

1. Serrà, A., Gómez, E., Vallés E., (2015) Facile electrochemical synthesis, using microemulsions with ionic liquid, of highly mesoporous CoPt nanorods with enhanced electrocatalytic performance for clean energy, *Int. J. Hydrog. Energy.*, 40(25), 8062-8070.

# Effect of Complete Dealumination on Acidic, Textural and Adsorption Properties of BEA Zeolite

M. Mihaylov\*, O. Lagunov, V. Zdravkova, E. Ivanova, I. Spassova, K. Hadjiivanov  
Institute of General and Inorganic Chemistry, Bulgarian Academy of Sciences, Sofia, Bulgaria

## Abstract:

BEA is an important zeolitic material from both a fundamental and industrial standpoint. It has found application as an adsorbent and catalyst for energy-efficient CO<sub>2</sub> management. BEA can be fully dealuminated without changing the structure. The catalytic and adsorption properties of zeolites largely depend on the content of Al, but the presence of additional porosity is also important for increasing the accessibility of active sites. In addition, dealumination has been reported as an effective post-synthetic method for enhancing the catalytic activity and thermal/hydrothermal stability of zeolites [1].

This work investigated the acidic, textural, and CO<sub>2</sub> adsorption properties of the proton form of zeolite BEA, AlBEA (Si/Al = 12.5), and [Si]BEA, obtained after complete removal of aluminum with concentrated nitric acid.

According to XRD and TEM, both samples consist of nanocrystalites, which are responsible for the formation of intercrystalline mesopores in accordance with the observed N<sub>2</sub> adsorption-desorption isotherms. Dealumination causes a significant increase in surface area and creates a larger total pore and micropore volume, which is associated with the formation of vacant T-sites and silanol netsts within them.

IR spectroscopy of the activated samples was utilized to ascertain the type, concentration, and localization of hydroxyl groups, whereas the spectra of adsorbed probe molecules were employed to determine their acidity and observe open Al<sup>3+</sup> cations.

Furthermore, IR spectroscopy provided information on the type, concentration, and strength of the adsorption centers for CO<sub>2</sub>. The strength of the centers in AlBEA decreases in the order of extra-framework Al<sup>3+</sup> centers ( $\nu_3(\text{CO}_2)$  at 2370 cm<sup>-1</sup>), Si(OH)Al (2356 cm<sup>-1</sup>), and SiOH groups (2347 cm<sup>-1</sup>). On [Si]BEA, only CO<sub>2</sub> bound to SiOH is observed, but at slightly lower frequencies (2343 cm<sup>-1</sup>), likely due to increased CO<sub>2</sub> adsorption onto silanol groups in the micropores.

Studies in the presence of moisture showed that water primarily blocks the strong centers and affects to a great extent the adsorption of CO<sub>2</sub> on AlBEA.

Figure 1 shows the adsorption isotherms of CO<sub>2</sub>. At low pressures, the isotherm of AlBEA is steeper, and the adsorbed amount of CO<sub>2</sub> is significantly higher, which is consistent with the presence of strong adsorption centers. At high pressures, the isotherm of AlBEA becomes flatter due to saturation of the strong centers. Above ~ 75 kPa, the amount of adsorbed CO<sub>2</sub> on [Si]BEA exceeds that on AlBEA. The reason for this is the increased surface area, volume of micropores, and additional SiOH sites generated in them after dealumination.

**Keywords:** adsorption, BEA, carbon dioxide, dealumination, FTIR spectroscopy, micro/mesoporosity, zeolites.

**Acknowledgements:** The financial support of the Bulgarian Science Fund under the project KII-06-H59/5/2021 is gratefully acknowledged.

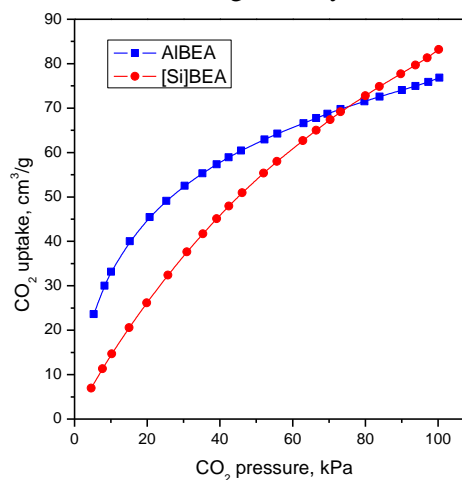


**Figure 1:** Adsorption isotherms of CO<sub>2</sub> at 273 K.

## References:

1. Minami, A., Takemoto, M., Yonezawa, Y., Liu, Z., Yanaba, Y., Chokkalingam, A., Iyoki, K., Sano, T., Okubo, T., Wakihara, T. (2022), Ultrafast dealumination of BEA zeolite using a continuous-flow reactor, *Adv. Powder Technol.*, 33, 103702.

# Oxidation of Hydrogen Sorbed in Reduced Nanoceria

E. Ivanova\*, M. Mihaylov, N. Drenchev, K. Chakarova, K. Hadjiivanov

Institute of General and Inorganic Chemistry, Bulgarian Academy of Sciences, Sofia, Bulgaria

## Abstract:

The key feature of ceria that determines its catalytic and bioactivity is associated with its redox chemistry. Therefore, detailed knowledge of the mechanism of reduction and oxidation of the ceria surface is extremely important.

In this work, we report on the *in situ* IR spectroscopic investigation of the interaction of reduced ceria nanoparticles with O<sub>2</sub> at different temperatures, starting from very low ones. We observed that an important part of Ce<sup>3+</sup> species and, more surprisingly, dissolved hydrogen can be oxidized even at 100 K. We also found that this hydrogen strongly affects the conversion pathway of superoxide species.

IR spectroscopy was employed as the primary investigative tool because it can not only observe adsorbed species but also track the concentration of Ce<sup>3+</sup> through its spin-orbit electronic transition. We estimated that the detection limit of Ce<sup>3+</sup> in our experiments is approximately 0.03% of the total amount of cerium. Furthermore, we found that the fine structure of the electronic Ce<sup>3+</sup> band, which is well-resolved at 100 K, can be associated with different environments such as nearby hydroxyls and residual carbonates. The formation of superoxide and peroxide species was confirmed using <sup>18</sup>O<sub>2</sub>. We found that the adsorption of O<sub>2</sub> at 100 K on ceria, which was H<sub>2</sub>-reduced and evacuated at 773 K, results in the rapid oxidation of almost half of the Ce<sup>3+</sup> sites, including all those bound to OH groups and carbonates. Simultaneously, superoxo species (~1130 cm<sup>-1</sup>) and peroxy species (890-810 cm<sup>-1</sup>) are formed. Upon heating to room temperature, most of the remaining Ce<sup>3+</sup> sites disappear, and about 10% of them vanish upon further heating to 348 K. These remaining sites are most likely subsurface situated. According to our results, the evolution of peroxy and superoxo species follows two independent pathways. The peroxide is likely formed with an oxygen vacancy, bridging two Ce<sup>3+</sup> ions, while the superoxide forms with an isolated Ce<sup>3+</sup> site. At higher temperatures, the peroxy species decompose directly, yielding lattice oxygen. Superoxides decompose through intermediate species into terminal OH groups.

Figure 1 shows that dosing O<sub>2</sub> at 100 K onto the reduced sample, evacuated at 573 K, results in the delayed development of the negative Ce<sup>3+</sup>

electronic band. This delay can be explained by assuming that a portion of the O<sub>2</sub> was consumed to oxidize Ce<sup>3+</sup> while another portion oxidized hydrogen dissolved in ceria. The oxidation of dissolved H<sub>2</sub> produces water, which is detected by the δ(H<sub>2</sub>O) modes and the appearance of broad absorbance in the ν(OH) region due to hydrogen-bonded water. Previous reports have indicated that hydrogen is stored on ceria below 773 K and released above this temperature [1]. These results demonstrate that hydrogen dissolved in ceria is highly reactive and can undergo oxidation even at 100 K in the absence of noble metals.

Analysis of the results revealed that peroxide species absorbing in the 850-810 cm<sup>-1</sup> spectral region are readily formed, particularly in samples containing a high concentration of dissolved hydrogen. Therefore, we propose that these species are hydroperoxides, formed as a result of the interaction of superoxide with dissolved hydrogen.

**Keywords:** ceria, hydrogen, hydroperoxide, IR spectroscopy, oxygen, peroxide, superoxide.

**Acknowledgements:** The financial support of the Bulgarian Science Fund under the project KII-06-H59/5/2021 is gratefully acknowledged.

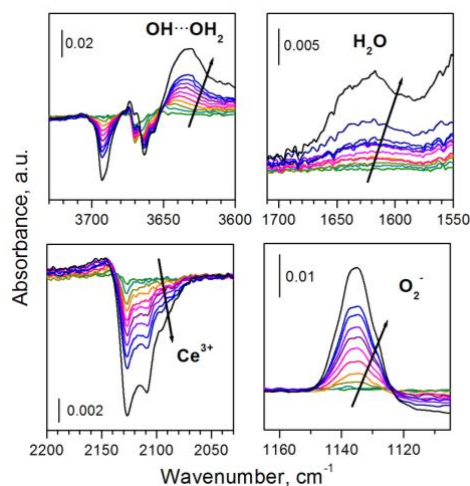


**Figure 1:** IR spectra recorded after O<sub>2</sub> dosing at 100 K on reduced nanoceria, evacuated at 573 K.

## References:

1. Kammert, J.; Moon, J., Wu, Z. (2020) A review of the interactions between ceria and H<sub>2</sub> and the applications to selective hydrogenation of alkynes, *Chin. J. Catal.*, 41, 901.

# Green synthesized Au-Ag core-shell nanoparticles as catalyst for reductive degradation of carmoisine

V. Moroşan<sup>1</sup>, B. Moldovan<sup>1</sup>, L. David<sup>1\*</sup>

<sup>1</sup> Department of Chemistry, “Babeş-Bolyai” University, Cluj-Napoca, Romania

## Abstract:

*Lycium barbarum L.* belonging to the Solanaceae family, native to South-Eastern Asian countries, has recently gained interest in European countries due to the properties of fruits produced by the shrub.<sup>1</sup> Antioxidant compounds found in goji berries, such as polyphenols, have been proved to present the ability to reduce and stabilize metal ions.

Bimetallic core-shell nanoparticles exhibit improved physicochemical properties (catalytic, biologic, optical and electronic activity) compared to the monometallic nanoparticles of the component metals.<sup>2</sup>

Synthetic dyes are used in large quantities in multiple industries such as textile, food, etc. due to their high coloring power, stability, and reduced price. As a result of textile processing processes, large quantities of waste are obtained, with a negative impact on soil, air, water and living organisms, presenting mutagenic and carcinogenic effects. Treatments of wastewater are the most common method used to reduce pollution when working with synthetic colorants. A large number of methods have been developed such as: dissolved air flotation, activated carbon adsorption, photocatalytic degradation, etc.<sup>3</sup> Photocatalytic degradation of dyes is a very effective method of reducing organic colorants amount from wastewaters; the use of metallic nanoparticles as catalysts for photodegradation has been investigated and proved to be useful.<sup>4</sup>

We report the green synthesis of bimetallic Au-Ag core-shell nanoparticles using goji berry extract as a source of reducing and stabilizing agents, as well as their catalytic activity on the reductive degradation of carmoisine (Figure 1).

**Keywords:** carmoisine degradation, gold nanoparticles, gold-silver core-shell nanoparticles, goji fruits

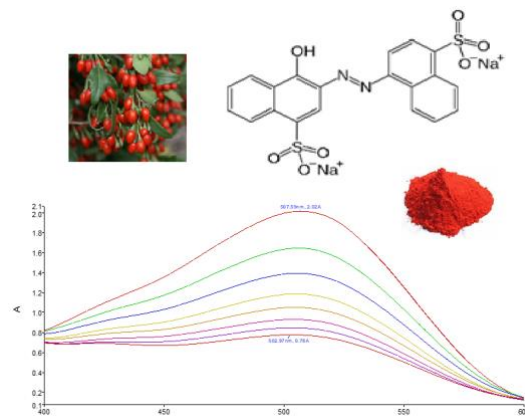


**Figure 1:** Reductive degradation process of carmoisine in the presence of Au-Ag core-shell nanoparticles as catalyst

## References:

1. Rocchetti, G., Chiodelli, G., Giuberti, G., Ghisoni, S., Baccolo, G., Blasi, F., Montesano, D., Trevisan, M., Lucini, L. (2018). UHPLC-ESI-QTOF-MS profile of polyphenols in Goji berries (*Lycium barbarum L.*) and its dynamics during *in vitro* gastrointestinal digestion and fermentation. *J. Funct. Foods*, 40, 564–572.
2. Alwhibi, M. S., Ortashi, K. M. O., Hendi, A. A., Awad, M. A., Soliman, D. A., El-Zaidy, M. (2022). Green synthesis, characterization and biomedical potential of Ag@Au core-shell noble metal nanoparticles. *J. King Saud Univ. Sci.*, 34, 102000.
3. Slama, H. B., Bouket, A. C., Pourhassan, Z., Alenezi, F. N., Silini, A., Cherif-Silini, H., Oszako, T., Luptakova, L., Golińska, P., Belbahri, L. (2021). Diversity of synthetic dyes from textile industries, discharge impacts and treatment methods. *Appl. Sci.*, 11, 6255.
4. David, L., Moldovan, B. (2020). Green synthesis of biogenic silver nanoparticles for efficient catalytic removal of harmful organic dyes. *Nanomaterials*, 10, 202.



# Comparative study of the graphene morphology on the effective electroelastic behavior of PVDF matrix composites

S. ELBARNATY<sup>1\*</sup>, W. AZOTI<sup>2</sup>, JPM.CORREIA<sup>1</sup>, S. AHZI<sup>1</sup>

<sup>1</sup> ICUBE, University of Strasbourg, Strasbourg, France, [\\*salah.elbarnaty@gmail.com](mailto:*salah.elbarnaty@gmail.com)

<sup>2</sup> ICA, University of Toulouse, CNRS UMR 5312, INSA, ISAE-Supaéro, INSA, IMT Mines Albi, UPS, France

## Abstract:

The Polyvinylidene fluoride PVDF, in its  $\beta$  phase, is a piezoelectric polymer that has garnered significant attention from researchers due to its superior performance compared to conventional piezoelectric materials [1], [2], [3]. In the context of climate change, PVDF stands out as a noteworthy alternative to lead-based piezoceramics, such as the PZT family. Besides its impressive piezoelectric properties, PVDF is thermally stable and possesses favorable mechanical characteristics [1] [Ref]. Naturally, PVDF is found in the non-electroactive Alpha crystalline phase. A transformation process is required to convert the alpha phase into the electroactive Beta phase, which is essential for piezoelectric applications [1]. This transformation can be achieved through various methods, including stretching, polarizing under high voltage, thermochemical treatments, or by using electrospinning to enhance the Beta phase.

Graphene, on the other hand is known as one of the strongest materials ever discovered. Therefore, it can greatly enhance a composite's properties even when added in small volume fractions. In the present work, we aimed to investigate the effect of Graphene's morphology on the effective elastic and piezoelectric properties of a PVDF matrix composite. For such a purpose, two morphologies were chosen to represent the Graphene, namely the Ribbon-like and platelet-like geometries (Figure 1). The Eshelby inclusion applied to the Mori-Tanaka micromechanics scheme [4] was used to compute the effective elastic and electroelastic properties of the composite. The computation process started by implementing the piezoelectric Eshelby tensors [5]. Next, the Mori-Tanaka scheme was computed to get the overall engineering constants. A comparative study was carried out to investigate the effect of both morphologies on the effective behavior. A significant difference was found between both geometries especially when it comes to the transverse properties.

**Keywords:** Piezoelectric, Homogenization, Micro-Mechanics, Mori-Tanaka, PVDF, GNR, GnP

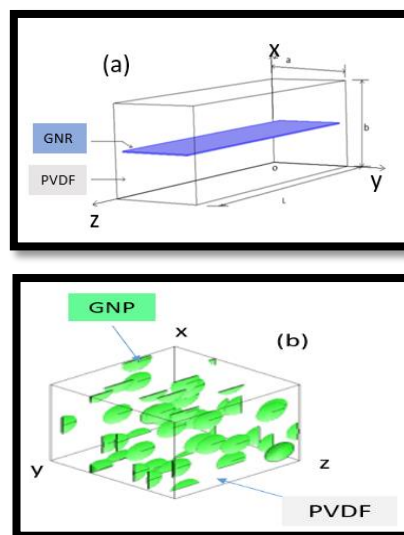


**Figure 1:** A schematic illustration of Graphene in PVDF matrix. (a): Graphene Nanoribbon (GNR). (b) Graphene nanoplatelets (GNP)

## References:

1. Juliette DEFEBVIN, "Thèse\_Defebvin\_PVDF," *Thèse*, Nov. 2015.
2. L. Laiarinandrasana, J. Besson, M. Lafarge, and G. Hochstetter, "Temperature dependent mechanical behaviour of PVDF: Experiments and numerical modelling," *Int J Plast*, vol. 25, no. 7, pp. 1301–1324, Jul. 2009, doi: 10.1016/j.ijplas.2008.09.008.
3. A. Vinogradov and F. Holloway, "Electromechanical properties of the piezoelectric polymer PVDF," *Ferroelectrics*, vol. 226, no. 1–4, pp. 169–181, 1999, doi: 10.1080/00150199908230298.
4. M. L. Dunn and M. Taya, "MICROMECHANICS PREDICTIONS OF THE EFFECTIVE ELECTRO ELASTIC MODULI OF PIEZOELECTRIC COMPOSITES," 1993.
5. Y. Mikata, "Determination of piezoelectric Eshelby tensor in transversely isotropic piezoelectric solids," 2000.

# Hydrogenated graphene superlattices: electronic and optical properties

V. A. Saroka<sup>1,\*</sup>, L. A. Chernozatonskii<sup>2</sup>, O. Pulci<sup>1</sup>

<sup>1</sup>Department of Physics, University of Rome Tor Vergata, Rome, Italy

<sup>2</sup>Emanuel Institute of Biochemical Physics, Russian Academy of Sciences, Moscow, Russia

## Abstract:

Contemporary mobile networks and emerging wireless technologies (internet of things etc.) require broadband channels to rapidly exchange a huge amount of data [1,2]. Harnessing frequencies from 0.1 to 10 THz has potential to increase the state-of-the-art high speeds by 2 orders of magnitude [3]. However, despite the latest advancements in THz technology [4], we still lack proper materials to realize suitable THz photonic components. The route to compact THz devices is seen in the usage of carbon nanostructures as building blocks for detectors, and emitters and passive components. Such carbon nanostructures, as nanotubes and graphene nanoribbons, exhibit unique electronic and optical properties that make them very promising candidates for THz components [5]. However, carbon nanotube and nanoribbon monolithic on-chip integration is challenging because it may result in significant change of their intrinsic properties after an embedment into a substrate. We investigate with first principles methods the successful integration of nanoribbons into a single-layer graphene and show that their electronic properties persist in the integrated structures forming a 2D graphene superlattice (Figure 1, left panel). Finally, we consider optical properties of the superlattices and their reinforcement with a monolayer hexagonal boron nitride (hBN) substrate (Figure 1, right panel).

This work is supported by EU HORIZON-MSCA-2021-PF-01 (project no. 101065500, TeraExc).

**Keywords:** 2D materials, superlattices, sandwich structures, patterned decoration, DFT, optical properties, THz radiation.

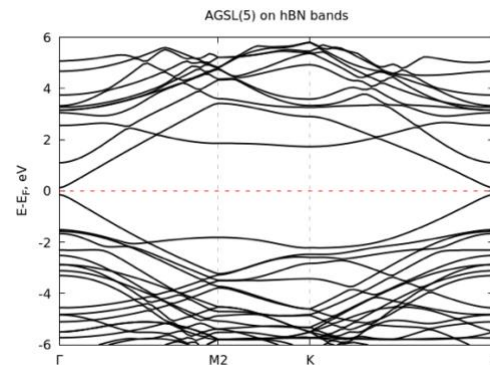
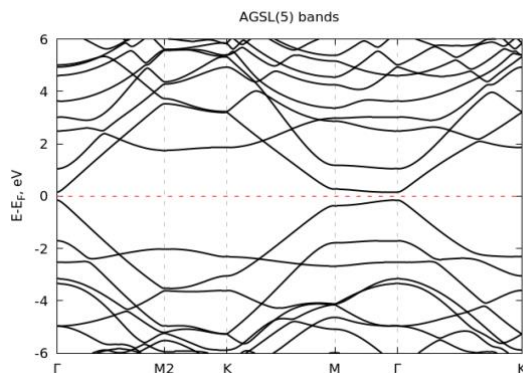


**Figure 1:** Electronic energy bands of hydrogenated graphene superlattice of armchair type (AGSL) with 5 C-C dimer chains in the unit cell without (top) and with (bottom) hBN substrate.

## References:

1. Hamza, A. S., Deogun, J. S., Alexander, D. R. (2019) Wireless Communication in Data Centers: A Survey, *IEEE Commun. Surv. Tutorials* 21, 1346.
2. Ghafoor, S., Boujnah, N., Rehmani, M. H., Davy, A. (2019), MAC Protocols for Terahertz Communication: A Comprehensive Survey, *arXiv* [arXiv:1904.11441]
3. Akyildiz, F., Jornet, J. M., Han, C. (2014), Terahertz band: Next frontier for wireless communications, *Phys. Commun.* 12, 16.
4. Dhillon, S. S. et al. (2017), The 2017 terahertz science and technology roadmap, *J. Phys. D: Appl. Phys.* 50, 043001.
5. Hartmann, R. R., Kono, J., Portnoi, M. E. (2014), Terahertz science and technology of carbon nanomaterials, *Nanotechnology* 25, 322001.



# pH sensor for the in-situ environmental measurements

N. Lenar\*, R. Piech, B. Paczosa-Bator

Faculty of Materials Science and Ceramics, AGH University of Krakow, Mickiewicza 30, PL-30059 Krakow, Poland

## Abstract:

Potentiometric sensor is defined as electrochemical sensor that transforms the effect of the electrochemical interaction between ion and membrane into a signal. The principle of electrochemical sensors is based on the interaction between "electricity" and "chemistry." The part of the sensor in which "chemistry" plays the key role is the receptor part, which is responsible for the specific interaction of the analyzed ions with the sensor. The other part of the sensor converts the received chemical signal into an electrical signal.

In this poster, the new construction of potentiometric sensor is presented and described. The new electrode's body was constructed, with two glassy carbon discs instead of one, and covered with  $H^+$  - selective polymeric membrane (Figure 1). The detailed preparation method and obtained results are included in the scope of the presented poster.

Research has shown that the presence of an additional membrane on the opposite side of the sensor allowed for the improvement of electrical properties of the sensors. Obtained results suggest that the ion-to-electron transduction processes are more efficient in the planar electrodes with two membranes instead of just one.

Hence, a higher electrical capacity and lower resistance were observed for the planar sensor, in contrast to the traditional single-membrane electrode. Consequently, due to the enhanced electrical properties, wider linear ranges, improved potential stability, and a shorter response time was recorded for the planar construction of pH sensor.

The new construction is particularly useful for in situ measurements in environmental samples. The planar construction with two membranes on the side surface of a sensor is more durable and resistant to the measurement environment in contrast to the coated-disc electrode. Furthermore, the sharp end of the body of an electrode makes it easier to place the electrode in the sample.

**Keywords:** ion sensing, pH detection, environmental monitoring, in-situ measurement,

ion-selective electrode, sensor design, polymeric membrane, soil, aqueous environment

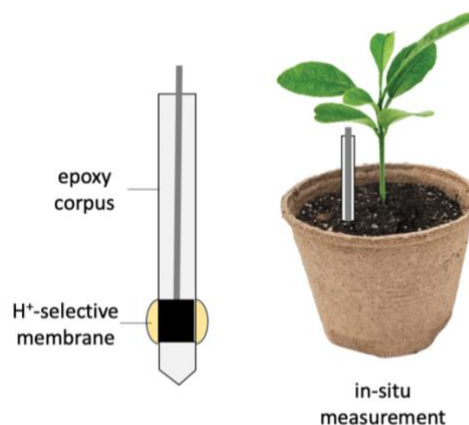


**Figure 1:** Planar  $H^+$  - selective sensor for in-situ measurements in soils and aqueous media.

## References:

1. Zdrachek, E., Bakker, E. (2019) Potentiometric sensing, *Anal. Chem.*, 91, 2-26.
2. Shao, Y., Ying, Y., Ping, J. (2020), Recent advances in solid-contact ion-selective electrodes: functional materials, transduction mechanisms, and development trends, *J. Chem. Soc. Rev.* 49, 4405-4465.
3. Lenar, N., Piech, R., Paczosa-Bator, B. (2024) A New Planar Potentiometric Sensor for In Situ Measurements, *Sensors* 24, 2492.

# FDM technology and the effect of printing parameters on the tensile strength of ABS parts

Mohamed Daly<sup>1,2</sup>, Mostapha Tarfaoui<sup>1,3,4</sup>, Manel Chihi<sup>2</sup>, Chokri Bouraoui<sup>2</sup>

<sup>1</sup> ENSTA Bretagne, IRDL UMR CNRS 6027, F-29200 Brest, France.

<sup>2</sup> University of Sousse, LMS ENISo, Sousse 4023, Tunisia.

<sup>3</sup> Green Energy Park (IRESEN/UM6P) km2 R206 Benguerir Morocco.

<sup>4</sup> Campus de Rouyn-Noranda, 445, Université du Québec en Abitibi-Témiscamingue, Rouyn-Noranda, QC J9X 5E4, Canada.

## Abstract:

This study examines how printing speed affects the tensile strength of acrylonitrile butadiene styrene (ABS) samples made by the fused deposition modeling (FDM) process. There were four different printing speeds used to assess the mechanical performance of FDM-ABS products: 10, 30, 50, and 70 mm/s. A numerical model was created by using the computer algorithms Abaqus and Digimat to replicate the experimental campaign. This paper also makes an effort to look into how printing factors affect ASTM D638 ABS specimens. To replicate the printing process and assess the quality of the printed object, residual stress, temperature gradient, and warpage were analyzed using a 3D thermomechanical model. Numerous Digimat printed parts were analyzed and contrasted numerically. We were able to measure the impact of several 3D printing factors, including printing direction, speed, and discretization method (layer by layer or filament), on warpage, residual stresses, deflection, and mechanical behavior by using a parametric research.

**Keywords** ABS Material, Fused deposition modelling, printing speed, Abaqus/Digimat coupling

# Advanced Deep Learning Framework for Damage Detection in 3D-Printed AEROSIL-Infused Polycarbonate Under Dynamic Loading

Youssef Qarssis<sup>1,2,\*</sup>, Ayoub Karine<sup>3</sup>, Mourad Nachtane<sup>2\*\*</sup>, Mostapha Tarfaoui<sup>1,6,7\*\*\*</sup>

<sup>1</sup> ENSTA Bretagne, IRDL – UMR CNRS 6027, F-29200 Brest, France.

<sup>2</sup> Mohammed VI Polytechnic University, LIMSET, km2 R206, Benguerir, Morocco.

<sup>3</sup> L@BISEN, ISEN Yncréa Ouest, 33 Quater Chemin du Champ de Manoeuvre, 44470 Carquefou, France.

<sup>4</sup> International University of Rabat, LERMA, Rabat, Morocco.

<sup>5</sup> University of Sousse, LMS ENISo, Sousse 4023, Tunisia.

<sup>6</sup> Mohammed VI Polytechnic University, GSMI, Green Energy Park, km2 R206, Benguerir, Morocco.

<sup>7</sup> University of Dayton, Department of Chemical Engineering, OH, United States.

\* Corresponding author: [youssef.qarssis@ensta-bretagne.org](mailto:youssef.qarssis@ensta-bretagne.org)

## Abstract:

3D printing of composites is a significant engineering advancement due to its robustness, ability to achieve complex geometries, and ease of use. Polycarbonate, especially when infused with AEROSIL, is an intriguing thermoplastic and a strong candidate for 3D printing with enhanced properties. This research aims to develop a deep learning-based framework for classifying and detecting damage in this material under dynamic loading conditions. A FASTCAM high-speed camera was positioned in front of the Split Hopkinson Pressure Bar (SHPB) test setup to capture dynamic damage events. The test results were then used as labeled inputs to train advanced deep learning algorithms, focusing on dense image recognition techniques for detailed damage analysis. The study explored fully convolutional networks (FCNs), evaluating semantic segmentation with U-Net and instance segmentation with frameworks like YOLOv8 and Mask R-CNN. Comparative analysis revealed that deep learning models outperform traditional methods, offering more efficient and accurate damage classification and detection. The U-Net model recognized shapes such as cubes and bars but faced challenges in detecting small-scale damage. YOLOv8 excelled in identifying significant damage but struggled with minor damage detection. This study enables efficient and accurate damage assessment, crucial for the reliability and safety of composite structures in various industries.

**Keywords:** Composite materials, 3D printing, Damage analysis, Deep learning, Dynamic loading

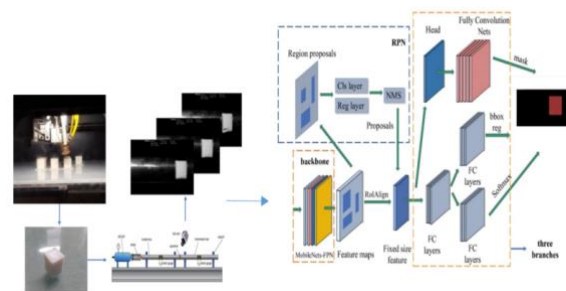


**Figure 1:** Illustration of the research framework for detecting damage in 3D-Printed AEROSIL-Infused Polycarbonate Composites.

## References:

1. QARSSIS, Youssef, KARINE, Ayoub, SAYED, Sirine, DALY, Mohamed, NACHTANE, Mourad et TARFAOUI, Mostapha. A Model-Based Deep Learning Framework for Damage Classification and Detection in Polycarbonate Infused with AEROSIL Under Dynamic Loading Conditions. *Composites Part B: Engineering*, 2024, article n° 111810. ISSN 1359-8368.



# Numerical Simulation for Assessing Wave Energy Converter Structural Resistance and Hydrodynamic Behavior

Mohammed Karkab<sup>1,2,3</sup>, Abdellatif Ghennioui<sup>3</sup>, Khalid Bouziane<sup>2</sup>, Omar Jellouli<sup>2</sup>, Mostapha Tarfaoui<sup>1,3,4</sup>

<sup>1</sup>ENSTA Bretagne, IRDL UMR CNRS 6027, F-29200 Brest, France.

<sup>2</sup>International University of Rabat, LERMA Lab, 11100 Sala El Jadida, Morocco.

<sup>3</sup>Green Energy Park (IRESEN/UM6P), km2 R206, Benguerir, Morocco.

<sup>4</sup>University of Dayton, Department of Chemical Engineering, OH, United States.

## Abstract:

Ensuring the structural integrity and efficiency of wave energy converters (WECs) against impact loads from varying sea wave conditions is paramount for their reliable operation and energy harvesting capability. This study explores the influence of waves on a WEC by analyzing its hydrodynamic and structural characteristics. A comprehensive numerical model has been developed to simulate the WEC's motion response and the stresses exerted on its structural elements. Two materials, steel and CF PETG, were used in this analysis to evaluate their respective performances. A novel numerical simulation technique has been devised to forecast the resistance stemming from the interaction between WECs and waves, bypassing the need to model the fluid domain directly. This innovative approach integrates an explicit finite element code, enabling detailed investigations into wave impact dynamics and facilitating comprehensive analyses of the device's hydrodynamic and structural responses. The hydrodynamic force acting on the WEC is quantified as a drag force, providing a robust basis for assessing its interaction with incoming waves. This simulation meticulously examines key hydrodynamic characteristics of the WEC, including heave, longitudinal oscillation, and energy extraction efficiency. By leveraging numerical simulations, the study offers insights into the device's motion response and the stresses imparted onto its structural components, which are crucial for ensuring operational safety, longevity, and optimal energy harvesting. The numerical results provide valuable insights into the complex interplay between WECs and varying wave conditions, offering a robust tool for the comprehensive design and optimization of wave energy conversion systems. This encompasses the geometric design of the WEC and its ability to effectively harness energy from anticipated wave models. Ultimately, this simulation tool holds promise for advancing the development of efficient and resilient wave energy conversion technologies, representing a

significant step forward in intelligent materials and energy harvesting systems.

**Keywords:** Wave Energy Converters, Structural Integrity, Numerical Simulation, Hydrodynamic Force, Finite Element Method, CF PETG

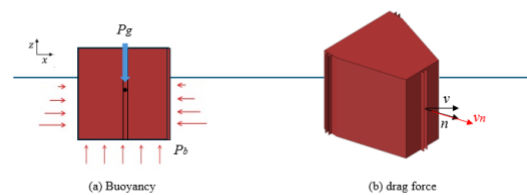


**Figure 1:** Representation of hydrostatic and hydrodynamic forces on the WEC system.

## References:

1. Ahamed, R., McKee, K., & Howard, I. (2020). Advancements of wave energy converters based on power take off (PTO) systems: A review. *Ocean Engineering*, 204, 107248.
2. Dai, S., Day, S., Yuan, Z., & Wang, H. (2019). Investigation on the hydrodynamic scaling effect of an OWC type wave energy device using experiment and CFD simulation. *Renewable Energy*, 142, 184–194.

# Polymethyl Methacrylate Fresnel Lenses to Focalize Ultrasound at Megahertz

M. Ghasemishabankareh\*, F. Torres, N. Barniol

<sup>1</sup> Dept. Enginyeria Electrònica, Universitat Autònoma de Barcelona, Cerdanyola del Vallès, Spain

## Abstract:

Ultrasound imaging is continuously improving its capabilities. Decreasing the size of ultrasound sources (using the so-called PMUTs or CMUTs) allows for an increase in the frequency of the sound, and thus, the ability to obtain high-resolution images. However, using these small sources has an important drawback related to omnidirectional energy radiation. Focusing the ultrasound at a focal point closer than the natural focus is crucial to overcome this drawback. Focusing can be achieved using arrays with beamforming, which leads to complex systems, or using lenses compatible with ultrasound [1-3]. Here, we present a Fresnel lens designed for a frequency in the megahertz range, fabricated using an inexpensive and simple method based on laser cutting machine and methacrylate (PMMA) as the base material.

We have designed (shown in figure A) and simulated (using the finite elements method, COMSOL software, shown in figure B) a Fresnel lens operating in the megahertz range (2 MHz) in water, with a millimeter focal point distance (12 mm), using a cheap and easily manipulable base material such as methacrylate and a laser cut machine as fabrication technique. The Fresnel lens is 2.3 mm thick and has an external radius of 8.3 mm. We have measured the speed of sound in this material, its density, and characterized the focal point created using an ultrasound source with a wide bandwidth (OPTEL) and a hydrophone (HNC-1500 ONDA).

First of all, the speed of sound in the methacrylate was measured, and a value of 2175 m/s was obtained, also for the density obtaining a value of 1200 kg/m<sup>3</sup>. Taking into account the speed of sound in water, the difference between the acoustic impedance of the methacrylate (2.6 Mrayl) and the water (1.5 Mrayl) is significant enough to ensure good focalization capability of the Fresnel lens. We placed our Fresnel lens between the OPTEL and the hydrophone (10 mm from OPTEL surface, at the beginning of its far field) and measured the signal received at the hydrophone while changing the distance between it and the lens surface in the Z-direction, showing a clear focal point (figure C). We also performed a characterization of the focal point in the plane

(figure D, in the X-direction). The obtained focal point is close to the desired position and has a width (at -3 dB) of 4 mm in the Z-direction and 1.8 mm in the X-direction, indicating an ellipsoidal shape for the focal point as predicted by the simulation (figure B).

This simple and inexpensive way to fabricate Fresnel lenses is feasible until 20 MHz of sound frequency (due to limitations in the the minimum dimensions fabrication of laser cut machine, 0.2 mm) and is complete flexible for focal point position needs.

**Keywords:** Ultrasound imaging and sensing. Fresnel lenses. Ultrasound focusing.

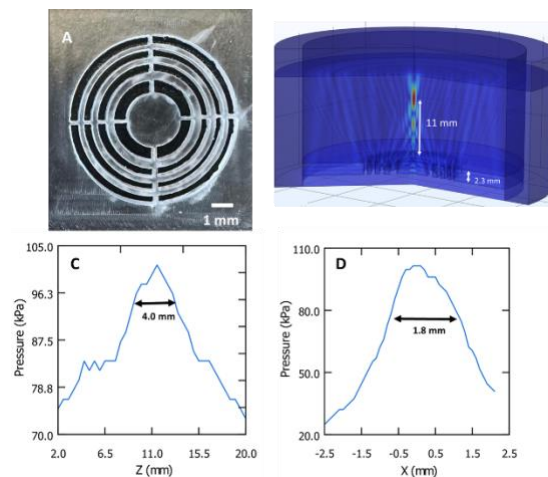


**Figure 1** (A) image of the Fresnel lens. (B) Comsol simulation. (C) Axial (Z-direction) measured pressure. (D) Focal point measurement in lateral direction (X-direction).

## References:

1. Jeong H. *et al.* (2019), Application of fresnel zone plate focused beam to optimized sensor design for pulse-echo harmonic generation measurements, *Sensors*, 19, 1373-1389.
2. Tarrazó-Serrano *et al.* (2019), Acoustic focusing enhancement in Fresnel zone plate lenses, *Scientific Reports*, 9, 7067-7077.
3. Chang C. *et al.* (2014), Acoustic lens for capacitive micromachined ultrasonic transducers, *J. Micromech. Microeng.*, 085007 (13pp).

# Investigation of a QCM sensing system using the concentration of low-concentration biomarker gas

H. Ito\*, S. Hashimoto, T. Katsuno  
Toyota Central R&D Labs., Inc., Nagakute, Japan

## Abstract:

Most lifestyle-related diseases are detected through regular checkups at medical institutions at intervals of several years, but if health conditions can be monitored more routinely and easily, early detection of diseases can be expected to prevent serious complications. We focused on the use of biomarker gas, a trace component of exhaled breath, as an invasive and simple method to detect low concentrations of acetone gas. We build up gas sensing system, in which low-concentration gases are converted to high-concentration gases in a concentrator, and the gases are detected by a detector (Figure 1).

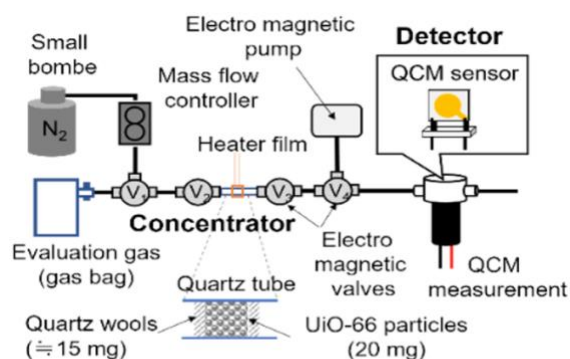


Figure 1 Prototype configuration

In this study, we targeted acetone gas, which is known as a biomarker in the breath of diabetes, a lifestyle-related disease. To detect the low-concentration acetone gas, we used UiO-66 metal-organic framework, which is reported to possess high acetone adsorption properties. For the concentrator, the UiO-66 particles were packed in a quartz tube and surrounded by heater film for heating. For the detector, we used QCM (Quartz crystal microbalance) sensor, coated with UiO-66 particles, was adopted to measure the sensor signal (resonant frequency) and the resonant resistance. The evaluation was conducted as follows: the evaluation gas (N<sub>2</sub>+ 0~5 ppm acetone gas, 2 L) was connected to the concentrator, which was then aspirated by the electromagnetic pump shown in the figure to adsorb the evaluation gas onto the UiO-66 particles in the concentrator. The acetone gas adsorbed on the UiO-66 particles is then desorbed by heating up to 200 °C. The gas desorbed by heating is passed through the concentrator to the detector by flowing N<sub>2</sub> gas from a small bombe, and the acetone component in the gas is acquired as a signal waveform by the QCM sensor.

The QCM signal variation of the detection section during the heating process of the concentrator is

shown in Figure 2. After the adsorption of the evaluation gas into the concentrator, when heating was performed (②) from the state (①), where the resonance frequency fluctuation was stabilized by N<sub>2</sub> flow after the adsorption of the evaluation gas into the concentrator, two kinds of peak (A and B) with a decrease in resonance frequency was detected. After the occurrence of this second peak, a fluctuation (C) with oscillation was also observed; the resonance frequency change in A corresponded to the fluctuation of the resonance resistance with the temperature rise of the concentration section, and for C, it corresponded to the temperature fluctuation of the concentration section. Therefore, these sensor signals can be judged as noise due to temperature fluctuations. On the other hand, for peak B, although a slight variation in resonance resistance is observed, a larger peak waveform is generated than for A, corresponding to the larger acetone concentration of the evaluated gas. This indicates that acetone gas at 0.5 ppm, the ppb level, can be detected using this system.

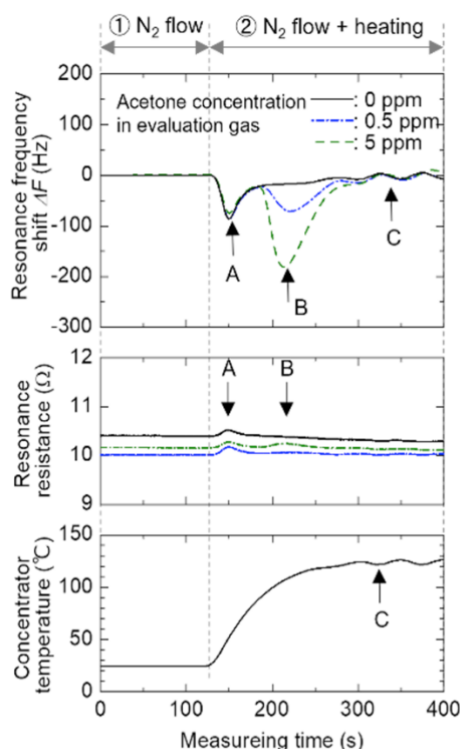


Fig. 2 QCM sensor signals and change in the concentrator temperature during heating of the concentrator with adsorbed evaluated gas.

**Keywords:** Health Care, Acetone Gas Sensing, Metal-organic Framework, Adsorption, Desorption

# Automatic skin cancer diagnosis using a robotic hyperspectral sensor.

Sáez C.<sup>1</sup>, Sanmartín O.<sup>2</sup>, García A., Díaz R.<sup>1</sup>

<sup>1</sup>Sensor and Robotic Department (Ainia), Valencia, Spain

<sup>2</sup>IVO (Valencian Institute of Oncology), Valencia, Spain

## Abstract:

Skin cancer is a pathology that affects more and more people as a consequence of climate change and the population's new habits. The two most harmful types of skin cancer are basal cell carcinoma and melanoma. Currently, early detection remains a significant challenge. In fact, there are limitations that affect the efficiency and precision in the detection of this type of cancer, which causes late diagnoses and more invasive interventions to eliminate the affected tissue.

Currently there are different techniques used in early detection, which are divided into two types: non-invasive (dermoscopy, confocal microscopy, OCT and LC-OCT) and invasive (biopsy).

Hyperspectral vision is a technique that allows obtaining the spectral signature in the infrared band of cellular tissues, being able to characterize them and discriminate between healthy epidermal cellular tissues and tumor cell tissues.

A medical device (Figure 1) has been developed based on a pushbroom hyperspectral sensor that is capable of characterizing the area of interest automatically. To do this, a stereoscopic vision sensor is used that analyzes the morphology of the area to be explored and, using a collaborative robotic arm, scans while maintaining the focal distance between the sensor and the skin, generating a hypercube of the epidermis area. explore even if it is not flat.

An observational study has been carried out with 2075 spectra from 20 patients who have been characterized using the medical device described and who have undergone a biopsy of a sample from the explored area (Figure 2).

The hypercube with the spectral information of the scanned tissue has been corrected spectrum by spectrum and subsequently analyzed using a SVM algorithm.

The results obtained have demonstrated precision, sensitivity and specificity above 96.6%, having left 20% of the samples for validation.

**Keywords:** hyperspectral, cancer, melanoma, basal cell carcinoma, support vector machine, spectroscopy, infrared, medical device, diagnosis, collaborative robot.



**Figure 1:** Figure illustrating the measurement process using the medical device developed. The head of the device integrates the luminaire, the stereoscopic sensor and the hyperspectral sensor that characterizes the area to be explored.

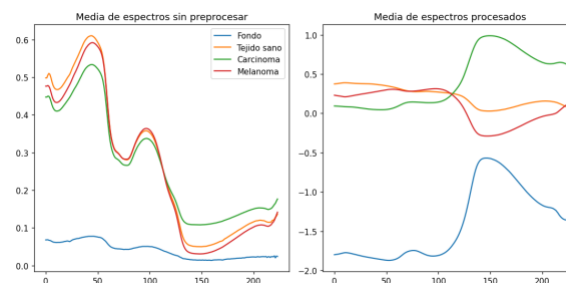


**Figure 2:** Figure showing the average spectra of healthy tissue, the basal cell carcinoma tissue and melanoma tissue, before and after pre-processing.

## References:

1. Petracchi B., Gazzoni M., Torti E., Marenzi E., Leporati F. (2023) Machine Learning-Based Classification of Skin Cancer Hyperspectral Images. *Procedia Computer Science*, 225, 2856-2865.



# Electrospun carbon nanofibers doped with metal nanoparticles used as sensors for high sensitive voltammetric drug determination

J. Smajdor<sup>1\*</sup>, M. Zambrzycki<sup>2</sup>, M. Marzec<sup>3</sup>, B. Paczosa-Bator<sup>1</sup>, R. Piech<sup>1</sup>

<sup>1</sup>Department of Analytical Chemistry and Biochemistry, Faculty of Materials Science and Ceramics, AGH University of Science and Technology, Al. Mickiewicza, 30-059 Krakow, Poland

<sup>2</sup>Department of Biomaterials and Composites, Faculty of Materials Science and Ceramics, AGH University of Science and Technology, Al. Mickiewicza, 30-059 Krakow, Poland

<sup>3</sup>Surface and Biomaterials Nanoengineering, Academic Centre for Materials and Nanotechnology, AGH University of Science and Technology, Al. Mickiewicza, 30-059 Krakow, Poland

## Abstract:

Electrospun carbon nanofibers (eCNF) and their hybrids with metallic and oxide nanoparticles are characterised by a set of favorable features that predispose this type of materials to electrochemical applications, including electroanalysis and storage and energy conversion [1]. They are characterised by a high share of  $sp^2$  bonds that ensure effective charge transport and good surface development, and their fibrous form and shape are particularly favourable from the point of view of the electrical percolation phenomenon. In hybrid systems, they primarily play the role of a substrate and a conducting network, and nanoparticles constituting electrocatalytically active centres are deposited on the surface of nanofibers. Electrochemical sensors based on eCNF nanocomposite systems do not require complicated and expensive equipment, while offering excellent detection limits, high sensitivity, a wide range of linearity, and a simple analytical procedure [2,3]. This work presents the results of research on electrochemical sensors based on hybrid systems based on electrospun carbon nanofibers for voltammetric drug detection. The morphology of the obtained layers is presented and the results obtained during quantitative measurements of selected organic compounds are presented.

**Keywords:** electrospun carbon nanofibers, metal nanoparticles, metal oxides, glassy carbon electrode, voltammetry, voltametric sensor, pharmaceutical analysis, biomedical application.

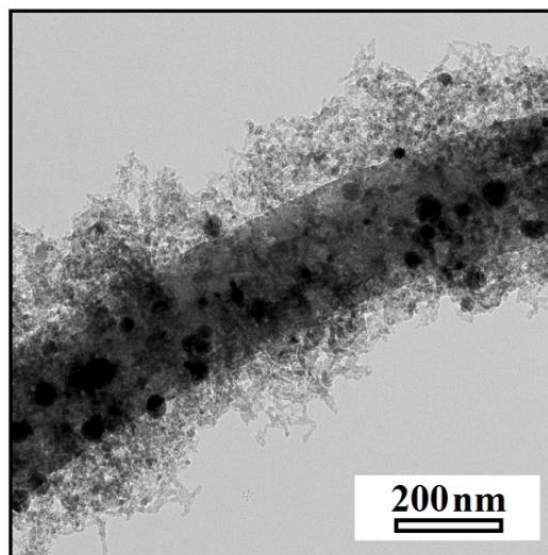


**Figure 1:** SEM images of hierarchical nanocomposite—carbon nanofibers/carbon nanotubes/NiCo nanoparticles (eCNF/CNT/NiCo) placed on the surface of glassy carbon electrode.

## References:

1. Zhang, B-T., Liu, H., Liu, Y., Teng, Y., Application trends of nanofibers in analytical chemistry, *Trends Anal. Chem.*, 131, 115992.
2. Smajdor, J.; Zambrzycki, M.; Paczosa-Bator, B.; Piech, R. (2022) Use of Hierarchical Carbon Nanofibers Decorated with NiCo Nanoparticles for Highly Sensitive Vortioxetine Determination, *Int. J. Mol. Sci.*, 23, 1-12.
3. Smajdor, J., Zambrzycki, M., Marzec, M., Paczosa-Bator, B., Piech, R. (2023) Electrochemical determination of thiethylperazine using semi-graphitized carbon nanofibers-MnO nanocomposite, *Microchim. Acta.*, 190, 1–12.

## Funding:

Research project supported by program “Excellence Initiative-Research University” for the AGH University of Science and Technology.



# Optimising Raman Spectroscopy for Early Detection of Microbial Spoilage in Meat

Debarati Bhowmik<sup>1</sup>, Jonathan Rickard<sup>2</sup> Professor Pola Goldberg Oppenheimer<sup>1,3\*</sup>

<sup>1</sup>Department of Chemical Engineering, University of Birmingham, Birmingham, UK

<sup>2</sup>Department of Physics, Cavendish Laboratory, University of Cambridge, Cambridge, UK

<sup>3</sup>Healthcare Technologies Institute, Institute of Translational Medicine, Birmingham, UK

## Abstract:

The rapid and accurate detection of microbial spoilage in meat products is crucial for ensuring food safety and quality. Traditional methods for identifying spoilage are time-consuming and often lack early detection sensitivity<sup>1</sup>. This study explores the potential of Raman spectroscopy, a non-destructive and sensitive analytical technique, for detecting microbial contamination in meat. By optimising Raman spectroscopic parameters and using advanced data processing algorithms, we aim to identify specific spectral markers associated with spoilage microorganisms, thereby enhancing food safety and quality control in the meat industry.

We systematically collected Raman spectra from meat samples under various spoilage conditions and used multivariate analysis techniques, like the Self-Optimising Kohonen Index Network (SKiNET)<sup>2</sup>, to correlate spectral features with the microbial load (Figure 1). Our results demonstrate that Raman spectroscopy can effectively distinguish between fresh and spoiled meat with high sensitivity and specificity. The identified spectral markers were consistent across different meat types and spoilage conditions, showcasing the technique's robustness.

The rapid acquisition of Raman spectra and real-time data processing allows for immediate meat quality assessment, enhancing food safety protocols, reducing spoilage waste and preventing food poisoning. Implementing Raman spectroscopy in the meat industry promises improved consumer confidence, more efficient supply chain management, and better regulatory compliance. This research has practical implications, as it paves the way for integrating Raman spectroscopy with automated systems for continuous monitoring and refining detection algorithms to enhance accuracy, thereby significantly improving food safety and quality control in the meat industry.

**Keywords:** food safety, machine learning, Raman spectroscopy, sustainable technology, SKiNET, resilience, sustainability, biosensor

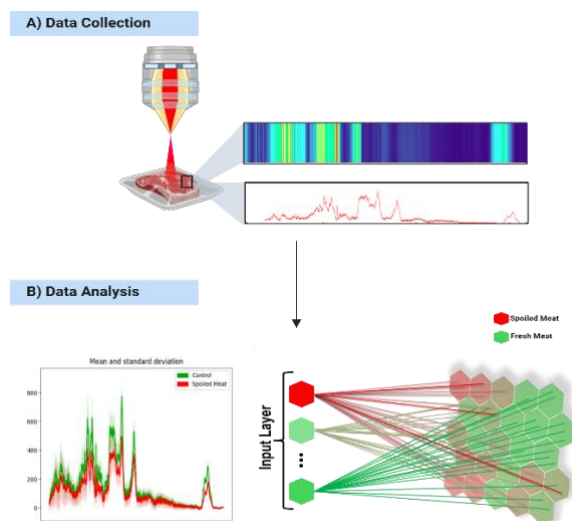


**Figure 1:** The figure illustrates the Raman spectra obtained from fresh and spoiled meat samples, highlighting distinct spectral markers indicative of microbial spoilage. It also depicts the use of the Self-Optimising Kohonen Index Network (SKiNET) to enhance detection sensitivity and accuracy, demonstrating the differentiation between fresh and contaminated meat samples.

## References:

1. Chen, J. et al. Critical review and recent advances of emerging real-time and non-destructive strategies for meat spoilage monitoring. *Food Chemistry* vol. 445 Preprint at <https://doi.org/10.1016/j.foodchem.2024.138755> (2024).
2. Banbury, C. et al. Development of the Self-Optimising Kohonen Index Network (SKiNET) for Raman Spectroscopy-Based Detection of Anatomical Eye Tissue. *Sci Rep* 9, (2019).

# Reliability Analysis of Hydrogen Pressure Sensor for Automotive Applications

H. Lee, C. Han, J. Lee, K. Lee, and H. Sagong\*

Reliability Technology R&D Dept., Korea Automotive Technology Institute (KATECH), Cheonan, Republic of Korea

## Abstract:

Fuel cell electric vehicles (FCEVs) have been widely studied as promising automotive solutions because of their environmental advantages, improved driving range, and versatile applications for heavy duty vehicles. Also, the global market of hydrogen sensors which are crucial for detecting hydrogen leakage and concentration in the vehicles to ensure the safety of hydrogen fuel cell systems has significantly grown. Specifically, hydrogen pressure sensors, typically positioned on manifolds and regulators of FCEVs, perform an important functions in proactively diagnosing safety issues arising from potential leaks.

In this paper, we studied silicon strain gauge-based pressure sensors (Figure 1), analyzing weakness points in real-world vehicle environments and failure mechanisms, and proposing process optimization methods. After environmental reliability tests, some failure samples were observed only in temperature and humidity cycle test with abnormal output voltage including both increases and decreases compared to normal samples (Figure 2). This results is also consistent with analysis of vehicle-level failure samples in the actual field.

These abnormal voltage fluctuation phenomenon can be described by corrosion mechanism of the printed circuit boards (PCBs) with high humidity and temperature conditions according to the Arrhenius–Peck model. Furthermore, we propose a simplified model driven by the formation of humidity-induced parasitic resistances to anticipate output voltage fluctuations from the signal processing IC within the sensor. This reliability model confirms that PCBs components exposed to humidity undergo corrosion, resulting in parasitic series or parallel resistances causing output voltage fluctuations (Figure 3).

Finally, through structural and elemental analysis, we propose the process improvement methods such as uniform PCB conformal coating to improve the corrosion vulnerabilities due to moisture exposure and confirms that the improved pressure sensors show no output voltage shift even after stress as shown in Figure

4. Utilizing these findings from the development phase, we can proactively mitigate and enhance the reliability and safety aspects of future automobiles, thereby preventing real-world field issues.

**Keywords:** electronic circuits, hydrogen pressure sensor, physics of failure, reliability, silicon strain gauges

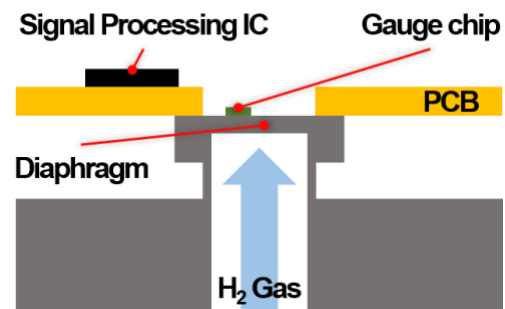


**Figure 1:** Schematic diagram of silicon strain gauge-based hydrogen pressure sensors

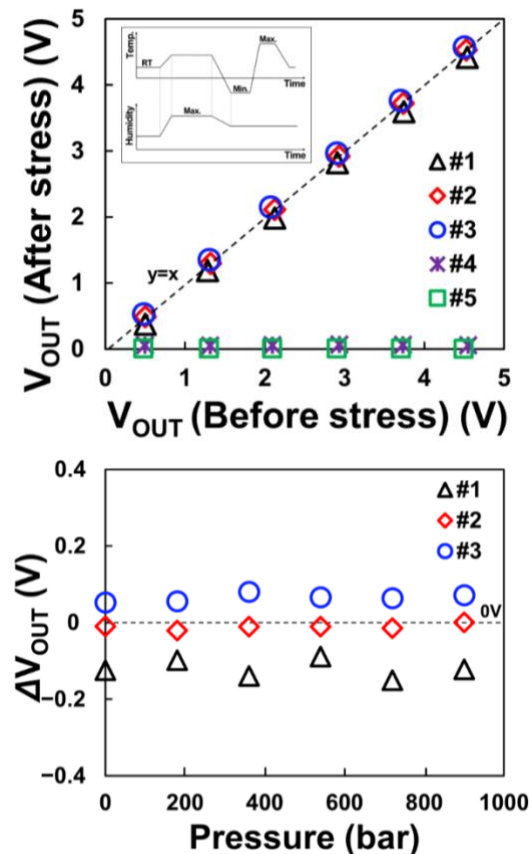


**Figure 2:** Comparison of pressure sensor's output voltage before and after temperature and humidity cycling stress: After the test, sample #1 to #3 show abnormal output voltage signals including both increases and decreases, sample #4 and #5 show no output voltage.  $V_{OUT}$  is output voltage,  $\Delta V_{OUT}$  is the  $V_{OUT}$  shift of subtracting  $V_{OUT}$  before stress from  $V_{OUT}$  after stress.

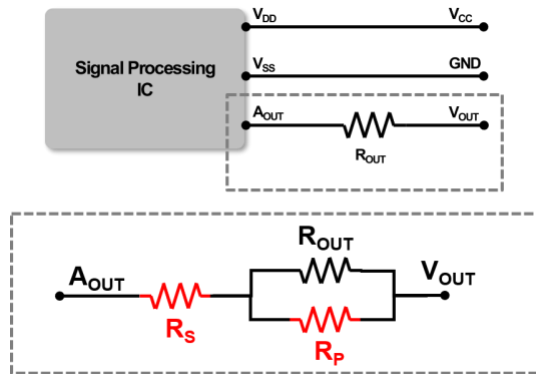


**Figure 3:** A simplified model driven by the formation of humidity-induced parasitic resistances to describe output voltage fluctuations:  $A_{OUT}$  is output voltage of signal processing IC,  $R_{OUT}$  is output resistance in the PCB,  $R_S$  is parasitic series resistance, and  $R_P$  is parasitic parallel resistance.  $R_S$  causes  $V_{OUT}$  decrease,  $R_P$  causes  $V_{OUT}$  increase, and both of resistance generation causes unexpected  $V_{OUT}$ .

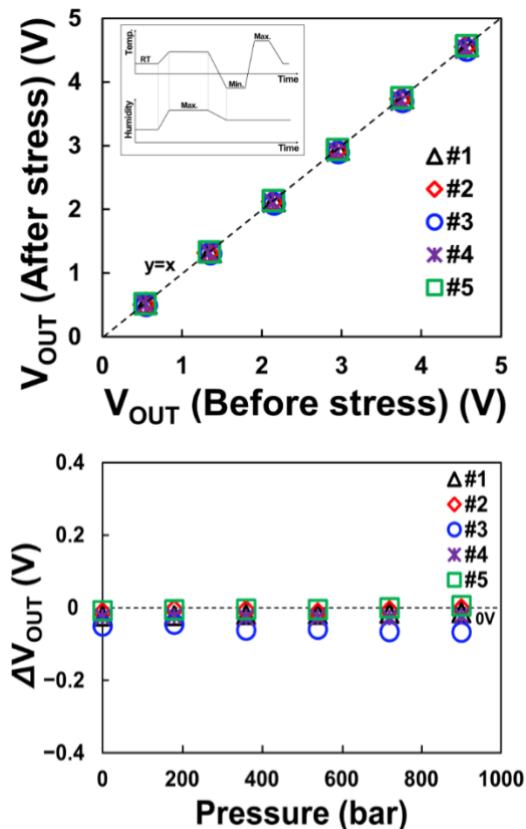


**Figure 4:** Comparison of output voltage before and after temperature and humidity cycling stress with improved pressure sensors: After the test, all samples show no significant  $\Delta V_{OUT}$ .

#### References:

1. Hubert, T., Boon-Brett, L., Black, G., Banach, U. (2011) Hydrogen sensors—A review, *Sens. Actuators B Chem.*, 157, 329-352
2. Hualiang, H., Xingpeng, G., Guoan, Z., Zehua, D. (2011), The effects of temperature and electric field on atmospheric corrosion behavior of PCB-Cu under absorbed thin electrolyte layer Protein helical structure enhancement in fluorinated-phosphonate nanoporous silica glasses characterized by circular dichroism spectroscopy, *Corros. Sci.*, 53, 1700-1707.

# Development of an Integrated Self-Diagnostic System for Water Quality Measurement Sensors

K.-Y. Hwang\*, S. Bae

Technology Research Institute, BLUESEN Co. Ltd., Daegu, Republic of Korea

## Abstract:

Recent declines in public trust in tap water in South Korea have prompted the Ministry of Environment to initiate 161 projects aimed at establishing Smart Water Management (SWM) infrastructure. The primary objective of these projects is to create a comprehensive monitoring and management system for the water supply process to prevent accidents and facilitate rapid response to incidents. This infrastructure includes the installation of real-time monitoring facilities, management systems, incident response mechanisms, and cleaning and drainage systems within the water supply network. As a result of these efforts, water quality measurement devices and automatic drain systems have been deployed throughout the network, significantly enhancing the monitoring and management functions of the tap water supply system. The increased number of water quality measurement devices necessitates precise maintenance and repair to ensure reliable monitoring and to optimize the use of water quality interpretation models. Currently, maintenance of these devices are conducted on a fixed schedule. However, due to the large-scale expansion of infrastructure, continuing with traditional maintenance frequency has become impractical and costly. This research focuses on developing sensor self-diagnosis technology that assesses the reliability of measurement values by monitoring variations in the sensor's unique characteristics and informs users of potential issues. The proposed self-diagnosis process involves exposing sensors, which are typically submerged in water, to air. The baseline signal of the sensor is read and stored, and after a specified period, this baseline is compared with the initially recorded value to detect any anomalies (Figure 1). This approach utilizes the correlation between the baseline signal, which changes slightly over time, and the current measurement values to assess whether the measurements fall within the acceptable error range.

**Keywords:** drinking water, water supply network, water quality, measuring device, self-diagnostic, sensor maintenance, sensor repair.

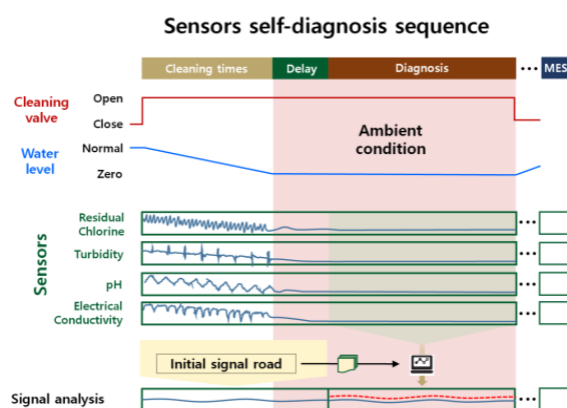


**Figure 1:** Sensor self-diagnosis system for water quality measurement devices: to facilitate sensor cleaning, water is drained from the sensor while its baseline signal is simultaneously recorded when exposed to air to establish an initial reference value, which is then compared with subsequent readings to detect anomalies and evaluate the sensor's operational status.

## References:

1. Haas, C.N., and Karra, S.B. (1984), Kinetics of waste chlorine demand exertion, *J. Water Pollution Cont. Fed.*, 56, 170-173.
2. Hua, F., West, J.R., Barker, R.A., Forster, C.F. (1999), Modelling of chlorine decay in municipal water supplies, *Water Res.*, 33, 2735-2746.

# Integrating Satellite, Ground Sensors, and AI for Surface Water Protection: The EcoNet Project

Gerardo Grasso<sup>1</sup>, Daniela Zane<sup>1</sup>, Bruno Brunetti<sup>1</sup>, Sabrina Foglia<sup>1</sup>, Giulio Ferrara<sup>1</sup>, Valeria La Pegna<sup>2</sup>, Davide De Santis<sup>2</sup>, Dario Cappelli<sup>2</sup>, Martina Frezza<sup>2</sup>, Iliaria Petracca<sup>2</sup>, Fabio Del Frate<sup>2</sup>, Giorgio Licciardi<sup>3</sup>, Patrizia Sacco<sup>3</sup>, Deodato Tapete<sup>3</sup>, Roberto Dragone<sup>1</sup>

<sup>1</sup>Istituto per lo Studio dei Materiali Nanostrutturati, Consiglio Nazionale delle Ricerche (CNR-ISMN), Rome, Italy

<sup>2</sup>Dipartimento Ingegneria Civile ed Ingegneria Informatica, Università degli Studi "Tor Vergata", Rome, Italy

<sup>3</sup>Agenzia Spaziale Italiana (ASI), Rome, Italy

## Abstract:

Human activities introduce contaminant mixtures, disrupting freshwater ecosystem balance. Monitoring surface freshwater is therefore crucial for safeguarding ecosystems and promoting sustainable development of (peri)urban areas. Current monitoring systems are discontinuous and do not meet timeliness requirements, making difficult to detect ecosystem changes before their impact on habitat and biodiversity.

The EcoNet project ([www.econet.cnr.it](http://www.econet.cnr.it)), funded by the Italian Space Agency under the "Innovation for Downstream Preparation for Science" program, aims to develop and demonstrate a sensoristic system with ground-based sensors and satellites data integrated using Artificial Intelligence (AI) for rapid diagnostic monitoring of variations in the natural state of surface waters (Figure 1). This multiparametric and flexible system combines a microalgae-based toxicity biosensor and satellite sensors for monitoring water parameters, alongside with multi/hyperspectral images from PRISMA, Sentinel-2, and Landsat 8/9 missions. Leveraging the synergy between these multisensory technologies, an Artificial Neural Network (based on a Multi-Layer Perceptron model) is implemented to effectively handle and analyze subtle data relationships. Overall, the proposed integrated sensor-driven system aims to overcome limitations of single ground or remote acquisition techniques. The results from ground bio/chemosensor measurements highlight significant variations in selected physico-chemical parameters among different water sampling points, attributed to agricultural and peri-urban anthropogenic pressures. Retrieval relevant parameters (e.g., concentration of Chlorophyll-a, Total Suspended Matter, Colored Dissolved Organic Matter, Total Phosphorus and Total Nitrogen) from satellite data is underway. Additionally, synthetic satellite images are being generated to expand the hyperspectral dataset used for the neural network algorithm training process. The Artificial Neural Network models development

proved to be interesting for estimating these parameters and assessing the natural state over entire surfaces of the tested water basins. Overall, EcoNet aims to establish a comprehensive downstream service to support user communities in managing protected areas, such as the Natura 2000 sites, and promotes environmental awareness through dissemination actions.

**Keywords:** Integrated Analytical Systems, PRISMA, Sentinel-2, Hyperspectral remote sensing, Bio/chemosensoristic devices, Artificial Intelligence, Freshwater ecosystems, Natura 2000

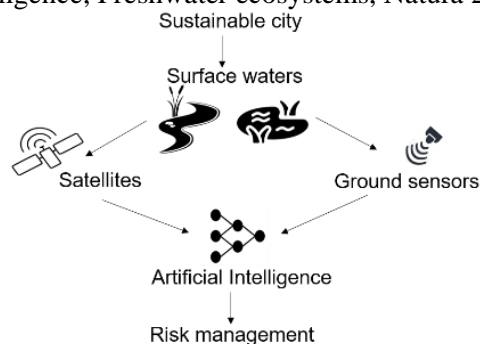


**Figure 1:** Schematic representation of EcoNet concept

## References:

1. Grasso, G., Zane, D., Dragone, R. (2022) Field and Remote Sensors for Environmental Health and Food Safety Diagnostics: An Open Challenge, *Biosens*, 285, 1-3.
2. Frezza, M., La Pegna, V., De Santis, D., Cappelli, D., Del Frate, F. (2023). Estimation of chlorophyll concentration on surface water bodies from hyperspectral satellite data. *IGD*, 7, 258-261.
3. Tapete, D. Coletta, A. (2022) ASI's roadmap towards scientific downstream applications of satellite data, In: *EGU General Assembly Conference Abstracts*, Vienna, EGU22-5643.



# Biosynthesis of cellulose using Antarctic bacterial strains

Maria Chiara Biondini<sup>1,3</sup>, Alberto Vassallo<sup>1</sup>, Martina di Sessa<sup>1,2,3</sup>, Marco Zannotti<sup>2</sup>, Rita Giovannetti<sup>2</sup>, Sandra Pucciarelli<sup>1</sup>

<sup>1</sup>School of Biosciences and Veterinary Medicine, University of Camerino, Via Gentile III da Varano, 1, 62032, Camerino (Italy)

<sup>2</sup>School of Sciences and Technology, University of Camerino, 62032, Camerino (Italy)

<sup>3</sup>IUSS Pavia, Palazzo del Broletto, Piazza della Vittoria, n.15, 27100, Pavia (PV)

## Abstract:

The demand for biopolymers is constantly increasing and is estimated to grow further especially to satisfy the urgent needs of companies to move towards more sustainable approaches and to find alternative solutions to decrease their environmental impact. Among the emerging biomaterials, bacterial cellulose is arousing great interest since it possesses peculiar characteristics which distinguish it from the vegetal counterpart (1). Despite the similarities in the chemical structures, indeed, bacterial cellulose showed higher purity, water holding capacity, and tensile strength resistance if compared to the plant-based one. While the production of this latter could be associated to deforestation and ecosystem degradation, bacterial cellulose can be obtained following green protocols which require unexpensive media, also including waste recycling. Although the scale-up of the production of this biomaterial remains a big challenge, its versatility paves the way towards many different applications, including papermaking, food, pharmaceutical, and biomedical sectors. Several bacterial strains have already been demonstrated to be cellulose producers. In this work, unique Antarctic bacteria isolated from a consortium associated to a ciliate organism were tested for cellulose production. Antarctic microorganisms developed extraordinary strategies of survival, involving the ability to resist against cold temperatures and UV radiations, to scavenge iron under limited concentrations, and to detoxify hazard compounds, such as heavy metals and pollutants (2). They also showed they could produce different biopolymers in response to the environmental stress factors. Thus, the aim of this project is to exploit the fascinating metabolism of Antarctic bacteria to produce cellulose with different shapes and properties, to optimize its biosynthesis, and to characterize it through chemical analyses.

**Keywords:** Biopolymers, microorganism metabolism, green protocol, industrial applications.

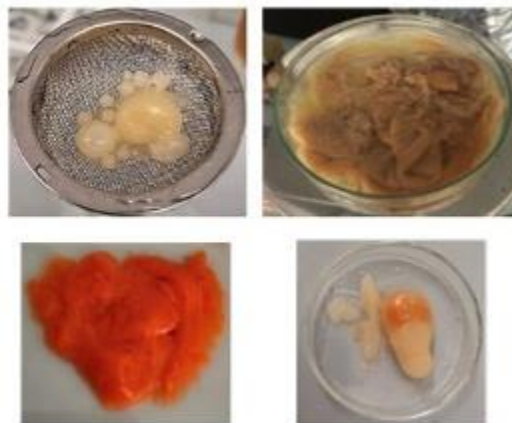


**Figure 1:** Cellulose synthesized by Antarctic bacteria grown under different conditions, obtaining cellulose-based biofilms of different shapes. Static incubation resulted in sheet-like structures, while under agitation spherical shapes were obtained. In the presence of additional stress factors, such as iron deficiency or UV light radiation, a pigmented cellulose was produced.

## References:

1. Lahiri D, Nag M, Dutta B, Dey A, Sarkar T, Pati S, Edinur HA, Abdul Kari Z, Mohd Noor NH, Ray RR. Bacterial Cellulose: Production, Characterization, and Application as Antimicrobial Agent. *Int J Mol Sci.* 2021 Nov 30;22(23):12984.
2. Ramasamy KP, Mahawar L, Rajasabapathy R, Rajeshwari K, Miceli C, Pucciarelli S. Comprehensive insights on environmental adaptation strategies in Antarctic . 1664-302X, 2023, Vol. 14.

# Characterization of a blue pigment isolated from an Antarctic *Rhodococcus* bacterial strain

Martina di Sessa<sup>1,2,3\*</sup>, Maria Chiara Biondini<sup>1,3</sup>, Alberto Vassallo<sup>1</sup>, Marco Zannotti<sup>2</sup>,  
Sandra Pucciarelli<sup>1</sup>, Rita Giovannetti<sup>2</sup>

<sup>1</sup>School of Sciences and Technology, Section Chemistry, University of Camerino, 62032, Camerino, Italy

<sup>2</sup>School of Biosciences and Veterinary Medicine, University of Camerino, Via Gentile III da Varano, 1, 62032, Camerino, Italy

<sup>3</sup>IUSS Pavia, Palazzo del Broletto, Piazza della Vittoria, n.15, 27100, Pavia (PV)

## Abstract:

Antarctic microorganisms adopted adaptive strategies that include the production of different compounds like biofilm, pigments, or antibiotics (1). For what concerns pigment's production, these are produced by particular processes like photo/chemo-synthesis, or as protection from solar light radiation (in particular UV light), a property that is particularly important in the Antarctic ecosystem due to the stratospheric ozone hole (1). Most of pigments that are produced are carotenoids, melanin, violacein, prodigiosin, pyocyanin, actinorhodin, and zeaxanthin.

This preliminary study focuses on the characterization of a novel pigment produced by the Antarctic bacterium *Rhodococcus* ef1 that shows important peculiarities. It was characterized among UV-Vis spectroscopy, HPLC analyses and Mass spectroscopy. Furthermore, some properties have been monitored, as pH behavior, solubility, and its thermal and photo stability. This new pigment displays different colour according to media conditions, i.e. it is blue in alkaline medium, while it is pink in acidic medium. The extraction in water is favoured by high temperatures (around 55°C) and, after extraction, it remains stable at room temperature for several days. This pigment, due to its peculiar features, might find interesting applications in various fields, in particular in medical or energy fields, as anticancer or as electron shuttle in microbial fuel cells.

**Keywords:** pyocyanin, antioxidant activity, pH, UV-Vis spectroscopy, HPLC analyses and Mass spectroscopy.

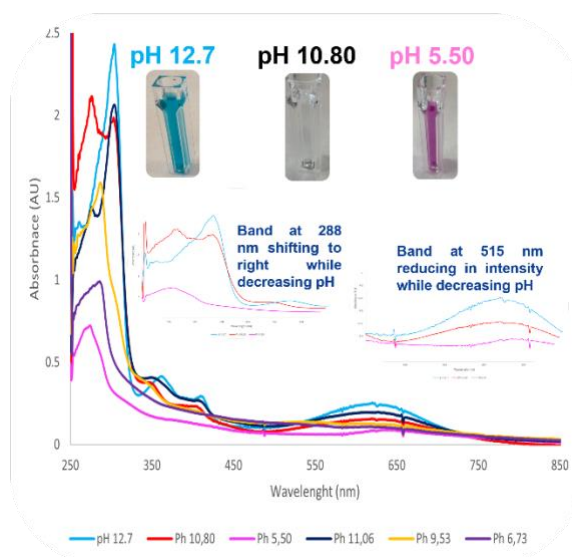


**Figure 1:** The UV-Vis adsorption properties of this pigment in water under different pH conditions was monitored. In high alkaline pH, all the bands are right-shifted, while at acidic pH, all the bands are shifted to the left. The most significant bands are present at 288 and 515 nm (acidic pH and pink colour) and at 303 and 617 nm (basic and blue colour). At a pH around 10 the pigment becomes completely transparent.

## References:

1. Comprehensive insights on environmental adaptation strategies in Antarctic . Ramasamy KP, Mahawar L, Rajasabapathy R, Rajeshwari K, Miceli C, Pucciarelli S. 1664-302X, 2023, Vol. 14.

# Antimicrobial effect on coated catheter surface

Á. Deák<sup>(1)</sup>, L. Janovák<sup>(1)</sup>, D. Szabó<sup>(2)</sup>, L. Rovó<sup>(2)</sup>, A. Zore<sup>(3)</sup>, A. Abram<sup>(4)</sup>, K. Bohinc<sup>(3)</sup>

<sup>(1)</sup> Department of Physical Chemistry and Materials Science, University of Szeged, H-6720, Rerrich Béla tér 1, Szeged, Hungary;

Principal Author's e-mail: agotadeak@chem.u-szeged.hu

<sup>(2)</sup> Department of Oto-Rhino-Laryngology and Head & Neck Surgery, University of Szeged, Tisza Lajos krt. 111, H-6724 Szeged, Hungary

<sup>(3)</sup> Faculty of Health Sciences, University of Ljubljana, Zdravstvena pot 5, 1000 Ljubljana, Slovenia

<sup>(4)</sup> Department for Nanostructured Materials, Jožef Stefan Institute, 1000 Ljubljana, Slovenia

## Abstract:

Catheters are used worldwide in diagnostic and therapeutic. The catheter is associated with the urinary tract where the infection caused by patient's microflora can take place. Studies

have shown that the following bacterial strains significantly contribute to the production of biofilms on the catheter surfaces for example *E. coli* (60%–80%) [1]. One type of self-cleaning surfaces is the photocatalytic coating which can chemically degrade organic materials when exposed to light [2,3].

The aim of this study was to investigate a durable composite coating on the catheter surfaces (Fig.1) that exert antimicrobial effects.

The structure and morphology of the synthesised nanoparticles/polymer coatings were examined by SEM and EDS - measurements. The surfaces were additionally characterized by measuring the roughness and hydrophobicity. The antimicrobial property of the coatings were also examined and the prepared coatings were exposed to bacterial suspension of *Escherichia coli* (Gram negative), *Streptococcus pyogenes* (Gram positive). According to our experiments the structure of the coatings becomes more and more structured and roughened with the increasing of nanoparticles (for eg. ZnO) in the nanocomposite content. The poly(ethyl acrylate-co-methyl methacrylate [p(EA-co-MMA)] polymer binder increase the mechanical durability of the composites. The results showed that surface roughness influenced the wetting properties of the hybrid layers and they have an important role on the bacterial adhesion and inactivation.

The surface roughness, wettability and bacterial adhesion properties can be varied by adjusting the loading of photocatalyst particles into the polymer matrix. The presence of ZnO decreases the bacterial adhesion.

## Acknowledgments:

Ágota Deák is very thankful for the National Research, Development and Innovation Office-NKFIH (Hungary) for support through program PD 142293. This work was also supported by the UNKP-23-5 (L.J.) and ÚNKP 23-4-SZTE-641 (Á.D.) New National Excellence Program of the Ministry for Innovation and Technology from the National Research, Development and Innovation Fund as well as by the János Bolyai Research Scholarship of the Hungarian Academy of Sciences (L.J.).

**Keywords:** catheter, coating, self-cleaning surfaces, antimicrobial property.

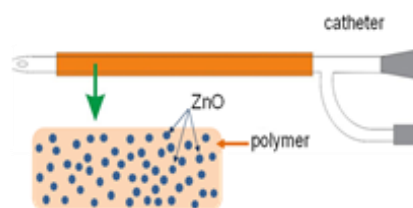


**Figure 1:** Durable composite coating on the catheter surface.

## References:

1. É. Campos Mota, A.C. Oliveira, *Vigil. Sanit. Debate*, 5, 116–122 (2017).
2. Á Deák, L. Janovák et al., *Applied Surface Science*. 389, 294 (2016).
3. Sz. P. Tallósy, L. Janovák, J. Ménesi et. al., *Environ Sci Pollut Res*, 21, 11155 (2014).

# Advancements in Biodegradable Magnesium-Based Implants: Enhancing Biocompatibility and Corrosion Resistance through Alloy Development

Tomasz Tański<sup>1</sup>, A. Woźniak<sup>2\*</sup>, Przemysła Snopiński<sup>1</sup>, Katarzyna Cesarz-Adreczke<sup>1</sup>, Mariusz Król<sup>1</sup>

<sup>1</sup> Department of Engineering Materials and Biomaterials, Silesian University of Technology, 18A Konarskiego Str., 41-100, Gliwice, Poland

<sup>2</sup> Research Laboratory. Faculty of Mechanical Engineering, Silesian University of Technology Konarskiego Street 18A, Gliwice, Poland

## Abstract:

The aging population and rising skeletal disorders have driven significant research into advanced implants. The Global Burden of Disease Study 2021 noted a 123.4% increase in musculoskeletal disorders from 1990 to 2020, with another 115% rise expected by 2050. Improving biomaterial functionality is crucial for better implant-tissue compatibility. Failure rates of endoprosthetic/implants reconstructions range from 40 to 73% over 5 to 15 years. Biodegradable magnesium-based materials hold promise for orthopedic implants due to their natural degradation in the body, reducing the need for removal surgeries and minimizing adverse reactions. They match bone's mechanical properties, support bone growth, and can be tailored to degrade at controlled rates through alloying and surface treatments. This work aimed to develop an Mg-based alloy with silver (Ag) and manganese (Mn) additions to enhance corrosion resistance, time of degradation, and in effect biocompatibility. This aims to improve implant performance, offering a balanced degradation that supports healing while integrating seamlessly with bone tissue.

The SEM analysis of the cast Mg-based alloys revealed that both ZK60 and modified ZK60xMn/Ag ( $x = 0.5, 1\%$ ) exhibited a dendritic microstructure with the  $\alpha$ -Mg phase (matrix), secondary phase particles, and eutectic structures. Potentiodynamic testing showed improved corrosion resistance in the ZK60 alloy with the addition of Ag and Mn. The Tafel plots for these samples shifted to more noble potentials with lower corrosion current densities. These results indicate that controlled degradation through chemical composition optimization is achievable. It was found that the best performance characteristics have been ZK60+1%Mn/Ag. Next, we conducted an ultrasonic atomization process to produce modified ZK60 powders suitable for additive manufacturing. SEM analysis and physical

property tests revealed that the powder particles were spherical and displayed a smooth surface, along with improved flowability. These findings highlight the potential of ZK60+1%Mn as a promising material for producing biodegradable orthopedic implants using 3D printing technology

**Keywords:** Mg-based alloy, EIS, corrosion, biodegradation, SEM.

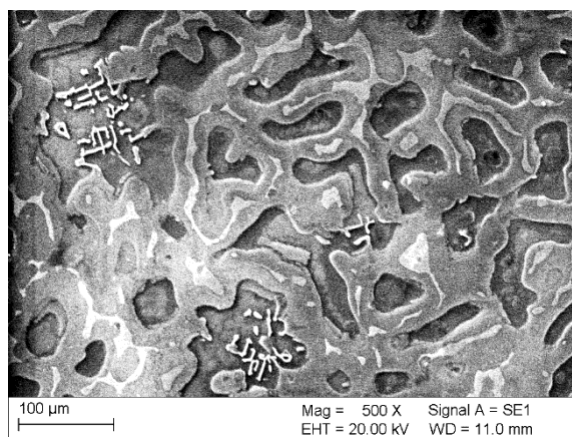


**Figure 1:** Example microstructure of ZK60+1%Ag alloy.

## References:

1. Zhang, Y. et al. (2021) The effect of enzymes on the in vitro degradation behavior of Mg alloy wires in simulated gastric fluid and intestinal fluid. *Bioact. Mater.* 7, 217–226.
2. Dong, H., Lin, F., Boccaccini, A. R. & Virtanen, S. (2021) Corrosion behavior of biodegradable metals in two different simulated physiological solutions: Comparison of Mg, Zn and Fe. *Corros. Sci.* 182, 109278.
3. Aljihmani, L. et al (2019). Magnesium-Based Bioresorbable Stent Materials: Review of Reviews. *J. Bio- Tribo-Corrosion* 5, 1–15.

**Founding:** POLTUR5/2022/27/3D-BioMg/2023



# Tailoring Fibrinogen Adsorption on Layer-by-Layer Films: the impact of hydrophilicity and film structure of cross linked PAA/PAH multilayers

B. Borisova<sup>1</sup>, T. Andreeva<sup>1,2,\*</sup>, R. Tzoneva<sup>1</sup>, R. Krastev<sup>2</sup>

<sup>1</sup> Institute of Biophysics and Biomedical Engineering, Bulgarian Academy of Sciences, Acad. G. Bonchev Str., Bl. 21, Sofia 1113, Bulgaria

<sup>2</sup> Faculty of Life Sciences, Reutlingen University, Alteburgstraße 150, 72762 Reutlingen, Germany

## Abstract:

Fibrinogen (FNG) adsorption is a crucial factor for biocompatibility of biomaterials for blood-contacting applications, as it can promote platelet adhesion and activation, which potentially can lead to thrombus formation (1). This study investigated FNG adsorption on surfaces targetly modified by layer-by-layer (LbL) constructed polyelectrolyte multi-layer (PEM) films, focusing on the interrelationship between surface properties and protein adsorption.

We used PEMs because they provide the possibility of fine and controlled modification of surface properties without affecting the surface microtopology and bulk properties of the material to which they are applied (2). The choice of polyelectrolyte pairs and the process parameters used in PEM fabrication (pH, addition of electrolytes, temperature, etc.) governs their physicochemical properties (2) and, consequently, protein adsorption and cell adhesion to PEM-coated surfaces, that can range from cytophilic to cytophobic (3).

In this study a pair of weak polyelectrolytes, polyacrylic acid / polyalilaminhydrochloride (PAA/PAH), was used to prepare PEM films. Films were assembled under different deposition conditions (pH change), with PAH and PAA as the surface layer, and were thermally cross-linked after assembly. Cross-linking of PEMs results in a polymer chain structure that is more compact and less aligned compared to the non-crosslinked films (4). The thickness of the films was quantified using ellipsometry, while the contact angle method was used to determine surface wettability. The Owens-Wendt-Rabel-Kaelble method was used to estimate surface energy. The Bradford assay was used to quantify FNG adsorption onto the different PEMs. The study contributes to the understanding of the impact of surface charge, hydrophilicity and film structure on protein adsorption, and biomaterial design techniques can be optimized to obtaine high biocompatibility. The results can be used in the development of medical implants, biosensors, and drug delivery systems.

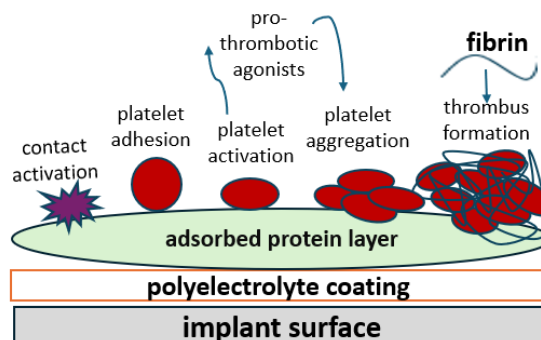


**Figure 1:** Thrombus formation on a biomaterial surface.

**Keywords:** protein adsorption, protein surface density, surface modification, weak polyelectrolytes, cross-linking, polyelectrolyte multilayers, biofunctionalization

## References:

1. Horbett, T. A. (2018) Fibrinogen adsorption to biomaterials, *J Biomed Mater Res A*, 106(10), 2777-2788.
2. Hartmann, H., Krastev, R. (2017) Biofunctionalization of surfaces using polyelectrolyte multilayers, *BioNanoMaterials*, 18(1-2), 20160015.
3. Mendelsohn, J. D., Yang, S. Y., Hiller, J., Hochbaum, I., Rubner, M. F. (2003) Rational design of cytophilic and cytophobic polyelectrolyte multilayer thin films, *Biomacromolecules*, 4(1), 96-106.
4. Jang, W. S., Jensen, A. T., Lutkenhaus, J. L. (2010) Confinement Effects on Cross-Linking within Electrostatic Layer-by-Layer Assemblies Containing Poly(Allylamine Hydrochloride) and Poly(Acrylic Acid), *Macromolecules*, 43, 9473– 9479.



# Development of a Novel Photothermal Material Using Gold Nanoparticles Synthesized Inside a Hydrogel for Biomedical and Biocatalytic Applications

M.J. Martínez-Tomé\*, A. Balah Tahiri, M. Rubio-Camacho, J. Gómez, C.R. Mateo, R. Esquembre  
Instituto de Investigación, Desarrollo e Innovación en Biotecnología Sanitaria de Elche (IDiBE),  
Universidad Miguel Hernández (UMH), Elche, Spain

## Abstract:

Photothermal materials, such as plasmonic nanoparticles, which convert light energy into heat, have emerged as promising tools in biomedical research for applications such as cancer therapy, drug delivery and tissue engineering. In addition, recently, reports have been published on plasmonic nanostructures as functional supports to simultaneously achieve enzyme immobilization and photothermal control of enzyme activity. This photothermal approach can perform the remote control of local heating in the reaction system, compared to other conventional methods which can just control the bulk temperature [1]. The few studies reported so far with this methodology, mainly carried out with lipases, have shown a local heating of the reaction system after Vis-NIR irradiation, consequently improving the lipolytic activity of the immobilized lipase. Taking these results into account, we are developing a project whose goal is the immobilization of enzymes in polyacrylamide-based hydrogels nanostructured with gold nanoparticles (AuNPs) to develop a platform for enzymatic degradation of toxic compounds. Within this project, we present here a remarkable breakthrough: the synthesis of AuNPs within a hydrogel matrix, which opens up a very novel potential for photothermal applications. The nanostructuring of the hydrogel with gold nanoparticles has been developed using a new methodology in which the hydrogel composition itself acts as a reducing agent for the gold salt, synthesizing the nanoparticles directly inside the hydrogel (Figure 1). The properties of this new material have been characterized (absorption spectra, photothermal capacity, drying and swelling cycles, etc.), as well as its ability to couple to different enzymes whose activity has been evaluated inside the material. Specifically, we are currently carrying out preliminary studies in which we are incorporating laccase into the photothermal nanocomposite hydrogel with satisfactory results.

**Keywords:** Photothermal hydrogel, plasmonic nanoparticles, nanocomposites, immobilization of enzymes, laccase

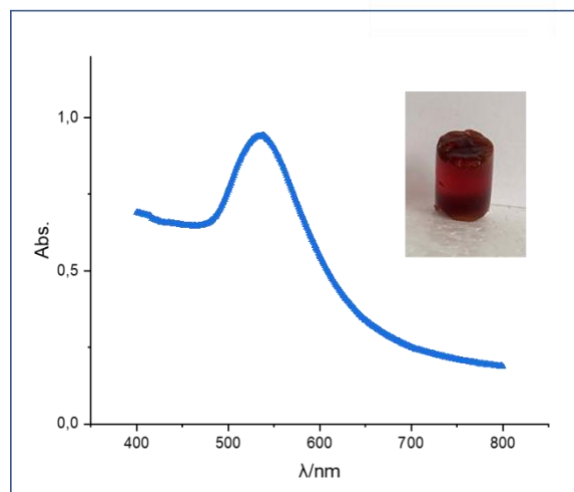


**Figure 1:** Absorption spectrum of AuNPs synthesized directly inside the hydrogel. Inset: Digital image of the photothermal hydrogel.

## References:

1. Zhu, Q., Song, J., Liu Z., Wu, K., Li, X., Chen, Z., Pang, H. (2022). Photothermal catalytic degradation of textile dyes by laccase immobilized on Fe<sub>3</sub>O<sub>4</sub>@SiO<sub>2</sub> nanoparticles. *J. Colloid Interface Sci.*, vol. 623, pp. 992–1001.

## Acknowledgments:

This work was supported by the project PID2022-138507OB-I00 (funded by MICIU/AEI/10.13039/501100011033).

# Antioxidant Effect of New Green Synthesized Bimetallic Nanoparticles using Phytocompounds from Goji Fruits

B. Moldovan<sup>1\*</sup>, V. Morosan<sup>1</sup>, L. David<sup>1</sup>, I. Baldea<sup>2</sup>

<sup>1</sup> Faculty of Chemistry and Chemical Engineering, "Babeş-Bolyai" University, Cluj-Napoca, Romania

<sup>2</sup> Faculty of Medicine, "Iuliu Hatieganu" University of Medicine and Pharmacy, Cluj-Napoca, Romania

## Abstract:

Nanobiotechnology facilitates the production and application of nanosize materials which interact with the human body with a high degree of specificity and can be tailored to achieve maximal therapeutic efficacy with minimal side effects. The use of bimetallic nanoparticles by controllable integration of two noble metals (e.g. gold and silver) into single nanostructures it's a great approach because the properties of both metals can be exploited and they also bring enhanced biological efficacy compared to single component materials, lower concentrations being required to achieve similar therapeutic effects [1]. Phenolic compounds from fruits can act both as reducing and capping agents for metal nanoparticles. Several studies revealed the presence of high amounts of polyphenolic compounds in goji fruits [2]. These compounds are well known free radical scavengers reducing damages generated by oxidative stress to the human body. Recent studies have also demonstrated that several types of inorganic nanoparticles can act as efficient antioxidants or free radical scavengers [3,4]. Therefore, functionalization of metal nanoparticles with natural antioxidants could reduce ROS production and protect the cell proteins and lipids. Herein, we aimed to elaborate an environmental-friendly method for the phytosynthesis of bimetallic nanoparticles and to evaluate their antioxidant capacity in order to establish their possible biological applications. The extracellular synthesis of a novel hybrid biomaterial based on core-shell Ag@Au nanoparticles using antioxidant compounds from Goji (*Lycium barbarum* L.), fruit extract as reducing and capping agent has been achieved. In order to obtain bimetallic nanoparticles with Ag core and Au coating, the silver nuclei were first obtained by reducing silver nitrate with bioactive compounds from goji berries, which later served as nucleation centers for the gold coating (Fig.1). UV-VIS and FT-IR spectroscopy, transmission electron microscopy (TEM) and X-ray diffraction technique (XRD) were used to characterize the obtained nanoparticles. The

TEM analysis of the synthesized Ag@Au NPs demonstrated their nearly spherical shape and a mean diameter of 11 nm. The *in vitro* protective role of phytosynthesized nanoparticles on hyperglycemia-induced oxidative stress on endothelial cells was evaluated, in order to establish their potential applications in the therapy of many diseases caused by ROS. The oxidative stress parameters: MDA as a marker of lipid peroxidation, CAT and SOD activities as markers of antioxidant defense, were assessed.

**Keywords:** bimetallic nanoparticles, goji berries, antioxidant activity

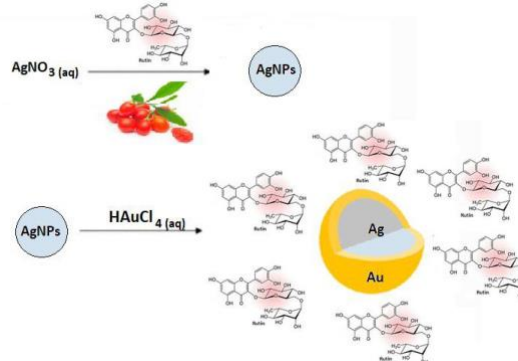


**Figure 1:** Synthesis of core-shell Ag@Au nanoparticles

## References:

1. Dahir, S.I., Arpita, R. (2023) Synthesis of Bimetallic Nanoparticles and Applications —An Updated Review, *Crystals*, 13(4), 637.
2. Zhao, W. H., Shi, Y. P. (2022), Comprehensive analysis of phenolic compounds in four varieties of goji berries at different ripening stages by UPLC–MS/MS, *J. Food Comp. Anal.*, 106, 104279.
3. Kim, T., Hyeon, T. (2013). Applications of inorganic nanoparticles as therapeutic agents, *Nanotechnology*, 25(1), 012001.
4. Naseem, K., Aziz, A., Khan, M. E., Ali, S., Khalid, A. (2024). Bioinorganic metal nanoparticles and their potential applications as antimicrobial, antioxidant and catalytic agents: a review, *Rev.Inorg. Chem.*, In Press.

# DESIGN AND DEVELOPMENT OF CYCLODEXTRIN NANOSPONGES-BASED *IN SITU* GELLING SYSTEMS TO CO-DELIVER POLYPHENOLS FOR CANDIDIASIS THERAPY

Sharanya V Paramshetti<sup>1</sup>, Mohit Angolkar<sup>1</sup>, Adel Al Fatease<sup>2</sup>, Riyaz Ali M Osmani<sup>1,2\*</sup>

<sup>2</sup>Department of Pharmaceutics, JSS College of Pharmacy,

<sup>2</sup>Department of Pharmaceutics, College of Pharmacy, King Khalid University

## Abstract:

Vaginal candidiasis (VC) is a clinical disease prone to about 80% of women at least once. Management therapy of VC includes the administration of both oral and local azole antifungal agents, often associated with undesirable side effects. Additionally, when taken orally, imidazole derivative agents exhibit relatively poor solubility in water and thus poor effectiveness. The current study aimed to develop cyclodextrin nanosponges (CD-NS) based mucoadhesive and thermosensitive *in situ* gel formulations that could be administered intravaginally to extend their residence time at the site of infection and provide the intended release of encapsulated active moieties for an enhanced and effective VC therapy. The NS was prepared by the hot melt method and optimized implying Box-Behnken design and then subjected to characterization by various analytical techniques. The optimized NS was gelled into thermosensitive *in situ* gel using two different grades of poloxamers and optimized using 3<sup>2</sup> Full Factorial design and were further evaluated. DSC and FT-IR studies revealed that the drug and excipients are compatible. SEM images revealed the spongy nature and roughly spherical shape of NS with the particle size of 354.2 nm and 375.8 nm for RES NS and QCT NS respectively. The entrapment efficiency of both the NS was 81.56 ± 1.23% and 80.76 ± 1.56 respectively. Within 12 h, the *in vitro* release profile of Resveratrol demonstrated a release rate of 77.56 % and Quercetin showed a release rate of 82.74 % indicating the prolonged nature of the gel. The effect of the optimized NS-based intravaginal *in situ* thermosensitive gel on *Candida albicans*

was assessed. Overall, the results proved that the developed NS-based intravaginal *in situ* gel shows potential for the effective local therapy of VC and could be a promising formulation approach for facilitated VC therapy in the near future.

**Keywords:** Vaginal candidiasis; nanosponge; cyclodextrin; *in situ* gel; resveratrol; quercetin; prolonged release; vaginal delivery

# Synthesis of Photo-crosslinked Nanoparticulate Polymer Supports Using Cyclodextrin and Chitosan Derivatives

Logigan Corina-Lenuta<sup>1</sup>, Cristian Peptu<sup>2</sup>, Catalina-Anisoara Peptu<sup>1</sup>

<sup>1</sup>Department of Natural and Synthetic Polymers, Faculty of Chemical Engineering and Environmental Protection “Cristofor Simionescu”, “Gheorghe Asachi” Technical University of Iasi, Romania

<sup>2</sup>“Petru Poni” Institute of Macromolecular Chemistry, Aleea Grigore Ghica Voda, 41A, 700487 Iasi, Romania

## Abstract:

This study employs the synthesis of new photo-crosslinked micro/nanoparticulate polymer supports using  $\alpha$ ,  $\beta$ ,  $\gamma$ - cyclodextrins and chitosan derivatives. Chitosan (CS) is the only naturally occurring primary polysaccharide and ranks second in abundance after cellulose. Chitosan nanoparticles have emerged as an innovative drug delivery system, offering enhanced drug stability, prolonged in vivo circulation time, improved drug utilization, and exceptional biocompatibility and biodegradability [1]. Chitosan has certain limitations, particularly in terms of water solubility and drug loading capacity. These challenges can be addressed through chemical modification of the polymer. By introducing thiol groups, various properties of CS can be tailored, and thiolated chitosan (CS-SH) can be synthesized either through direct substitution or by attaching a thiol-bearing ligand [2]. Cyclodextrins (CDs) are a family of  $\alpha$ -1,4-linked cyclic oligosaccharides characterized by a hydrophobic cavity and a hydrophilic outer surface rich in hydroxyl groups. This unique structure enables CDs to encapsulate various guest molecules within their hydrophobic cavity, facilitating the solubilization, stabilization, and transport of hydrophobic drugs. To create water-soluble CD polymers, different approaches have been employed, including reacting functionalized CD derivatives with preexisting polymers, incorporating CD units into linear polymer backbones, and forming branched polymers by coupling CDs with bifunctional crosslinking agents such as epichlorohydrin, anhydrides, and epoxides [3]. The primary goal of this study is to synthesize photo-crosslinked nanoparticulate polymer supports based on  $\alpha$ -CD,  $\beta$ -CD,  $\gamma$ -CD derivative, and CS-SH. Thiolated chitosan (CS-SH) was obtained by covalently attaching homocysteine thiolactone to the chitosan backbone, while  $\alpha$ -CD,  $\beta$ -CD, and  $\gamma$ -CD were functionalized with double bonds through a reaction with 2-hydroxyethyl acrylate and isophorone diisocyanate (resulting in  $\alpha$ -CDdb,  $\beta$ -CDdb, and  $\gamma$ -CDdb). The resulting

nanoparticulate supports (Figure 1) were characterized structurally and morphologically using various techniques, including infrared spectroscopy, laser diffractometry, and scanning electron microscopy. Additionally, the impact of each polymer ( $\alpha$ -CDdb,  $\beta$ -CDdb,  $\gamma$ -CDdb, and CS-SH) on the final particle structure was thoroughly investigated.

**Keywords:** functionalized cyclodextrins, thiolated chitosan, thiol-ene coupling, micro and nanoparticles.

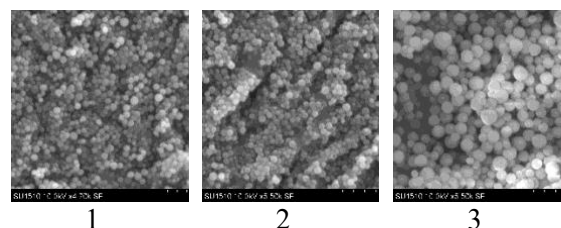


**Figure 1.** Photo-crosslinked Nanoparticles based on: 1.  $\alpha$ -CD, 2.  $\beta$ -CD, 3.  $\gamma$ -CD derivative, and CS-SH

## References:

1. A. Enriquez de Salamanca, Y. Diebold, M. Calonge, et al. Chitosan nanoparticles as a potential drug delivery system for the ocular surface: toxicity, uptake mechanism and in vivo tolerance Invest. Ophthalmol. Vis. Sci., 47 (2006), pp. 1416-1425
2. Nikhil K. Singha and Helmut Schlaad, First Edition. Edited by Patrick Theato and Harm-Anton Klok., pp. 64-86
3. M. Zhang, X. Wei, X. Xu, Z. Jin, J. Wang. Synthesis and characterization of water-soluble  $\beta$ -cyclodextrin polymers via thiol-maleimide ‘click’ chemistry, European Polymer Journal, 128, 2020, pp.109603.

## Acknowledgment:

This work was supported by a grant from the Ministry of Research, Innovation and Digitization, CNCS—UEFISCDI, project number PN-III-P4-PCE-2021-1365, within PNCDI III, (contract number PCE 115/2022)

# Innovative Nanoparticulate Polymer Supports via Thiol–Ene Polymer Conjugation for Enhanced Drug Delivery

Catalina-Anisoara Peptu<sup>1</sup>, Cristian Peptu<sup>2</sup>, Logigan Corina-Lenuta<sup>1</sup>

<sup>1</sup>Department of Natural and Synthetic Polymers, Faculty of Chemical Engineering and Environmental Protection “Cristofor Simionescu”, “Gheorghe Asachi” Technical University of Iasi, Romania

<sup>2</sup>“Petru Poni” Institute of Macromolecular Chemistry, Aleea Grigore Ghica Voda, 41A, 700487 Iasi, Romania

## Abstract:

Recent research has underscored the successful conjugation of polymers with low molecular weight compounds through thiol–ene radical chemistry. This method efficiently combines functional polymers with bi- or multifunctional thiol/ene systems, often requiring an excess of the low molecular weight compound to achieve optimal results [1].

Chitosan, a natural polysaccharide, has shown significant potential as a drug delivery system due to its beneficial properties, such as enhanced drug stability, extended circulation time, and excellent biocompatibility. However, its limitations, including poor water solubility and limited drug loading capacity, can be addressed through chemical modifications, such as the introduction of thiol groups to form CS-SH [2]. Poly(ethylene glycol) (PEG), known for its distinctive physicochemical and biological properties, acts as a non-ionic hydrophilic polymer used for functionalization. Weipu et al. introduced a simple method to create biodegradable and biocompatible PEG hydrogels via the thiol–ene “click” reaction under physiological conditions, successfully synthesizing PEG copolymers with multi-thiol or multi-ene groups using scandium trifluoromethanesulfonate as a highly efficient catalyst (PEG-SH) [3]. Cyclodextrins are cyclic oligosaccharides with a structural ability to encapsulate and transport hydrophobic drugs, facilitating solubilization and stabilization [4]. This study focuses on the synthesis of novel photo-crosslinked nanoparticulate polymer supports, incorporating various cyclodextrins (modifying  $\alpha$ -CD,  $\beta$ -CD, and  $\gamma$ -CD) and thiolated chitosan (CS-SH) blended with poly(ethylene glycol-co-thiomaleate) (PEG-SH).

The nanoparticulate supports were characterized using infrared spectroscopy, laser diffractometry, and scanning electron microscopy to assess their structural and morphological properties. The research investigates how each polymer influences the resulting particle structure,

providing insights into their potential applications in drug delivery systems.

**Keywords:** Poly(ethylene glycol-co-thiomaleate), thiolated chitosan, functionalized cyclodextrins, thiol-ene coupling, nanoparticles.

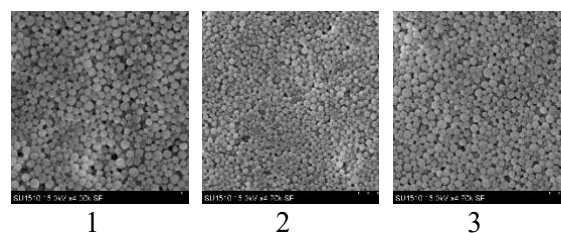


**Figure 1.** Nanoparticles via thiol-ene polymer conjugation based on: 1.  $\alpha$ -CD db-CS-SH-PEG-SH, 2.  $\beta$ -CD db-CS-SH-PEG-SH, 3.  $\gamma$ -CD db-CS-SH-PEG-SH

## References:

1. Lowe, A. B. Thiol–ene “click” reactions and recent applications in polymer and materials synthesis: a first update. *Polymer Chemistry*, 2014,5, 4820-4870.
2. A. Enriquez de Salamanca, Y. Diebold, M. Calonge, et al. Chitosan nanoparticles as a potential drug delivery system for the ocular surface: toxicity, uptake mechanism and in vivo tolerance Invest. Ophthalmol. Vis. Sci., 47 (2006), pp. 1416-1425
3. Zhu, W., Gao, L., Luo, Q., Gao, C., Zha, G., Shen, Z. and Li, X. (2014) Metal and light free, click, hydrogels for prevention of post-operative peritoneal adhesion. *Polymer Chemistry*, 5, 2018-2026
4. M. Zhang, X. Wei, X. Xu, Z. Jin, J. Wang. Synthesis and characterization of water-soluble  $\beta$ -cyclodextrin polymers via thiol-maleimide ‘click’ chemistry, *European Polymer Journal*, 128, 2020, pp.109603.

## Acknowledgement

This work was supported by a grant from the Ministry of Research, Innovation and Digitization, CNCS—UEFISCDI, project number PN-III-P4-PCE-2021-1365, within PNCDI III, (contract number PCE 115/2022)



# Novel Egg Protein-Based Nanoplatfoms as Drug Delivery Sytems for Personalized Medicine

F. Seidita<sup>1</sup>, F. Barrino<sup>1</sup>, M. Mangione<sup>2</sup>, P. Picone<sup>3</sup>, D. Nuzzo<sup>3</sup>, A. Girgenti<sup>3</sup>, D. Chmielewska<sup>4</sup>, M. Walo<sup>4</sup>, S. Cabo Verde<sup>5</sup>, C. Dispenza<sup>1</sup>

<sup>1</sup>Dipartimento di Ingegneria Chimica, Università degli Studi di Palermo, Viale delle Scienze 6, 90128, Palermo, Italia

<sup>2</sup>Centro Nazionale delle Ricerche, Istituto di Biofisica, Via Ugo La Malfa 153, 90146, Palermo, Italia

<sup>3</sup>Centro Nazionale delle Ricerche, Istituto per la Ricerca e l'Innovazione Biomedica (IRIB), Via Ugo La Malfa 153, 90146, Palermo, Italia

<sup>4</sup>Institute of Nuclear Chemistry and Technology (INCT), Dorodna 16, 03-195, Warszawa, Polonia

<sup>5</sup>Centro de Ciências e Tecnologias Nucleares (C2TN), Instituto Superior Técnico, Universidade de Lisboa, 2695-066 Bobadela LRS, Portugal

[federica.seidita01@unipa.it](mailto:federica.seidita01@unipa.it)

## Abstract:

Over the past two decades, nanoparticles have become crucial in various fields, especially personalized medicine, addressing the limitations of free therapeutic compounds and biological barriers<sup>1</sup>. These nanoparticles, made from a wide range of organic and inorganic materials, can be synthesized through various methods. Among these, electron-beam irradiation stands out for its versatility, using ionizing radiation from radioisotopes or accelerators to precisely manipulate chemical structures. This method allows for the tailored fabrication of nanoparticles in aqueous solutions or as protein powders. Electron-beam irradiation offers advantages such as lower energy use, reduced reliance on hazardous chemicals, and streamlined production processes. Moreover, materials produced this way are inherently sterile, making them ideal for medical applications. This approach not only advances nanoparticle synthesis but also improves drug delivery systems and biomedical interventions through precise chemical modifications<sup>2</sup>.

This study focuses on the design and characterization of innovative functional organic nanoplatfoms derived from egg white proteins. The product undergoes rigorous examination to assess its chemical and biological properties. Detailed exploration of its chemical interactions aims to enhance compatibility with chemotherapeutics or natural drugs through precise bioconjugation techniques. These nanoplatfoms are designed to function as carriers for both traditional chemotherapeutics and organic compounds, specifically targeting cancer treatment. By functionalizing these nanoplatfoms, the goal is to optimize drug delivery mechanisms, potentially enhancing

therapeutic outcomes while minimizing adverse effects.

**Keywords:** drug delivery system, personalized medicine, cancer therapy, nanoparticles, nanotechnology, radiation chemistry, high-energy irradiation, egg proteins.

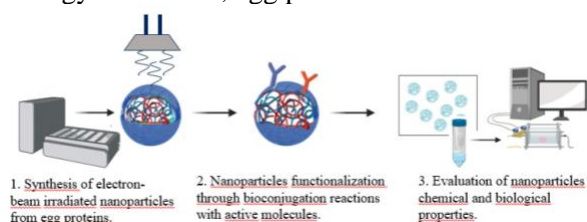


**Figure 1:** Schematic representation of the steps of the present research.

## References:

1. Alghamdi MA, Fallica AN, Virzì N, Kesharwani P, Pittalà V, Greish K. The Promise of Nanotechnology in Personalized Medicine. *J Pers Med.* 2022 Apr 22;12(5):673.
2. Dispenza C, Grimaldi N, Sabatino MA, Soroka IL, Jonsson M. Radiation-Engineered Functional Nanoparticles in Aqueous Systems. *J Nanosci Nanotechnol.* 2015 May;15(5):3445-67.

**Acknowledgments:** The author wishes to acknowledge RaDiation harvesting of bioactive peptides from egg prOteins and their integration in adVanced functional products (RADOV) project for the contribution in this research.

# Reprogramming human ferritin nanoparticles for multivalent inhibition of PCSK9: a novel strategy to enhance LDL cholesterol clearance.

Chiara Cappelletti<sup>1</sup>, Alessio Incocciati<sup>1</sup>, Silvia Masciarelli<sup>2</sup>, Francesca Liccardo<sup>2</sup>, Roberta Piacentini<sup>1,4</sup>, Sofia Botta<sup>1</sup>, Lucia Bertuccini<sup>3</sup>, Barbara De Berardis<sup>3</sup>, Francesco Fazi<sup>2</sup>, Alberto Boffi<sup>1</sup>, Alessandra Bonamore<sup>1</sup>, Alberto Macone<sup>1</sup>

<sup>1</sup>Department of Biochemical Sciences, Sapienza University of Rome, Rome, Italy

<sup>2</sup>Department of Anatomical, Histological, Forensic & Orthopaedic Sciences, Section of Histology and Medical Embryology, Sapienza University of Rome, Rome, Italy

<sup>3</sup>Core Facilities, Microscopy Area, and National Center for Innovative Technologies in Public Health, Istituto Superiore di Sanità, Rome, Italy

<sup>4</sup>Center for Life Nano Science@Sapienza, Istituto Italiano di Tecnologia, Rome, Italy

## Abstract:

Hypercholesterolemia, characterized by elevated levels of LDL cholesterol, significantly increases the risk of cardiovascular disease. Proprotein convertase subtilisin/kexin type 9 (PCSK9) plays a crucial role in cholesterol regulation by mediating the degradation of LDL receptors (LDLR), making it an important target for therapies aimed at reducing hypercholesterolemia. In our research, we engineered human H ferritin to serve as a scaffold for displaying multiple peptides that target PCSK9. Our objective was to inhibit the interaction between PCSK9 and LDL receptors to enhance LDL clearance from the bloodstream.

We incorporated a 13-amino acid peptide (Pep2-8), known as the smallest PCSK9-inhibitor peptide, at the N-terminus of human H ferritin (HFn-Pep2-8). By exploiting ferritin's quaternary structure, we designed nanoparticles displaying 24 copies of the targeting peptide on their surface to achieve a multivalent binding effect (Figure 1). Biochemical analyses confirmed that the nanoparticles' size and morphology were precisely controlled, and they demonstrated strong binding affinity to PCSK9, with a dissociation constant in the high picomolar range. Experiments with HepG2 liver cells showed that these engineered ferritin nanoparticles effectively countered the PCSK9-induced reduction in LDL receptor expression on cell surfaces, thereby enhancing LDL uptake. Our results demonstrate the potential of ferritin-based nanoparticles as versatile tools for targeting PCSK9 in the management of hypercholesterolemia. This study not only advances ferritin-based therapeutics but also opens new strategies for treating cardiovascular diseases. Furthermore, given PCSK9's involvement in various physiological

and pathological conditions, including liver diseases, infectious diseases, autoimmune disorders, and cancer, this innovative ferritin-based nanoparticle holds promise for therapeutic applications beyond cardiovascular disorders.

**Keywords:** Ferritin, protein nanoparticles, LDL, Cholesterol, hypercholesterolemia, LDL receptor, PCSK9, Pep2-8, HepG2.

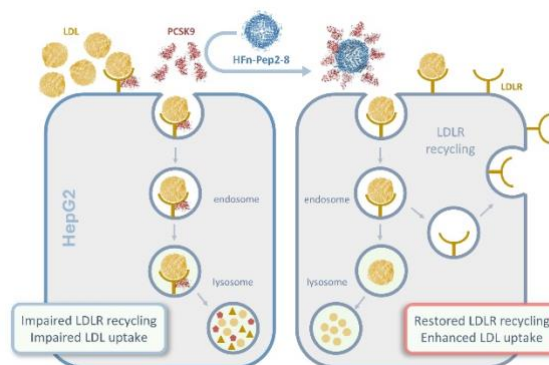


**Figure 1:** Scheme showing the interaction between PCSK9 and the LDLR on HEPG2 cells' surface (left panel) and how HFn-Pep2-8 nanoparticle can disrupt this interaction, sequestering PCSK9 and restoring both the LDLR recycling and LDL uptake (right panel).

## References:

1. Incocciati, A., Cappelletti, C., Masciarelli, S., Liccardo, F., Piacentini, R., Giorgi, A., Bertuccini, L., De Berardis, B., Fazi, F., Boffi, A., Bonamore, A., Macone, A.; (2024) Ferritin-based disruptor nanoparticles: A novel strategy to enhance LDL cholesterol clearance via multivalent inhibition of PCSK9–LDL receptor interaction. *Protein Science*, In Press.

# ROS responsive dextran-thioketal conjugate nanocarriers for the delivery of various low and high molecular weight hydrophilic payloads

S. Nayak<sup>1\*</sup>, E. Pirlet<sup>2</sup>, N. Caz<sup>3</sup>, E. Wolfs<sup>3</sup>, A. Bronckaers<sup>2</sup>, W. Maes<sup>4</sup>, A. Ethirajan<sup>1</sup>

<sup>1</sup>Nanobiophysics and soft matter interfaces (NSI), IMO-IMOMEC, Hasselt University, Diepenbeek, Belgium

<sup>2</sup>Laboratory for research in ischemic stroke, stem cells & angiogenesis (LISSA), BIOMED, Hasselt University, Diepenbeek, Belgium

<sup>3</sup>Laboratory for Functional Imaging & Research on Stem Cells (FIERCE), BIOMED, Hasselt University, Diepenbeek, Belgium

<sup>4</sup>Design & Synthesis of Organic Semiconductors (DSOS), IMO-IMOMEC, Hasselt University, Diepenbeek, Belgium

## Abstract:

Nanocarriers (NCs) based on stimuli responsive polymers have gained attention owing to their ability to undergo degradation and phase transition under the influence of various physical, chemical and biological stimuli, leading to drug release. Excess reactive oxygen species (ROS) production is characteristic of many disease conditions (e.g., tumor, inflammation, wound healing) and thus NCs designed for cargo release at the target sites that produce excessive ROS has evoked enormous interest.[1]

In our study, a ROS-responsive water soluble dextran conjugate was synthesized and studied for reactivity to different ROS stimulus. Various hydrophilic payload containing NCs were formulated using interfacial polymerization employing the miniemulsion technique.[2] In here, the thioketal moieties serve as a ROS-responsive linker. NCs were successfully synthesized varying several reaction parameters and subsequently characterized. The encapsulation efficiencies of the various hydrophilic payloads in the NCs were between 79-91%. The release kinetics systematically studied under different ROS conditions showed a clear stimulus responsive release trend.

The NCs were tested for the delivery of small therapeutic molecule (e.g., Doxorubicin) as well as high molecular weight growth factor (e.g., VEGF). The responsiveness, crosslinking density etc. of the NCs were tuned to release the diverse payloads. Biocompatibility and cellular uptake experiments using oral squamous carcinoma cells (head and neck cancer) and Human umbilical vein endothelial cells (HUVEC) were successfully carried out (Figure 1). The promising results highlight the huge potential of ROS-responsive NCs to deliver hydrophilic therapeutics to treat various diseases.

**Keywords:** nanocapsules, dextran, reactive oxygen species, growth factor, drug delivery systems

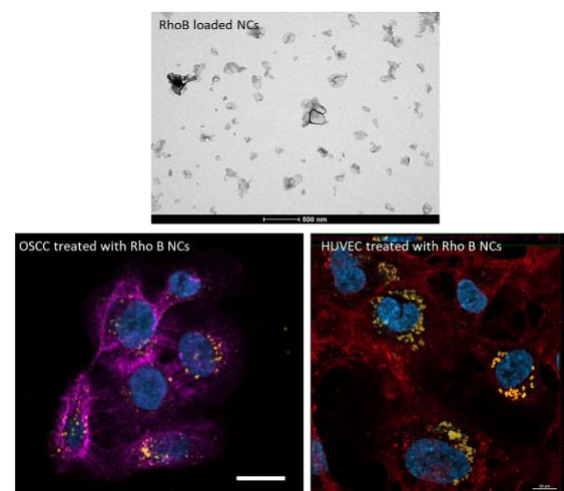


**Figure 1:** TEM image of the NCs (top row) and confocal fluorescence microscopy images showing uptake of ROS responsive dextran NCs loaded with a fluorescent dye (RhoB) by head and neck cancer cells and HUVEC cells (bottom row).

## References:

1. G. Saravanakumar, J. Kim, W. J. Kim, *Advance Science*, 2017, 4, 1600124.
2. S. Seneca, S. Pramanik, L. D'Olieslaeger, G. Reekmans, D. Vanderzande, P. Adriaensens, A. Ethirajan, *Materials Chemistry Frontiers*, 2020, 4, 2103-2112.

# Fluorometholone loaded Solid Lipid Nanoparticles: a new strategy for ocular delivery of anti-inflammatory drugs

Da Ana. Raquel <sup>1,2,\*</sup>, Fonseca. Joel,<sup>1</sup> Cravo. Sara <sup>3,4</sup>, Faezeh. Fathi<sup>5</sup>, Sanchez-Lopez. E.<sup>6,7</sup>, Oliveira, M. Beatriz <sup>5</sup>, Garcia. Maria L.<sup>6,7</sup>, Souto. Eliana B. <sup>1,2</sup>

<sup>1</sup> Department of Pharmaceutical Technology, Faculty of Pharmacy, University of Porto, Porto, Portugal  
UCIBIO, Faculty of Pharmacy, University of Porto, Porto, Portugal

<sup>3</sup> Laboratory of Organic and Pharmaceutical Chemistry (LQOF), Department of Chemical Sciences, Faculty of Pharmacy, University of Porto, Porto, Portugal

<sup>4</sup> Interdisciplinary Centre of Marine and Environmental Research (CIIMAR), Porto, Portugal

<sup>5</sup> REQUIMTE/LAQV, Department of Chemical Sciences, Faculty of Pharmacy, University of Porto, Porto, Portugal

<sup>6</sup> Department of Pharmacy, Pharmaceutical Technology and Physical Chemistry, Faculty of Pharmacy and Food Sciences, University of Barcelona, Barcelona, Spain

<sup>7</sup> Institute of Nanoscience and Nanotechnology (IN2UB), University of Barcelona, Barcelona, Spain

## Abstract:

Fluorometholone (FML) is a glucocorticoid drug, widely used for the treatment of inflammatory eye diseases, namely for the anterior segment of the eye, due to its high pharmacological potency. The drug is however hydrophobic consequently showing low bioavailability. Lipid nanoparticles are nanocarriers based on the use of physiological and biocompatible lipids with exceptional properties, such as safety profile and bioadhesion, with potential to increase drug bioavailability and patients' compliance due to a sustained and targeted drug release.

In this work, cationic Solid Lipid Nanoparticles (SLN) formulation, composed of Compritol 888 ATO, Poloxamer 188, and cetyltrimethylammonium bromide (CTAB) was optimized using the sonication method. FML was dispersed in the lipid phase, in two different concentrations: 0.05% (commercial dosage) and 0.1%. The obtained results showed that the drug was successfully encapsulated, resulting in particles with a mean size ( $z$ -Ave) of  $139.5 \pm 1.012$  nm and  $133.9 \pm 1.639$  nm, and polydispersity index (PI) of 0.269 and 0.275, respectively. Encapsulation Efficiency (E.E.) higher than 99% for both drug concentrations. The high Zeta Potential (ZP), higher than 60 mV is a very representative characteristic of cationic nanoparticles, providing great stability and makes them suitable use for ophthalmic delivery. SLN containing FML were characterized regarding their physicochemical properties, considering the crystallinity profiles, rheological behavior, morphology, and release profile. The encapsulation of FML allows the reduction of undesirable effects related to the use of this corticoid, providing, at the same time, the increase

of bioavailability, safety, and sustained release, through the use of a biocompatible and biodegradable nanosystem, SLN.

**Keywords:** Fluorometholone; ocular drug delivery; nanosystems; solid lipid nanoparticles; ophthalmic administration; eye inflammatory diseases; sustained release; bioavailability increasing; biocompatibility and biodegradation; encapsulation of hydrophobic drugs.

## References:

1. Ana, R. d., Fonseca, J., Karczewski, J., Silva, A. M., Zielińska, A., & Souto, E. B. (2022). Lipid-Based Nanoparticulate Systems for the Ocular Delivery of Bioactives with Anti-Inflammatory Properties. *International Journal of Molecular Sciences*, 23(20), 12102
2. Ana, R. d., Gliszczynska, A., Sanchez-Lopez, E., Garcia, M. L., Krambeck, K., Kovacevic, A., & Souto, E. B. (2023). Precision Medicines for Retinal Lipid Metabolism-Related Pathologies. *Journal of Personalized Medicine*, 13(4), 635
3. Fernandes, A. R., Sanchez-Lopez, E., Santos, T. D., Garcia, M. L., Silva, A. M., & Souto, E. B. (2021). Development and Characterization of Nanoemulsions for Ophthalmic Applications: Role of Cationic Surfactants. *Materials (Basel)*, 14(24)
4. Gonzalez-Pizarro, R., Carvajal-Vidal, P., Halbaut Bellowa, L., Calpena, A. C., Espina, M., & García, M. L. (2019). In-situ forming gels containing fluorometholone-loaded polymeric nanoparticles for ocular inflammatory conditions. *Colloids and Surfaces B: Biointerfaces*, 175, 365-374



# Innovative Gold-Liposome Nanohybrids: Revolutionizing Photothermal Nanoplatforms with Tunable Plasmonic Properties

M. Rubio-Camacho <sup>1,\*</sup>, C. Cuestas-Ayllón <sup>2</sup>, R. Esquembre <sup>1</sup>, M.J. Martínez-Tomé <sup>1</sup>, Jesus M. de la Fuente <sup>2</sup>, C. R. Mateo <sup>1</sup>

<sup>1</sup> Instituto de Investigación, Desarrollo e Innovación en Biotecnología Sanitaria de Elche (IDiBE), Universidad Miguel Hernández (UMH), Elche, Spain

<sup>2</sup> Instituto de Nanociencia y Ciencia de Materiales de Aragón, CSIC – Universidad de Zaragoza, Zaragoza, Spain

## Abstract:

The development of effective photothermal agents is crucial to advance in different fields of knowledge, particularly in the biomedical area. This study introduces a rapid and environmentally friendly methodology for the in situ synthesis of gold nanoparticles (AuNPs) with tunable plasmons on thermosensitive liposomes. By manipulating lipid phase states, charge, and synthesis temperatures, we achieved nanohybrids with tunable plasmon modes in the visible/near-infrared (NIR) region. Specifically, fluid-phase liposomes produced discrete AuNPs with plasmon peaks in the visible spectrum, whereas gel-phase liposomes favored the formation of nanoclusters, shifting the plasmon bands towards the NIR as synthesis temperature decreased [1] (Figure 1). The role of the unsaturated fatty amine oleylamine in liposomes for plasmon modification and the implementation of other types of gold structures in these nanohybrids such as nanoprisms (AuNPrs) have also been explored (Figure 1). All these nanohybrids retained light-to-heat conversion efficiency and enhanced photothermal properties, positioning them as promising candidates to control enzyme activity of certain temperature-dependent enzymes. Furthermore, these nanohybrids preserved the intrinsic physical properties of the liposomes, such as fluidity and cooperativity, maintaining transition temperatures within the mild-hyperthermia range essential for drug delivery and therapeutic applications. Our findings emphasize the potential of lipid phase modulation or composition to fine-tune the plasmonic properties of AuNP-liposome hybrids, paving the way for innovative approaches in controlling enzymatic activity, cancer treatment and other medical applications.

**Keywords:** gold nanoparticles, plasmonic nanohybrids, thermosensitive liposomes, tunable LSPR, light-mediated therapies, photothermal therapy

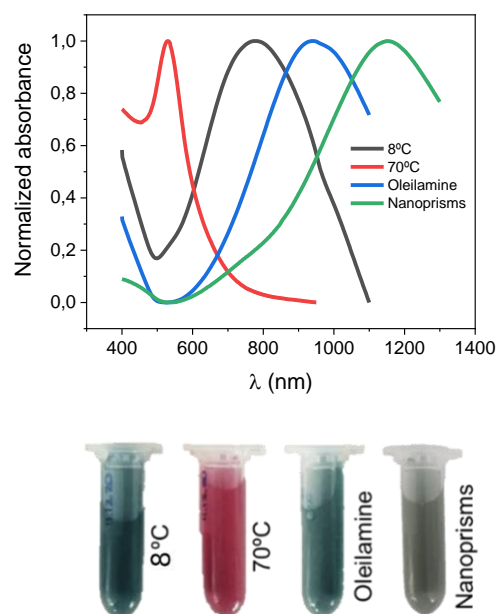


**Figure 1:** Normalized absorption spectra of AuNPs synthesized in situ in dipalmitoyl phosphocholine (DPPC) liposomes, at 8°C (-) and at 70°C in the absence (-) and presence of oleylamine (-), compared to that of AuNPrs covalently bound to liposomes (-).

## References:

1. Rubio-Camacho, M., Martínez-Tomé, M.J., Cuestas-Ayllón, C., Martínez de la Fuente, J., Mateo Martínez, C.R. (2023) Tailoring the plasmonic properties of gold-liposome nanohybrids as a potential powerful tool for light-mediated therapies, *Colloids Interface Sci. Commun.*, 52, 100690.

## Acknowledgments:

This work was funded by Project PID2022-138507OB-I00 and PID2020-118485-RB-I00, from Spanish MICIN



# Optimization of Lipid Nanoparticles for RNA Encapsulation: Influence of the Nature and Content of Ionizable Lipid

M. Frohly<sup>1</sup>, C. Favre<sup>1</sup>, E. Lacazette<sup>2</sup>, F. Montury<sup>1</sup>, L. Sanchez Gonzalez<sup>1</sup>

<sup>1</sup>CEA, NanO'up Platform, Labège, France

<sup>2</sup>UMR 1048-I2MC, Inserm, Université de Toulouse, UPS, Toulouse, France

**Abstract:** Lipid nanoparticles (LNP) appears as promising systems for vaccines and gene therapy. The composition of LNP includes neutral and helper lipids (phospholipid, cholesterol), lipid-anchored polyethylene glycol (PEGylated lipid) and ionizable lipids (Figure 1). PEGylated lipids give colloidal stability by introducing a steric barrier at the surface of nanoparticles and increase pharmacokinetic, biodistribution of LNPs by protecting their surface from blood components. Helper lipids have different functions, including particle structure, encapsulation and cellular delivery. At low pH, ionizable lipids can interact electrostatically with polyanionic RNA during the microfluidic assembly, which facilitates cell transfection with an enhanced endosomal escape. LNPs were formulated by microfluidic mixing technique, more precisely an staggered herringbone micromixer, which offers advantages over other the conventional microfluidic hydrodynamic focusing devices (faster mixing, higher throughput, and lesser dilution) [1].

The ionizable lipid is a key parameter to optimize LNP for nucleic acid delivery [2]. Under acidic conditions, ionizable lipids are positively charged, whereas they are neutral at physiological pH. Formulation of LNPs is carried out at room temperature and acidic conditions to enable establishment of electrostatic bonds between ionizable lipids and negatively charged mRNAs to improve encapsulation efficiency.

Two ionizable lipids, N-(4-carboxybenzyl)-N,N-dimethyl-2,3-bis(oleoyloxy)propan-1-aminium (DOBAQ) and 1,2-dioleoyloxy-3-dimethylaminopropane (DODMA), were compared in this study, with molar ratios ranging from 30 to 50. LNPs formulated by microfluidic mixing were characterize in terms of size, polydispersity, charge and encapsulation efficiency. Transfection assays were carried out in parallel on cell line HEK 293, transfection ratio was analysed quantitatively by flow cytometry.

In this study, significant differences were observed in terms of physico-chemical properties

and transfection ratio depending the nature and the content of ionizable lipid used in LNPs formulation.

**Keywords:** lipid nanoparticles (LNP), mRNA, drug delivery, gene therapy, vaccines, microfluidic mixing, DOBAQ, DODMA.

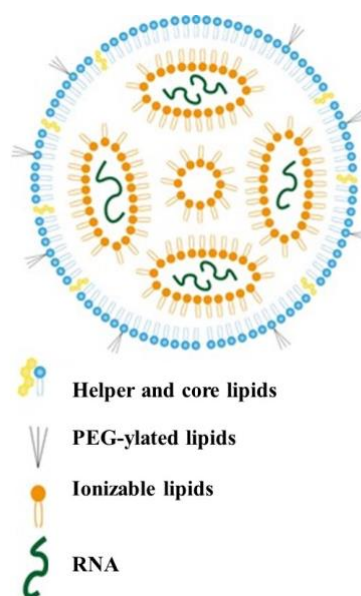


**Figure 1:** Composition of Lipid Nanoparticles for RNA encapsulation

## References:

1. Cheung, C.C.L., Al-Jamal, W.T. (2019). Sterically stabilized liposomes production using staggered herringbone micromixer: Effect of lipid composition and PEG-lipid content, *Int.J.Pharm.*, 566, 687–696
2. Han, X., Zhang, H., Butowska, K., Swingle, K.L., Alameh, M.G., Weissman, D., Mitchell, M.J. (2021). An ionizable lipid toolbox for RNA delivery, *Nat Commun*, 13;12(1):7233.

# Improving antibiotics quantification using label-free SERS-based microfluidic platform. Challenges of therapeutic drug monitoring at intensive care units.

R. Slipets, M. Pytlarz

Center for Intelligent Drug Delivery and Sensing Using Microcontainers and Nanomechanics (IDUN), Department of Health Technology, Technical University of Denmark, Kongens Lyngby 2800, Denmark.

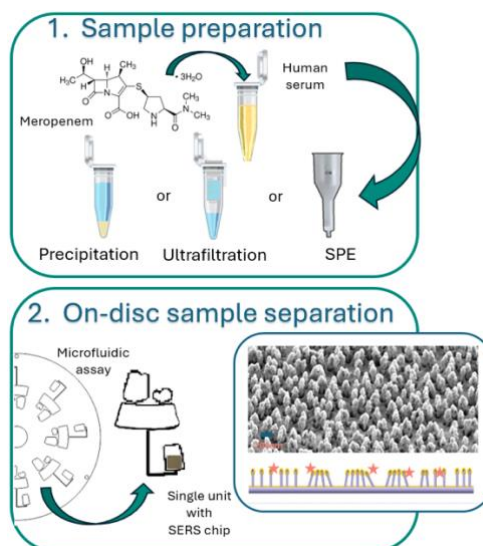
## Abstract:

Sepsis is a leading cause of death in infectious diseases, particularly in intensive care units (ICUs), where optimal antibiotic treatment and careful monitoring of drug dosage are crucial<sup>1</sup>. Therapeutic drug monitoring (TDM) is essential for improving clinical care, especially when using drugs with pharmacokinetic variability and a narrow therapeutic window.

Label-free SERS is an efficient technique for identifying analytes based on their unique molecular Raman fingerprints. Detection is achieved by observing specific Raman bands from the analyte<sup>2</sup>. However, for high sensitivity and specificity in analyte quantification using label-free SERS, effective surface-molecule interaction and minimal interference from other molecules in the sample are required<sup>3</sup>. To achieve this, optimal matrix cleanup procedures, such as protein precipitation (PP), ultrafiltration (UF), liquid-liquid extraction, or solid-phase extraction (SPE), can be integrated with the SERS assay to improve drug quantification in complex biological matrices.

We present an automated method for detecting antibiotics in serum samples using label-free SERS. Silver-coated nanopillar (AgNP) SERS substrates serve as both a sample pretreatment and detection platform. Also, we demonstrate implementation of the sample pretreatment techniques to enhance the separation of the target analyte from the sample matrix and conduct a performance evaluation of the entire measurement system, with a focus on its relevance and potential impact for clinical applications in the intensive care units.

**Figure:** 1) Sample collection and preparation including PP, UF, and ms-SPE off disc; 2) Utilizing microfluidic platform enabling migration of the analyte on the SERS nanopillar chip within the sensing chamber through centrifugal forces



**Key words:** antibiotic, nanopillar, therapeutic drug monitoring, SERS

## References:

1. Fleischmann-Struzek, C.; Mellhammar, L.; Rose, N.; Cassini, A.; Rudd, K. E.; Schlattmann, P.; Allegranzi, B.; Reinhart, K. Incidence and Mortality of Hospital- and ICU-Treated Sepsis: Results from an Updated and Expanded Systematic Review and Meta-Analysis. *Intensive Care Med* 2020, 46 (8), 1552–1562. <https://doi.org/10.1007/S00134-020-06151-X/FIGURES/4>.
2. Laing, S.; Jamieson, L. E.; Faulds, K.; Graham, D. Surface-Enhanced Raman Spectroscopy for in Vivo Biosensing. *Nature Reviews Chemistry* 2017 1:8 2017, 1 (8), 1–19. <https://doi.org/10.1038/s41570-017-0060>.
3. Soufi, G.; Dumont, E.; Göksel, Y.; Slipets, R.; Altaf Raja, R.; Schmiegelow, K.; Bagheri, H.; Boisen, A.; Zor, K. Discrimination and Quantification of Methotrexate in the Presence of Its Metabolites in Patient Serum Using SERS Mapping, Assisted by Multivariate Spectral Data Analysis. 2023. <https://doi.org/10.1016/j.biosx.2023.100382>.

# Microphysiological systems based on liver on chip for drug discovery and testing.

E. Guerrero<sup>1</sup>, A. Rigat<sup>1</sup>, P. Monterde<sup>1</sup>, X. Barceló<sup>1</sup>, J. M. Cabot<sup>1</sup>

<sup>1</sup> Diagnostic Devices Group, Department of Advanced Engineering, Leitat (Barcelona, Spain)

## Abstract:

Organ-on-a-chip are microfluidic platforms that recapitulate human physiology at the microscale. Compared to traditional cell culture systems, these systems allow for the creation of more relevant models with the potential to replace or be integrated into non-clinical studies, helping to significantly reduce costs and the use of animals.

Despite 3D liver models like liver organoids can reproduce some aspects and functions of *in vivo* tissue, their static and isolated nature does not reproduce the complex intercommunication for biochemical exchange or *in vivo* pharmacodynamics, pharmacokinetics, and physiology. Cell differentiation can be incomplete, and cell organization is random, leading to lower reproducibility. Herein, we aim to develop liver-on-chip devices to better recapitulate the physiology and functionality of the human liver for drug discovery. These devices could also be more relevant than current gold standard methods for drug testing, as they can be adapted to capture the heterogeneity of the different metabolisms of the population through multi-donor pooling for more representative data.

Decellularized liver-derived extracellular matrix (ECM) has shown improved hepatocyte functionality and metabolism. By incorporating liver-specific ECM into hydrogels, we aim to improve the *in vitro* viability and support the functionality of primary human hepatocytes. Converging advanced bioprinting technologies with 3D liver models based on liver-derived bioinks into microphysiological systems will allow not only the development of reliable *in vitro* models for drug screening but also to create scalable systems with potential for personalized medicine.

To achieve this, we have designed a microfluidic device that can be parallelized following the international standard for a 6-well plate (Figure 1A,B). This device is composed of two independent channels with a central chamber where the liver model will be placed. The bioengineered tissue is obtained by bioprinting an ECM-derived bioink using a 3D-printed

pluronic support (Figure 1C-E). Finally, the assembled device has been tested for its use, demonstrating good perfusion throughout the system (Figure 1F). The next steps will involve the incorporation of human-derived hepatocytes into the system to evaluate its functionality.

**Keywords:** organ-on-chip, liver-on-chip, microfluidics, bioprinting.

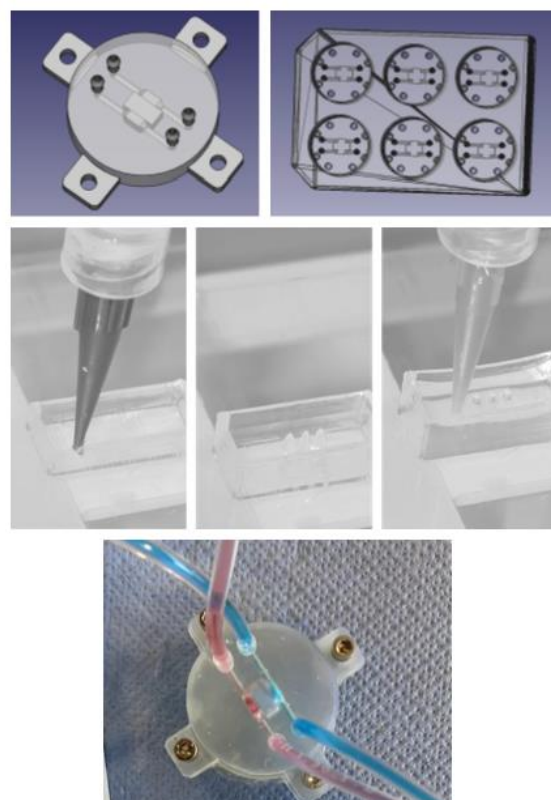


**Figure 1. Liver on chip microphysiological system.** Computer-aided design (CAD) of the microfluidic system. (A) Single device with two perfusion channels, and a central platform to locate the liver-derived model; (B) Scaled-up system into a 6-well plate format following international standard ANSI/SBS: 3D bioprinting process of the liver-derived model. (C) First, pluronic ink is used to create a template with three perfusion channels (D) before depositing the liver-derived bioink (E); (F) Assembled microphysiological system with the perfusion of two different fluids. Red and blue colorants are used for representation.

# Influence of the Nature and Content of Bile Salts on the Properties of Bilosomes Developed for Nose-to-brain Applications

J. Aussourd<sup>1</sup>, C. Favre<sup>1</sup>, F. Montury<sup>1</sup>, L. Sanchez Gonzalez<sup>1</sup>

<sup>1</sup>CEA, NanO'up Plateform, Labège, France

**Abstract:** The nasal-to-brain route shows promise for improving drug delivery to the central nervous system, avoiding the need to cross the blood-brain barrier (BBB). Intranasal administration is non-invasive, easy to apply, and also prevents gastrointestinal enzymatic degradation and hepatic first-pass metabolism. Further the intranasal delivery shows rapid absorption with quick onset of action. However, nose-to-brain delivery also has many challenges. Factors such as limited residence time due to high mucociliary clearance, enzymatic degradation, pH compatibility with the nasal mucosa and limited dispensed volumes need to be taken into account when developing an intranasal formulation [1]. To increase the bioavailability of therapeutic molecules through nasal route, particularly hydrophobic actives, the use of lipid vectors is an interesting strategy. Thanks to their small size and the presence of emulsifiers, these particles are highly stable and capable of penetrating biological membranes. Previous work based on nanoparticles has demonstrated their ability to encapsulate neurodrugs [2], although active compounds such as diazepam can naturally cross the BBB. Among the lipid nanoparticles studied, bilosomes appear to be promising vectors for drug delivery. These nanocarriers are composed of a bilayer of non-ionic surfactants and bile salts (Figure 1). The composition of bilosomes includes helper lipids (phospholipid, cholesterol and lipid-anchored polyethylene glycol (PEGylated lipid)); targeting agents can also be added to the particle surface. Previous studies reported bilosomes are more elastic, flexible, and deformable than conventional liposomes [3].

Curcumin, natural hydrophobic compound extract from *Curcuma longa*, present interesting properties as antioxidant, anti-inflammatory or anti-angiogenic effects. Curcumin present a very low water solubility associated with poor bioavailability especially through BBB. Therapeutic applications of curcumin are therefore limited. Nano-encapsulation is an interesting approach to improve bioavailability of this high-potential natural compound.

In this study, bilosomes-curcumin formulated by nanoprecipitation were characterized in terms of size, polydispersity, charge and encapsulation efficiency. Significant differences were observed in

terms of curcumin encapsulation efficiency depending the nanoparticle composition (nature and content of bile salts). The use of nanobilosomes for curcumin delivery is a promising system.

**Keywords:** nose-to-brain, nanocarriers, lipid nanoparticles, bile salt, curcumin, nanoprecipitation, drug delivery, intranasal.

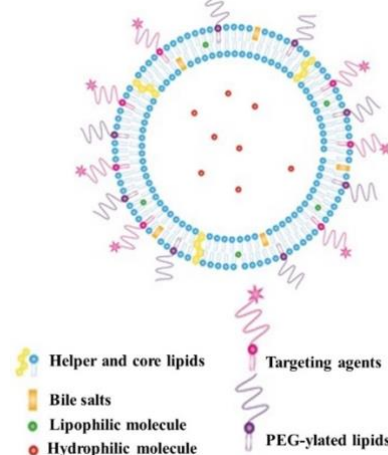


**Figure 1:** Bilosomes composition

## References:

1. Erdo, F., Bors, L.A., Farkas, D., Bajza, A., Gizurarson, S. (2018) Evaluation of intranasal delivery route of drug administration for brain targeting, *Brain Res. Bull.*, 143,155-170.
2. Costa, C.P., Cunha, S., Moreira, J.N., Silva, R., Gil-Martins, E., Silva, V., Azevedo, L., Peixoto, A.F., Sousa Lobo, J.M., Silva, A.C. (2021) Quality by design (QbD) optimization of diazepam-loaded nanostructured lipid carriers (NLC) for nose-to-brain delivery: Toxicological effect of surface charge on human neuronal cells. *Int J Pharm*, 607:120933.
3. Abbas, H., El-Feky, Y.A., Al-Sawahli, M.M., El-Deeb, N.M., El-Nassan, H.B., Zewail, M. (2022) Development and optimization of curcumin analog nano-bilosomes using 2<sup>1</sup>.3<sup>1</sup> full factorial design for anti-tumor profiles improvement in human hepatocellular carcinoma: *in-vitro* evaluation, *in-vivo* safety assay. *Drug Deliv.*, 29(1), 714-727.



# Development of photosensitizing nanoparticles of nanodiamonds using femtosecond lasers

R. C. Queiroz<sup>1,2</sup>, C. R. Hurtado<sup>3</sup>, G. R. Hurtado<sup>4</sup>, A. M. dos Santos<sup>3</sup>, M. F. Diniz<sup>5</sup>, H. C. Junqueira<sup>6</sup>, A. U. Fernandes<sup>7</sup>, H. Besser<sup>2</sup>, W. Pflöging<sup>2</sup>, D. B. Tada<sup>1</sup>.

<sup>1</sup>Institute of Science and Technology, Federal University of São Paulo (UNIFESP), São José dos Campos, Brazil.

<sup>2</sup>Institute for Applied Materials (IAM-AWP), Karlsruhe Institute of Technology (KIT), Karlsruhe, Germany.

<sup>3</sup>Federal Institute of São Paulo (IFSP), São José dos Campos, Brazil.

<sup>4</sup>Institute for Advanced Studies of the Sea, São Paulo State University (UNESP), São José dos Campos, Brazil.

<sup>5</sup>Institute of Aeronautics and Space (ITA), São José dos Campos, Brazil.

<sup>6</sup>Institute of Chemistry, University of São Paulo (USP), São Paulo, Brazil.

<sup>7</sup>Anhembi Morumbi University, São José dos Campos, Brazil.

## Abstract:

Photodynamic therapy (PDT) has emerged as an useful therapeutic treatment of cancer and infections alternative to other commonly used therapies such as chemotherapy and radiotherapy, which have several unpleasant side effects<sup>1</sup>. PDT requires the presence of photosensitizers (PS) that are able to generate reactive oxygen species after exposure to light of a specific wavelength. Coupling PS with nanoparticles has proven to be as a great strategy to improve tumor targeting and to enhance PS photoactivity. In this work, photosensitizing nanoparticles have been developed by coupling the photosensitizers hypericin and dimethyl-8,13-divinyl-3,7,12,17-tetramethyl-21H,23H-porphyrin-2,18-dipropionate dimethyl ester (Pmet) to diamond nanoparticles (NDs). The use of NDs as human anticancer agents and in health products has shown promising results for future development<sup>2</sup>. NDs have been investigated to be used as therapeutic agents, diagnostic probes, drug delivery vehicles for cancer or gene therapy, antiviral and antibacterial agents, tissue regeneration scaffolds, and as new medical devices such as nanorobots. Along with their excellent biomedical compatibility, high adsorption capacity and large surface area, one of the most important characteristics of NDs is the presence of sp<sup>2</sup> carbon atoms on their structure. This is because, in the ND structure, the sp<sup>3</sup> diamond core is covered with some layers of sp<sup>2</sup> carbon, thus allowing the surface to be functionalized, allowing the obtation of organic ND hybrid materials<sup>3</sup>. For this reason, in the present work a femtosecond laser ( $\lambda=1030\text{nm}$ , 7W) was applied to modify the surface of NDs and increase the amount of sp<sup>2</sup> carbons, which

provided enhanced binding of photosensitizers to NDs<sup>4</sup>. Reactions were carried out to couple the laser-treated NDs with the Pmet and with hypericin. Laser-treated NDs showed greater toxicity to metastatic tumor cells (murine melanoma - B16F10-Nex2) than NDs without this treatment. Therefore laser-treated NDs show great potential in the development of new anticancer agents. The integration of NDs in photodynamic therapy may offer an efficient and less toxic alternative for cancer treatment.

**Keywords:** nanodiamonds, photosensitizer, femtosecond-laser, biocompatibility.

## References:

1. Sun, C.C., Bodurka, D.C., Weaver, C.B., et al. (2005) Rankings and symptom assessments of side effects from chemotherapy: Insights from experienced patients with ovarian cancer. *Support Care Cancer* 13: 219-227.
2. Hurtado, C. R., Hurtado, G. R., de Cena, G. L., Queiroz, R. C., et al. (2021) Diamond Nanoparticles-Porphyrin mTHPP Conjugate as Photosensitizing Platform: Cytotoxicity and Antibacterial Activity. *Nanomaterials*, May 25;11(6):1393.
3. Dias, L.D., Rodrigues, F.M.S., Calvete M.J.F., et al. (2020) Porphyrin–Nanodiamond Hybrid Materials — Active, Stable and Reusable Cyclohexene Oxidation Catalysts. *Catalysts* 10:1402.
4. Fraczyk, J., Rosowski, A., Kolesinska, B. et al. (2018) Orthogonal Functionalization of Nanodiamond Particles after Laser Modification and Treatment with Aromatic Amine Derivatives. *Nanomaterials*. 8, 908.



# Lipophilic molecular rotor to assess the viscosity of oil core in nano-emulsion droplets

Mohamed Elhassan,<sup>a,b</sup> Carla Faivre,<sup>a,c</sup> Halina Anton,<sup>d</sup> Guillaume Conzatti,<sup>a</sup> Pascal Didier,<sup>d</sup> Thierry Vandamme,<sup>a</sup> Alteyeb S. Elamin,<sup>e</sup> Mayeul Collot,<sup>c</sup> Nicolas Anton<sup>a,\*</sup>

<sup>a</sup>INSERM (French National Institute of Health and Medical Research), UMR 1260, Regenerative Nanomedicine (RNM), FMTS, Université de Strasbourg, F-67000 Strasbourg, France.

<sup>b</sup>Department of Pharmaceutics, Faculty of Pharmacy, University of Gezira, Wad Medani 21111, Sudan.

<sup>c</sup>Chemistry of Photoresponsive Systems, Laboratoire de Chémo-Biologie Synthétique et Thérapeutique (CBST) UMR 7199, CNRS, Université de Strasbourg, F-67400 Illkirch, France

<sup>d</sup>Laboratory of Biophotonic and Pathologies, CNRS UMR 7021, Université de Strasbourg, Faculté de Pharmacie, 74, Route du Rhin, 67401 Illkirch, France.

<sup>e</sup>Omdurman Islamic University, faculty of pharmacy, department of pharmaceutics, Khartoum 00249, Sudan.

Correspondance Author: Nicolas Anton, [nanton@unistra.fr](mailto:nanton@unistra.fr)

## Abstract:

Characterization of nanoscale formulations is a continuous challenge. Size, morphology and surface properties are the most common characterizations. However, physicochemical properties inside the nanoparticles, like viscosity, cannot be directly measured. Herein, we propose an original approach to measuring dynamic viscosity using a lipophilic molecular rotor solubilized in the core of nano-emulsions. These molecules undergo conformational changes in response to viscosity variations, leading to observable changes in fluorescence intensity and lifetime, allowing them to sense the volume properties of nanoscale formulations. The lipophilic molecular rotor (BOPIDY derivatives) was specifically synthesized and characterized as oil viscosity sensing in large volumes. A second part of the study compares these results with rBDP-Toco in nano-emulsions (Figure 1). The objective is to evaluate the impact of the formulation, droplet size and composition on the viscosity of the droplet's core. The lipophilic rotor showed a universal behavior, whatever the oil composition, giving a master curve. Applied to nano-formulations, it discloses the viscosity in the nano-emulsion droplets, enabling the detection of slight variations between reference oil samples and the nano-formulated ones. This new tool opens the way to the fine characterization of complex colloids and multidomain nano and microsystems, potentially applying hybrid materials and biomaterials.

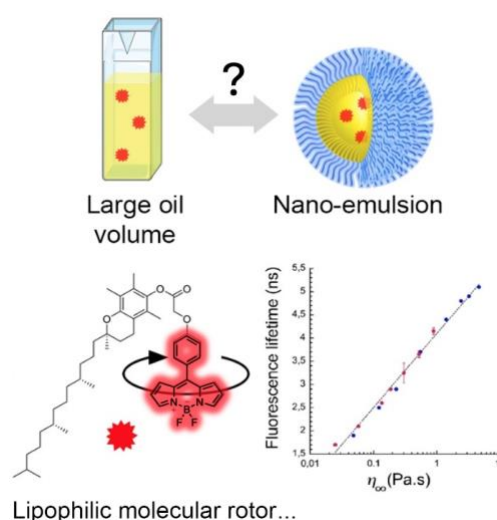


**Figure 1:** Illustrates the measurements of viscosity in large native oil and inside the nano-formulation core using a lipophilic molecular rotor (BOPIDY), the lipophilicity was enhanced by coupling with the lipid tocopherol.

**Keywords:** molecular rotors; nano-emulsions; viscosity sensor; surfactant; fluorescence intensity; fluorescence lifetime.

## References:

1. Ashokkumar, P.; Ashoka, A. H.; Collot, M.; Das, A. A fluorogenic BODIPY molecular rotor as an apoptosis marker, *Chem. Commun.*, 2019, 55, 6902-6905.
2. S. Ding, B. Mustafa, N. Anton, C.A. Serra, D. Chan-Seng, T.F. Vandamme, Production of lipophilic nanogels by spontaneous emulsification, *International Journal of Pharmaceutics* 585 (2020) 119481.

# Nanovehicles for a combined cell differentiation therapy and cancer stem cell-targeting drugs: towards a new way to prevent resistance and tumor recurrence in glioblastoma (TARG-DIFFERENT).

T. Fernandez-Cabada<sup>1</sup>, P. Melón<sup>1,2</sup>, M. Mulero-Acevedo<sup>2,1,3</sup>, P. Alfonso-Triguero<sup>1,4</sup>, A. P. Candiota<sup>2,1,3</sup>, J. Lorenzo<sup>1,2,3</sup>

<sup>1</sup> Institut de Biotecnologia i Biomedicina, Universitat Autònoma de Barcelona, Spain

<sup>2</sup> Departament de Bioquímica i Biologia Molecular, Unitat de Biociències, Universitat Autònoma de Barcelona, Spain

<sup>3</sup> Centro de Investigación Biomédica en Red: Bioingeniería, Biomateriales y Nanomedicina, Spain

<sup>4</sup> Institut Català de Nanociència i Nanotecnologia, Spain

## Abstract:

Glioblastoma (GBM; World Health Organization grade IV glioma) is the most aggressive and prevalent primary brain tumor with the worst prognosis. Despite aggressive treatment strategies, including maximal surgical resection followed by concurrent radiation therapy and chemotherapy with temozolomide (TMZ), median patient survival remains only 15 to 18 months<sup>1</sup>. A key challenge in GBM therapy is the presence of cancer stem cells (CSCs) that present characteristics such as self-renewal, contributing to tumor initiation and resistance to conventional therapies. Consequently, effective therapeutic approaches targeting CSCs are urgently needed to prevent tumor recurrence and improve patient outcomes.

One promising alternative therapy to traditional chemotherapy and radiotherapy is based on differentiation therapy, which aims to reactivate endogenous differentiation programs in tumor cells promoting their conversion to less aggressive phenotypes. In general, differentiation agents tend to have less toxicity than conventional cancer treatments. Recently, drugs that trigger differentiation in primary tumor cells (such as bone morphogenetic proteins (BMPs<sup>2</sup>) and all-trans retinoic acid (ATRA)<sup>3</sup>) have been identified, suggesting that they are clinically safe and effective. However, these agents alone often fail to fully differentiate tumor cells, allowing for GBM recurrence. Therefore, it is necessary to combine cell differentiation therapies with other therapies that are specifically directed against CSCs<sup>4</sup>. In this context, repurposed drugs such as curcumin and disulfiram have emerged as promising candidates for CSC-specific targeting, effectively eliminating CSC populations while minimizing the adverse effects associated with conventional chemotherapeutics.

Our working hypothesis is based on the possibility of combining cell differentiation therapies with

therapies directed specifically against CSCs in GBM (high targeting anti-CSCs) within a nanocarrier system (Figure 1) for a controlled drug release. This study presents some preliminary results on the efficacy of differentiation-inducing agents and repurposed drugs in the complete eradication of GBM CSCs using both immortalized GBM cell lines and patient-derived models.

**Keywords:** Cancer stem cells, glioblastoma, cell differentiation therapy, cancer stem cell targeting drugs, nanocarrier, controlled drug release

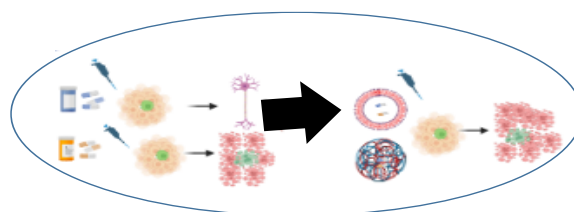


**Figure 1:** Schematic representation of the current and future steps on TARG-DIFFERENT: separate *in vitro* testing of differentiation-inducing agents and CSC targeting drugs on GBM cells, followed by the synthesis of nanoplatforms with optimized with the most effective drug combinations for GBM CSC eradication.

## References:

1. Schiffer et al. (2018), Glioblastoma: Microenvironment and Niche Concept, *Cancers*, 11, 5.
2. Koguchi et al. (2020), BMP4 induces asymmetric cell division in human glioma stem-like cells, *Oncol. Lett.* 19, 1247–1254.
3. Wang et al. (2019), All-trans retinoic acid therapy induces asymmetric division of glioma stem cells from the U87MG cell line, *Oncol Lett* 18: 3646-3654.
4. Xia et al. (2024), Drug repurposing for cancer therapy. *Sig Transduct Target Ther* 9, 92.

# Shining Light on Cancer Treatments: Integrated Photonic Biosensors for Immunotherapy Monitoring

Anjara Morgado Benítez<sup>1,#</sup>, Violeta Gil-Ocaña<sup>1,#</sup>, Laura Rueda Calzada<sup>1</sup>, Yara Aceta<sup>1</sup>, Antonio Conde-González<sup>1</sup>

<sup>1</sup> Bioherent S.L., Calle Severo Ochoa 34, 29590 Málaga, Málaga, Spain

# Equal contribution

## Abstract:

Bevacizumab (anti-VEGF antibody) is a key drug in oncological immunotherapy. Fast and precise immunotherapy monitoring is essential to tailor drug dosing to individual patient responses, detect early signs of adverse reactions like immune-related toxicities, and manage drug resistance. Real-time data allow for personalized medicine and adaptive treatments that can improve outcomes and reduce side effects.

Photonic biosensors are transforming healthcare by enabling real-time, label-free biomolecule quantification with cost-effective, user-friendly and highly versatile instrumentation. In this work, we present the development of an integrated photonic biosensor for monitoring immunotherapy treatments such as Bevacizumab. At the core of this biosensor is an optimized biorecognition layer, which plays a critical role in enhancing the biosensor's selectivity, sensitivity and overall performance. Our optimized biorecognition layer enables target detection in complex environments, such as serum, with little sample preparation. Our layer introduces carboxylic acid moieties for both enhancing detection and enabling formation of stable anchoring of anti-Bevacizumab *via* amide coupling. Overall, our system detects Bevacizumab in human serum under 10 ng/mL and 60 min, offering a significantly better performance than conventional reference ELISA immunoassays (30 ng/mL and 2-3h).

**Keywords:** surface chemistry, biorecognition layer, smart materials, biosensors, immunotherapy, precision medicine

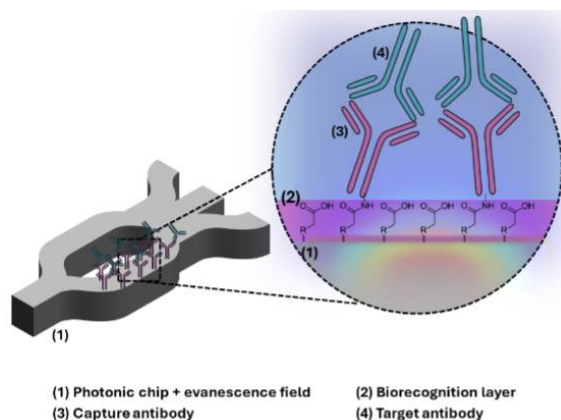


**Figure 1:** Figure illustrating the biorecognition layer on a (1) biosensor. The (2) biorecognition layer is assembled on top of the biosensor surface with the (3) capture antibody anchored via formation of stable amide. Evanescence field, which penetrates few 100 nm in the biorecognition layer, can detect the anchoring of the capture antibody and (4) target antibody.

# NIR responsive gold nanorod for targeted cancer photothermal therapy

Shagufta Gul<sup>1</sup>, Francesco Barbero<sup>2</sup>, Aurora Bellone<sup>2</sup>, Guido Perrone<sup>2</sup>, Roberto Mazzoli<sup>3</sup>, Ivana Fenoglio<sup>1\*</sup>

<sup>1</sup> Department of Chemistry, University of Turin, Turin, Italy

<sup>2</sup> Department of Electronics and Telecommunications, Politecnico di Torino, 10129 Torino, Italy

<sup>3</sup> Department of Department of Life Sciences and Systems Biology, University of Turin, Turin, Italy

## Abstract:

Advancements in nanotechnology are revolutionizing cancer therapy, offering new avenues for targeted and efficient treatments. Gold nanorods (AuNRs) have been extensively explored, due to their well-defined anisotropy, unique optical properties, which provide enhanced photothermal conversion efficiency and deeper tissue penetration under near-infrared (NIR) laser irradiation, that allow their use in various nanomedicine applications (Zhou, Zhang et al. 2022) (reference). The synthesis of GNRs typically involves the use of cetyltrimethylammonium bromide (CTAB), a cationic surfactant that forms a bilayer structure on the surface of AuNRs which plays a crucial role in controlling the size, shape, growth of rods and maintain their good dispersibility in an aqueous phase (Mosquera, Wang et al. 2023) (reference). For medical applications, CTAB needs to be removed due to its cytotoxicity. However, simple purification of CTAB-stabilized GNRs induces the loss of colloidal stability.

In the present study the synthesis of AuNRs has been optimized. The nanorods have been characterized by UV-Vis-NIR spectroscopy to examine their optical properties, including surface plasmon resonance and transmission electron microscopy TEM to observe their size, shape, and structural integrity. Several strategies have been apply to remove CTAB, such as ligand exchange, surface functionalization with biocompatible proteins and inorganic coatings, have been attempted selecting those able to maintain good plasmonic properties and good colloidal stability.

AuNRs demonstrated strong absorption in the NIR region, making them ideal for photothermal therapy. Upon NIR laser irradiation (915 nm), the AuNR efficiently produced localized heat, showcasing their potential for photothermal therapy. Moreover, the nanorods appeared stable during time.

One of the possible strategy to improve the biocompatibility and promote the targeting into tumors is to coat AuNRs with carbon shel via

hydrothermal method and then the inclusion of AuNR@C in extracellular vesicles (EVs). While these methods have shown promise in previous studies, achieving optimal loading efficiency and maintaining EV integrity remains a critical objective. In the present study the integration of AuNRs and AuNR@C has been attempted using methods such as electroporation, sonication, and co-incubation.

**Keywords:** Extracellular vesicles, Gold nanorods, photothermal therapy,

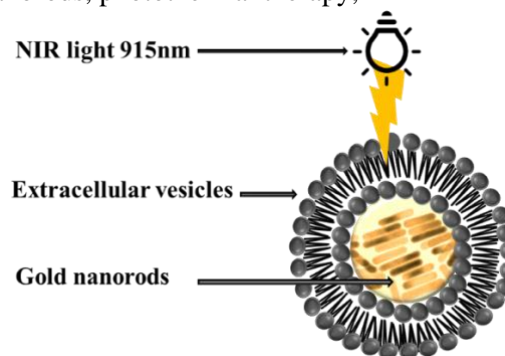


**Figure 1:** Figure illustrating the integration and application of GNR@C-loaded extracellular vesicles (EVs).

## References:

1. Kaneti, Y.V., Chen, C., Liu, M., Wang, X., Yang, J.L., Taylor, R.A., Jiang, X., Yu, A., 2015. Carbon-Coated Gold Nanorods: A Facile Route to Biocompatible Materials for Photothermal Applications. *ACS Applied Materials & Interfaces* 7, 25658-25668.
2. Kim, H.I., Park, J., Zhu, Y., Wang, X., Han, Y., Zhang, D., 2024. Recent advances in extracellular vesicles for therapeutic cargo delivery. *Experimental & Molecular Medicine* 56, 836-849.
3. Mosquera, J., et al. (2023). "Surfactant Layers on Gold Nanorods." *Accounts of chemical research* 56(10): 1204-1212.
4. Zhou, R., et al. (2022). "Gold Nanorods-Based Photothermal Therapy: Interactions Between Biostructure, Nanomaterial, and Near-Infrared Irradiation." *Nanoscale Research Letters* 17(1): 68.



# Self-targeted magnetic nanoparticles for combined magnetothermal therapy and immunotherapy in cancer treatment

Xulin Xie <sup>1,2</sup>, Chi-Chun Fong <sup>1,2</sup>, Mengsu Yang <sup>1,2,\*</sup>

<sup>1</sup>Department of Biomedical Sciences and Tung Biomedical Sciences Centre, City University of Hong Kong, Hong Kong SAR, China

<sup>2</sup>Department of Precision Diagnostic and Therapeutic Technology, City University of Hong Kong Shenzhen Futian Research Institute, Shenzhen, China

## Abstract:

Magnetic hyperthermia therapy (MHT) is non-invasive and has excellent tissue penetration for deep-seated tumors, but unfortunately, suffers from low therapeutic efficacy due to insufficient intratumoral accumulation of conventional intravenously injected magnetic nanoparticles. Such a disadvantageous characteristic is expected to be solved by specially designed tumor-targeted magnetic nanoparticles. A kind of antibody-modified iron oxide superparamagnetic nanoparticles with penetrating peptide modification was synthesized, which exhibits excellent and highly controllable magnetic hyperthermia performance for effective MHT at the local tumor site. The controllable mild MHT at 43-44 °C based on the tailored magnetic nanoparticles shows almost complete inhibition of breast cancer cell proliferation and tumor growth. More importantly, the mild MHT-treated breast cancer cells are able to activate immune cells. As a result, the growth of both xenograft breast tumors was almost completely suppressed under mild MHT via induced immunocyte-related anti-tumor immunity in vivo. This work not only demonstrates the great potential of mild MHT but also elucidates the underlying immunity activation mechanism in the treatment of breast cancer by mild MHT.

**Keywords:** Magnetic hyperthermia therapy, Cancer treatment, Immunotherapy, Liposome

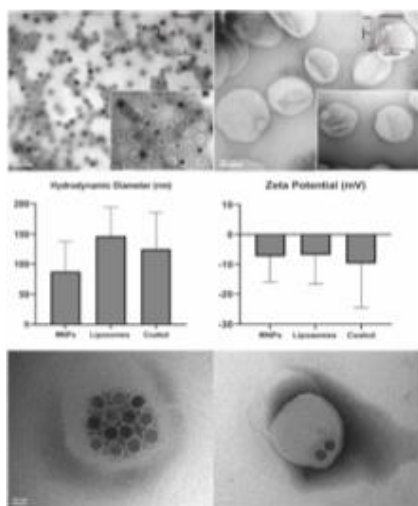


**Figure 1:** Low and high magnification TEM images (Scale bar: 20 nm and 100 nm), size distribution, and Zeta potential of A) magnetic nanoparticles (MNPs) and B) liposomes. C-D) Low magnification TEM images (Scale bar: 20 nm) of coated MNPs.

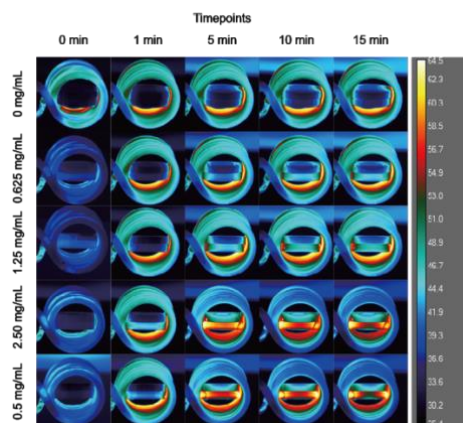


**Figure 2:** Thermal images of MNPs in different concentrations at various time points.

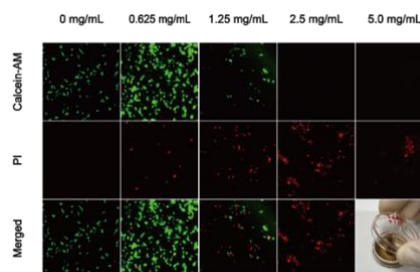


**Figure 3:** CLSM images of CAM- and PI-stained MDA-MB-231 cells after MHT of various MNP concentrations (Scale bar: 50  $\mu$ m).

## MHT performance on MDA-MB-231 cell line

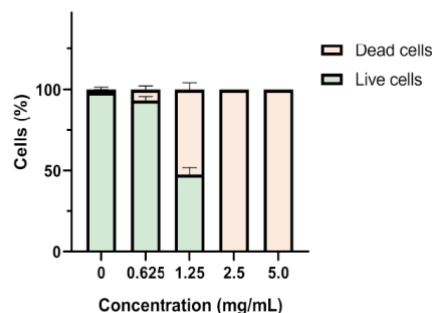


**Figure 4:** Relative cell viability of MDA-MB-231 cells after MHT of various MNP concentrations.



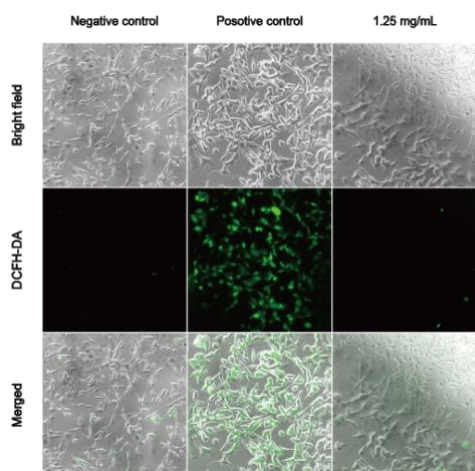


**Figure 5:** Ferroptosis assay after MHT of 1.25 mg/ml MNP group.

**References:**

1. Giaquinto AN, Sung H, Miller KD, Kramer JL, Newman LA, Minihan A, Jemal A, Siegel RL. (2022), Breast Cancer Statistics, 2022. *CA Cancer J Clin.*, 72(6):524-541.
2. Lei G, Zhuang L, Gan B. (2022), Targeting ferroptosis as a vulnerability in cancer. *Nat Rev Cancer.*, 22(7):381-396.

# New Insight in the radius of influence in Electric Force Microscopy

L. Lehnert <sup>1</sup>, R. Thoelen <sup>2</sup>, H. Möbius <sup>1</sup>

<sup>1</sup> Department of Computer Sciences and Micro Systems Technology,  
University of Applied Sciences Kaiserslautern, Zweibrücken, Germany

<sup>2</sup> Institute for Materials Research, Hasselt University, Hasselt, Belgium

## Abstract:

Electrostatic Force Microscopy (EFM) is a well-established technique for characterizing local electrostatic material properties in the nanometer range. In EFM, tip and substrate form a capacitor with a capacitance sensitive to changes of charge distribution or dielectric properties while scanning the surface. This capacitance can theoretically be modelled using analytical calculations of the tip substrate interaction, complex 3D-FEM simulations or the model of a parallel plate capacitor characterized by a so-called radius of influence ( $r_{inf}$ ) [1-3]. Common to all calculations is the consideration of the contact potential difference ( $V_{CPD}$ ) between tip and substrate material as an additional voltage opposite to the voltage applied.

In this work we developed a new measuring method which allows the determination of the radius of influence based on a nanoparticle model system. To avoid topographic crosstalk the tip substrate distance is kept constant (linear mode) while measuring above a dielectric nanoparticle (polystyrene). The electrostatic force gradient corresponding to the second derivative of the capacitance of the parallel plate capacitor is proportional to the phase shift of the oscillating tip. The only fitting parameter is the radius of influence which was investigated as a function of the applied voltage ( $V_{Tip}$ ).

From theory a zero phase shift is expected when the applied voltage equals the contact potential difference  $V_{CPD}$ , which is in contrast to measurements in several works. Our measurements reveal the radius of influence to be constant only for voltages significantly larger than the contact potential difference. We observed that the radius of influence increases with decreasing applied voltage showing a maximum when  $V$  reaches  $V_{CPD}$ . The fact of a non-zero phase shift when the applied voltage reaches  $V_{CPD}$  as well as the result of the dramatically increasing radius of influence approaching  $V_{CPD}$  show the necessity of taking into account the different origin of the voltage applied and  $V_{CPD}$  in the theoretical models.

**Keywords:** Electrostatic Force Microscopy, polymer nanoparticle, radius of influence, contact potential difference

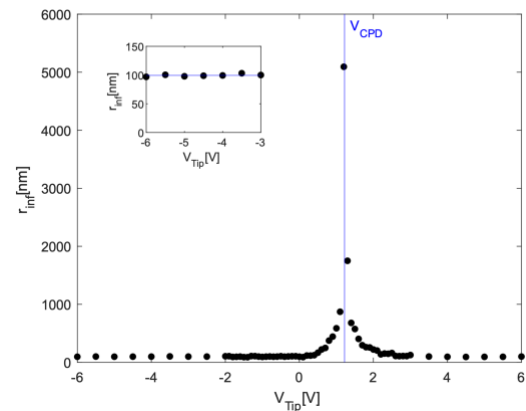


**Figure 1:** Radius of influence as function of applied voltage (126 nm polystyrene nanoparticle, CoCr coated tip, 33 nm tip radius)

## References:

1. M. Fuhrmann, A. Musyanovych, R. Thoelen, and H. Moebius, "Determination of the dielectric constant of non-planar nanostructures and single nanoparticles by electrostatic force microscopy," *Journal of Physics Communications*, vol. 6, no. 12, 2022, doi: 10.1088/2399-6528/aca87b.
2. S. Belaidi, P. Girard, and G. Leveque, "Electrostatic forces acting on the tip in atomic force microscopy: Modelization and comparison with analytic expressions," *Journal of Applied Physics*, vol. 81, no. 3, pp. 1023-1030, 1997, doi: 10.1063/1.363884.
3. L. Fumagalli, D. Esteban-Ferrer, A. Cuervo, J. L. Carrascosa, and G. Gomila, "Label-free identification of single dielectric nanoparticles and viruses with ultraweak polarization forces," *Nat Mater*, vol. 11, no. 9, pp. 808-16, Sep 2012, doi: 10.1038/nmat3369.

# Hydrogen-like atoms with shielded ions in the tight-binding approximation.

Freinkman B.G., Independent researcher, Moscow, Russia

## Abstract:

The simplest model of multi-electron atoms is the model of independent electrons [1] and in particular the model of a hydrogen-like atom. In [2], based on the Thomas-Fermi theory, the distribution of electrons in shielded atoms ions with an arbitrary nuclear charge was obtained. This electron distribution was used in [3] as a model of the carbon atom to calculate the emission characteristics of grfen. It was assumed that of the four valence electrons, three electrons in bonds have little effect on the emission process, which is mainly determined by the fourth weakly bound electron, strongly interacting with the field of the environment. The use of this model to calculate the ionization potential of light atoms [4] gave good agreement with the experiment.

In this paper, the interaction of a hydrogen-like atom with a shielded ion with an external quasi-static field is investigated. An analytical expression for the distribution of the binding energy of an electron with an ion in this field is obtained. It is used to calculate the cross section of the interaction of this atom with a quasi-static field in the Brandt-Lundquist local plasma frequency approximation [5,6].

## References

1. W. Fano, L. Fano Physics of Atoms and Molecules Science 1980
2. W. Brandt, M. Kitagawa. Effective stopping-power charges of swift ions in condensed matter // Phys. Rev., 1982, v. B25, n. 9, p. 5631-5637.
3. B. G. Freinkman. Model of the pseudopotential of a carbon atom in a graphene lattice // Mathematical Modeling, 2015, vol. 27, no. 7, pp. 122-128. (in Russia)
4. B. G. Freinkman. Coulomb Interactions in the Model of an Isolated Atom with a Screened Ion Mathematical Models and Computer Simulations, 2022, Vol. 14, No. 5, pp. 710–715.
5. W. Brandt, S. Lundqvist Atomic Oscillations in the Statistical Approximation Phys. Rev. 1965. V. 139, p. A612–A617.
6. V. A. Astapenko Interaction of Radiation with Atoms and Nanoparticles. Publishing House “Intellect” Dolgoprudny, 2010 (in Russia)

# A miniaturized, wireless and implantable sensory system to screen bone healing.

E. Guerrero SanVicente <sup>1</sup>, C. Hennemann <sup>2</sup>, J. Disser <sup>2</sup>, R. Grinyte <sup>1</sup>, N. Marjanovi <sup>2</sup>, J. M. Cabot <sup>1</sup>

<sup>1</sup> Diagnostic Devices, LEITAT, Barcelona, Spain

<sup>2</sup> Electronics, CSEM, Neuchatel, Switzerland

## Abstract:

The monitoring of bone regeneration after large bone fractures is still a challenge that needs to be addressed. Therefore, in this project a novel solution was proposed in order to help and screen bone healing. This goal was accomplished by a combination of a bone scaffold and an implantable sensory system (Figure 1) entitling the following challenges:

- Sensors to monitor the most significant parameters of bone regeneration and infection presence: pH, Temperature (T), strain-gauge and biosensors for Transforming Growth Factor (TGF $\beta$ 1).
- Biocompatible and implantable, a feature that was ensured by conducting in-vitro cytotoxicity in cells and in-vivo tests in animal models.
- Flexible for implantation (Kapton as base material) at the same time as cost-effective.
- Wireless so it incorporated a battery, and the biosensors used the Differential Pulse Electrochemical technique that is label and reagent free for being inside the body.
- Continuous and real-time measurement which was done via Bluetooth and smartphone readout.

Each sensor was developed individually in the laboratory environment, and then integrated in a full system divided into a hard PCB (microcontrollers, battery, bluetooth, transceiver) and flex PCB (biosensors and sensors). The whole system was coated with Parylene-F, then moulded into a medical grade silicon and sterilized with hydrogen peroxide plasma. Furthermore, all the necessary in-vitro cytotoxicity tests were done in cell before the *in vivo* biocompatibility and performance studies in sheep models were conducted.

**Keywords:** implantable sensors, pH sensor, temperature sensor, strain gauge sensor, biosensors, smart wireless system, bone regeneration.

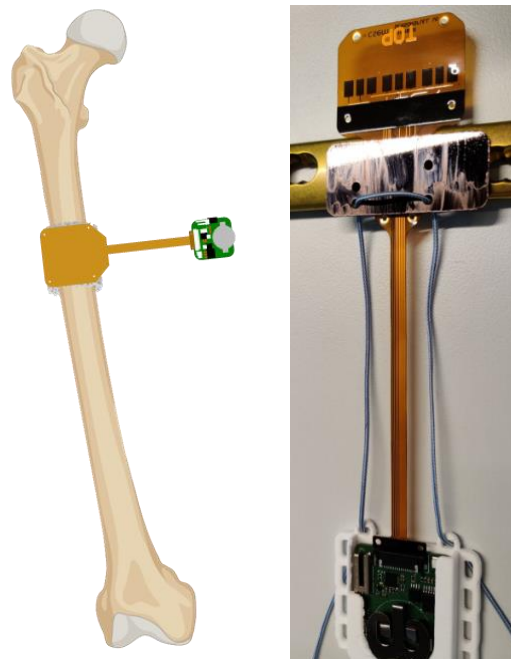


**Figure 1:** Illustration of the concept idea for wireless monitoring of bone regeneration with a scaffold in the bone defect and a sensor on top (left) and a picture of the integrated system built with pH, T, strain-gauge sensors and biosensors for its application (right).

## References:

1. K. C. McGilvray, E. Unal, K. L. Troyer, B. G. Santoni, R. H. Palmer, J. T. Easley, H. V. Demir, C. M. Puttlitz, "Implantable Microelectromechanical Sensors for Diagnostic Monitoring and Post-Surgical Prediction of Bone Fracture Healing" *Journal Of Orthopaedic Research* October, pp. 1439-1446, 2015.
2. M. Graya, J. Meehanb, C. Warda, S.P. Langdonb, I.H. Kunklerb, A. Murrayd, D. Argylea, "Implantable biosensors and their contribution to the future of precision medicine," *The Veterinary Journal*, vol. 239, pp. 21–29, 2018..



**SETCOR**  
Conferences & Exhibitions